Multi-mode Active Vibration Control Using H_∞ Optimization MIMO Positive Position Feedback Based Genetic Algorithm

by

Zhonghui WU *B.Eng(Electrical)*

School of Computer Science, Engineering and Mathematics, Faculty of Science and Engineering

31/03/2014

A THESIS SUBMITTED IN FULFILMENT OF THE REQUIREMENT FOR THE DEGREE OF MASTER OF ENGINEERING

Adelaide, South Australia, 2014

Contents

List of Figures

List of Tables

Abstract

In this thesis, experimental, analytical and numerical analysis three kinds of methods are used for distributed parameter plate structure modeling, an infinite-dimensional and a very high-order plate mathematical transfer function model is derived based on modal analysis and numerical analysis results. A feed-through truncated plate model which minimizing the effect of truncated modes on spatial low-frequency dynamics of the system by adding a spatial zero frequency term to the truncated model is provided and numerical software MATLAB is used to compare the feed-through truncated plate model with traditional balanced reduction plate model which is used to decrease the dimensions and orders of the infinite-dimensional and very high-order plate model. Active vibration control strategy is presented for a flexible plate structure with bonded three self-sensing magnetic transducers which guarantee unconditional stability of the closed-loop system similar as collocated control system. Both multi-mode SISO and MIMO control laws based upon positive position feedback is developed for plate structure vibration suppression. The proposed multi-mode PPF controllers can be tuned to a chosen number of modes and increase the damping of the plate structure so as to minimize the chosen number of resonant responses. Stability conditions for multi-mode SISO and MIMO PPF controllers are derived to allow for a feed-through term in the model of the plate structure which is needed to ensure little perturbation in the in-bandwidth zeros of the model. A minimization criterion based on the H_∞ norm of the closed-loop system is solved by a genetic algorithm to derive optimal parameters of the controllers. Numerical simulation and experimental implementation are performed to verify the effectiveness of multi-mode SISO and MIMO PPF controllers vibration suppression for the feed-through truncated plate structure.

List of Abbreviations

SISO	Single Input Single Output
MIMO	Multiple Input Multiple Output
T.F	Transfer Function
PDE	Partial Derivative Equation
ODE	Ordinary Differential Equation
PPF	Positive Position Feedback
IMSC	Independent Modal
FSS	Flexible Spacecraft Simulator
AVA	Active Vibration Absorber
SRF	Stain Rate Feedback
LQR	Linear Quadric Regulator
NNP	Neural Network Predictive
LQG	Linear Quadratic Gaussian
PACE	Planar Articulating Controls Experiment
RCGA	Real Coded Genetic Algorithm
SIMO	Single Input Multiple Output
FXLMS	Filtered-X Least Mean Square
AVC	Active Vibration Control
MISO	Multiple Input Single Output
FEM	Finite Element Method
MDF	Medium Density Fibreboard

Certification

I certify that this work does not incorporate without acknowledgment any material previously submitted for a degree or diploma in any university; and that to the best of my knowledge and belief it does not contain any material previously published or written by another person except where due reference is made in the text.

Flinders University may lend this thesis to other institutions or individuals for the purpose of scholarly research;

Flinders University may reproduce this thesis by photocopying or by other means, in total or in part, at the request of other institutions or individuals for the purpose of scholarly research.

Adelaide, 31 March 2014

Zhonghui WU

Acknowledgement

I am heartily thankful to Associate Professor Fangpo He, whose guidance and support at the initial and medium level.

To Dr. Lei Chen, who is from the mechanical engineering school of Adelaide University, thanks a lot for your willingness to help and your availability time for long discussions and helpful suggestions.

To S. O. R. Moheimani, thanks a lot for your contributions to vibration control theory. I felt that I was just like under your supervision to finish my thesis after read your books and thesis.

To Siyang Yu, thanks for your help and discussion the ANSYS model with me.

Finally, I wish to thank my family, my father-in-law, mother-in-law, my mum, and my daughter Hanzhen , Hanen, especially to my wife Clare, whom I mostly in debt, thank you so much for your constant love, support, patience, and encouragement during the whole study time of master degree at Flinders University, without whom I would be unable to complete my degree, thanks a million, love you forever!

Also thanks all the people who giving help:
Miss Natalie Hills
Ms Kylie Sappiatzer
Ms Vanesa Duran Racero
Prof Sonia Kleindorfer,
Professor Paul Calder,
Dr Peter Anderson,
Ms Anne Hayes
Ms Lisa O'Neill
Prof Mark Taylor
Prof John Roddick

Prof Warren Lawrance

Prof Carlene Wilson

Prof Jeri Kroll

Chapter 1

Introduction

This chapter discusses the motivation for the research described in this thesis. The research methodology is presented, followed by a literature review. Finally, an outline of the thesis is given along with a list of original contributions.

1.1 Motivation

In order to improve dynamic performance, the operating efficiency, and the amount of material which is used in mechanical structures, many designers employ lightweight materials to reduce the cross sectional dimensions of those structures [4].

However, one side-effect of employing lightweight materials and reducing the cross sectional dimensions is that the structures become more flexible. Flexible structures are more susceptible to the detrimental effects of unwanted vibration, particularly when they operate at or near their natural frequencies or when they are excited by disturbances that coincide with their natural frequencies [4].

The design and implementation of a high performance vibration controller for a flexible structure can be a difficult task. The difficulty is due to the following factors but not limited:

i. A major difficulty in control of flexible structures is due to the fact that they are distributed parameter systems. Consequently, these structures have a very large number of vibration modes and their transfer functions contain many poles close to the jω axis [1]. High-frequency modes also contribute to the dynamics at low frequencies. Thus, a model may have to include a relatively high number of high-f requency modes to capture the low frequency dynamics with acceptable accuracy. This yields a model with a relatively high order and the systems are generally difficult to control [2].

ii. In most cases, a small number of in-bandwidth modes of the structure are required to be controlled, and it is possible that some in-bandwidth modes are not targeted to be controlled at all. The presence of uncontrolled modes can lead to the problem of spill-over. That is, the control energy is channeled to the residual modes of the system and this process may destabilize the closed-loop system. In particular, the spill-over effect is of major concern at higher frequencies where obtaining a precise model of the structure is rather difficult [3]. Normally there are two types of spill-over: control spill-over and observation spill-over. Control spill-over occurs when the control force excites unmodeled dynamics. The excitation of these unmodeled dynamics can degrade the performance of the system. Observation spill-over refers to the measurement error caused by the contribution of excluded modes to the sensor measurements. While control spill-over leads to poor performance, observation spill-over can lead to instability [4].

iii. To control a flexible structure that has widely separated multi-mode vibration a wide-band controller is needed. However, the design of a high performance wide-band controller is difficult. The difficulty is due to the design trade-off between the error reduction in one frequency band and the increase of sensitivity at other frequencies, as explained in Bode's theorem [5] .

Given these requirements, the question is how to design and implement a suitable controller. Seeking the answer to this questions is the motivation for the research described in this thesis.

1.2 Research Methodology

The research methodology includes of four steps:

In the first step, a literature review overviews the relevant existing methods for controlling the vibration of flexible structures, and discusses the relevant shortcomings or gaps in those methods. Based on the gaps that are found in the existing methods, new control methods are proposed.

In the second step, an experimental plant that can be used as a tool for the design and evaluation of the effectiveness of the proposed control methods, is designed and implemented. The plant chosen must represent a real application and have the essential

characteristics of a flexible structure. A flexible two dimensions plate with three transducers which are treated as supporting feet is chosen as the experimental plant.

In the third step, analytical and numerical analysis three kinds of methods are used for modeling, an infinite-dimensional and a very high-order plate mathematical transfer function model is derived based on modal analysis and numerical analysis results. A feed-through truncated system model which minimizing the effect of truncated modes on spatial low-frequency dynamics of the system by adding a spatial zero frequency term to the truncated system model is provided and numerical software MATLAB is used to compare the feed-through truncated system model with traditional balanced reduction model which is used to decrease the dimensions and orders of the infinite-dimensional and very high-order model.

In the fourth step, SISO and MIMO PPF controllers were designed based on the H_∞ norm of the closed-loop system by a genetic algorithm to derive optimal parameters of the controller.

In the fifth step, simulation models of the experimental plant are implemented, and computer simulations are exercised. These simulations reduce the design time, increase the success rate of the real-time implementation, and help in the evaluation of the performances of the proposed controllers prior to their use with the experimental plant.

In the sixth step, the proposed controllers are used with the experimental plant and the effectiveness of the proposed control methods are evaluated.

1.3 Vibration Control of Structure

Vibration control is applied with respect to avoid the unwanted vibration of the structure. Vibration control can be categorized into two major techniques: passive control and active control.

Passive Control

For passive control, vibration is attenuated or absorbed by traditional vibration dampers, shock absorbers, and base isolation. However, it has two major drawbacks.:

i. Firstly, it is ineffective at low frequencies. The natural frequency is inversely proportional to the square root of the spring compliance and to the mass of the damper. Hence, at low frequencies, the volume and mass requirements are often impractically large for many applications where physical space and mass loading are critical.
ii. Secondly, the passive technique only works effectively for a narrow band of frequencies and is not easy to modify [6].

Active Control

For active vibration control, it is the active application of force in an equal and opposite fashion to the forces imposed by external vibration.In contrast with passive control, active control works effectively over a wide bandwidth where the working band does not depend on the characteristics of the structure, and is limited only by the bandwidth of the actuators. Furthermore, the actuators are less sensitive to the characteristics of the structures and the vibration sources. Therefore, the same actuators can be used even if the characteristics of the structures or the vibration sources are changed. To maintain the system performance, the electronic controller might need to be modified, but this modification is relatively easy, especially with digital controllers [7].

From the above discussion, it is clear that active control shows better potential comparing with passive control. So this thesis will focus on the design of active controllers.

1.4 Active Vibration Control of Structure

1.4.1 open-loop and closed-loop control

Active control can be classified as open-loop and closed-loop.

Open-loop Control

An open-loop control system uses a controller and an actuator to obtain the desired response and it is a system without feedback [8]. In general, an open-loop system relies on the model of the plant to obtain a command input that, supplied to it, causes the output to follow a desired pattern. This strategy requires very good knowledge of the

dynamics of the controlled system and is usually applied only as a feed-forward component in conjunction with a feedback controller [9].

advantages:

- simplicity and stability: they are simpler in their layout and hence are economical and stable too due to their simplicity.
- construction: since these are having a simple layout so are easier to construct [9].

disadvantages:

- accuracy and reliability: since these systems do not have a feedback mechanism, so they are very inaccurate in terms of result output and hence they are unreliable too.
- due to the absence of a feedback mechanism, they are unable to remove the disturbances occurring from external sources [9].

Closed-loop Control

In contrast to an open-loop control system, a closed-loop control system utilizes an additional measure of the actual output to compare the actual output with the desired output response. The measure of the output is called the feedback signal. A feedback control system is a control system that tends to maintain a prescribed relationship of one system variable to another by comparing functions of these variables and using the difference as a means of control. With an accurate sensor, the measured output is a good approximation of the actual output of the system [8].

advantages:

- accuracy: they are more accurate than open-loop system due to their complex construction. They are equally accurate and are not disturbed in the presence of non-linearities.
- noise reduction ability: since they are composed of a feedback mechanism, so they clear out the errors between input and output signals, and hence remain unaffected to the external noise sources [8].

disadvantages:

- construction: they are relatively more complex in construction and hence it adds up to the cost making it costlier than open-loop system.
- since it consists of feedback loop, it may create oscillatory response of the system and it also reduces the overall gain of the system.
- stability: it is less stable than open loop system but this disadvantage can be striked off since we can make the sensitivity of the system very small so as to make the system as stable as possible [8].

In order to achieve better performance, the design control method discussed in this thesis will concentrate on closed-loop control.

1.4.2 Feed-forward and Feedback Control

Active control can be classified as feed-forward or feedback control depending on the derivation of the error signal.

Feed-forward Control

Feed-forward is a term describing an element or pathway within a control system which passes a controlling signal from a source in its external environment, often a command signal from an external operator, to a load elsewhere in its external environment. A control system which has only feed-forward behavior responds to its control signal in a pre-defined way without responding to how the load reacts; it is in contrast with a system that also has feedback, which adjusts the output to take account of how it affects the load, and how the load itself may vary unpredictably; the load is considered to belong to the external environment of the system [10].

In a feed-forward system, the control variable adjustment is not error-based. Instead it is based on knowledge about the process in the form of a mathematical model of the process and knowledge about or measurements of the process disturbances [10].

For the feed-forward system[11,12,13], it has some advantages [14]:

- wider bandwidth
- works better for narrow-band disturb

also include disadvantages [14]:

- reference needed
- local method (response may be amplified in some part of the system)
- large amount of real time computations

Feedback Control

In feedback control, the error signal, which is the difference between the desired response and the controlled output, is fed to the controller. The controller then generates control signals to drive the error signal to zero. With feedback control, stability becomes a major concern because the feedback modifies the characteristic of the original plant [14].

advantages [14]:

- guaranteed stability when collocated
- global method
- attenuates all disturbances within ω_c (bandwith)

disadvantages [14]:

- effective only near resonances
- limited bandwidth
- disturbances outside ω_c (bandwith) are amplified
- spill-over

Due to the excitation signal in the flexible plate, feed-forward control is not suitable for application with this system. Therefore, the design control method discussed in this thesis mainly focuses on feedback control.

1.4.3 Wave Control and Modal Control

Active control can also be classified according to the model descriptions upon which the control design is based. The most common descriptions of the vibration of continuous systems are in terms of waves and modes of motion [15]. These two descriptions lead to two different approaches for active control: wave control and

modal control.

Wave Control

In a structure where the flow of vibrational energy from one part to another is significant and needs to be reduced, wave control is normally used. Wave control design makes use of the wave equation of a structure and the local properties at and around the control region. Since inherently the local properties of the structure are less sensitive to system properties wave control has a good robustness. However, because it does not take into account global motion, global behaviour can adversely affect the amount of control achieved [4].

Difficulty in realizing an active wave control system is that all components in the system are expressed as non-causal and irrational functions of Laplace variable s. Therefore, in a practical case, the wave controllers are approximately realized to a limited extent [16].

Modal Control

Modal control of flexible structures has been of great interest for several decades among vibration control engineers. In general, modal analysis and control refer to the procedure of decomposing the dynamic equations of a system into modal coordinates and designing the control system in this modal coordinate system [17]. The principle behind it is that it somehow extracts a target mode signal from the structural response and controls it in modal domain in a similar way to controlling a single degree-of-freedom oscillator. Advantages are as follows: controller design is easy as it is conducted in modal domain, a global vibration reduction over the whole structure can be achieved by suppressing modes at a number of discrete positions (i.e., global control using local feedback), and the designed controller is inherently very robust to the dynamics of uncontrolled modes [18].

Because of the implement limitation, in this thesis, the design control method will follow on collocated control.

1.4.4 SISO Control and MIMO Control

A single-input and single-output (SISO) system is a simple single variable control system with one input and one output. Systems with more than one input and more than one output are known as multi-input multi-output (MIMO) systems. Normally SISO systems are typically less complex than MIMO systems, and SISO system is also easier to be constructed and implemented.

Due to the increasing complexity of the system under control and the interest in achieving optimum performance, the importance of control system engineering has grown in the past decade. Furthermore, as the systems become more complex, the interrelationship of many controlled variables must be considered in the control scheme [4].

In order to make the clearly comparison, in this thesis, both SISO and MIMO methods will be invested later.

1.4.5 Collocated Control and Uncollocated Control

Collocated Control

A collocated control system is a control system where the actuator and the sensor are attached to the same d.o.f.(degree of freedom). It is not sufficient to be attached to the same location; they must also be dual, that is, a force actuator must be associated with a displacement (or velocity or acceleration) sensor, and a torque actuator with an angular (or angular velocity) sensor, in such a way that the product of the actuator signal and the sensor signal represents the energy (power) exchange between the structure and the control system [3].

The structure of the collocated system allows for the design of feedback controllers, with specific structures, that guarantee unconditional stability of the closed-loop system. Such controllers are of interest due to their ability to avoid closed-loop instabilities arising from the spill-over effect [3].

Uncollocated Control

Non-collocation of sensor and actuator is often unavoidable due to installation convenience of transducers or is even recommendable for high degrees of observability and controllability. However, non-collocated control is generally known to be more involved than collocated control as the plants are no longer minimum phase [18].

For non-collocated control, one major reason for this is a modeling difficulty, since it is impossible to model an infinite number of modes existing in a flexible structure. Those controllers designed based on a few low order modes may thus seriously suffer from the control spillovers associated with un-modeled but often non-negligible high order modes. Another is due to the non-minimum phase characteristic of the plant, and thus the modes excited by a control actuator will not all be the same in phase, when measured at a non-collocated sensor location [18].

Based on the information, in this thesis, the design control method will pay close attention on collocated control.

1.5 Modal Based Controller for Multi-mode Vibration Control

There are three main modal control methods that can be found in the literature for controlling multi-mode vibration in flexible structures: independent modal space control (IMSC) , resonant control and positive position feedback (PPF) control.

1.5.1 Independent Modal Space Control (IMSC)

Meirovitch [19,20] established the independent modal space control (IMSC) which allows the control design for each single mode to be implemented independently, hence there is little spillover to the residual modes. However, this method requires as many sensors/ actuators as the number of modes to be controlled, and thus it can only control a limited number of modes. Furthermore, the control system is vulnerable to uncertainties such as parameter fluctuation. To overcome this problem, the application of the robust control techniques to active vibration control problem has been discussed in the past two decades [16].

1.5.2 Resonant Control

The resonant control method proposed by Moheimani et al. [21,22,23,24,25,26] is based on the resonant characteristic of flexible structures. The controller applies high gain at the natural frequency and rolls off quickly away from the natural frequency thus avoiding spillover. It is also described as having a decentralized characteristic from a modal control perspective [27], thereby making it possible to treat each of the system's modes in isolation. One of the issues with resonant controllers is their limited performance in terms of adding damping to the structure [3].

1.5.3 Positive Position Feedback (PPF) Control

Positive position feedback (PPF) was devised by Goh and Caughey [28,29], the stability was proved by Fanson J. L. [30,31], it has several distinguished advantages [32]. It has been shown to be a solid vibration control strategy for flexible systems with smart materials, particularly with the PZT (lead zirconium titanate) type of piezoelectric material [28,29,30].

PPF controller development

After the PPF controller theory was provided, lots of people did the simulations and experiments using PPF theory for active vibration, for example:

[31] developed the method further and showed that PPF was capable of controlling the first six bending modes of a cantilever beam. The second order PPF filter was simple to implement and had global stability conditions, which were easy to fulfill even in the presence of actuator dynamics.

[33,34] introduced a first order PPF filter eliminating one of the three filter parameters. They also combined the positive position feedback with independent modal space control.

[35] realized that effective vibration control with PPF depends on the accuracy of the modal parameters used in the control design. They extended the original feedback technique with an adaptive estimation procedure to identify the structural parameters.

[36] implemented PPF in both discrete and continuous systems, showed that an exact knowledge of the natural frequencies of the structure is not required in order to design an effective control system.

[37] presented the effectiveness of the optimal modal positive position feedback algorithm in damping out two vibration modes of a cantilever beam with one piezoelectric actuator and three position sensors.

[38] illustrated that an adaptive first order PPF filter can successful damp vibration of a cantilever beam even if the first mode changes by 20%.

[39] provide PPF controller employing multiple actuators instead of a single one for any particular vibration mode.

[40] designed a combined scheme of PD feedback controller for AC servo motor and PPF controller for PZT actuators to suppress multi-mode vibration applied to experimental single-link flexible manipulator.

[41] implemented a single mode PPF and also a multi-mode PPF controller under single channel control scheme for vibration of beam

[42] introduced PPF to increase the stability margins and allow higher control bandwidth, compensated for the coupled fuselage-rotor mode of a Rotary wing Unmanned Aerial Vehicle (RUAV).

[43] PPF controllers are designed based on the identified results and investigated active vibration control of a beam under a moving mass using a pointwise fiber Bragg grating (FBG) displacement sensing system.

[44] indicated a multi-mode controllable SISO PPF controller, a non-collocated sensor/ moment pair actuator, and tuned to different vibration modes of beam based on the results of the parametric study for the design parameters.

Modified PPF (MPPF)

based on the performance has already achieved, some researchers modify the structure of PPF, [45] provided a modified compensator which enhanced flexibility actively

changing damping and stiffness of flexible structures. [46] constructed a new MPPF which consists of first order and second order two SISO parallel compensators, and find the optimal parameters through experimental way. [47] combined PPF and an output feedback sliding mode control (AOFSMC) for vibration and attitude control. [48] designed suboptimal positive position feedback (SOPPF) and output feedback sliding mode control (OFSMC). [49] provided negative position feedback (NPF) and positive position feedback (PPF) to reduce multi-mode vibration of a lightly damped flexible beam using a piezoelectric sensor and piezoelectric actuators. [50] proposed positive velocity and position feedback (PVPF) controller and achieved high-amplitude actuation of a piezoelectric tube. [51] extended the linear modal control to nonlinear modal control by using quadratic modal positive position feedback (QMPPF) control algorithm to suppress forced vibrations in distributed parameter structures.

Robust PPF

Expect the normal advantages, some people also showed the robust ability of PPF controller.

PPF control system is robust and performs significantly well at the target frequency, because the high control action can be generated at the resonance of the controller due to the tuning stated in literatures [52,53]. [54] presented the experimental results robustness study of vibration suppression of a cantilevered beam with PZT sensors and PZT actuators using PPF control. PPF controllers were implemented for single-mode vibration suppression and for multimode vibration suppression. Experiments found that PPF control is robust to frequency variations for single-mode and for multimode vibration suppressions. [55] considered PPF which derived from solving a group of LMIs with adjustable parameters with respect to the inaccurate structure modal frequencies and a simulation was presented to illustrate the effectiveness of the proposed robust PPF controller design method.

Adaptive PPF

In order to control vibration of structures with varying parameter, an adaptive PPF controller was put into the consideration. [56] presented an adaptive modal control algorithm, utilized only modal position signals, fed through first-order filters to damp

out the vibration, [57,58,59] proposed the use of GA for tuning PPF controller for grid structure, [60] proposed a new APPF based on gradient-descent approach for beam structure, [61] provided a SISO PPF controller with RLS and Bairstow combined online frequency estimator, [62] designed a SISO PPF controller for a simulation study with RLS estimator for the first two natural frequencies of a beam structure, [63,64] developed RLS estimator with SISO PPF controller for the beam structure, [65] through system identification, a two-mode SISO PPF controller was designed for beam structure based on GA which was designed to minimize the H∞-norm and choose PPF optimal parameters.

PPF combine with Genetic Algorithms (GA)

During the PPF controller design, in order to achieve better performance, some designer used Genetic Algorithms (GA) to choose the placement of sensor and actuator. [66] applied GA to find efficient location of sensor and actuator of a cantilevered composite plate, showed significant vibration reduction for the first three modes (controlled modes) has been observed using the coupled PPF in the vibration control experiment. and the closed loop has been observed to robust with respect to system parameter variations. [67] presented GA method of optimal placement for the cantilever plate. Simulations and experimental results on the actual process have shown that the proposed control method by combining PPF and PD can suppress the vibration effectively, especially for vibration decay process and the smaller amplitude vibration.

PPF compare with other controllers

In order to compare the performance with other controllers, some researchers did simulations and experiments, such as [68] compared with AVA controller at SISO and MIMO situation, [69] conducted simulations and experiments for SISO PPF case compared with LQG controller for suppressing the single and multi- modes vibration of flexible spacecraft simulator (FSS). [70] showed that a PPF controller may be formulated as an output feedback controller both in centralized and decentralized situation. [71,72,73,74] compared PPF with stain rate feedback(SRF), [75]compared PPF with velocity feedback. [76] compared Positive position feedback (PPF) control, linear quadric regulator (LQR) control and neural network predictive (NNP) control

strategies. [77] compared negative imaginary feedback controllers (PPF, Resonant Controllers, Integral Resonant Controllers) with state feedback controller. [78] compared velocity feedback controller, the integral resonant controller (IRC), the resonant controller, and the positive position feedback (PPF) controller. [79] gave a PPF controller for controlling the first mode of vibration, a decentralized controller which used three independent PPF filters for suppressing the first three modes of vibration and a MIMO linear quadratic Gaussian (LQG) for the vibration of USAF Phillips Laboratory's Planar Articulating Controls Experiment (PACE)

MIMO PPF

In order to achieve better performance, and because the complicated coupled relations between controllers, only some designer provided MIMO PPF controller.

For beam structure

[1,3] reported experimental implementation of MIMO PPF controller on an active structure consisting of a cantilevered beam with bonded collocated piezoelectric actuators and sensors through pole placement and H_∞ optimization. [65] designed MIMO PPF controller on a flexible manipulator and based on GA method to find controller parameters to optimize H_∞ result.

For grid structure

[57, 58,59] proposed the use of GA method for tuning MIMO PPF controller for grid structure. [80] designed MIMO PPF controller for grid structure based on the block-inverse technique.

For plate structure

[81] designed MIMO PPF controller for plate structure based on the pseudo-inverse technique.

For shell structure

[82] studied MIMO PPF controller for shell structure for the first two vibration mods based on the block-inverse technique.

1.6 Plate or Shell Structure Vibration Control

In the following, we will summarize the vibration control method for plate or shell structure in the literature. It can be divided to three methods: SISO vibration control, decentralized MIMO vibration control and MIMO vibration control.

SISO vibration controller for plate or shell structure

[83] studied two SISO control algorithms: constant-gain negative velocity feedback and constant-amplitude negative velocity feedback for plate. [84] designed SISO direct feedback control and Lyapunov control for the vibration of shell. [85] proposed SISO H_∞ based robust control for bending and torsional vibration modes of a flexible plate structure. [86] designed SISO velocity proportional feedback to control the vibration of a cross-stiffened plate with a very small laminated piezoelectric actuator (LPA) under low voltage. [87] presented the development of an active vibration control (AVC) mechanism using real-coded genetic algorithm (RCGA) optimization. The approach is realized with single-input single-output (SISO) and single-input multiple-output (SIMO) control configurations in a flexible plate structure.

decentralized MIMO vibration controller for plate or shell structure

[88] gave a decentralized MIMO experimental compensation method based on PPF theory which is applied to switched reluctance machine (SRM). [89] provided the optimal placements of three acceleration sensors and PZT patches actuators are performed to decouple the bending and torsional vibration of such cantilever plate for sensing and actuating. A nonlinear MIMO PPF control method is presented to suppress both high and low amplitude vibrations of flexible smart cantilever plate. [90] provided MIMO PPF, PPF and PD combined controller to control the decoupled bending and torsional modes of plate. [91] implemented decentralized velocity feedback control on panel structure. [92] studied the decentralized multiple velocity feedback loops on a flat panel.

MIMO vibration controller for plate structure

For MIMO vibration control design, it can be divided to following methods:

[93,94,95] studied MIMO adaptive filtered-x least mean square (FXLMS) feed-forward control method for the vibration of plate structure and obtained a good performance.

[96] presented the development of an active vibration control (AVC) mechanism using Genetic Algorithms, Particle Swarm Optimization and Ant Colony Optimization method. The approach is realized with multipl-input multiple-output (MIMO) and multiple -input single-output (MISO) control configurations in a flexible plate structure.

[97,98,99,100,101,102,103,104] designed H_2, H_∞ and μ-synthesis robust MIMO controller for the plate vibration. The result of the simulation showed that the control method and the controller designed in the paper was useful

[105,106,107,108,109,110] gave linear MIMO LQR & LQG controller for the vibration of plate structure. The control method was verified by experiment and achieve better performance.

[111,112] provided MIMO Sliding Mode controller to the vibration control of plate structure. According to MATLAB/Simulink platform, the simulation results clearly demonstrated an effective vibration suppression.

Based on the literature review, the author will adopt optimal MIMO PPF controller based H_∞ optimization through GA searching for multi-mode vibration control of a flexible plate structure, similar method application only can be found on beam structure.

1.7 Aim of the Thesis

The aim for this research can be summarized as:

i. set up model of the mechanical plate structure using experimental, mathematical and numerical method ;

ii. truncate the model of the mechanical plate structure comparing with model reduction and model correction method;
iii. select an actuator/sensor system suitable for active control;
iv. increase damping of resonant vibration modes of the mechanical plate structure using multi-mode SISO and MIMO PPF controller;
v. develop an algorithm to tune the multi-mode SISO and MIMO PPF controller parameters;
vi. analyze and compare the performance of closed-loop dynamics between shaker and plate with the open-loop dynamics;

1.8 Outline of the Thesis

This thesis presents the design and implementation of the optimal multi-mode SISO and MIMO PPF controller based H_∞ optimization through GA searching for attenuating vibration of plate structure.

A detailed outline of the thesis structure is given below.

In Chapter 2, the model of the plate structure is derived in three ways: experimental method, analytical method and numerical method. The author also set up the transfer function matrix of plate simulation model, MATLAB plot figure about SISO and MIMO plate simulation model is given in this chapter.

In Chapter 3, the model reduction and spatial H_∞, H_2 norm is given. In order to truncate the plate model into lower order, the balanced reduction method is proposed. MATLAB plot figures are also given for SISO and MIMO plate model.

In Chapter 4, model correction method is introduced, and the MATLAB plot figures are given for SISO and MIMO plate model, comparing with the result of SISO and MIMO balanced reduction plate model.

In Chapter 5, multi-mode SISO and MIMO PPF controllers are given. The stability of controllers are derived. In order to achieve better performance, controller parameters are selected based on H_∞ optimization through GA searching, MATLAB plot figures

are given.

In Chapter 6, simulation results of multi-mode SISO and MIMO PPF controllers are given in time and frequency domain. According to comparing the performance of multi-mode SISO and MIMO PPF controllers.

In Chapter 7, experimental implement results of multi-mode SISO and MIMO PPF controllers are given in time and frequency domain. According to comparing the performance result of multi-mode SISO and MIMO PPF controllers, final conclusion is given.

In Chapter 8, a summary and a conclusion obtained from the research are presented and recommendations for further continuation of the research are given.

Chapter 2

Model of Flexible Plate Structure

Normally, there are three methodologies, analytical analysis, experimental method and numerical calculation, could be implemented to describe a system. In this chapter, the design and implementation of the experimental plant, the analytical and numerical models used to simulate the experimental plant are discussed. The purpose for the modeling is outlined and the reasons for choosing the experimental plant, and the modeling steps are given. The plate used in the experimental plant is followed by a description of the analytical and numerical method used to obtain the mathematical model of the plant. The model derivation itself is not original and can also be found in [113,4,117,118,119,120].

2.1 Introduction

As mentioned in Chapter 1, in order to design and evaluate the proposed controller, an experimental plant together with its mathematical representations is need to obtained.

Modeling methods can be applied to find models which represent the experimental plant after the experimental plant is decided. According to these models, it is easy for us to study the dynamics of the plant. As all of the proposed control methods employ natural frequency as the controller parameter, the most important part of the modeling is that how to find the models with accurate representations of the natural frequencies of the systems [4].

Physical and mathematical theories such as Newton's laws, Hooke's laws, Lagrange's equations, Hamilton's principle, etc will be used to obtain the analytical model. The mathematical model that is adopted is known as the equation of motion, which is usually given in the form of a Partial Differential Equation (PDE). To determine the dynamics of the model, the solution of the PDE needs to be found. Normally there are

two common methods used to find the solution of the PDE: the analytical method and the numerical method [4].

The analytical method gives an exact solution of the PDE. The solution is in a closed form and is expressed in terms of known functions. Although analytical methods can be used to very accurately describe the dynamics of structures, the types of applications where this method can be applied are limited. The analytical method is only applicable for systems that are characterized by uniformly distributed parameters and simple boundaries [114]. In many cases, even though closed-form solutions may be possible, great effort and time are required to obtain them. Therefore in practice the analytical method has fewer application areas than the numerical method [4].

In numerical method, a discrete version of the model is produced. The spatial dependence in the solution of the PDE is eliminated by applying spatial discretization and the differential eigenvalue problems are transformed into an algebraic form [115]. Several methods exist for constructing the discrete model [114,115]: Rayleigh's method, Rayleigh-Ritz's method, Galerkin's method, assumed- modes method, collocation method, Holzer's method, Myklestad's method and the finite element method (FEM). FEM is currently the most widely used method for representing discrete models [115]. The FEM package ANSYS is used here to study the dynamics of the structures. Due to the use of approximation, numerical methods do not give the same exact results as analytical methods. However, approximation algorithms have led to accuracy improvements for the numerical method.

Simulation is an important step in the control system design process. It provides a flexible and relatively inexpensive means by which to study the dynamics of a plant, design controllers, and evaluate the performances of the controllers prior to their implementation in an actual system. The simulation tool Mablab Simulink is used for that purpose. Using MATLAB Simulink, simulation models, which are derived from the modification of the mathematical models which is obtained from the analytical method or from the modification of the numerical models which is obtained from the numerical method, need to be implemented [4].

The implementation of the models is undertaken in four steps. In the first step, the experimental plant (experimental models), which describes the mechanical system is

built. In the second step, analytical models of the experimental models are derived. In the third step, numerical models of the experimental models are built using ANSYS. Then the numerical models are compared with the analytical models and the experimental models to determine their accuracy. In the fourth step, the numerical models are used to construct the simulation models in MATLAB Simulink.

2.2 Description of Experimental Plant

(Experimental Model)

Plate structure can be served as a basic representative model for a number of flexible structures such as solar panels of the aerobat and aircraft wings [116]. This plant was built, analyzed, and designed by [139]. With using energy dissipation structure, vibration control was achieved in 2010 using the shunt control by [139] in simulation and experiment study. With using three SISO controllers, vibration control was achieved in 2012 by [138]in simulation study.

The schematic of the experimental plant is shown in Fig. 2.1. An uniform AL6061-T6 plate is mounted with screw on the MDF board using three electromagnetic transducers (anticlockwise number 1, 2, 3)which are called 'Response CS2277 Power Bass Rocker', normally used for vibrating car seats while playing music as to enhance the experience of the low frequency range. Another electromagnetic transducer is mounted on the MDF board with screw as a disturbance noise shaker. The MDF board is placed on the table with four rubber legs which are screwed on the MDF board. [139].

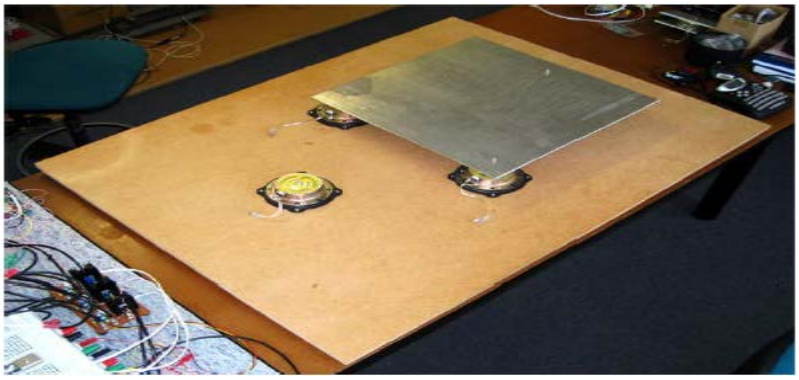

Figure 2.1 A thin plate in transverse vibration

Figure 2.2 shows a cross section of the transducer. This transducer is quite similar in structure to a normal loudspeaker. It consists of a coil which produces a magnetic field when a current is fed through. This will move the core magnet which is mounted inside the coil and supported by a flexible structure. The model used for this transducer is shown in Figure 2.2b [139].

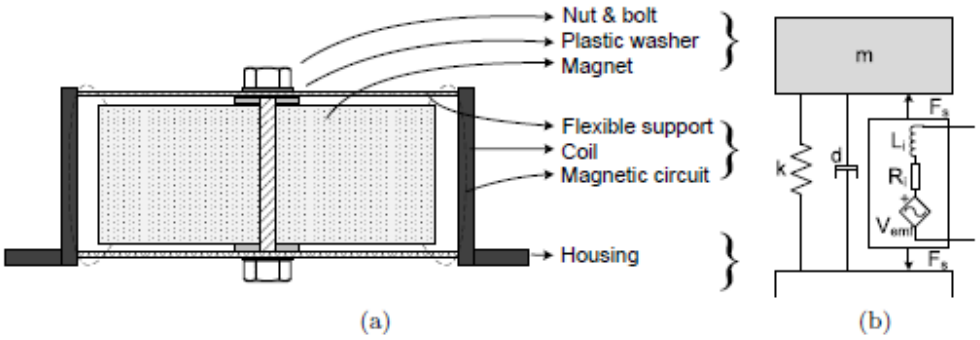

Figure 2.2 Transducer cross section (a) and model (b)

It is basically a mass-spring-damper system with an electrical port consisting of a coil, a series resistance and a voltage source modeling the back-emf voltage. The transducers mass-spring-damper system with an electrical port consisting of a coil, a series resistance and a voltage source modeling the back-emf voltage. The transducers were assumed mechanically identical. Table 2.1 shows the measured mechanical parameters of the transducers [139].

Parameter	Symbol	Value
Spring constant	k	19037 N/m
Core mass	m	0.323 kg
Damping ratio	ζ	$3.39 \cdot 10^{-2}$
Damping Coefficient	d	5.32 Ns/m
Damped resonance frequency	ω_d	38.63 Hz
Resonance frequency	ω_c	38.65 Hz

Table 2.1: Mechanical parameters of the transducers

The frequency range at which actuation is possible was found to be 20 Hz to 200 Hz for all transducers. However, they were not found to be electrically identical. Table 2.2 shows the measured electrical parameters of the transducers used for control. For a detailed description of the measurement procedures [139].

As stated in 1.5.3 of Chapter 1, PPF combine with Genetic Algorithms (GA), the optimal control position of the three control transducers can be derived through GA calculation. The author did not derived that because the limited time, the other reason is that during the implementation, for some mechanical plant systems, some optimal positions may not be used due to the physical conditions. Expect the analytical GA calculation, the other easier method is that set up the model and do the simulation using the numerical software such as ANSYS. It is easier to find and confirm the minimum displacement of the observation position according to different control transducer position.

Parameter	Symbol	T 1	T 2	T 3
Impedance at 50 Hz	$Zi[\Omega]$	3.6170	3.7204	3.8442
Inductance at 50 Hz	$L_i[\mu H]$	518	533	597
Resistance at 50 Hz	$R_i[\Omega]$	3.6133	3.7166	3.8396
Current-Force coupling at 26.9 Hz	$C_{iF}[N/A]$	2.0523	3.6361	3.6996
Velocity-Voltage coupling at 26.9 Hz	$C_{vV}[Vs/m]$	2.0523	3.6361	3.6996

Table 2.2: Electrical parameters of the three transducers (T 1, 2 and 3)

The natural frequencies of the experimental models are the most important parameters to be considered for the proposed control methods. Therefore, a series of experiments are undertaken to measure the natural frequencies of the experimental model. The natural frequencies are obtained by applying a sweep signal to experimental model. The amplitude of the vibration is then measured against the frequency of the signal. The frequencies where the amplitude of vibration forms a peak are the natural frequencies of the experimental model. In the experiment, a sweep signal from a signal generator is amplified by a 50 W Jay Car amplifier and the output from the amplifier is applied to the disturbance noise transducer. The attenuation is necessary in order to make the signal level suitable for input to the analog-to-digital converter. The amplitude of the vibration is measured by accelerometers then it is shown on Agilent 54621A oscilloscope. Experiments show that the dominant modes for all the experimental models are the first four modes. The frequencies for the first four modes are shown in

Table 2.3 [139].

In the next section analytical models of the experimental model will be de rived.

Mode	Natural frequency (Hz)
1	27.1
2	34.4
3	40.5
4	49.2

Table 2.3: The first four natural frequencies of the experimental model

2.3 Numerical Solution Using ANSYS

(Numerical Model)

In practice, especially for complex structures, a software tool such as ANSYS can be used to find the natural frequencies of the structures. ANSYS uses the finite-element method (FEM) to solve the underlying governing equations and the associated problem-specific boundary conditions. FEM tools are used widely in industry to simulate the responses of a physical system to structural loading, and thermal and electromagnetic effects. In this research, ANSYS software version 14.0 is used to find the natural frequencies of the plate structure. The results are validated through comparison with the results from the experimental and analytical method [4]. This numerical model was built, analyzed, and designed by [139], and also studied by [138]. Due to the limitation of the transducers, the author adjusted the thickness of the top plate and MDF board, and other relevant parts in the numerical model to make sure that the first natural frequency of the top plate is within the frequency range of the transducers.

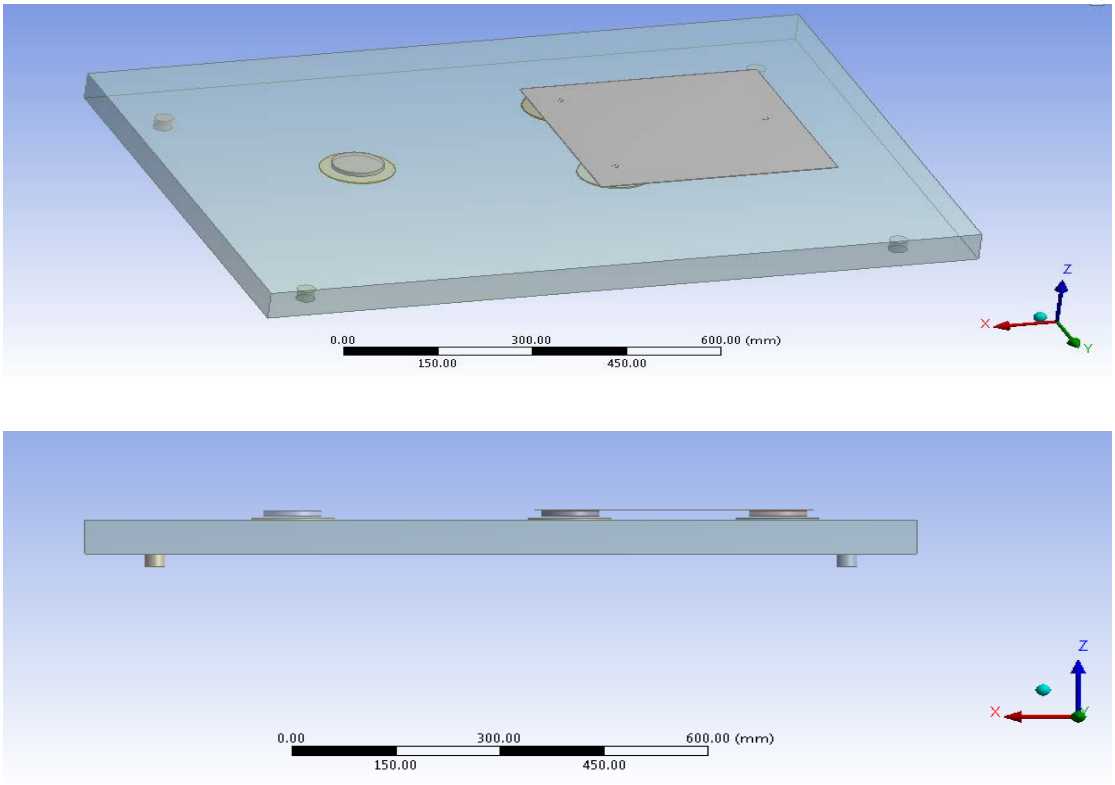

Figure 2.3 System model shown in isometric view and side view

2.3.1 Resonance Frequency

Normal mode, an inherent property of the system, is characterized with a specific natural frequency, damping ratio and mode shape, and it can be applied to describe the system motion called resonance which is approximate equal to the natural frequency[117,118,119]. For any system, modes are totally independent with each other so that they have different modal parameters including natural frequencies, damping ratios and mode shapes (even if the same value). Those modal parameters normally depend on the system structure, materials and boundary conditions. Hence, the excitation of one mode of a system would not cause the motion of different mode. In ANSYS, the modal analysis module is able to be used for computing the resonant frequencies and corresponding mode shapes [4].

Resonance frequency (or natural frequency) refers to a certain frequency that is able to lead the significant magnitude of the oscillation. To determine the dynamics on the top plate, start with modal analyses so that the resonance frequencies can be found.

In the simulation the model is supposed to be analyzed in range of [0, 200 Hz] due to

following three reasons [139].

i. In practice, the transducers used in the mechanical structure can only sense the signal which frequency is from 20 Hz to 200 Hz. To guarantee that there is no mode below 20 Hz is omitted, the simulation should be analyzed the mode from 0 Hz instead of the lower limit of the transducer detecting range.
ii. More serious, since the modes with low natural frequencies would normally cause more significant response than the ones with high frequencies, it is necessary to ensure if there is a mode invisible when the modes were detected experimentally, especially for the natural frequency below the physical detection range.
iii. On other hand, as the magnitude of the response declines with the frequency increasing, it might be worthless to sense any natural frequencies above 200 Hz.

The resonant frequencies from virtual simulation are shown in the right column of Table 2.5. To verify the simulation results, detecting the natural frequencies of the physical system has been implemented experimentally. Apply sine swept which was the disturbance signal from 20 Hz to 200 Hz to the shaker on the bottom plate and observe the acceleration at the top plate. To measure the acceleration, the PCB Piezotronics 353B17 accelerometer is used to sense the natural frequencies which have the acceleration peak values. The physical measurement results are also listed in the Table 2.4. For comparison purposes, the first four natural frequencies of the model are shown below. From the comparison, it can be seen that the difference between the results from the experimental, analytical method and the results from ANSYS [139].

Mode	Experimental Model natural frequencies (Hz)	Analytical Model natural frequencies (Hz)	Numerical Model natural frequencies (Hz)
1	27.1	25.94336	27.195
2	34.4	31.39146	35.01
3	40.5	31.39146	37.467
4	49.2	50.22634	46.202

Table 2.4 natural frequencies comparison

From this comparison it can be concluded that the ANSYS results are more accurate

cause the deformation is more complex and the deformation equation which had been derived from theoretical analysis can not exactly predict the deformation. Based on the accuracy of the results, numerical model from ANSYS will be used here to form simulation model for the experimental plant.

2.3.2 Mode Shape

Mode shape, one of the mode parameters, describes a deflection pattern associated with a particular natural frequency. Same as the natural frequency, mode shape is independent with the ones with other modes. The actual deformation or displacement at arbitrary point of the structure is the summation of all the mode shapes of that system[118,119]. Basically, the pure mode shapes can be generated and observed as the displacement if the external harmonic excitations have the same frequencies as the system modes. Conversely, the excitations with random frequencies tend to produce an arbitrary “shuffling” of all the structural mode shapes superposition. The mode shape can be treated as the inherent dynamic property when the system is in free vibration without any external force applying. In another word, the mode shapes can be considered as the superposed deflection of the all parts in the system [139].

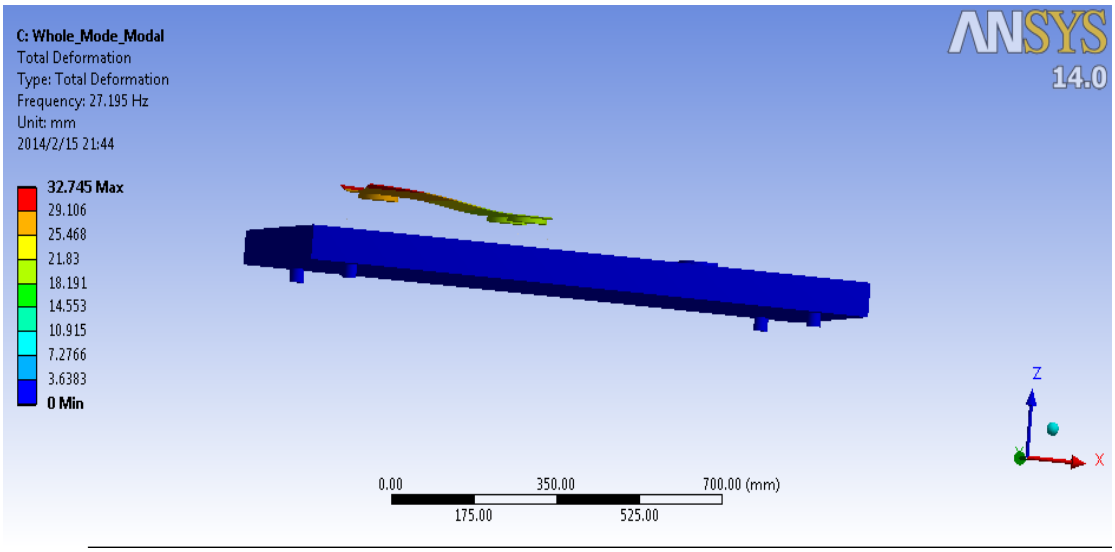

Figure 2.4 Modal Analysis mode shape of first mode

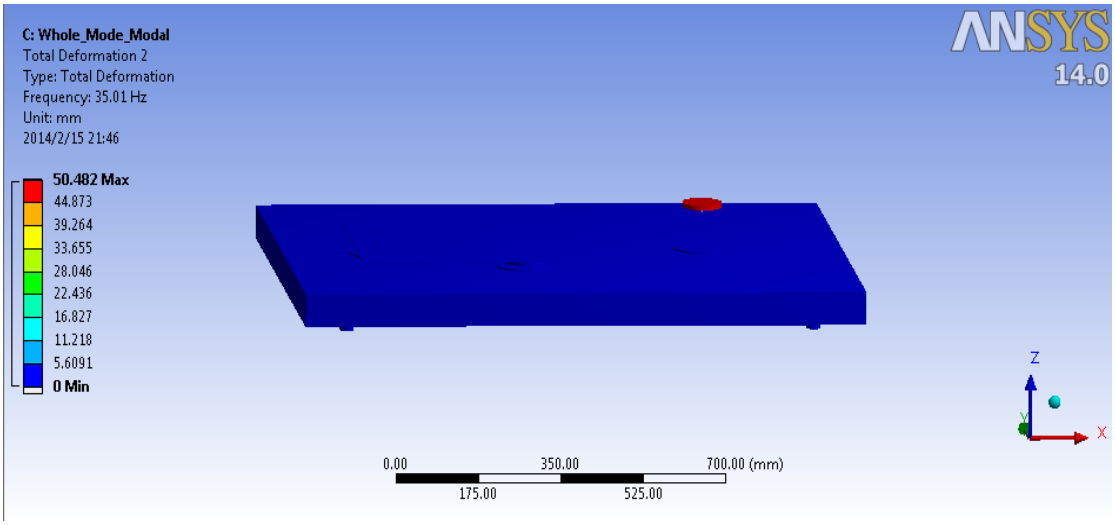

Figure 2.5 Modal Analysis mode shape of second mode

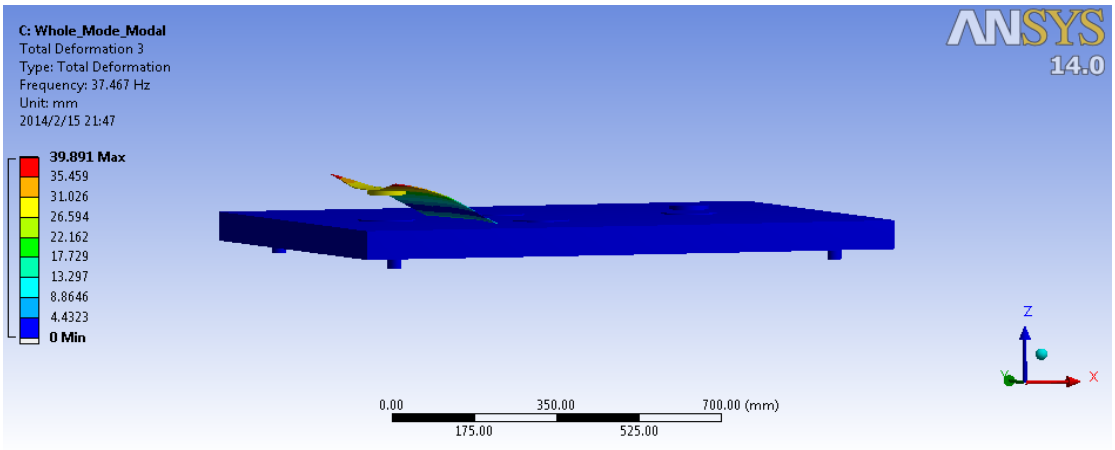

Figure 2.6 Modal Analysis mode shape of third mode

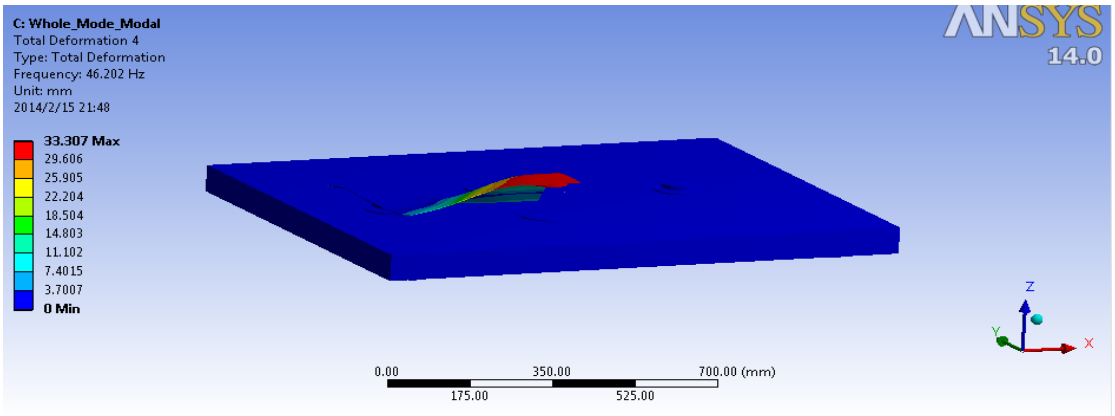

Figure 2.7 Modal Analysis mode shape of forth mode

In ANSYS, the mode shapes can be obtained by implementing the modal analysis such as Fig 2.4−2.7. With the given mode which has been determined before, the modal shape is computed and represented as maximum deformation or displacement.

2.3.3 Harmonic Response Analysis

Instead of computing the transient vibrations which exists at the beginnings the excitation, the ANSYS harmonic response analysis technique calculates the steady – state response of the linear structure system to loads that vary harmonically [118,119]. That is, harmonic analysis can be applied with given (range of) frequency (frequencies) when the structure is in forced vibration. In the harmonic analysis, once the input has been determined, the corresponding output could be computed. Note that the dynamic between input and output which is characterized by natural frequency, damping ratio and mode shape, is the inherent property of the existed system. It means that the system dynamic would not change whatever the external excitation is applied unless the system itself has been changed. To determine the dynamic between shaker and any positions on the top plate, apply 1N force through the shaker and collect the results given as deflections from the top plate. For instance, as shown in Figure 2.8, the 1N force, which is the user-defined input, has been applied to the shaker with specific natural frequency. The amplitude and phase response result of the whole top plate is shown in Figure 2.9 and 2.10. The harmonic analysis is also able to present the corresponding deflections at the position of each transducer. The same implementation can be applied to the shaker, while other three transducers (transducer 1, 2, 3 and the shaker) are considered as outputs [139].

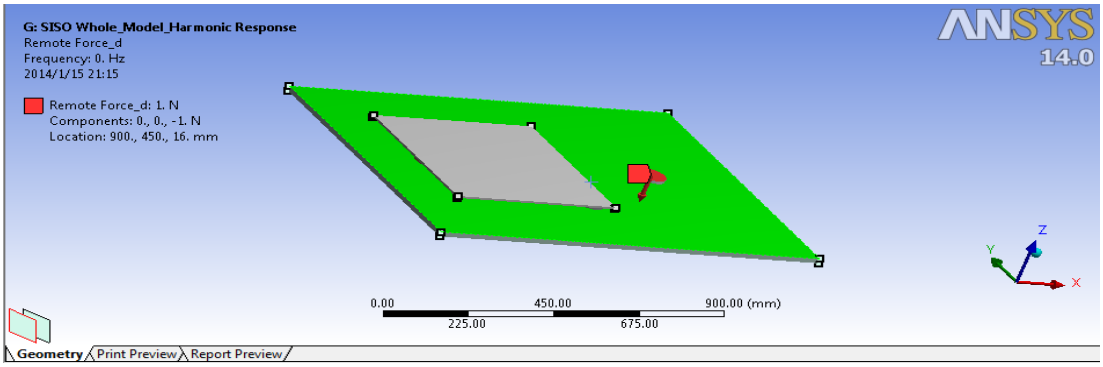

Figure 2.8 Harmonic Analysis Example

With applying 1N force via the shaker (input), respectively, the corresponding deflection of transducer in millimetre (output) only depends on that single input and its related dynamic. The harmonic analysis results is shown at Figure 2.11.

It is shown that for Fig 2.11(a), at transducer 1, the mode shape of mode 2 and 4 are very small. For Fig 2.11 (b) and (c), only three modes can be seen because the mode shape of mode 2 is very small

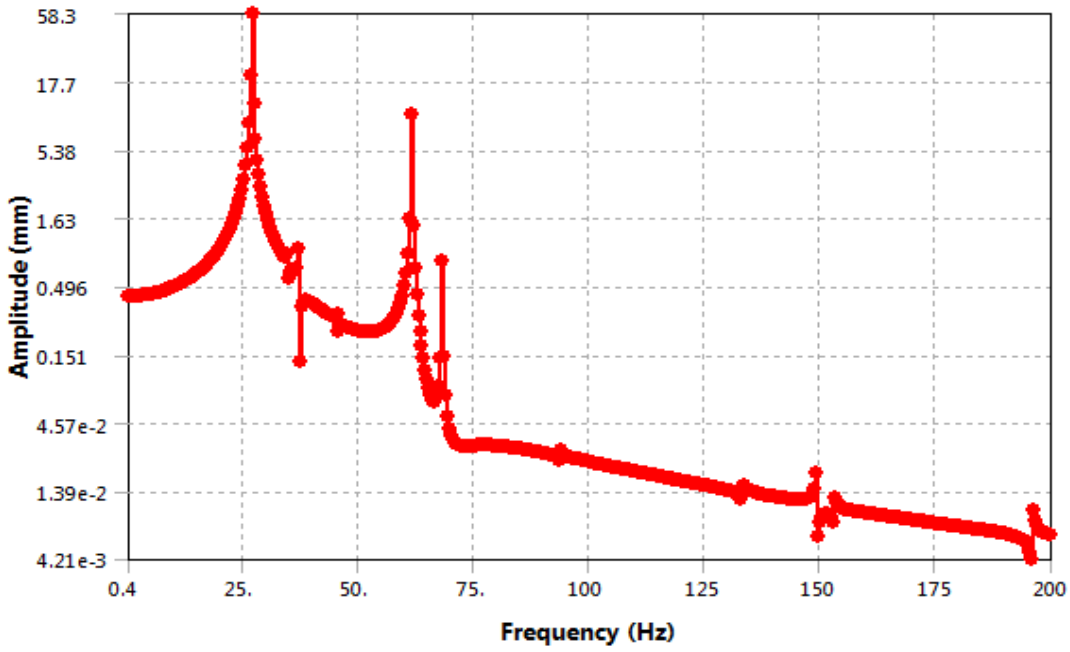

Figure 2.9 Amplitude Response of whole top plate to a harmonic disturbance at shaker

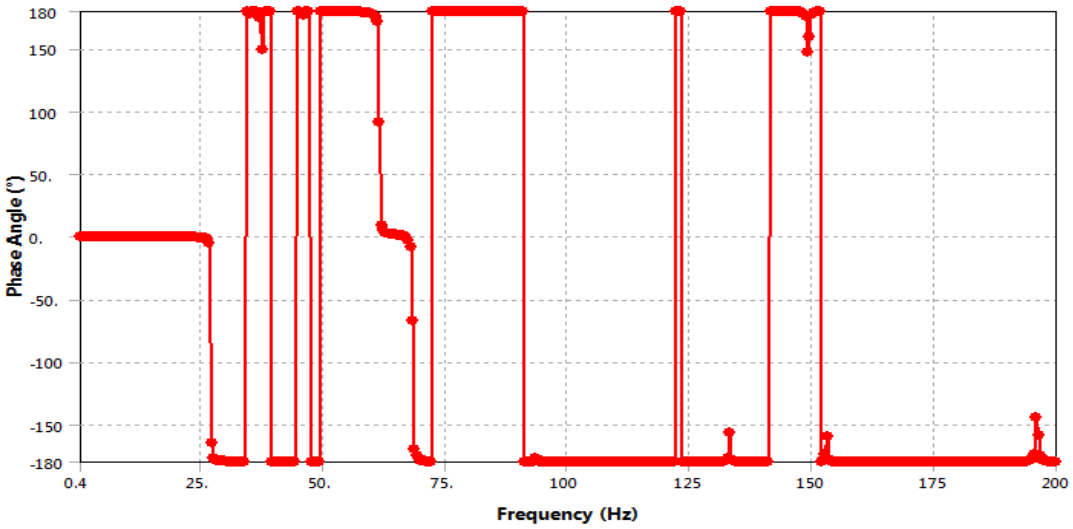

Figure 2.10 Phase Response of whole top plate to a harmonic disturbance at shaker

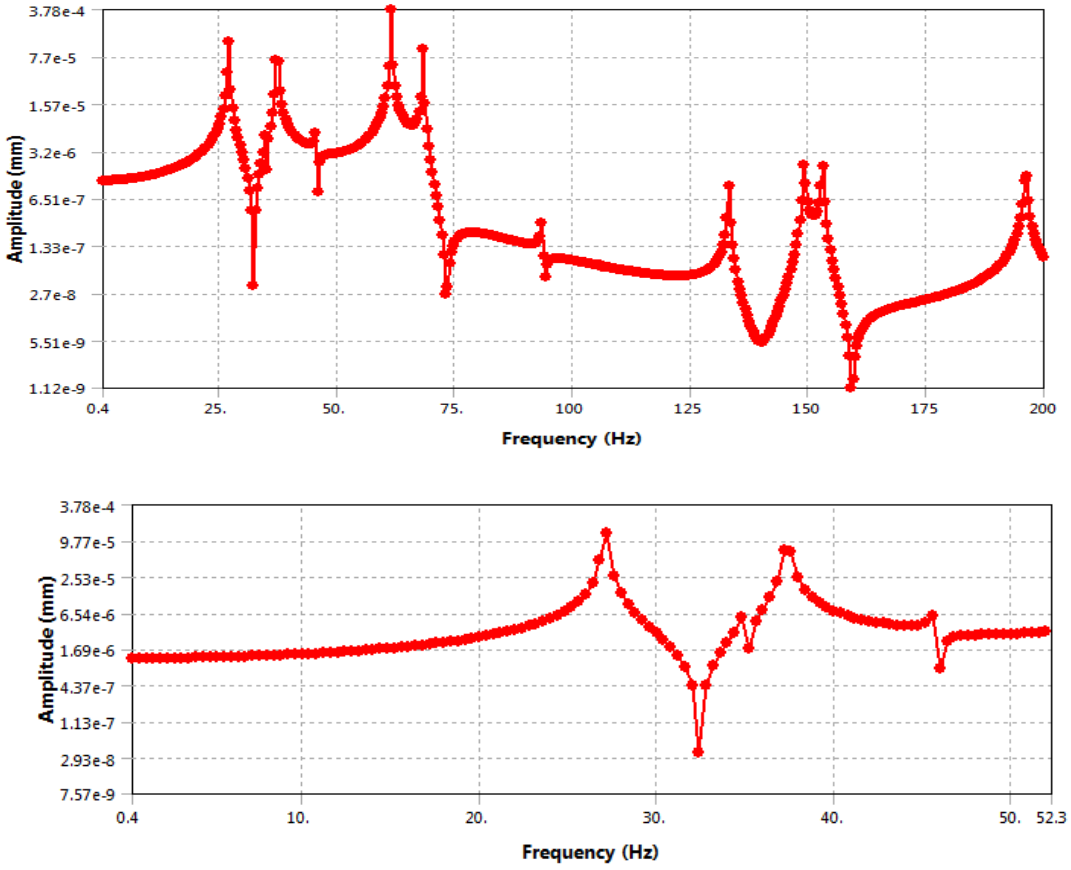

(a) Transducer 1 resonant peaks

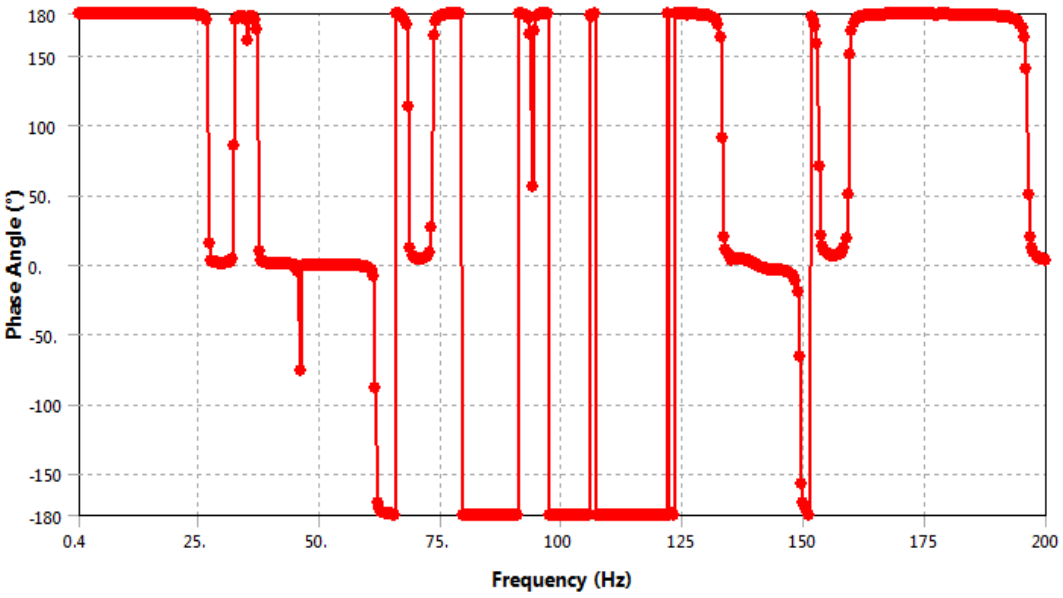

(b) Transducer 1 resonance phase

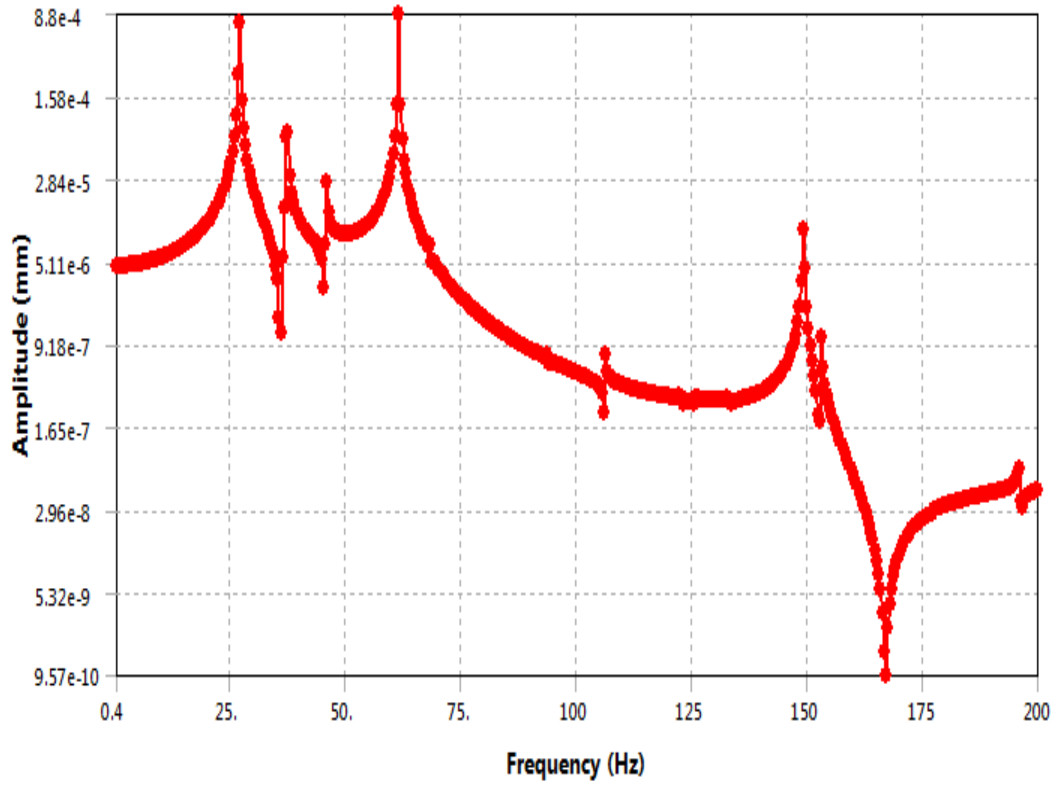

(c) Transducer 2 resonance peaks

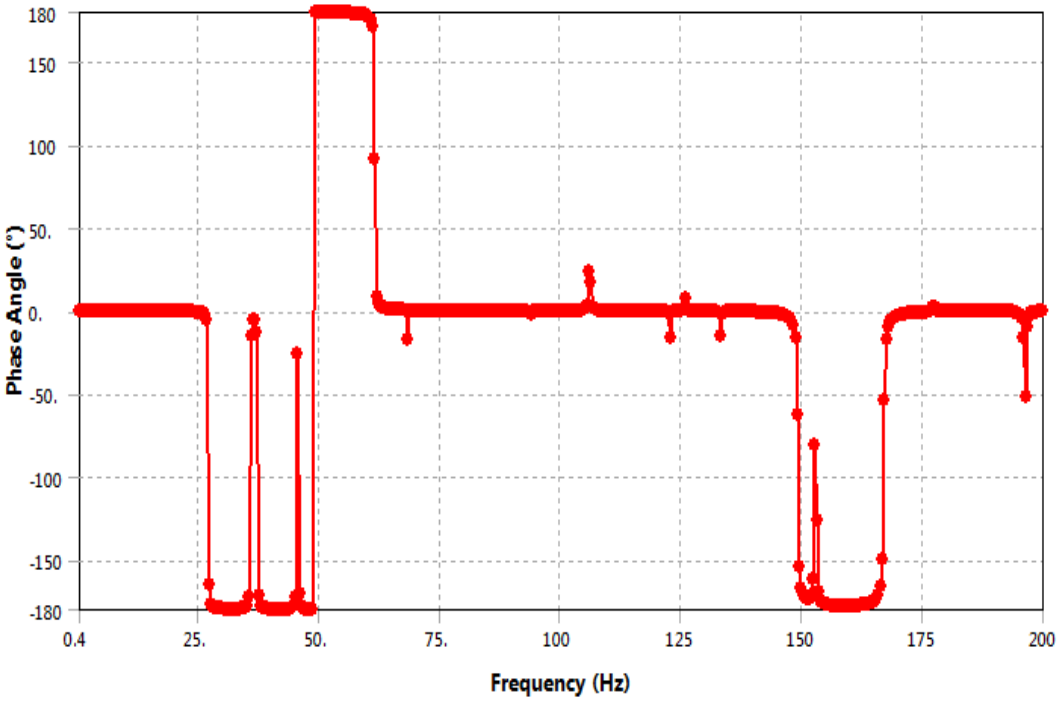

(d) Transducer 2 resonance phase

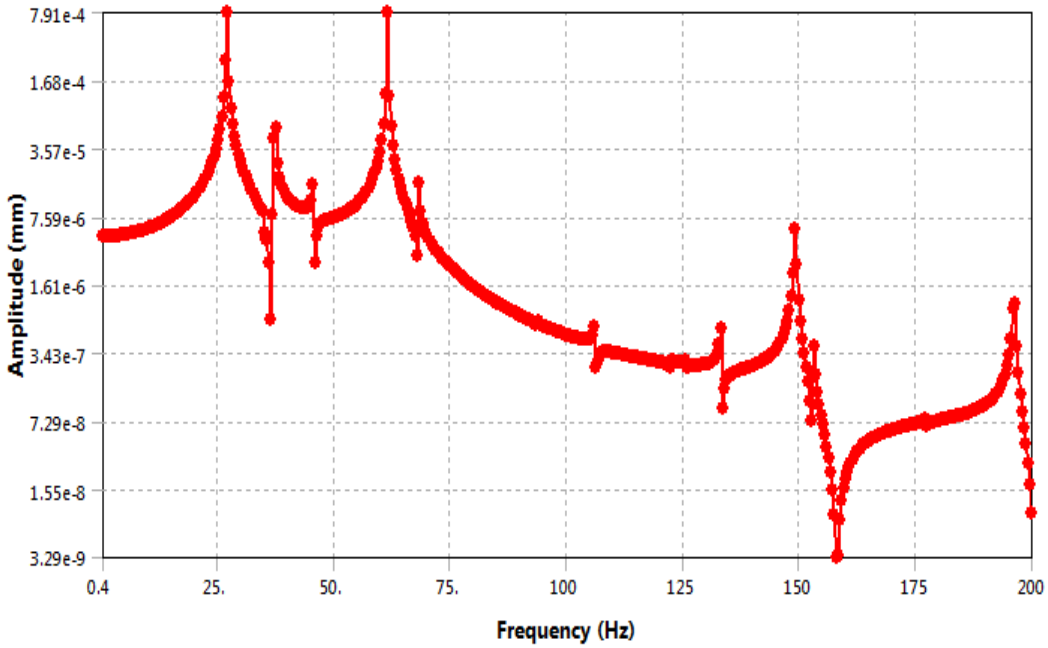

(e) Transducer 3 resonance peaks

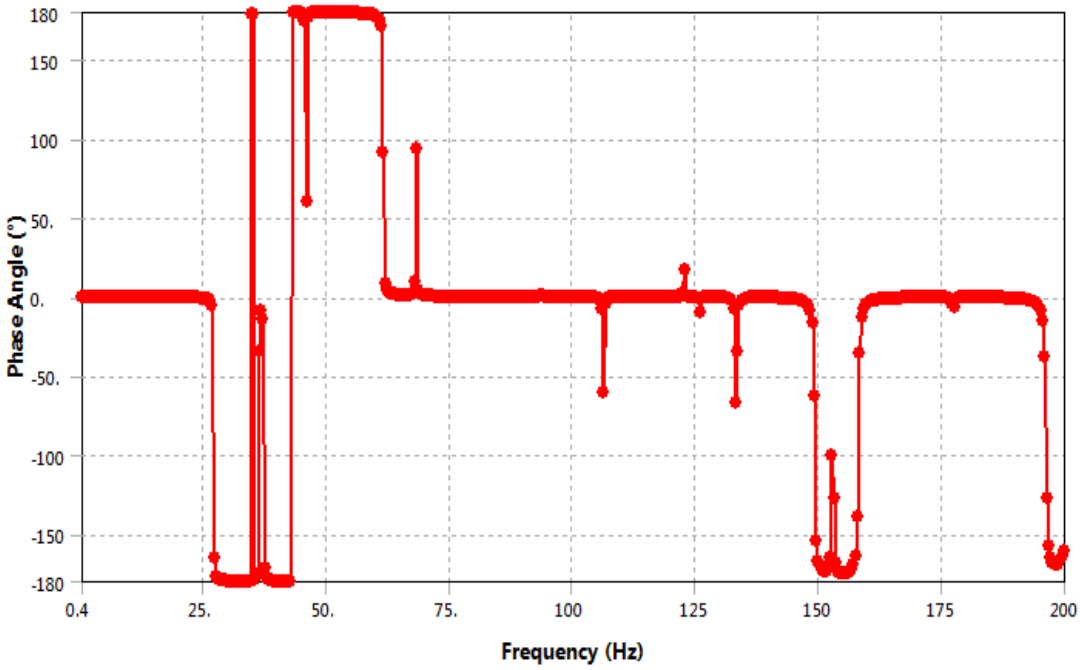

(f) Transducer 3 resonance phase

Figure 2.11 Simulated harmonic disturbance at shaker and measured resonant peaks and phase of top plate at transducer 1 (a, b), transducer 2 (c, d) and transducer 3 (e, f).

2.4 Simulation Model of The plate

Simulation plant model using Simulink is used to design and evaluate the proposed controllers. The simulation results are then used as a benchmark for real-time implementation of the proposed controllers in the experimental plant. To use Simulink as a simulation platform, the numerical model from ANSYS need to be modified into simulation model in the form of transfer functions or state space equations [138].

In this section simulation plate model to represent the experimental plant is designed and implemented. The simulation plate model is created in transfer functions form.

By following the plant physically set up in the laboratory, the system is modeled and analyzed using FEM simulation software ANSYS. Random disturbance signal is applied to the shaker, and the signal will be transmitted to the top plate through the base plate and then subjected to the three coupled transducers labeled as 1, 2 and 3 in counterclockwise in Figure 2.3. So we use the same locations where the three transducers connect to the top plate as the observation points [139]. Therefore this system is considered as MIMO with three inputs and three outputs as shown in Figure 2.12.

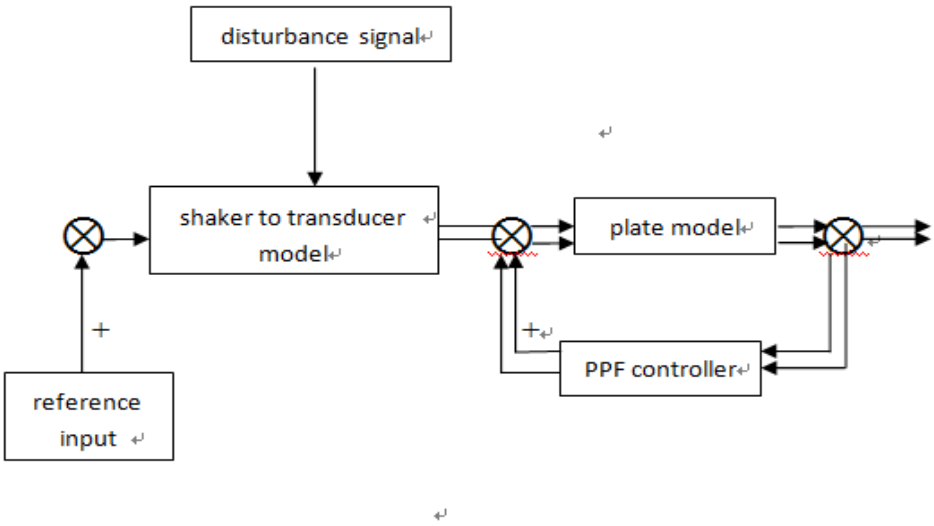

Figure 2.12 Block diagram representation of the PPF control problem

Due to the MIMO properties, any one of the outputs on the top plate is induced by superposing all the inputs and their related dynamics. Hence, the fully description of the dynamics of the system can be expressed using open – loop system superposition

technology.

$$Y_1(s)=Y_{11}(s) + Y_{12}(s) + Y_{13}(s) + Y_{1d}(s) = T_{11}(s)\,U_1(s) + T_{12}(s)\,U_2(s) + T_{13}(s)\,U_3(s) \quad (2.1a)$$

$$Y_2(s)=Y_{21}(s) + Y_{22}(s) + Y_{23}(s) + Y_{2d}(s) = T_{21}(s)\,U_1(s) + T_{22}(s)\,U_2(s) + T_{23}(s)\,U_3(s) \quad (2.1b)$$

$$Y_3(s)=Y_{31}(s) + Y_{32}(s) + Y_{33}(s) + Y_{3d}(s) = T_{31}(s)\,U_1(s) + T_{32}(s)\,U_2(s) + T_{33}(s)\,U_3(s) \quad (2.1c)$$

The equations (2.130a-2.130c) can be illustrated using matrix form

$$\begin{bmatrix} Y_1(s) \\ Y_2(s) \\ Y_3(s) \end{bmatrix} = \begin{bmatrix} T_{11}(s) & T_{12}(s) & T_{13}(s) \\ T_{21}(s) & T_{22}(s) & T_{23}(s) \\ T_{31}(s) & T_{32}(s) & T_{33}(s) \end{bmatrix} * \begin{bmatrix} U_1(s) \\ U_2(s) \\ U_3(s) \end{bmatrix} \quad (2.2)$$

where

$$\begin{bmatrix} U_1(s) \\ U_2(s) \\ U_3(s) \end{bmatrix} = \begin{bmatrix} D_1(s) \\ D_2(s) \\ D_3(s) \end{bmatrix} * U_d(s) \quad (2.3)$$

U_i – input through the transducer i to the top plate, i = 1, 2, 3

U_d – input to shaker

Y_i - output at the position on the top plate, i = 1, 2, 3

D_i - dynamic between the shaker and transducer

T_{mn} - dynamic between transducer m and n, m = 1, 2, 3, n = 1, 2, 3

When the three transducers are treated as three SISO system, the only difference is that only the diagonal elements exist, other elements are equal to zero.

Based all the information before, we could set up the simulation model of the plate

plant in MATLAB, the model include SISO model and MIMO model.

Due to fact that there is no available spectrum analyzer in the laboratory and workshop, no budget to buy or rent the equipment, we could not plot the numerical result and compare with the experimental result, according to [120], we hope that we can adopt 150 modes plate model as the simulation model, and compare the truncated model which used balanced truncation method with the 150 modes simulation model.

When simulation model was calculated by the MATLAB software, we found that if there is more than 47 modes in the plate model, the parameter in the denominator would be too small that MATLAB could not recognize and treat it as infinite small.

So what we can do is that we adopt 47 modes in the plate model and take it as the simulation model.

SISO 47 modes plate model is shown in Figure 2.13-2.16. MIMO 47 modes plate model is shown in Figure 2.17-2.26.

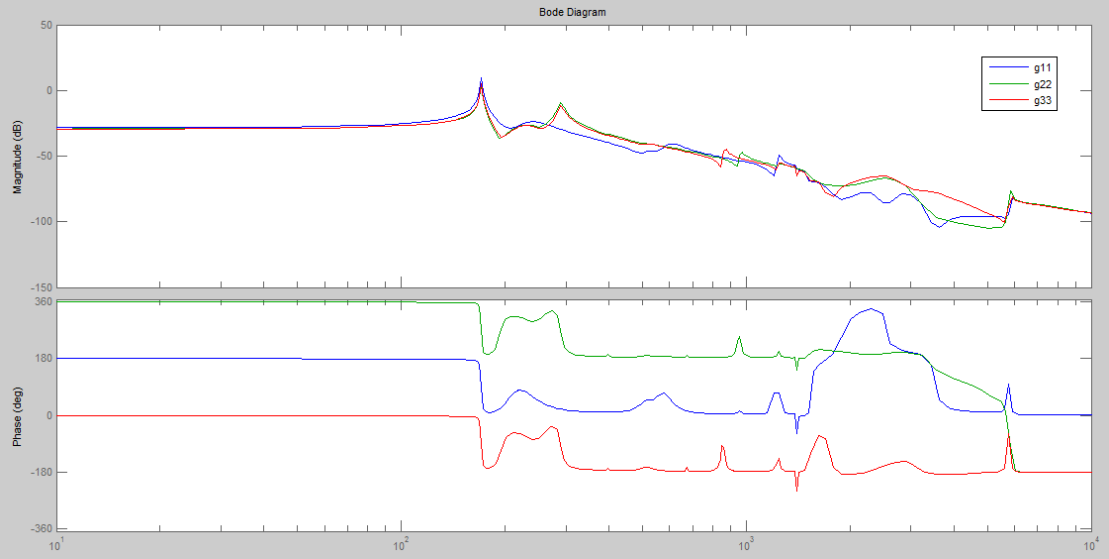

Figure 2.13 three SISO (g11,g22,g33) 47 modes plate model

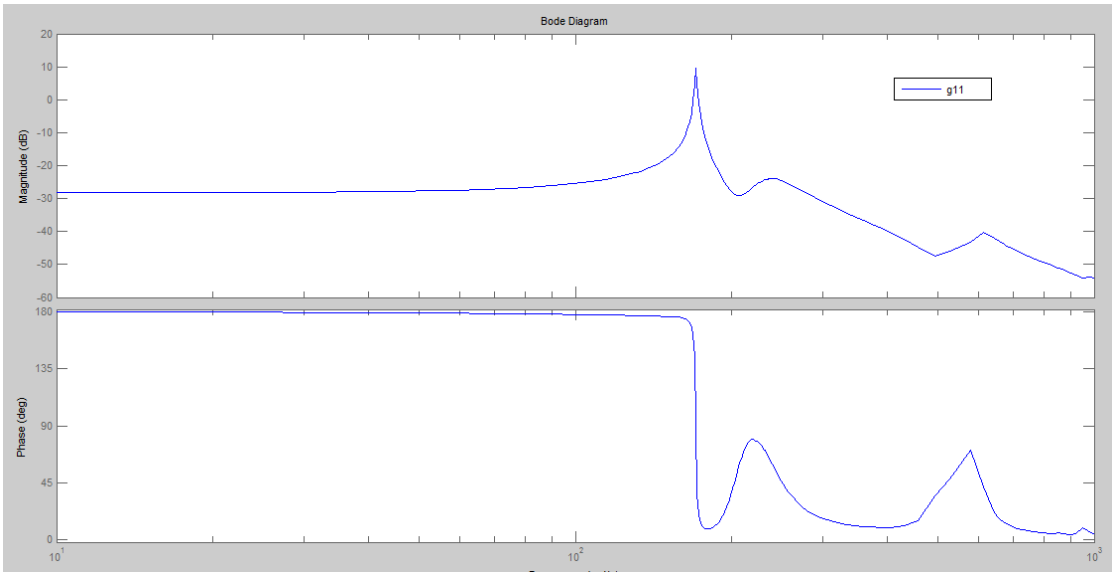

Figure 2.14 SISO (g11) 47 modes plate model at transducer 1

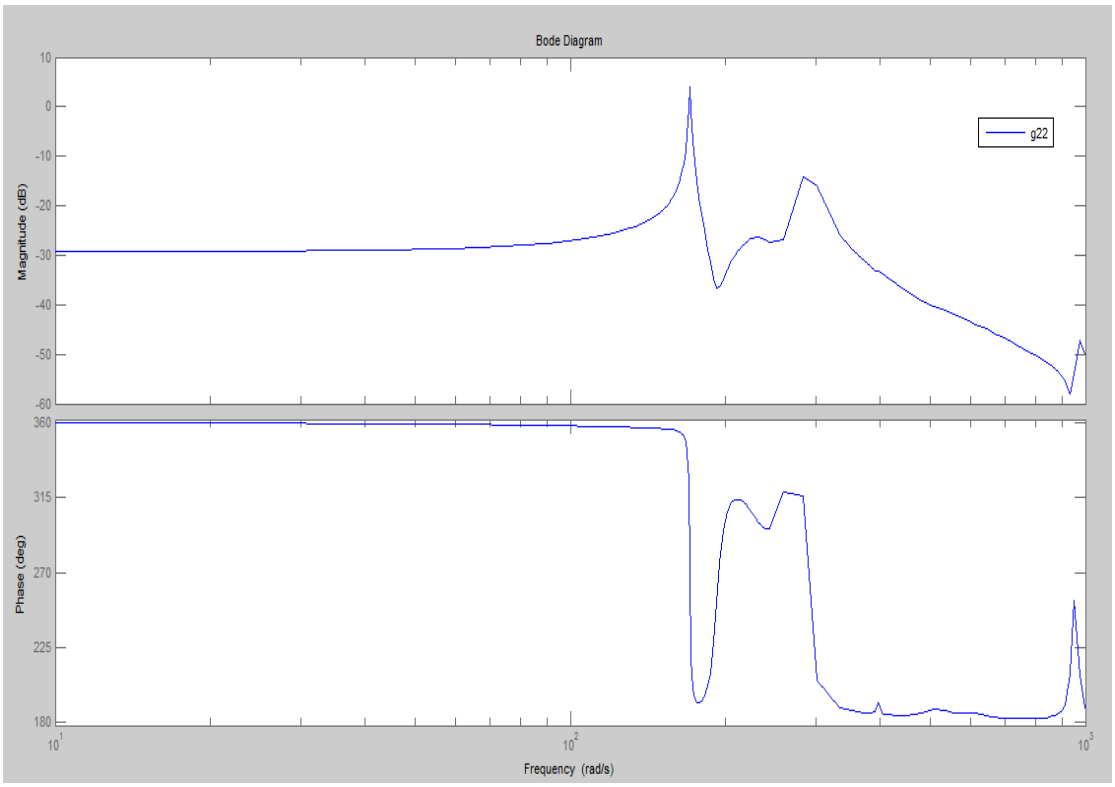

Figure 2.15 SISO (g22) 47 modes plate model at transducer 2

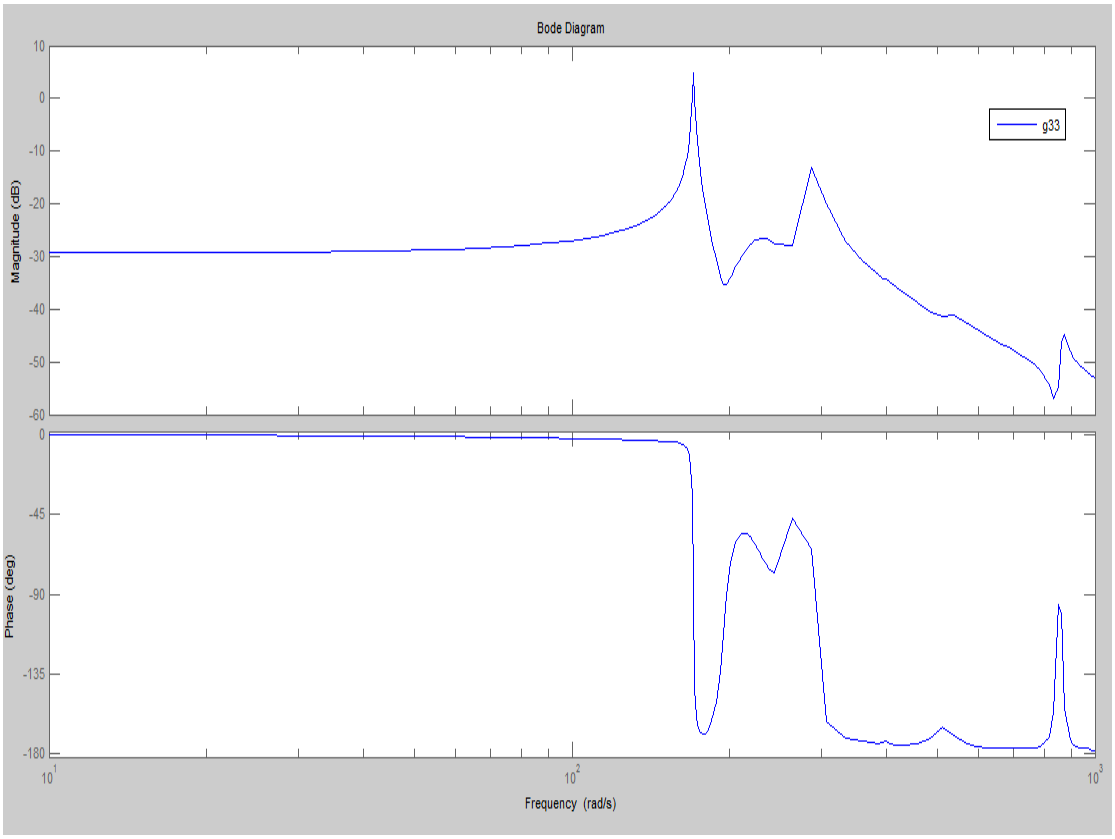

Figure 2.16 SISO (g33) 47 modes plate model at transducer 3

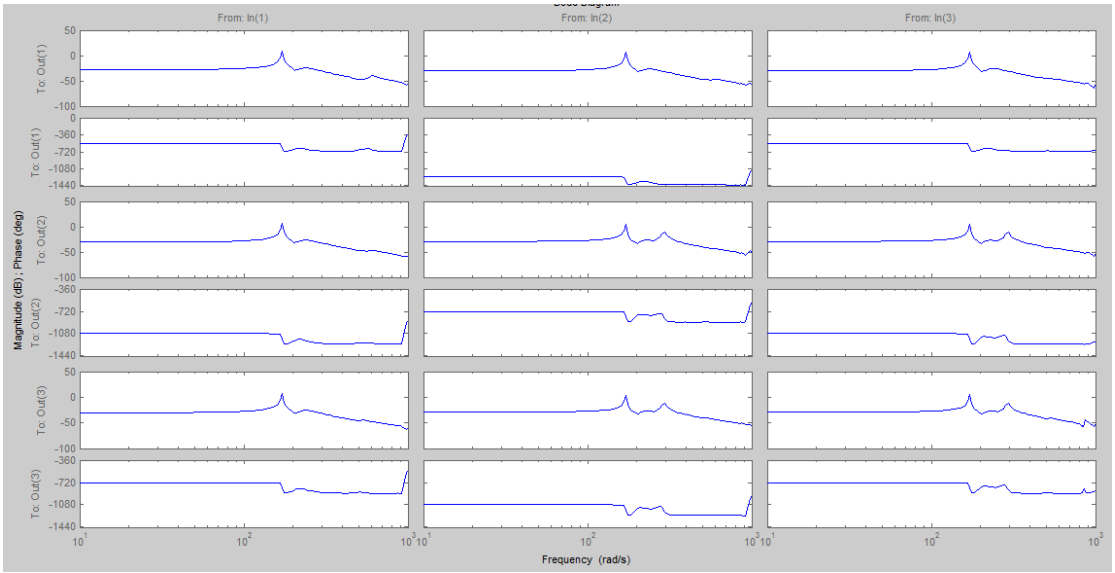

Figure 2.17 MIMO 47 modes plate model

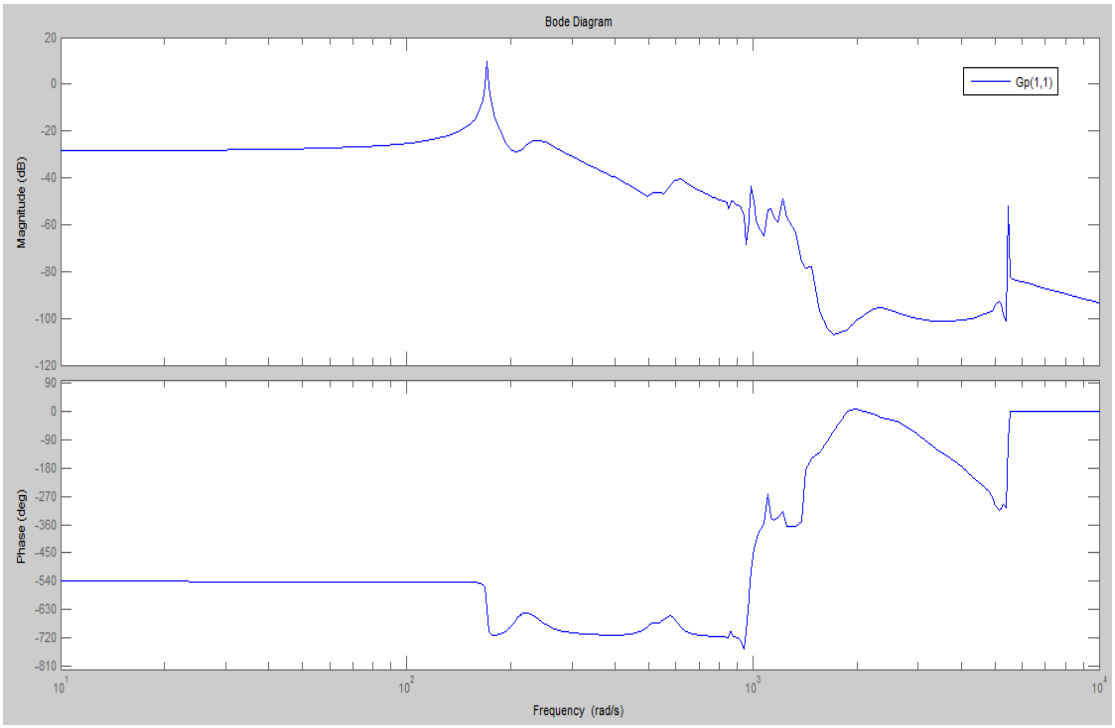

Figure 2.18 MIMO (Gp(1,1)) 47 modes plate model

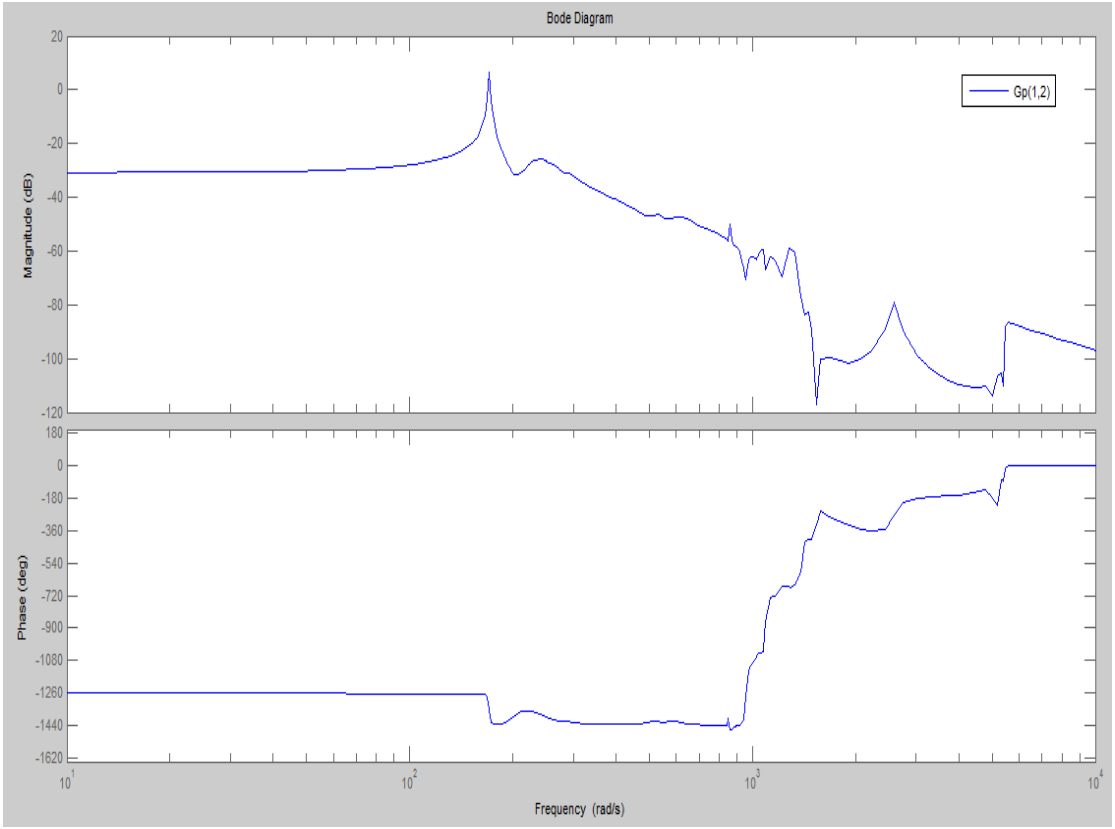

Figure 2.19 MIMO (Gp(1,2)) 47 modes plate model

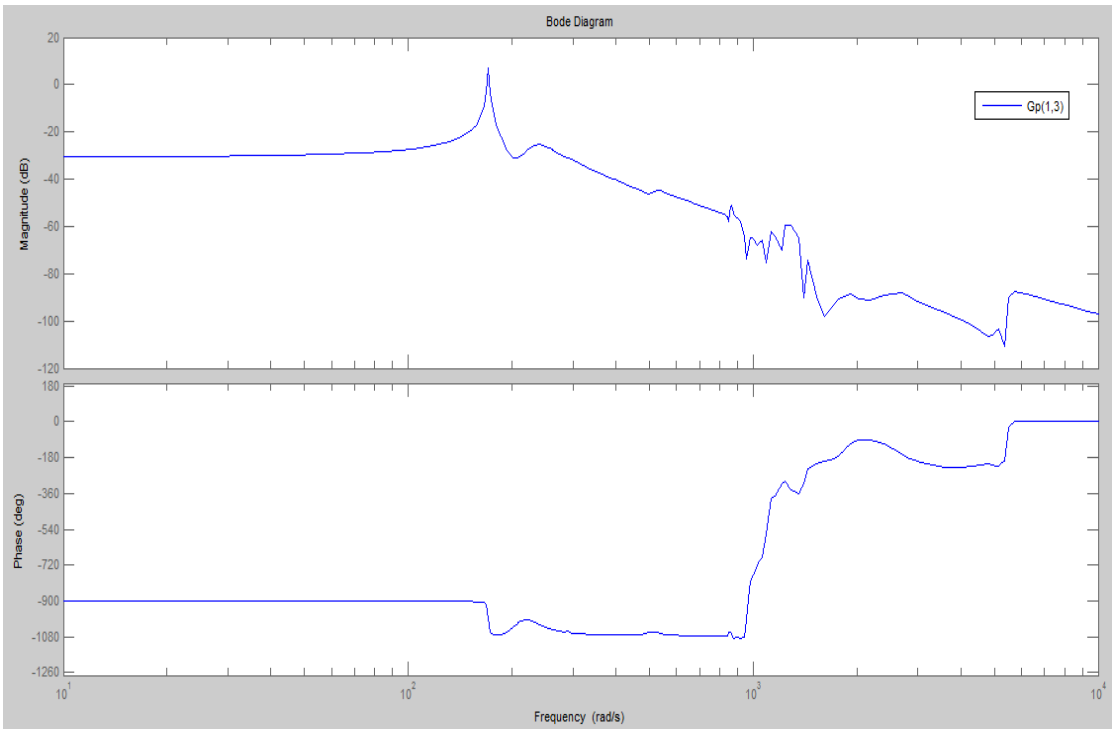

Figure 2.20 MIMO (Gp(1,3)) 47 modes plate model

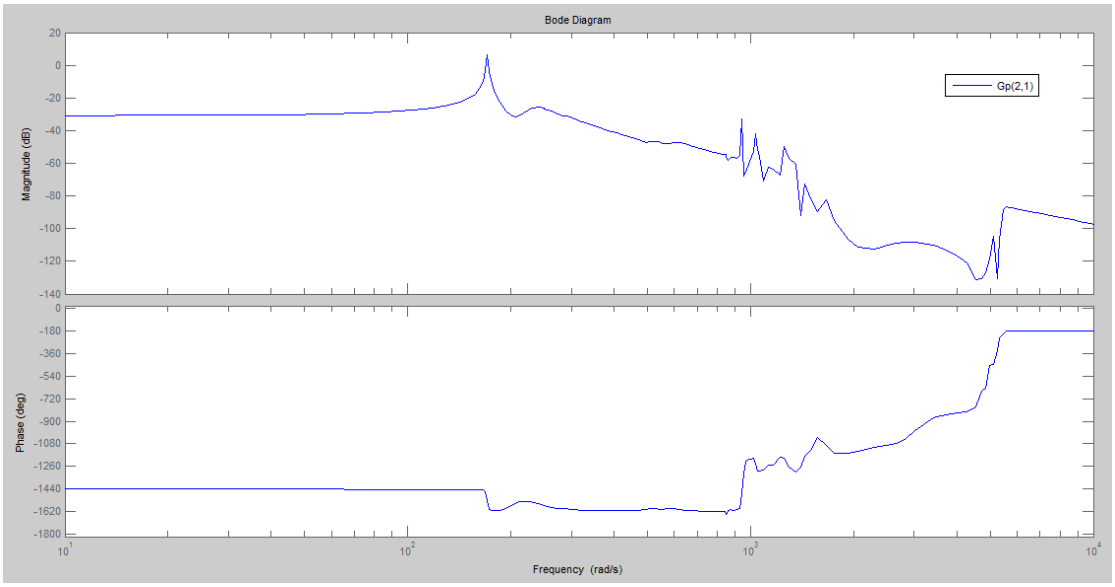

Figure 2.21 MIMO (Gp(2,1)) 47 modes plate model

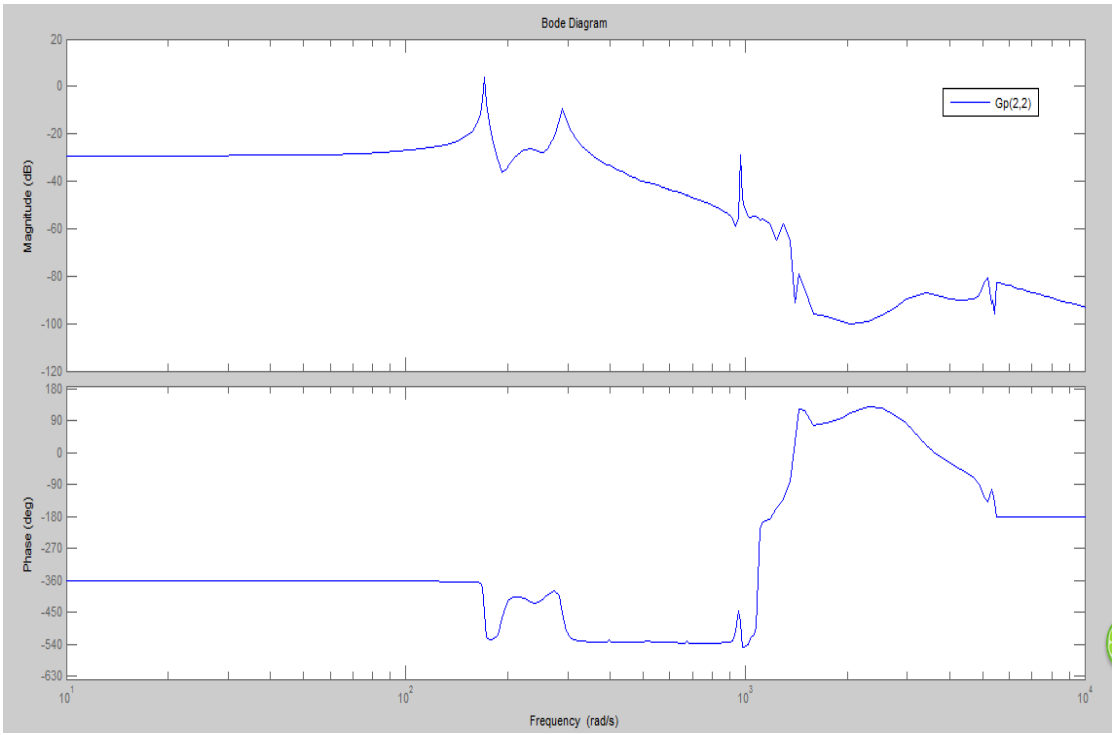

Figure 2.22 MIMO (Gp(2,2)) 47 modes plate model

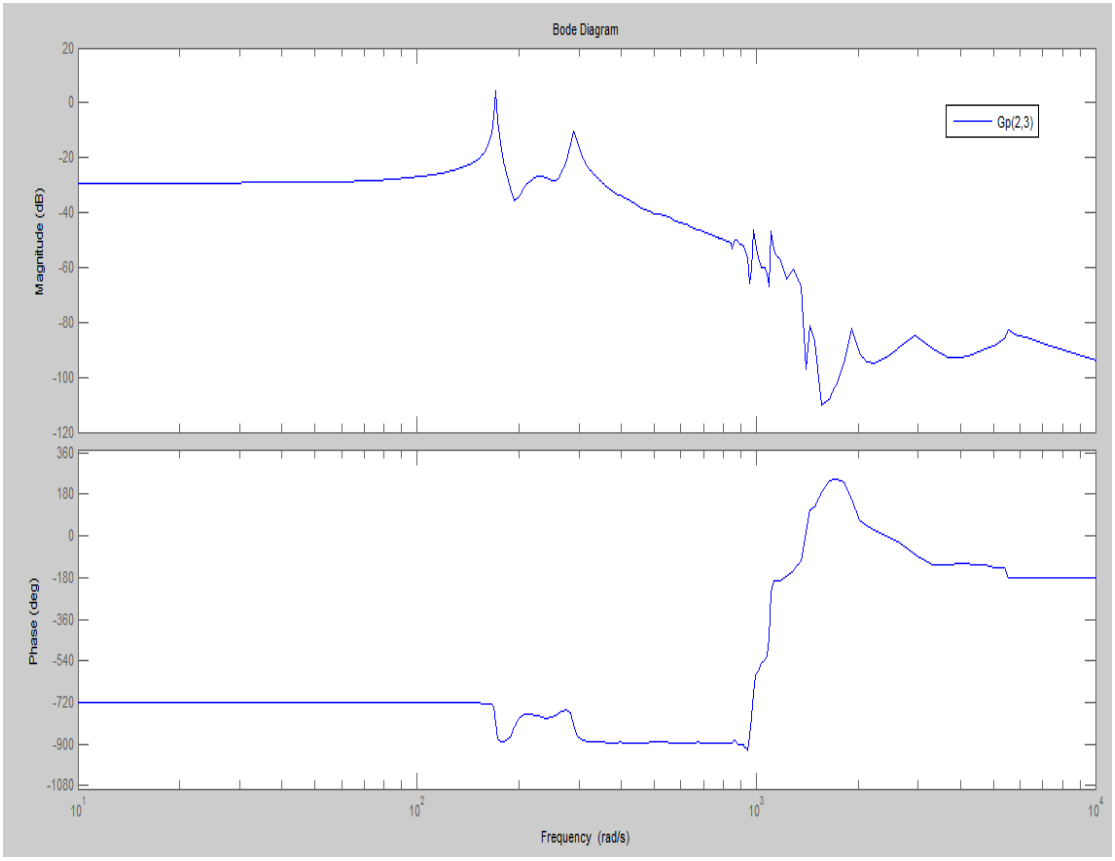

Figure 2.23 MIMO (Gp(2,3)) 47 modes plate model

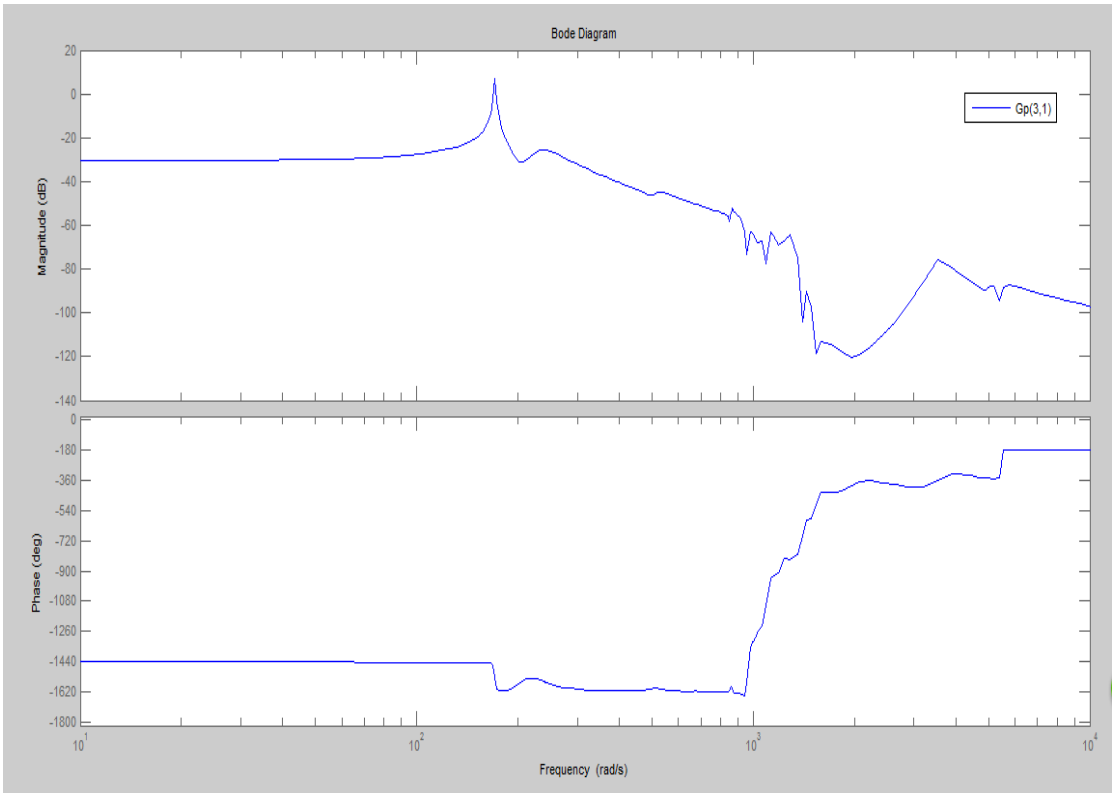

Figure 2.24 MIMO (Gp(3,1)) 47 modes plate model

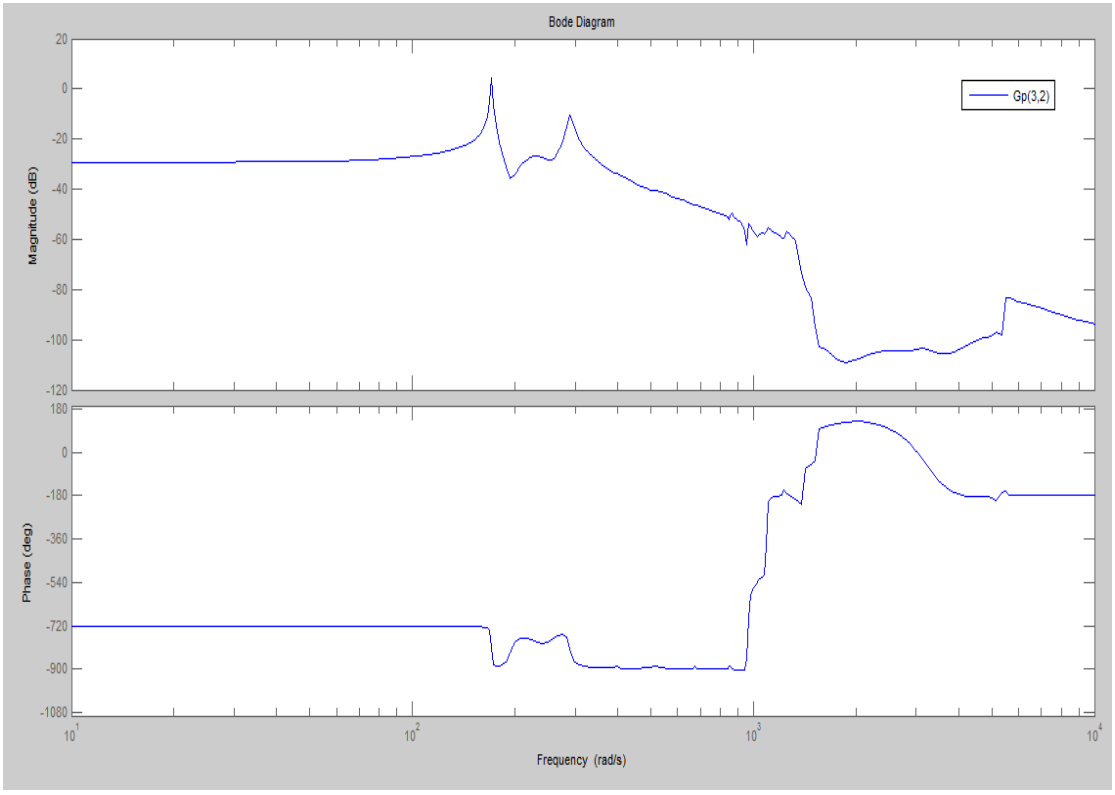

Figure 2.25 MIMO (Gp(3,2)) 47 modes plate model

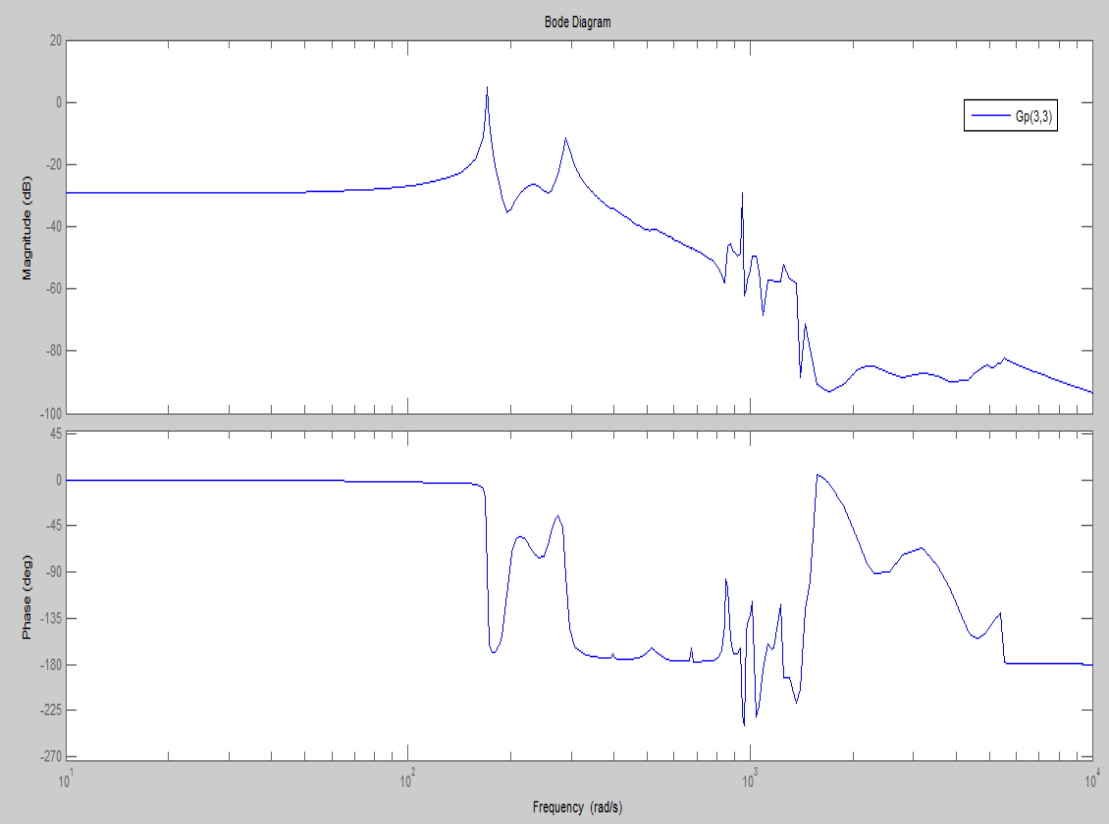

Figure 2.26 MIMO (Gp(3,3)) 47 modes plate model

2.5 Summary

In this chapter we studied the dynamics of plate structure with specific boundary conditions. The majority of system in this chapter was flexible structure with regular shape and well-defined boundary conditions, whose eigenvalue problems can be solved analytically. We derived transfer functions that represent the behavior and capture the spatially distributed nature of the system. Comparing the accuracy of the natural frequencies of the model which obtained from experimental method and numerical calculation. We also set up the simulation model of the plate.

Chapter 3

Spatial Norm and Model Reduction

3.1 Introduction

Modeling of physical systems often results in high order models. It is desirable to reduce such a high-order model to a simpler model of lower dimension. The problem of model reduction is important since the majority of modern controller design techniques (such as H_∞ and LQG design methods) result in a controller of dimension equal to that of the plant. Hence, a controller design based on a suitable reduced model would result in a lower order controller which would reduce implementation problems [113]. In order to use the model in analysis and synthesis problems, we need to define suitable performance measures that take into account their spatially distributed nature. Traditional performance measures, such as H_2 and H_∞ norms, only deal with point-wise models for such systems. In this chapter, we extend these performance measures to include the spatial characteristics of spatially distributed systems [113].

Another topic that is covered in this chapter is that of model reduction by balanced truncation. The problem of model reduction for dynamical systems has been studied extensively throughout the literature; see, for example, [121,122] Here, we address the problem for spatially distributed linear time-invariant systems, following [123].

3.2 Plate Model Reduction and Balanced Realization

3.2.1 SISO Plate Model Reduction and Balanced Realization

Based on the knowledge in [113], we can use spatial H_2 and H_∞ norm for spatially distributed systems. This norm can be used as measures of performance in certain analysis and synthesis problems. In some cases, it can be beneficial to add a spatial weighting function to emphasize certain regions [113]. In this section, we extend those definitions to allow for spatially distributed weighting functions. So we can reduce the

plate model order by the balanced method: Fig 3.1-3.8 are shown the SISO plate model reduction by balanced truncation method.

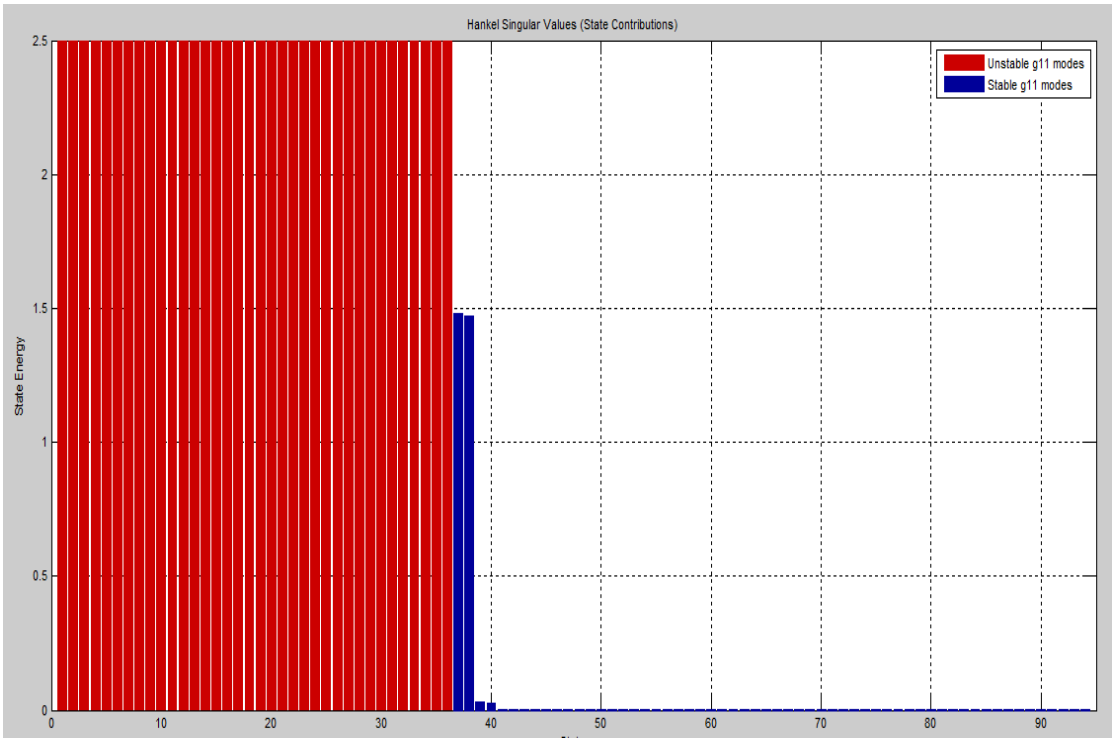

Figure 3.1 SISO Plate (g11) at transducer 1 Hankel singular values

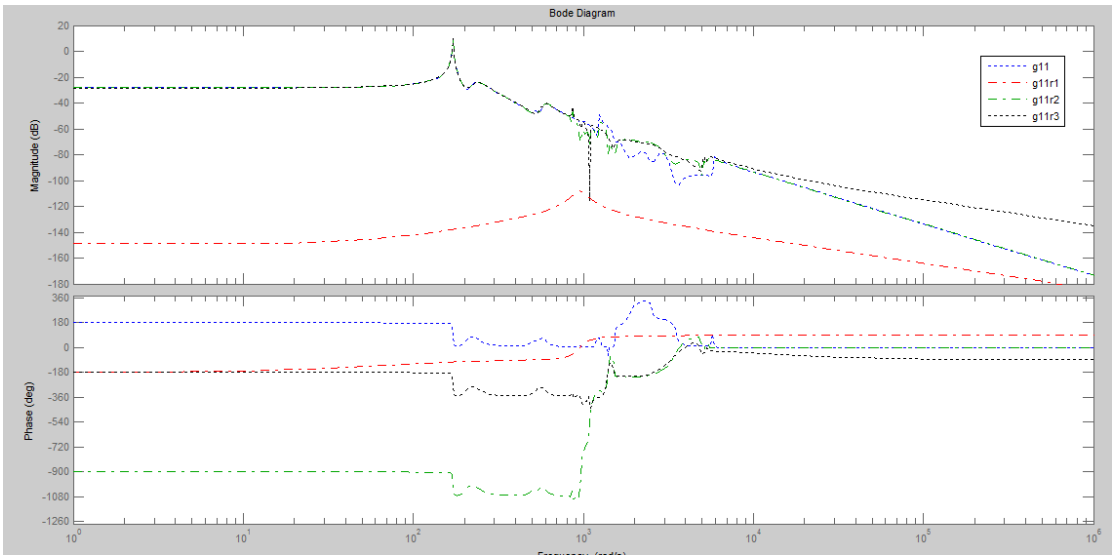

Figure 3.2 SISO Plate (g11) at transducer 1 model reduction and balanced realization frequency domain compare

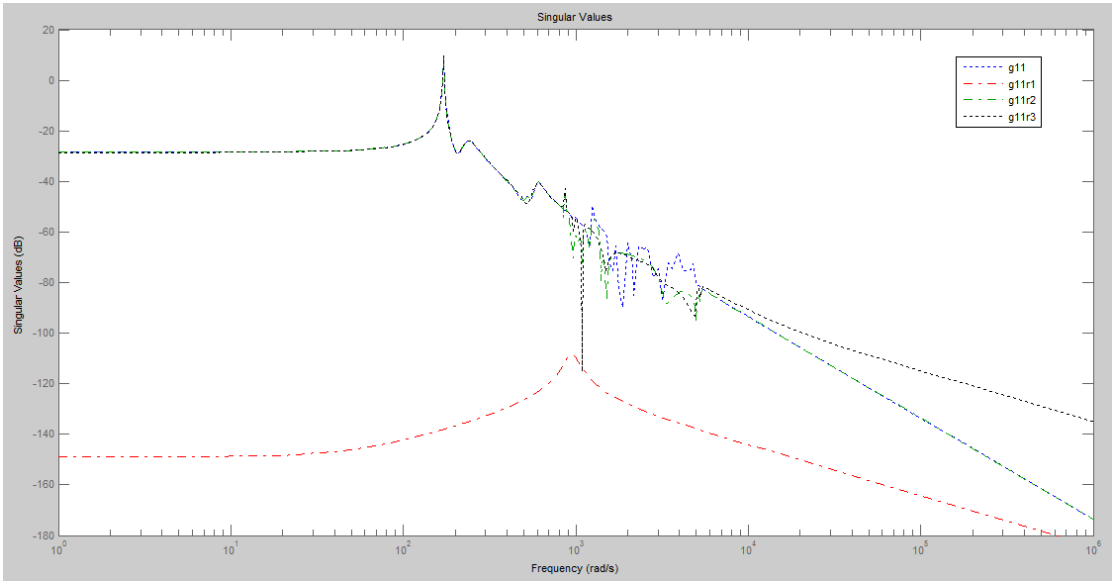

Figure 3.3 SISO Plate (g11) at transducer 1 model reduction and balanced realization singular values compare

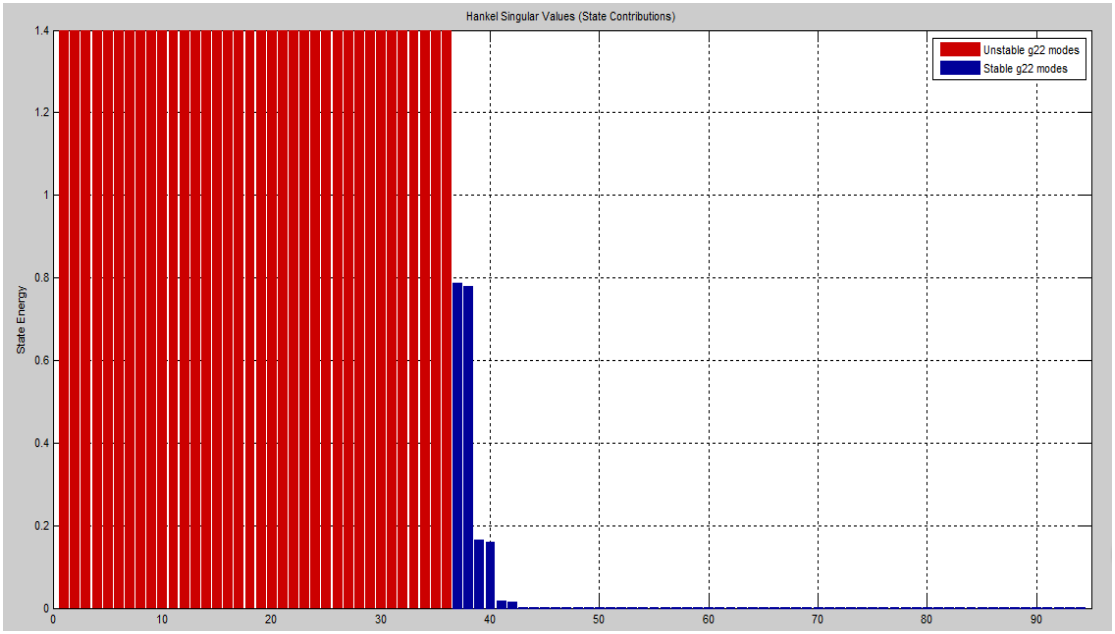

Figure 3.4 SISO Plate (g22) at transducer 2 Hankel singular values

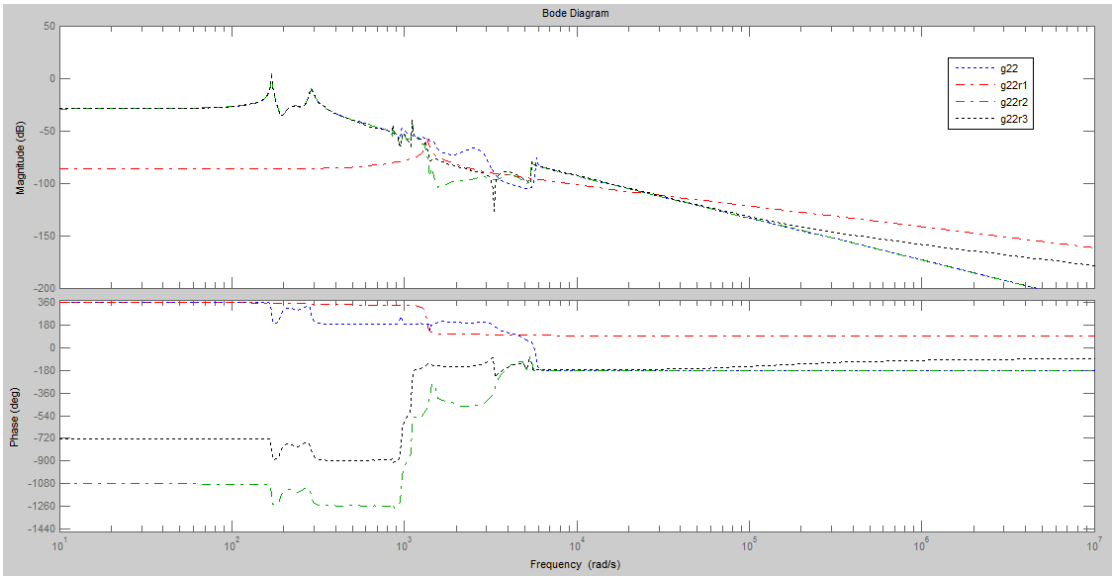

Figure 3.5 SISO Plate (g22) at transducer 2 model reduction and balanced realization frequency domain compare

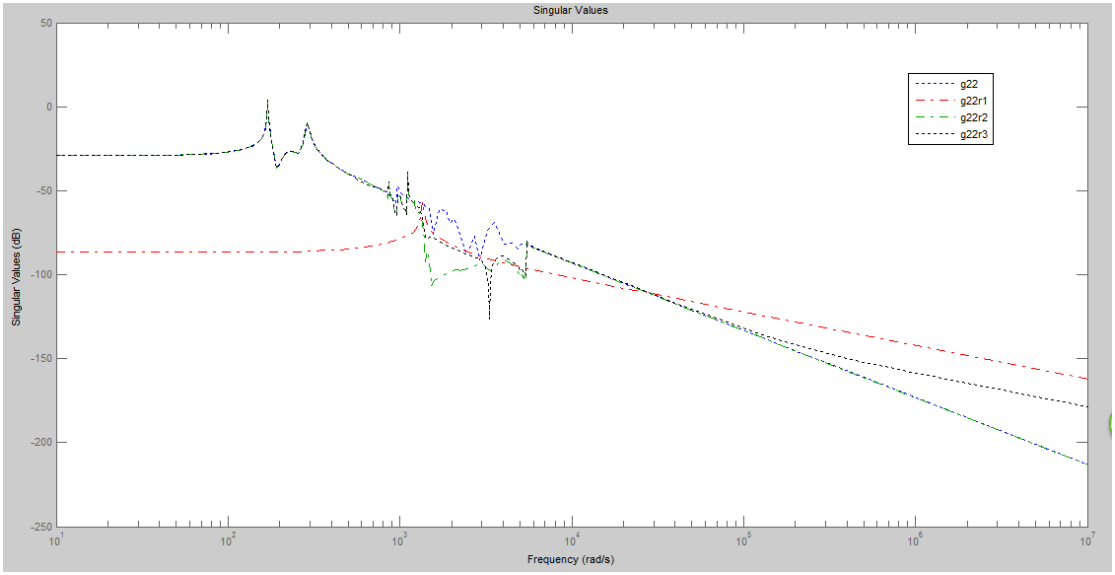

Figure 3.6 SISO Plate (g22) at transducer 2 model reduction and balanced realization singular values compare

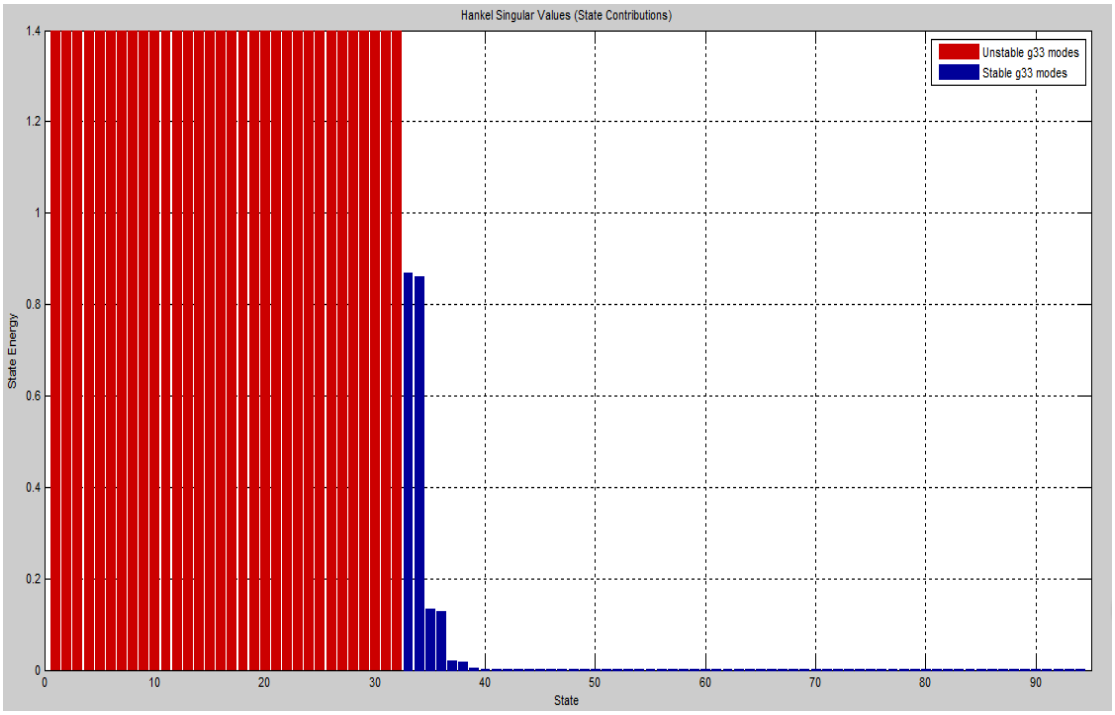

Figure 3.7 SISO Plate (g33) at transducer 3 Hankel singular values

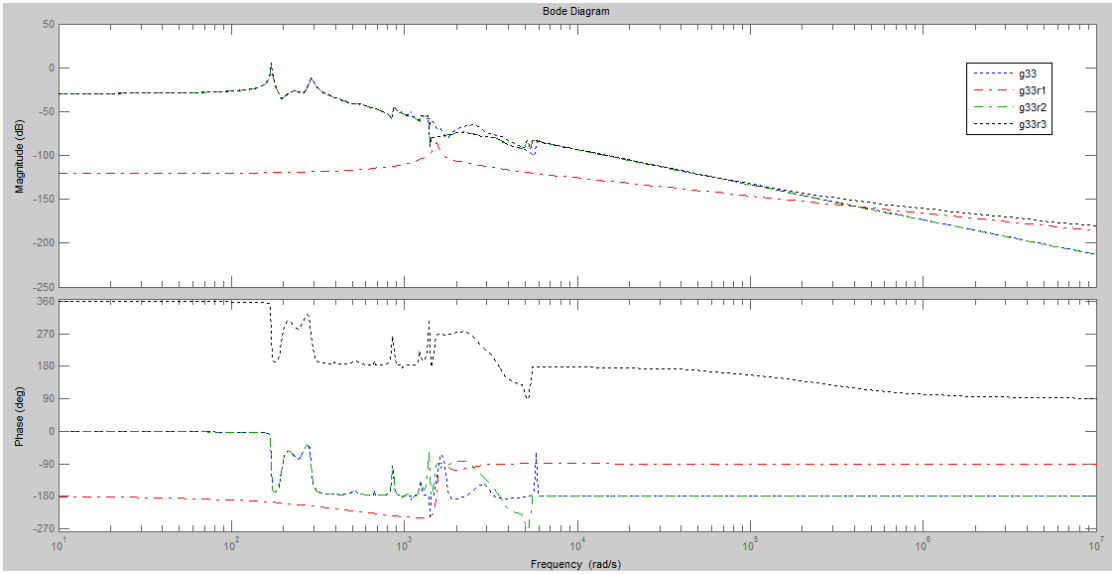

Figure 3.8 SISO Plate (g33) at transducer 3 model reduction and balanced realization frequency domain compare

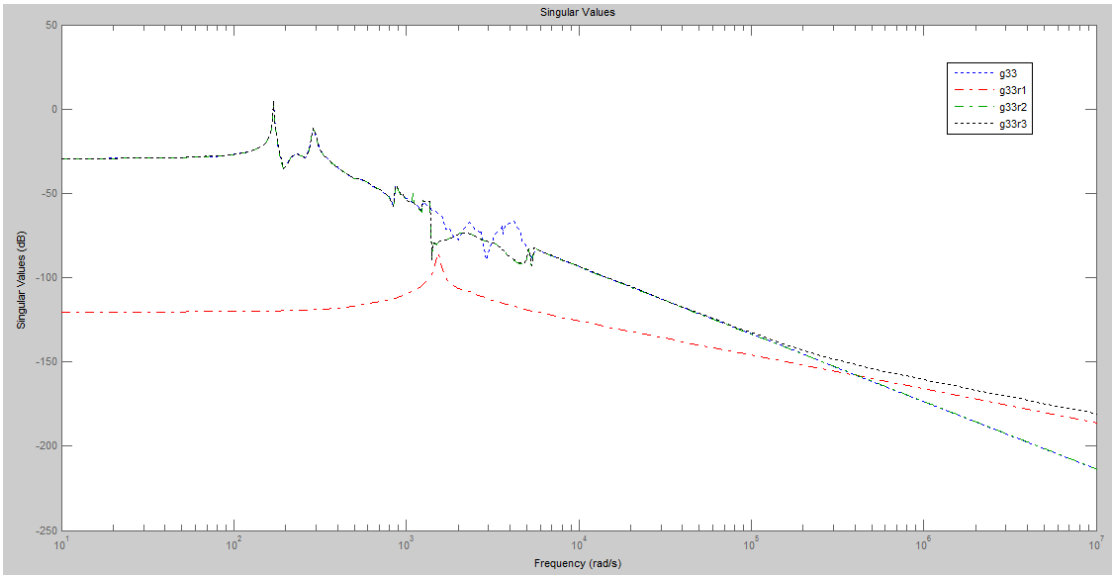

Figure 3.9 SISO Plate (g33) at transducer 3 model reduction and balanced Realization singular values compare

We can see that, according to Hankel singular values, first 44 states of g11, first 36 states of g22, first 32 states of g33 are all unstable states, so if we want to reduce the order of the model, we need to obtain all the unstable states. It can be seen that the "balreal" method is better compare to others.

3.2.2 MIMO Plate Model Balanced truncation

Fig 3.10-3.12 are shown the MIMO plate model reduction by balanced truncation method.

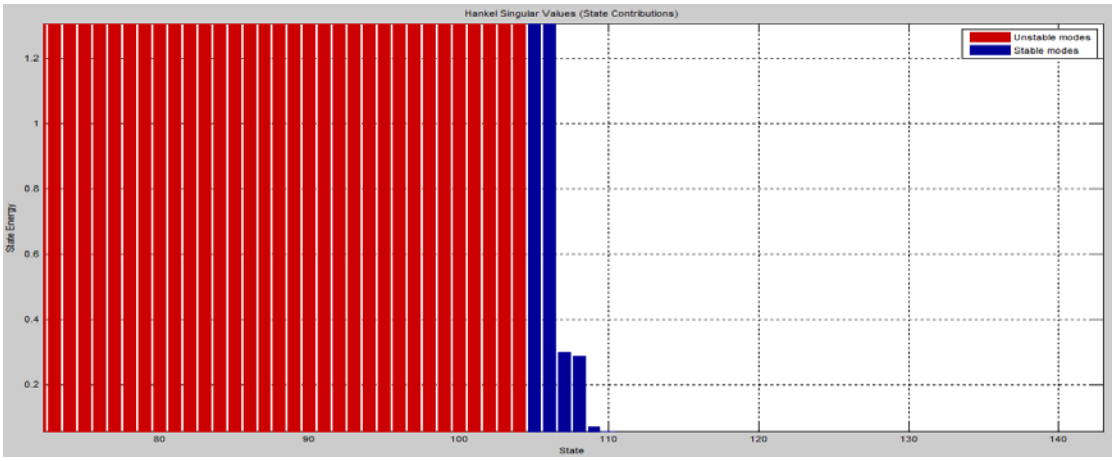

Figure 3.10 MIMO Plate Hankel singular values

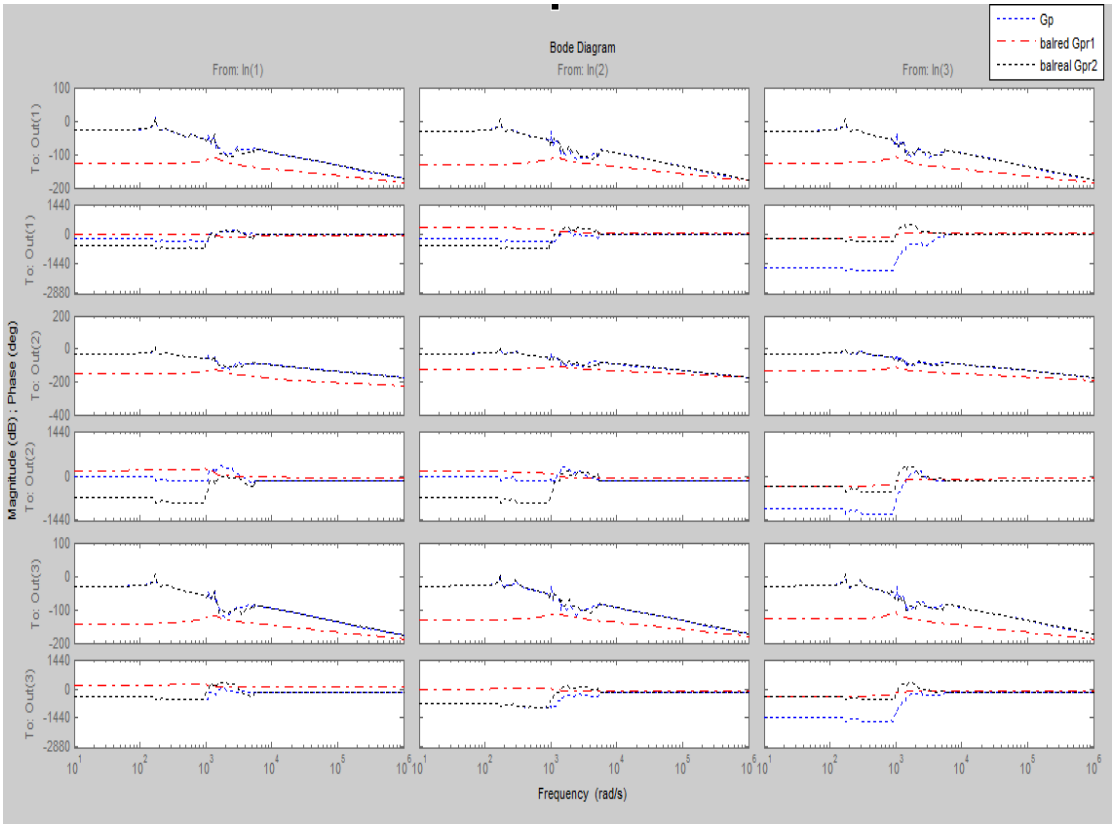

Figure 3.11 MIMO Plate model reduction and balanced realization frequency domain compare

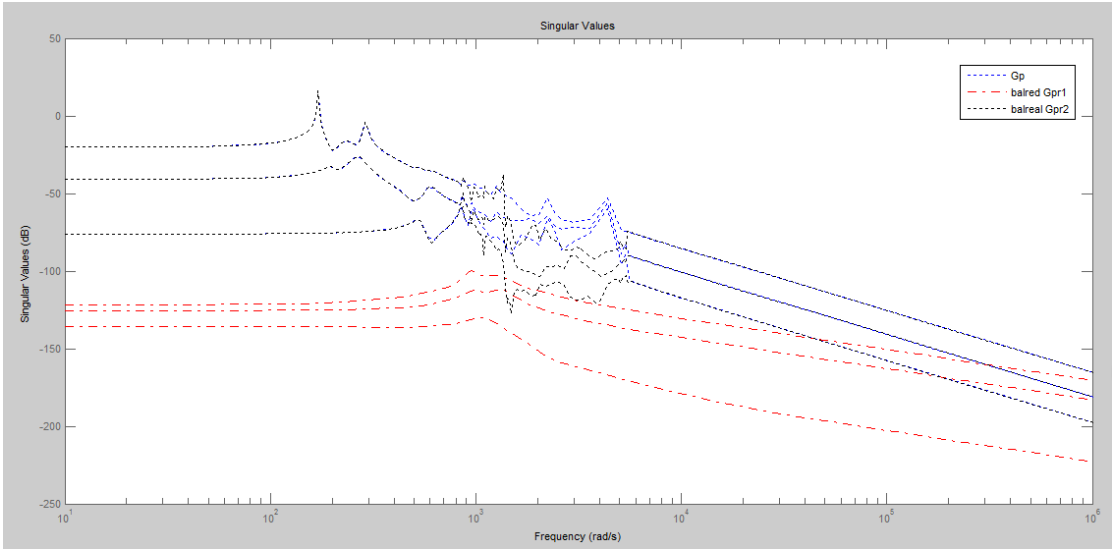

Figure 3.12 MIMO Plate model reduction and balanced realization singular values compare

It can be seen that the "balreal" method is better compare to others.

3.3 Summary

In this chapter, we showed the method to reduce the model order by balanced truncation method, and also introduce the spatial norm of model. We gave the performance of "balred", "balreal" and "modred" for SISO plate model, the performance of "balred" and "balreal" and for MIMO plate model, and according to compare the performance, we gave the decision that "balreal" balanced truncation method is better both for SISO and MIMO plate model, but for some cases caused too big phase angle.

Chapter 4

Model Correction

4.1 Introduction

Dynamics of flexible structures and some acoustic systems consist of an infinite number of modes. For control design purposes these models are often approximated by finite-dimensional models via truncation. Direct truncation of higher order modes results in the perturbation of zero dynamics and hence generates errors in the spatial frequency response of the system. If the truncated model is then used to design a controller which is implemented on the system, say in the laboratory, the closed loop performance of the system can be considerably different from the theoretical predictions. This is mainly due to the fact that although the poles of the truncated system are at the correct frequencies, the zeros can be far away from where they should be. Therefore, it is natural to expect that a controller designed for the truncated [113].

Reference [124] discusses the effect of out of bandwidth modes on the low-frequency zeros of the truncated model. There, it is suggested that the effect of higher frequency modes on the low frequency dynamics of the system can be captured by adding a zero frequency term to the truncated model to account for the compliance of the ignored modes [133]. The model correction method that is proposed allows for a spatially distributed DC term to capture the effect of truncated modes in an optimal way. In this chapter, we take a similar approach in the sense that we allow for a zero frequency term to capture the effect of truncated modes. However, this constant term is found such that the H_2 norm of the resulting error system is minimized [113].

4.2 Plate Correction Model

As discussed in Chapter 3, Fig 3.1, 3.4, 3.7, 3.10 showed that there are unstable states in the Hankel singular values, so we could not choose the state which we want to save and truncate as normal, so we just focus on the first four modes in this study.

4.2.1 SISO Plate Model Correction

Figure 4.1-4.4 show the model correction result for SISO plate and compare with "balreal" balanced truncation method. Compare to "balreal" balanced truncation method, model correction method is better because

i. the transfer function of correction model is simple, for example, if we only focus on the first four modes of the plate, there are only 8 states of correction model comparing to 94 states of balanced truncation model.
ii. there is no big phase angle.
iii. it is very easy to implemented in MATLAB or simulink.

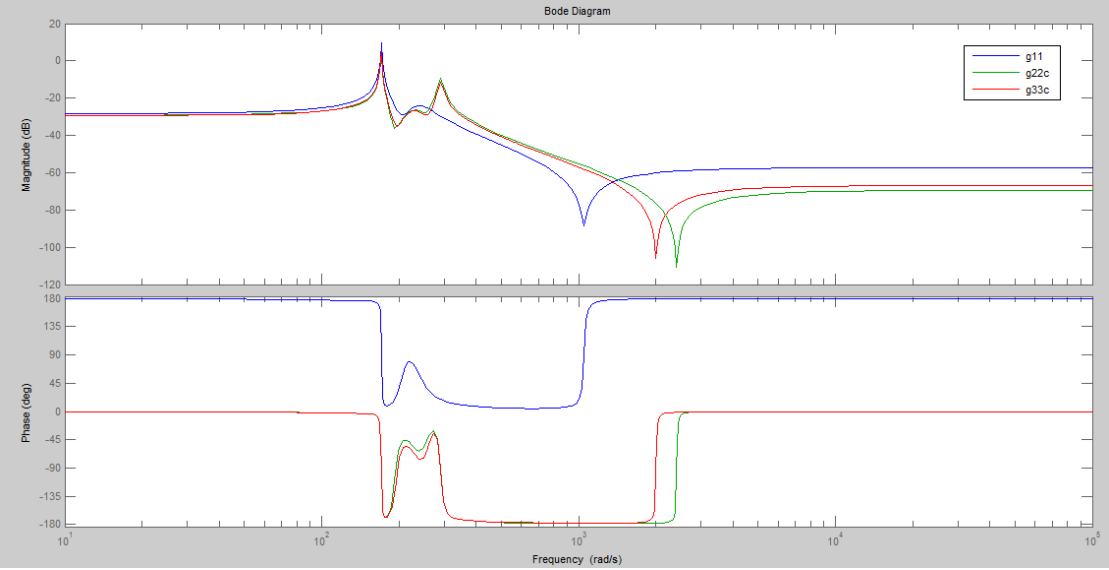

Figure 4.1 SISO plate model correction result

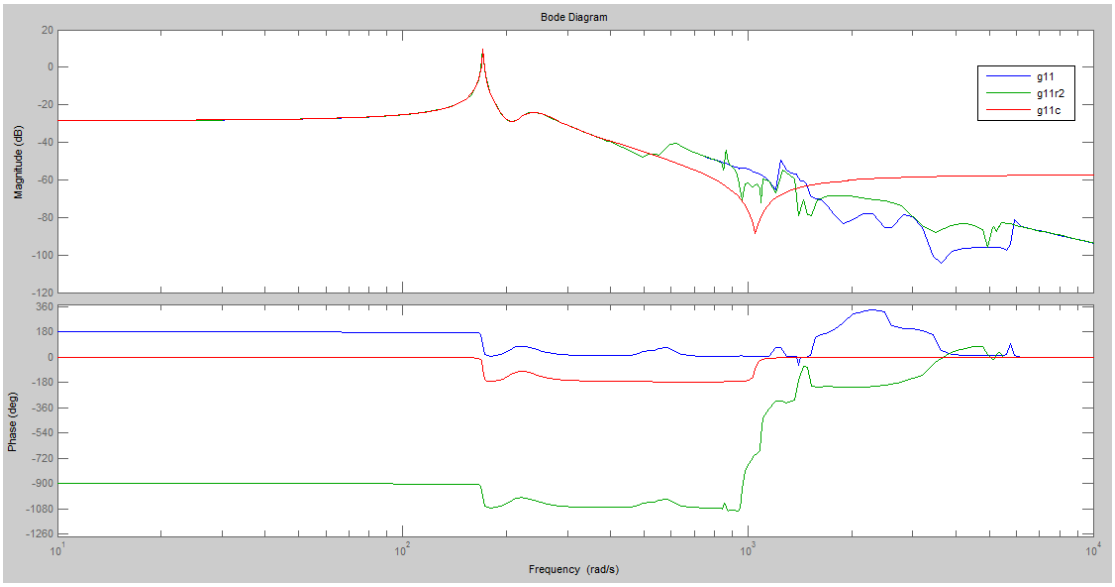

Figure 4.2 SISO plate (g11) model reduction result compare (balreal and correction)

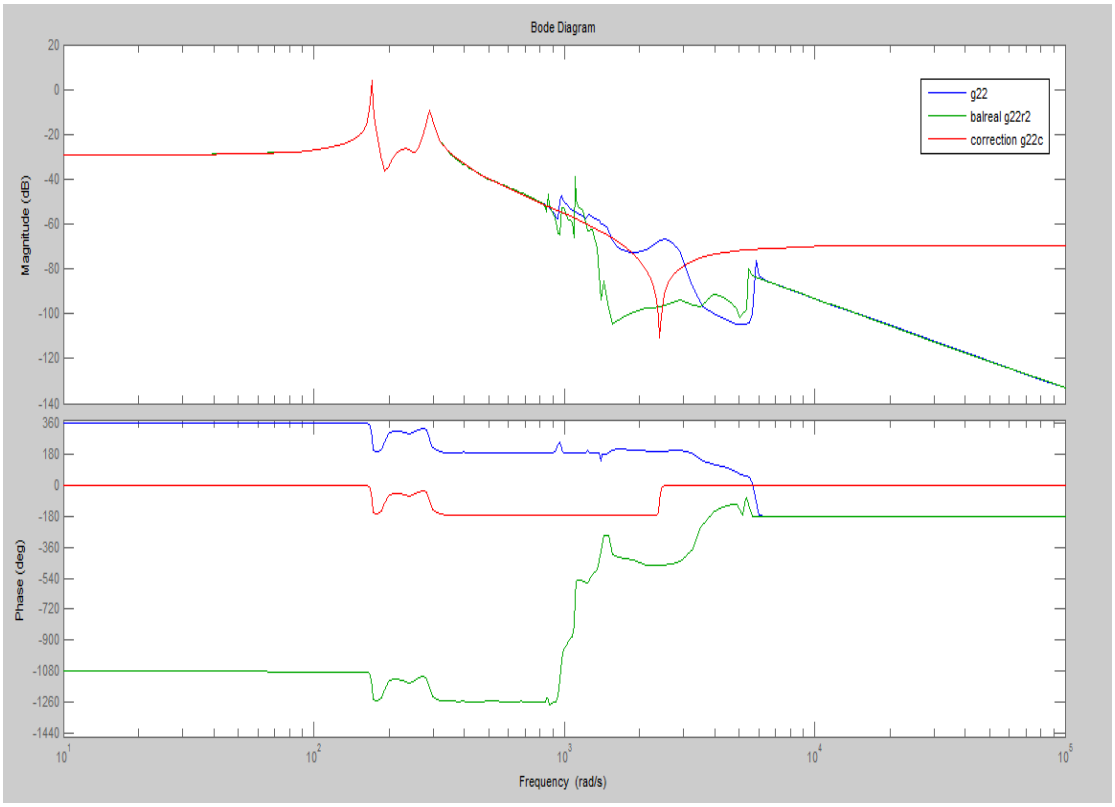

Figure 4.3 SISO plate (g22) model reduction result compare (balreal and correction)

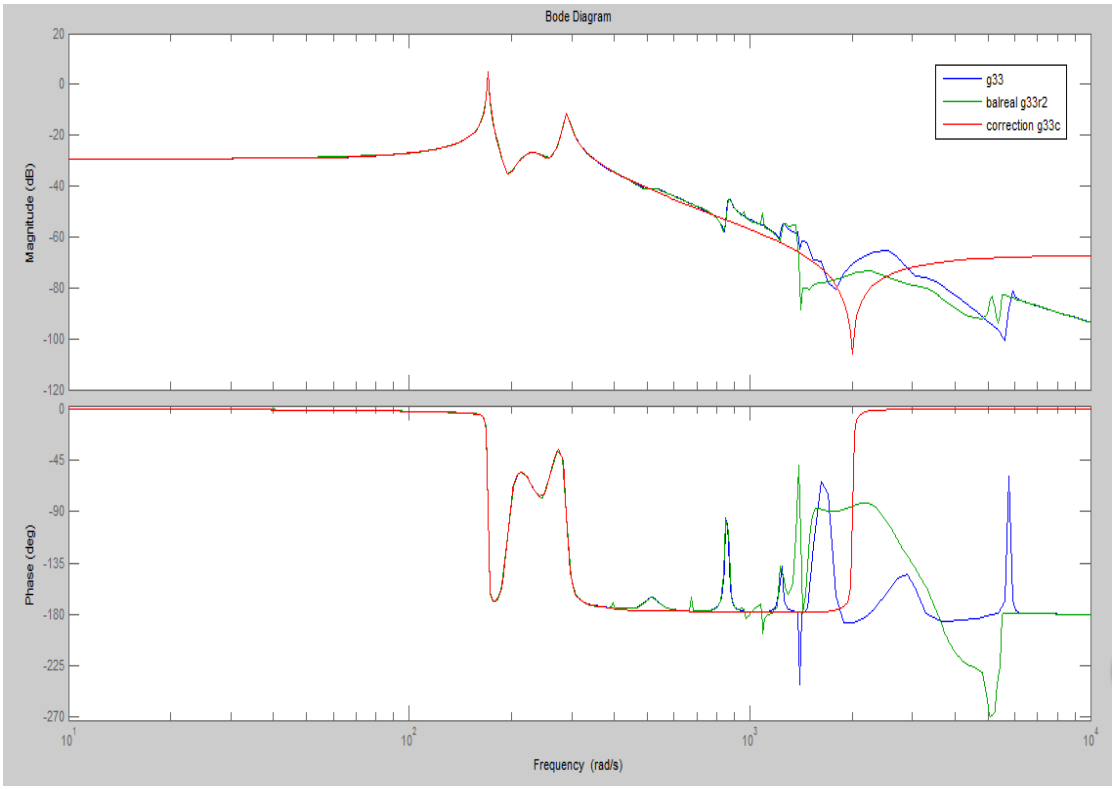

Figure 4.4 SISO plate (g33) model reduction result compare (balreal and correction)

4.2.2 MIMO Plate Model Correction

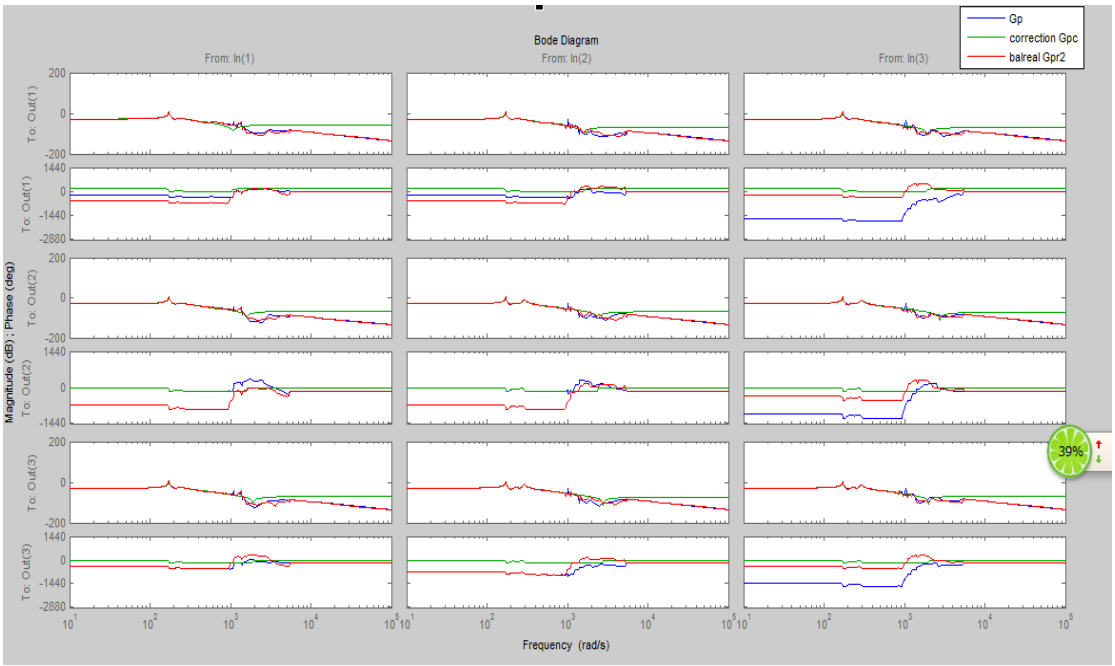

Figure 4.5 MIMO plate model reduction result compare (balreal and correction)

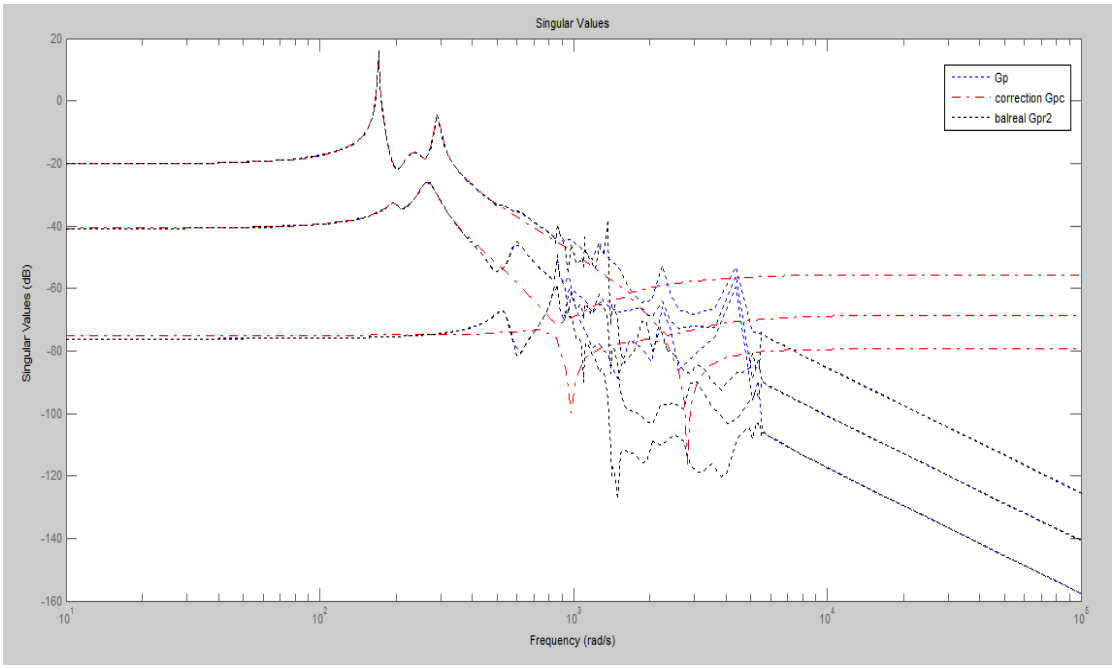

Figure 4.6 MIMO Plate model correction and balanced truncation singular values compare

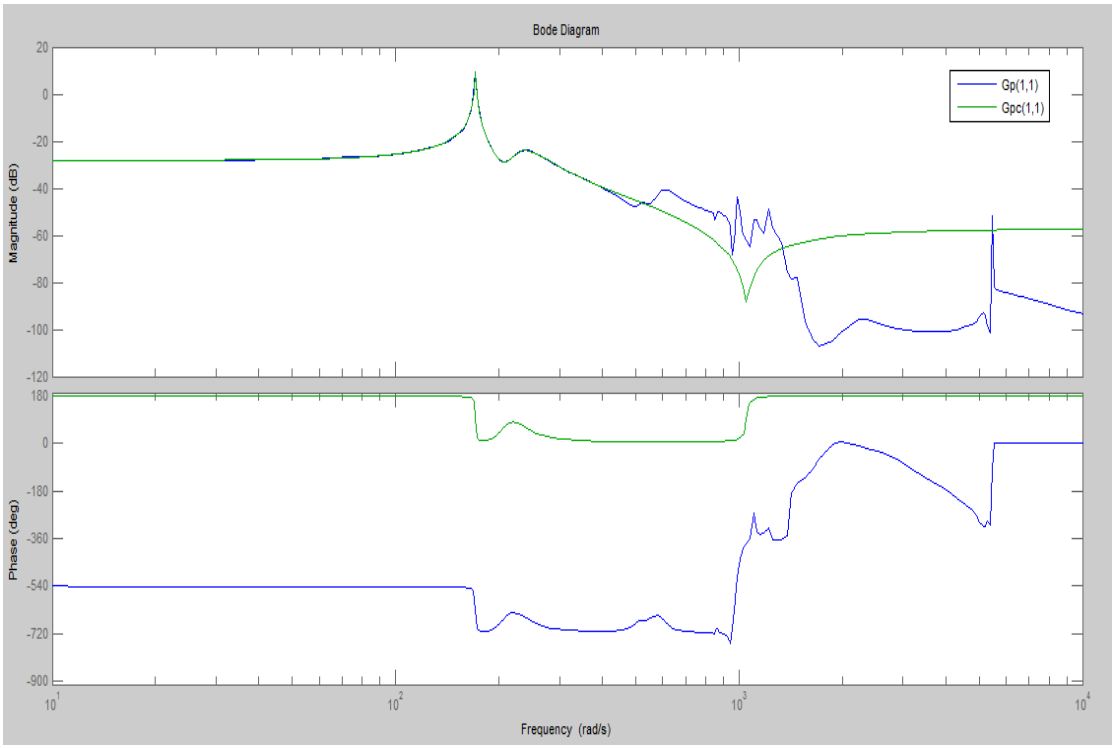

Figure 4.7 MIMO (Gpc(1,1)) plate model correction result

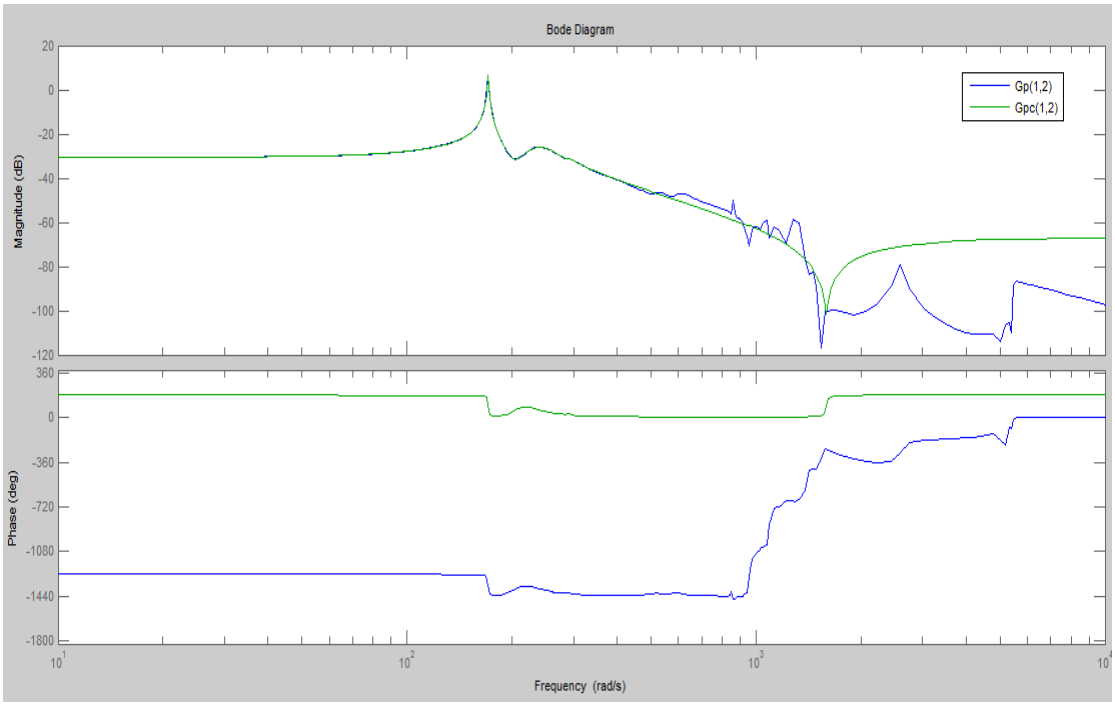

Figure 4.8 MIMO (Gpc(1,2)) plate model correction result

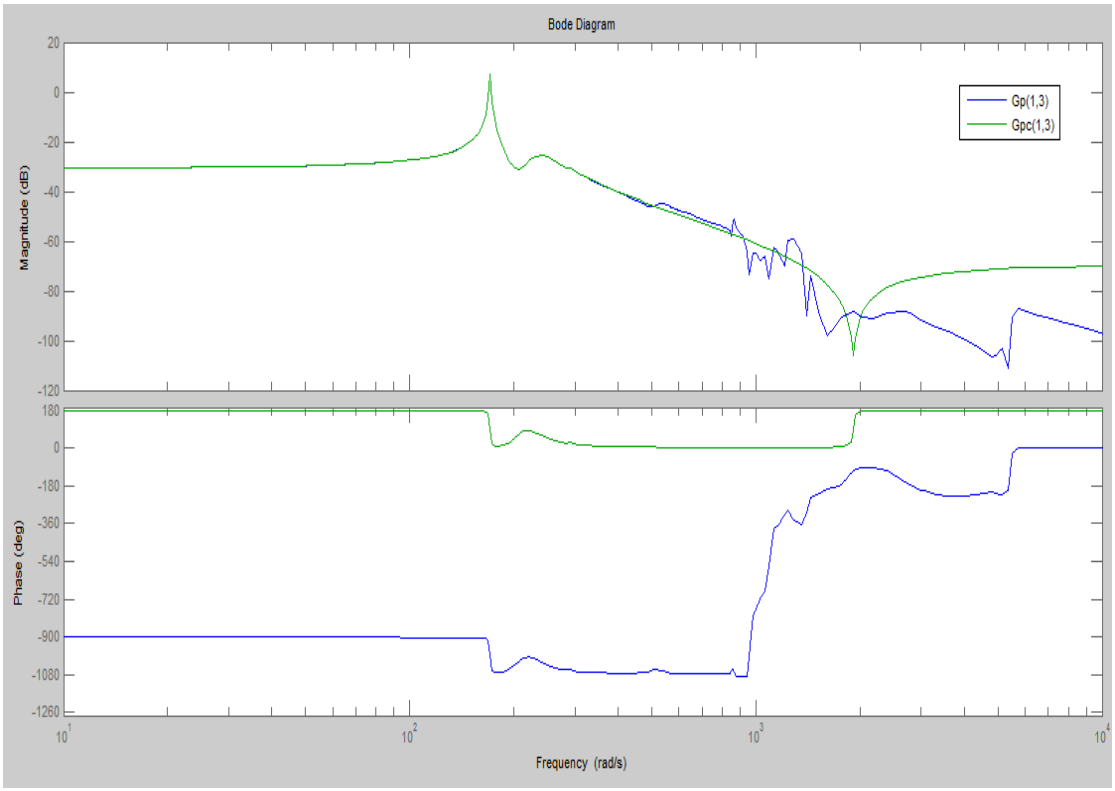

Figure 4.9 MIMO (Gpc(1,3)) plate model correction result

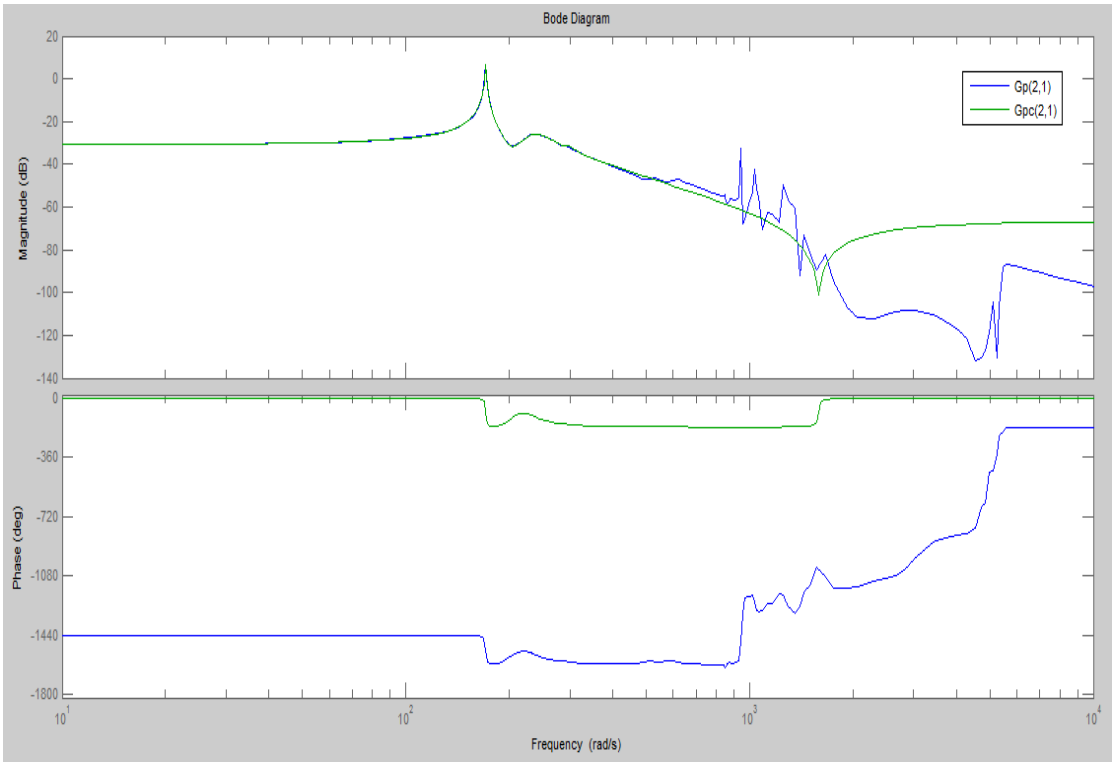

Figure 4.10 MIMO (Gpc(2,1)) plate model correction result

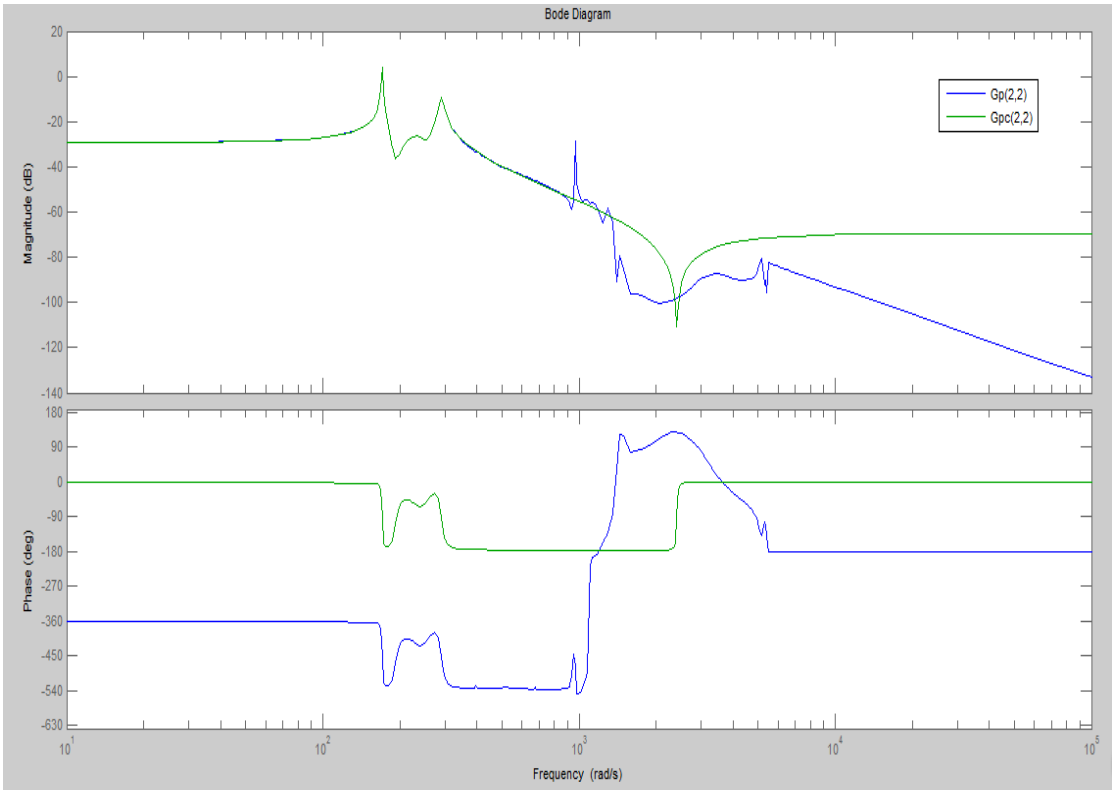

Figure 4.11 MIMO (Gpc(2,2)) plate model correction result

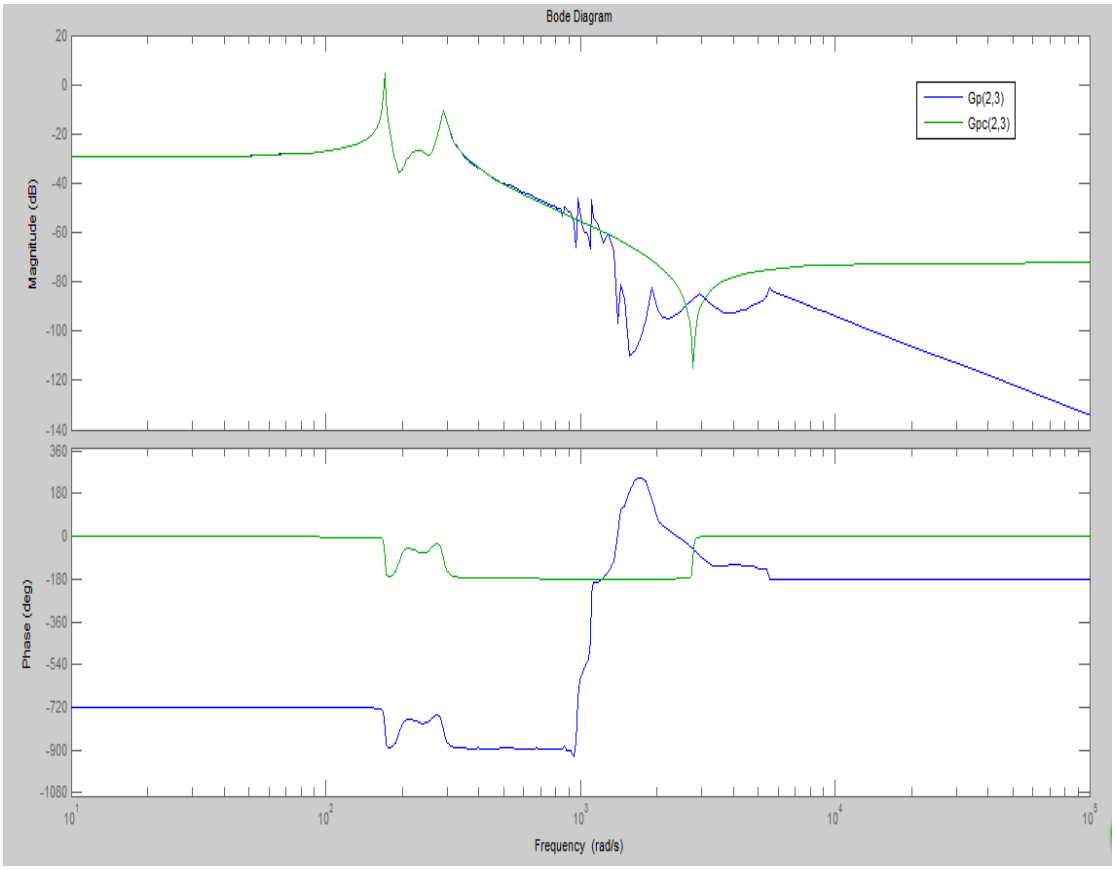

Figure 4.12 MIMO (Gpc(2,3)) plate model correction result

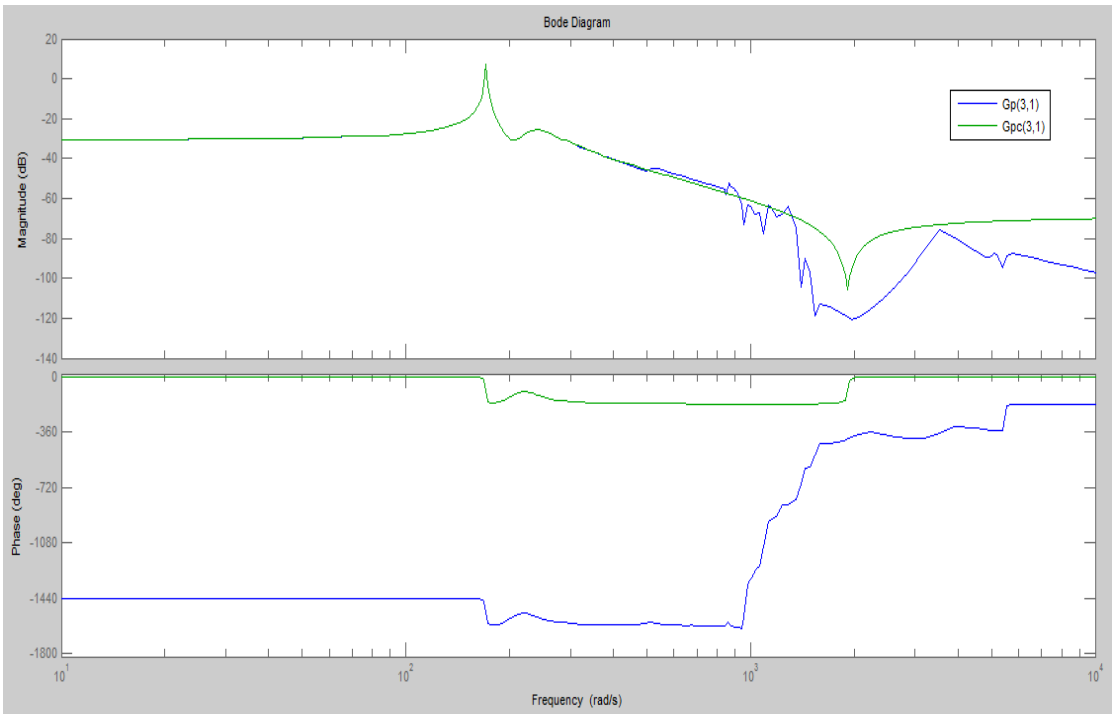

Figure 4.13 MIMO (Gpc(3,1)) plate model correction result

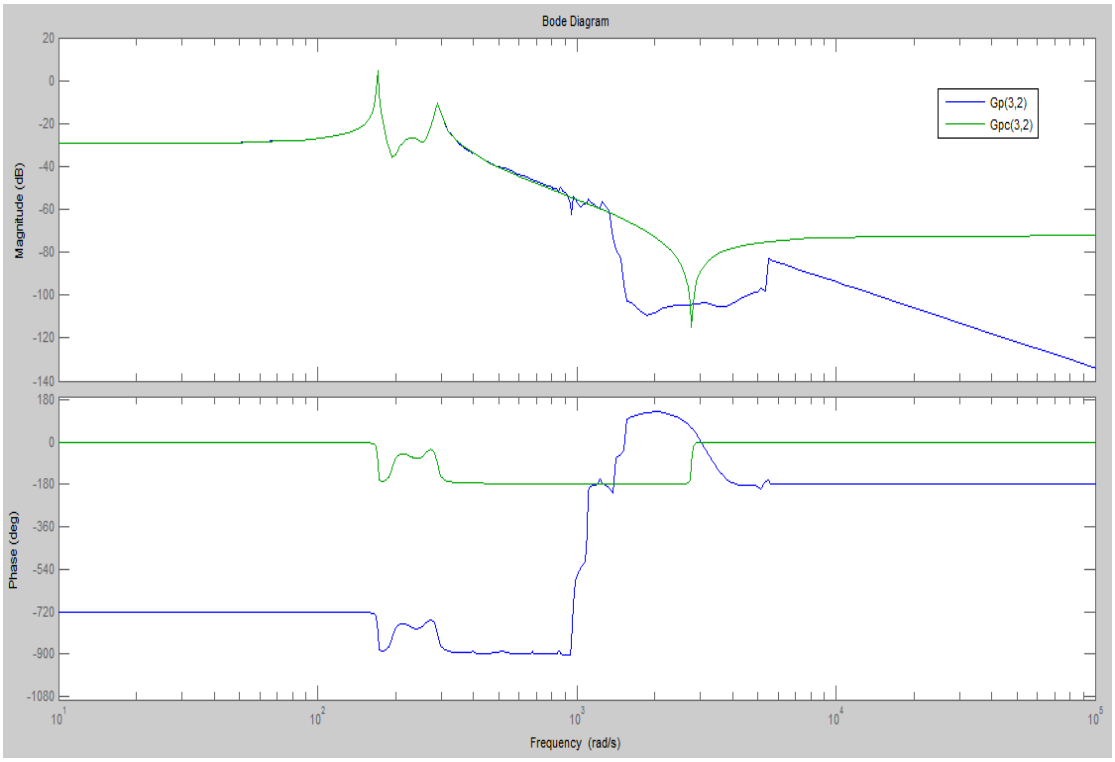

Figure 4.14 MIMO (Gpc(3,2)) plate model correction result

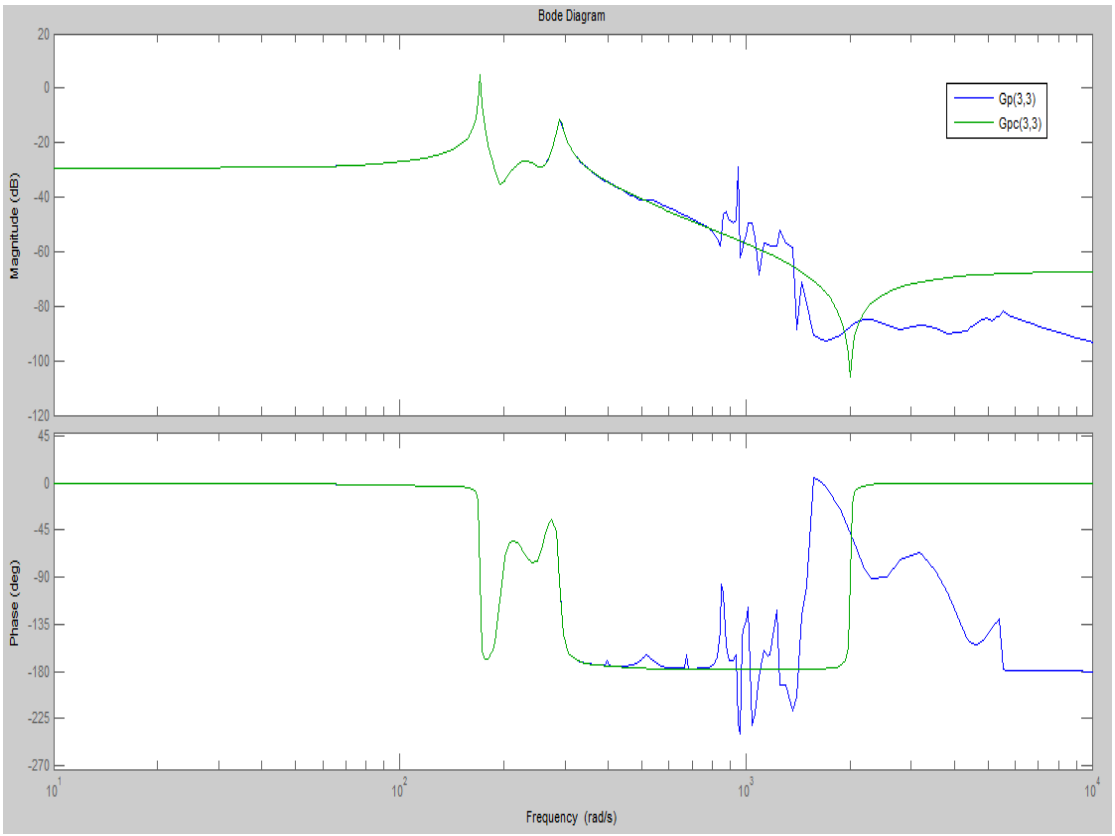

Figure 4.15 MIMO (Gpc(3,3)) plate model correction result

4.3 Summary

In this chapter, we reported the method to truncate the model order by correction method. We gave the performance of "balreal" balanced truncation and model correction for SISO and MIMO plate model. According to compare the performance, we made the decision that model correction method is better both for SISO and MIMO plate model.

Chapter 5

Multi-mode SISO and MIMO PPF Controller

This chapter provides an overview of the positive position feedback (PPF) technique. In the first two section general information and structure about PPF is given. The third section shows the PPF controller stability derivation. This derivation itself is not original and can also be found in [125,1,3]. The following section shows the selection method of the optimal controller parameters and MATLAB simulation result.

5.1 Introduction

As shown in Chapter 2, one of the characteristics of flexible structures is their highly resonant nature. For the case of the plate used in this research this characteristic is made evident by the relatively large vibration at or near to the natural frequencies of the structure, as shown in Fig. 2.5. From the figure, it is clear that suppressing the vibration of a structure at or very close to the natural frequencies of the structure is more important than suppressing the vibration at other frequencies. However, suppressing the vibration at one or more natural frequencies may excite or amplify other natural frequencies. Therefore, one important design requirement for flexible structure control is to achieve high attenuation for modes of interest without driving the other modes into instability or exciting and amplifying the vibration of other modes [4].

As stated in Chapter 1, a resonant PPF controller has necessary characteristics that satisfy the design requirements for multi-mode vibration attenuation of flexible structures investigated in this research. Exploiting the highly resonant characteristic of the flexible structure, the resonant PPF controller only applies high gain at or close to the natural frequencies of interest, and is therefore able to suppress the vibration at those frequencies without causing adverse effects at other frequencies. In the

following section, a further analysis on the characteristics of a PPF resonant controller is presented [133].

5.2 PPF Controller Structure

The technique of positive position feedback (PPF) control was first introduced by Caughey and Goh in a Dynamics Laboratory Report in 1982. Its simplicity and robustness has led to many applications in structural vibration control [29,30]. Unlike other control laws, positive position feedback is insensitive to the rather uncertain natural damping ratios of the structure [29]. The terminology positive position is derived from the fact that the position measurement is positively fed into the compensator and the position signal from the compensator is positively fed back to the structure [31]. This property makes the PPF controller very suitable for collocated actuator/sensor pairs. Equations 3.1 and 3.2 show the structure and compensator equations in the scalar case [29]:

Structure: $$\ddot{\varepsilon} + 2\xi\omega\dot{\varepsilon} + \omega^2\varepsilon = g\omega^2\eta \quad (5.1)$$

Compensator: $$\ddot{\eta} + 2\xi_f\omega_f\dot{\eta} + \omega_f^2\eta = \omega_f^2\varepsilon \quad (5.2)$$

where g is the scalar gain (positive), ε is the modal coordinate (structural), η is the filter coordinate (electrical), ω and ω_f are the structural and filter frequencies, respectively, and ζ and $2\xi_f$ are the structural and filter damping ratios, respectively. This non-dynamic stability criterion is characteristic for the positive position feedback system. Figure 5.1 illustrates the connection of Equations (5.1) and (5.2) in a block diagram.

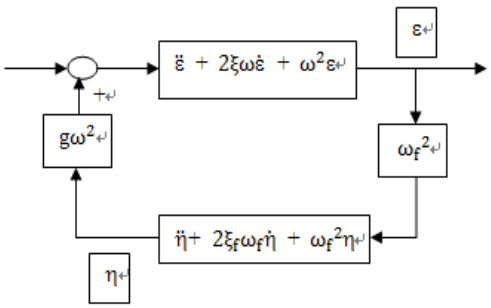

Figure 5.1 Block Diagram of a Second-Order System with Positive Position Feedback

The second-order transfer function in Equation (5.3) also represents the PPF compensator. The transfer function form will be used in this text for deriving the properties of the control system [29].

$$G_{ppf}(s) = \frac{g\omega_f^2}{s^2 + 2\xi_f\omega_f s + \omega_f^2} \tag{5.3}$$

Another feature of the compensator equation, its second-order low-pass characteristic, led to the terminology PPF filter. Figure 5.3 presents a Bode plot of a typical PPF filter. In effect, a PPF filter behaves much like an electronic vibration absorber for the structure except that a mechanical vibration absorber can never destabilize a structure[133,124].

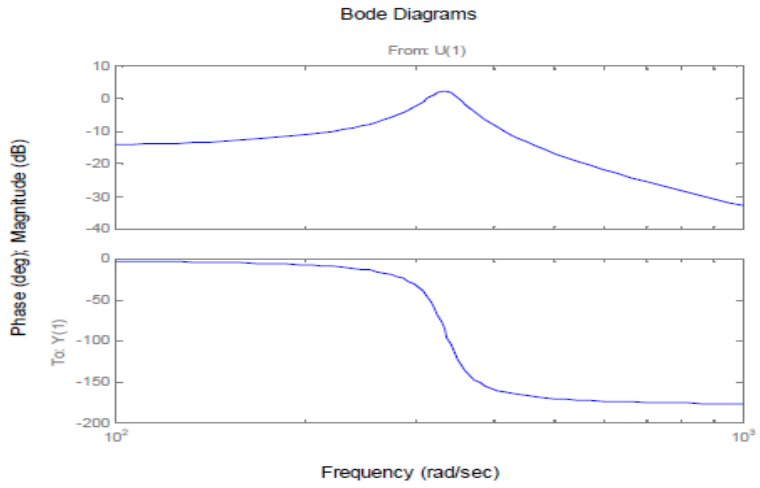

Figure 5.2 Bode Plot of a Typical PPF Filter Frequency Response Function

The roll-off character of the PPF filter is one of the advantages of using a PPF controller. Structural poles with frequencies higher than the filter frequencies are hardly affected by the compensator. This is especially useful when complicated structures with many resonance poles are to be controlled. PPF is able to add damping to lower frequency poles while leaving the possibly unmodeled high frequency poles unchanged [133,124].

Since one PPF filter tuned to a certain frequency only adds damping to one certain pole of the structure, the possibilities of multiple PPF were investigated by many authors [28]. Multiple PPF filters allow that each filter is tuned to add damping to one structural pole while only using one actuator/sensor pair.

Unfortunately, the stability criterion is not as simple as for the one PPF filter case but experiments have shown that for widely spaced poles with up to three PPF filters the stability is usually not a problem [29].

5.3 PPF Controller Closed -loop Stability

5.3.1 Scalar Case

Considering the scalar case first, PPF can be described by two coupled differential equations where the first equation describes structure, and the second describes the compensator as[29]

$$\ddot{\varepsilon}+\beta\dot{\varepsilon}+\omega^2\varepsilon=g\omega^2\eta \tag{5.4}$$

$$\ddot{\eta}+\beta_f\dot{\eta}+\omega_f{}^2\eta=\omega_f{}^2\varepsilon \tag{5.5}$$

where ε is the system coordinate, η is the actuator coordinate, $\varepsilon, \eta \in R$, β and β_f are the system damping and actuator damping ratios, ω and ω_f are the structural natural frequency and filter frequency, and g is the scalar gain, $g > 0$.

Theorem 5.1

The combined system and actuator of (5.4) and (5.5) are Liapunov asymptotic stable iff $g < 1$. (Also serves as the stability boundary.)

Proof :

Taking the Laplace transform of the second-order equation (5.4) and (5.5)

$$(s^2+\beta s+\omega^2)\cdot\varepsilon(s)=g\omega^2\cdot\eta(s) \tag{5.6}$$

$$(s^2+\beta_f s+\omega_f{}^2)\cdot\eta(s)=\omega_f{}^2\cdot\varepsilon(s) \tag{5.7}$$

So we can get

$$\frac{\varepsilon(s)}{\eta(s)}=\frac{g\omega^2}{s^2+\beta s+\omega^2}=\frac{s^2+\beta_f s+\omega_f{}^2}{\omega_f{}^2} \tag{5.8}$$

The closed loop characteristic equation for (1) and (2) is

$$(s^2 + \beta s + \omega^2) \cdot (s^2 + \beta_f s + \omega_f{}^2) - g\omega^2\omega_f{}^2 = 0 \quad (5.9)$$

Then we can achieve

$$s^4 + (\beta + \beta_f)\, s^3 + (\omega^2 + \omega_f{}^2 + \beta\, \beta_f)\, s^2 + (\beta_f\omega^2 + \beta\omega_f{}^2)\, s$$

$$+ (1 - g)\, \omega^2\omega_f{}^2 = 0 \quad (5.10)$$

A sufficient and necessary condition for stability is that all the principal minors of the corresponding Routh - Hurwitz array be greater than zero. The principal minors of (7) can be easily show to be

s^4:	1	$\omega^2 + \omega_f{}^2 + \beta\, \beta_f$	$(1- g)\, \omega^2\omega_f{}^2$
s^3:	$\beta + \beta_f$	$\beta_f\omega^2 + \beta\omega_f{}^2$	0
s^2:	$\frac{(\beta+\beta_f)*(\omega^2+\omega_f{}^2+\beta\,\beta_f)-(\beta_f\omega^2+\beta\omega_f{}^2)}{\beta+\beta_f}$	$(1- g) * \omega^2 * \omega_f{}^2$	0
s^1:	$\frac{[\beta\omega^2+\beta_f\omega_f{}^2+\beta\beta_f(\beta+\beta_f)]*(\beta_f\omega^2+\beta\omega_f{}^2)-(\beta+\beta_f)^2*(1-g)*\omega^2*\omega_f{}^2}{\beta\omega^2+\beta_f\omega_f{}^2+\beta\beta_f(\beta+\beta_f)}$	0	
s^0:	$(1- g) * \omega^2 * \omega_f{}^2$		

$$M_1 = \beta + \beta_f \quad (5.11)$$

$$M_2 = \beta\omega^2 + \beta_f\omega_f{}^2 + \beta\beta_f(\beta + \beta_f) \quad (5.12)$$

$$M_3 = \beta\beta_f\left[\left(\omega^2 - \omega_f{}^2\right)^2 + \left(\beta + \beta_f\right)\left(\beta\omega_f{}^2 + \beta_f\omega^2\right)\right] + g(\beta + \beta_f)^2\omega^2\omega_f{}^2 \quad (5.13)$$

$$M_4 = (1- g) * \omega^2 * \omega_f{}^2 \quad (5.14)$$

Thus for positive g, $M_1, M_2, \& M_3$ are unconditionally positive. M_4 is positive iff $g < 1$, and the proof is complete.

5.3.2 Multivariate Case

Having understood the scalar system, the idea of position feedback can be easily generalized into the multivariate system. The equations governing position feedback (collocated actuators and sensors) control of a quasi-distributer parameter system with actuator dynamics are given by[1,133,124]

$$M\ \ddot{y} + D\ \dot{y} + K\,y = S^{T} C\,u \tag{5.15}$$

$$\ddot{u} + \beta_a\ \dot{u} + \omega_a^2(u - S\,y) = 0 \tag{5.16}$$

where $y \in \mathbb{R}^{N}$ is the system state vector and $u \in \mathbb{R}^{N_A}$ the actuator state vector. The $N_A x N_A$ gain matrix C is positive definite and can be factorized, using its square root $C^{1/2}$ as follows:

$$C^{T/2}\ C^{1/2} = C \tag{5.17}$$

The modal form of the system is obtained by applying the following transformation

$$y = \phi\xi \tag{5.18}$$

$$\eta = \frac{1}{\omega_a}\ C^{1/2}\ u \tag{5.19}$$

so that

$$\ddot{\xi} + D\dot{\xi} + \Omega\xi = \omega_a \phi^{T} S^{T} C^{T/2}\eta \tag{5.20}$$

$$\ddot{\eta} + \beta_a\dot{\eta} + \omega_a^2\eta = \omega_a C^{1/2} S\,\phi\xi \tag{5.21}$$

or

$$\begin{bmatrix}\ddot{\xi}\\ \ddot{\eta}\end{bmatrix} + \begin{bmatrix}D & 0\\ 0 & \beta_a I_{N_A}\end{bmatrix}\begin{bmatrix}\dot{\xi}\\ \dot{\eta}\end{bmatrix} + \begin{bmatrix}\Omega & -\omega_a \phi^{T} S^{T} C^{T/2}\\ -\omega_a C^{1/2} S & \omega_a^2 I_{N_A}\end{bmatrix}\begin{bmatrix}\xi\\ \eta\end{bmatrix} = 0 \tag{5.22}$$

Theorem 5.2

The combined system and actuator dynamics as represented by (5.19) are Liapunov asymptotic stable if

$\Omega - (1+ \varepsilon)$ B is positive definite (5.23)

where ε is some arbitrarily small positive quantity and B is the modal gain matrix given by

$B = \phi^T S^T C S \phi$ (5.24)

Theorem 5.3

For a second order multivariate dynamical system described by

$I\ddot{Z}+\mathcal{Q}\dot{Z}+\mathcal{P}Z = 0$ (5.25)

where Z, $\mathcal{Q}$, $\mathcal{P}$ are of appropriate dimension and $\mathcal{Q}$ is positive definite, a sufficient and necessary condition for Liapunov asymptotic stability is that

$\mathcal{P}$ is positive definite (5.26)

Theorem 5.4

The system in (5.19) is LAS iff the modiffied stiffenss matrix

$$P = \begin{bmatrix} \Omega & -\omega_a \phi^T S^T C^{T/2} \\ -\omega_a C^{1/2} S \phi & \omega_a^2 I_{N_A} \end{bmatrix} \text{ is positive definite} \quad (5.27)$$

Note that the sufficient condition for stability (5.20) is equivalent to

$K - (1 + \varepsilon)\ S^T C S$ is positive definite

5.3.3 Multivariate PPF Controller implemented with feed-through plant

Based on Chapter 4, addition of feed-through term to the truncated model is quite important, if the truncation is not to substantially alter open-loop zeros of the system. Although the truncation does not perturb open-loop poles of the system, it has the potential to significantly move the open-loop zeros, particularly when the actuators and sensors are collocated. Consequently, if a feedback controller is designed for the truncated model, and then implemented on the real system, the performance and stability of the closed loop system could be adversely affected [1].

Normally PPF techniques which we talked before do not allow for a feed-through term in the plant model. However, it is essential to include this in the design phase, if the implemented

controller is to perform in a satisfactory manner. Closed-loop performance of a controlled system is highly dependent on open-loop zeros of the plant. Inclusion of a feed-through term in the model ensures that closed-loop performance of the controller, once implemented, is in close agreement with theoretical predictions [3]. The derivation below are from [1,133,124].

If we are concerned with designing high-performance feedback controllers for multivariable resonant systems of the form

$$G(s)= \sum_{i=1}^{M} \frac{\psi_i \psi_i'}{s^2 + 2\xi_i \omega_i s + \omega_i^2} \tag{5.28}$$

where ψ_i is an mx1 vector, and $M \to \infty$. In practice, however, the integer is finite, but possibly a very large number which represents the number of modes that sufficiently describe the elastic properties of the structure under excitation

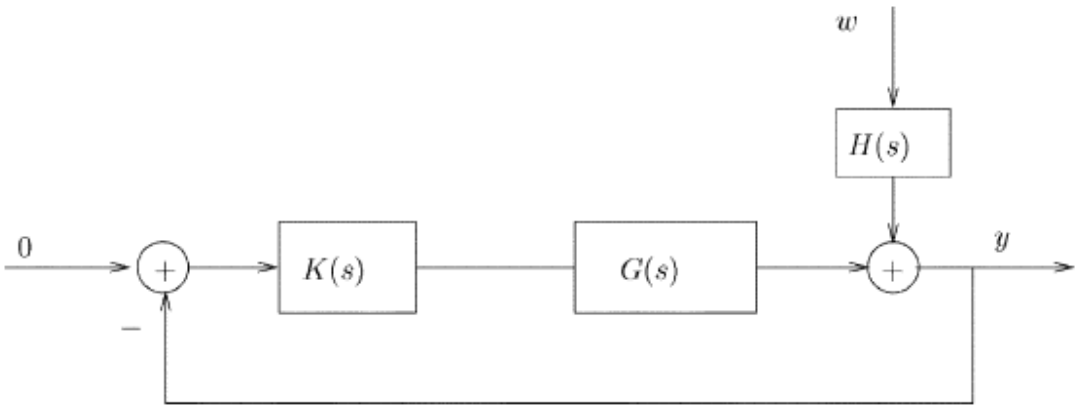

Figure 5.3 Feedback control system associated with a flexible structure with collocated actuator/sensor pairs, and subject to disturbance w

For a system of the form (5.41), a positive position feedback controller is defined as

$$K_{pp}(s) = \sum_{i=1}^{\tilde{N}} \frac{-\gamma_i \gamma_i'}{s^2 + 2\delta_i \tilde{\omega}_i s + \tilde{\omega}_i^2} \tag{5.29}$$

where $\gamma_i \in \mathbb{R}^{mx1}$ for i = 1, 2, ..., N.

where $\gamma_i \in R^{mx1}$ for i = 1, 2, ..., $\tilde{N}$

As illustrated in Fig. 5.3, due to the existence of the negative sign in all terms of (5.35), the overall system resembles a positive feedback loop. Also, the transfer function matrix (5.34) is

similar to that of the force to displacement transfer function matrix associated with a flexible structure, hence, the terminology positive position feedback.

An important property of PPF controllers is that to suppress one vibration mode requires only one second-order term, as articulated in (5.35). Consequently, one can choose the modes, within a specific bandwidth, that are to be controlled and construct the necessary controller.

To derive stability conditions for this control loop, the series in (5.36) is first truncated by keeping the first N modes($N < M$) that lie within the bandwidth of interest, and then incorporating the effect of truncated modes by adding a feed-through term to the truncated model. That is, to approximate (5.35) by

$$G^N(s) = \sum_{i=1}^{N} \frac{\psi_i \psi_i'}{s^2 + 2\xi_i \omega_i s + \omega_i^2} + D \qquad (5.30)$$

To derive stability of (5.43) under (5.42), the following theorem is needed.

Theorem 5.5: Consider the following second-order multivariable dynamical system:

$$\ddot{x}(t) + D\,\dot{x}(t) + K\,x(t) = 0 \qquad (5.31)$$

where $D, K \in R^{NxN}$ and $x \in R^{Nx1}$. Furthermore, assume that $D = D' > 0$. Then (5.37) is exponentially stable if and only if $K = K' > 0$. Proof same as **Theorem 5.3.**

The following theorem gives the necessary and sufficient conditions for closed-loop stability under positive position feedback. First, we need to make the following definitions:

$$Z = \begin{bmatrix} \xi_1 & & & \\ & \xi_2 & & \\ & & \ddots & \\ & & & \xi_N \end{bmatrix} \quad \Omega = \begin{bmatrix} \omega_1 & & & \\ & \omega_2 & & \\ & & \ddots & \\ & & & \omega_N \end{bmatrix}$$

$$\Psi = [\psi_1 \quad \psi_2 \quad \dots \quad \psi_N]$$

and

$$\Delta = \begin{bmatrix} \delta_1 & & & \\ & \delta_2 & & \\ & & \ddots & \\ & & & \delta_{\bar{N}} \end{bmatrix} \qquad \tilde{\Omega} = \begin{bmatrix} \tilde{\omega}_1 & & & \\ & \tilde{\omega}_2 & & \\ & & \ddots & \\ & & & \tilde{\omega}_{\bar{N}} \end{bmatrix}$$

$$\Gamma = [\gamma_1 \quad \gamma_2 \quad \dots \quad \gamma_{\bar{N}}]$$

Furthermore, we assume that

$$\Delta > 0 \tag{5.32}$$

Theorem 5.6: The negative feedback connection of (5.43) and (5.42) with (5.45) is exponentially stable if and only if

$$\widetilde{\Omega}^2 - \Gamma' D \Gamma > 0 \tag{5.33}$$

and

$$\Omega^2 - \Psi' \Gamma (\widetilde{\Omega}^2 - \Gamma' D \Gamma)^{-1} \Gamma' \Psi > 0 \tag{5.34}$$

5.4 Multi-mode SISO and MIMO PPF Controller Parameter Selection

5.4.1 MATLAB Optimization toolbox and GA Optimization Search

In order to find the minimum value of H_∞ norm, we need to use MATLAB Optimization Toolbox, which provides widely used algorithms for standard and large-scale optimization. These algorithms solve constrained and unconstrained continuous and discrete problems. The toolbox includes functions for linear programming, quadratic programming, binary integer programming, nonlinear optimization, nonlinear least squares, systems of nonlinear equations, and multi-objective optimization. We can use them to find optimal solutions, perform tradeoff analyses, balance multiple design alternatives, and incorporate optimization methods into algorithms and models [140].

Key Features[140]:

i. Interactive tools for defining and solving optimization problems and monitoring solution progress
ii. Solvers for nonlinear and multi-objective optimization
iii. Solvers for nonlinear least squares, data fitting, and nonlinear equations
iv. Methods for solving quadratic and linear programming problems
v. Methods for solving binary integer programming problems

In the toolbox, it contains several functions, such as GlobalSearch, MultiStart, Genetic Algorithm, Direct Search, Simulated Annealing. For Genetic Algorithm, it is a method for

solving both constrained and unconstrained optimization problems that is based on natural selection, the process that drives biological evolution. The genetic algorithm repeatedly modifies a population of individual solutions. At each step, the genetic algorithm selects individuals at random from the current population to be parents and uses them to produce the children for the next generation. Over successive generations, the population "evolves" toward an optimal solution. Genetic algorithm can be applied to solve a variety of optimization problems that are not well suited for standard optimization algorithms, including problems in which the objective function is discontinuous, nondifferentiable, stochastic, or highly nonlinear. The genetic algorithm can address problems of mixed integer programming, where some components are restricted to be integer-valued [140].

The genetic algorithm uses three main types of rules at each step to create the next generation from the current population [140]:

i. Selection rules select the individuals, called parents, that contribute to the population at the next generation.
ii. Crossover rules combine two parents to form children for the next generation.
iii. Mutation rules apply random changes to individual parents to form children

The genetic algorithm differs from a classical, derivative-based, optimization algorithm in two main ways in the following table 5.1 [140]:

Classical Algorithm	Genetic Algorithm
Generates a single point at each iteration. The sequence of points approaches an optimal solution.	Generates a population of points at each iteration. The best point in the population approaches an optimal solution.
Selects the next point in the sequence by a deterministic computation.	Selects the next population by computation which uses random number generators.

Table 5.1 classical algorithm and genetic algorithm comparison

Because the limited space, more details about Genetic Algorithm optimization toolbox please refer to MATLAB user guide.

5.4.2 Multi-mode SISO PPF Controller Optimal Parameter Selection

Based the dynamics model between shaker and plate, the results of multi-mode SISO PPF

controller optimal parameters are shown below.

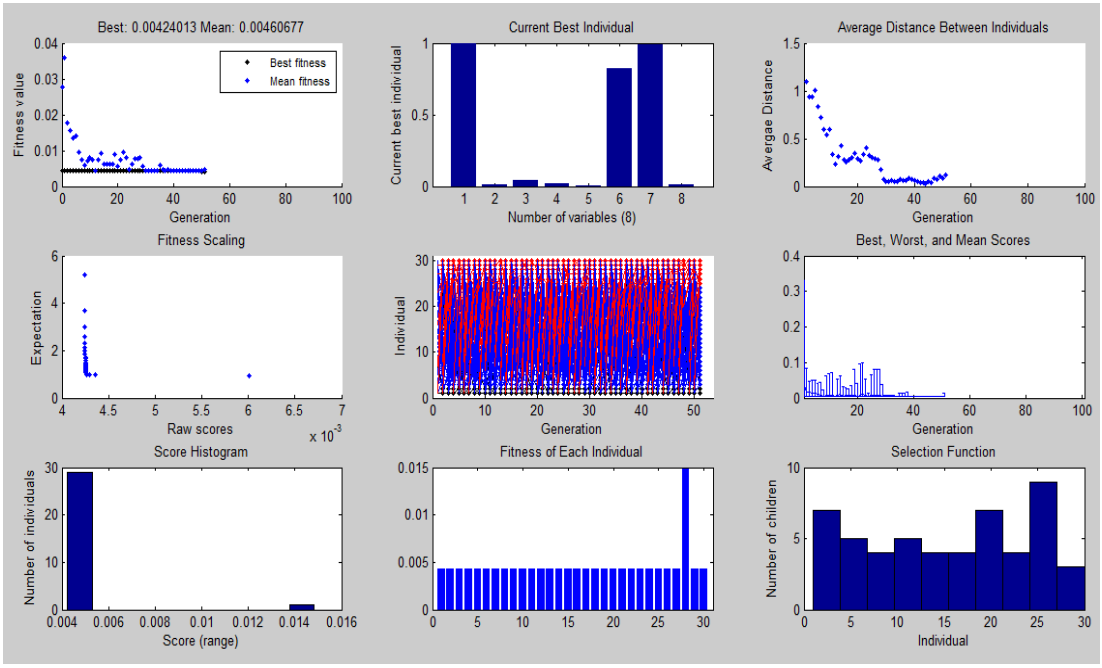

Figure 5.4 multi-mode SISO PPF controller K11 optimal parameter result through GA search

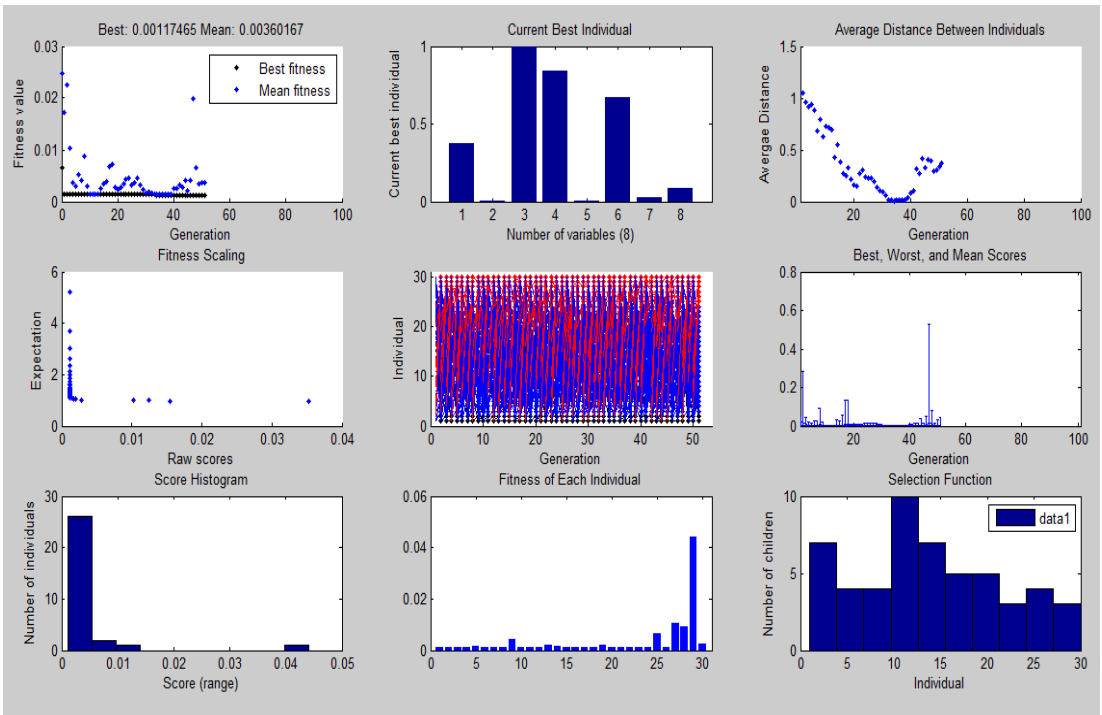

Figure 5.5 multi-mode SISO PPF controller K22 optimal parameter result through GA search

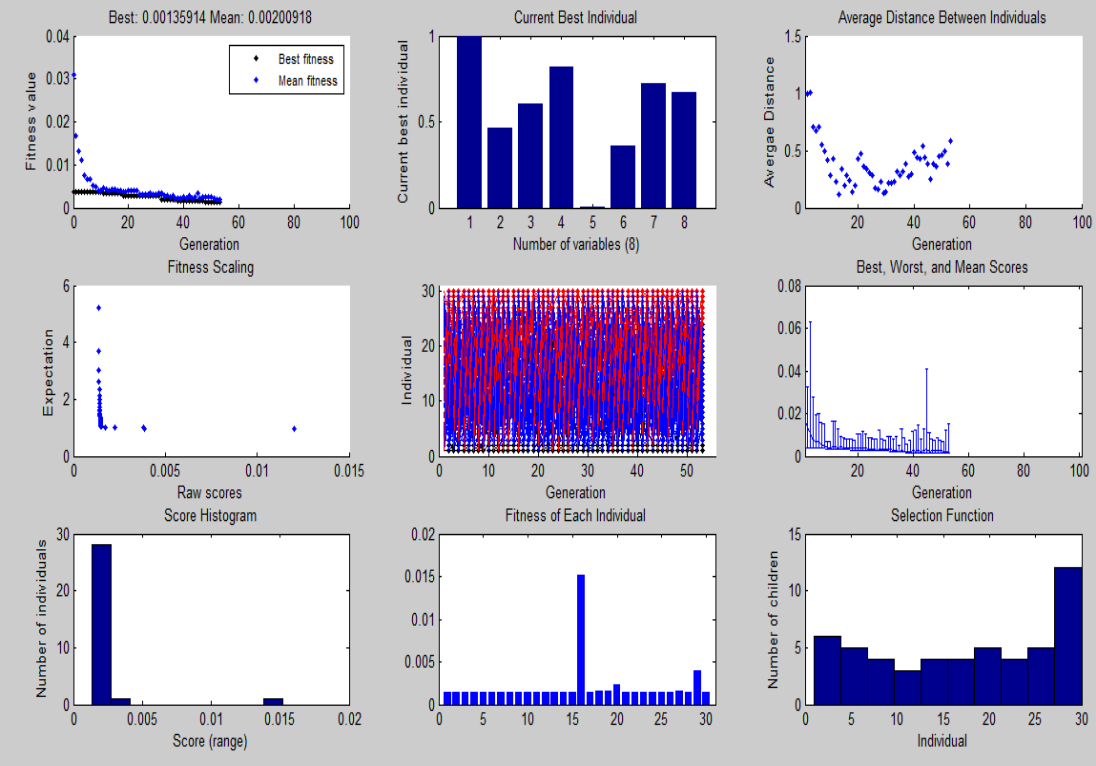

Figure 5.6 multi-mode SISO PPF controller K33 optimal parameter result through GA search

		Mode 1	Mode 2	Mode 3	Mode 4
Controller K11	control gain	g1=0.981	g2=0.033	g3=0.016	g4=0.099
	damping	zc1=0.029	zc2=0.953	zc3=0.807	zc4=0.987
Controller K22	control gain	g5=0.997	g6=0.979	g7=0.915	g8=0.962
	damping	zc5=0.005	zc6=0.004	zc7=0.441	zc8=0.72
Controller K33	control gain	g9=0.993	g10=0.462	g11=0.6	g12=0.816
	damping	zc9=0.006	zc10=0.356	zc11=0.724	zc12=0.673

Table 5.2 multi-mode SISO PPF controller optimal parameter result

5.4.3 Multi-mode MIMO PPF Controller Optimal Parameter Selection

Based the dynamics model between shaker and plate, the results of multi-mode MIMO PPF controller optimal parameters are shown below.

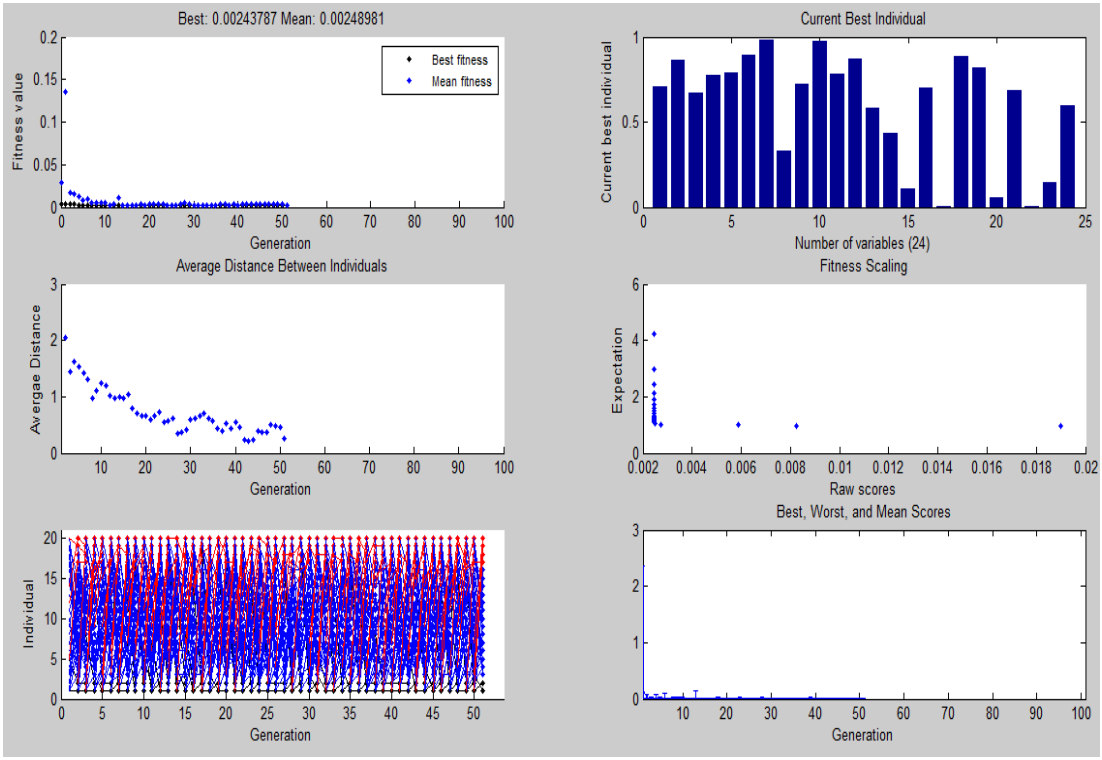

Figure 5.7 multi-mode MIMO Controller optimal parameter result through GA search

		Mode 1	Mode 2	Mode 3	Mode 4
Controller 1	control gain	g1=0.709	g2=0.861	g3=0.674	g4=0.776
	damping	zc1=0. 538	zc2=0. 437	zc3=0. 11	zc4=0.703
Controller 2	control gain	g5=0.791	g6=0.892	g7=0.981	g8=0.327
	damping	zc5=0.004	zc6=0.888	zc7=0.818	zc8=0.053
Controller 3	control	g9=0.722	g10=0.974	g11=0.778	g12=0.872

	gain				
	damping	zc9=0.683	zc10=0.005	zc11=0.146	zc12=0.596

Table 5.3 multi-mode MIMO PPF controller optimal parameter result

5.5 Summary

In this chapter, we reported the structure of PPF controller, derived the stability of scalar case, multivariate case controller and multivariate case controller with feed-through plant. We gave the selection method of parameters of controller. According to MATLAB simulation, we get the final results of controller parameters which can be used in the next chapter.

Chapter 6

Simulation

In the following simulation studies, the resonant multi-mode SISO and MIMO PPF controller are applied to control the plate vibration when applying a disturbance sine wave signal at shaker.

Based the method in Chapter 2, 3 and 4, we can easily derive the dynamics correction model from shaker to transducer.

The objectives of the simulation study of the PPF control method are to demonstrate that:

1. PPF control is able to attenuate multi-mode vibration using only a single sensor-actuator pair(explained before in this experiment test, sensor and actuator is the same one).

2. PPF control has an independent characteristic, in the sense that the controller is able to control a particular mode without destabilising other modes.

6.1 Multi-mode Three SISO PPF Controller Simulation

Three SISO PPF controller are used to control the first four vibration modes of simulation plate structure model using MATLAB. Firstly, simulation plate structure model and three SISO PPF controller are connected as feedback closed-loop system. Secondly, dynamics correction model from shaker to transducer is connected to feedback closed-loop system as in Fig2.21. Thirdly, the parameters of the controller are chosen as Tab 5.2. Fourthly, sinusoid signals which contain resonant frequencies of first four modes of simulation plate structure model are applied to the shaker. Fifthly, Open-loop dynamics which is between shaker to plate without controller is compared to closed-loop dynamics which is between shaker to plate with controller. Time domain and frequency domain cases are designed to test the ability of three

SISO PPF controller to attenuate multi-mode vibration when the controller centre frequencies match the resonant frequencies of the plate.

The simulation results show that the open-loop and closed-loop dynamics between shaker and plate.

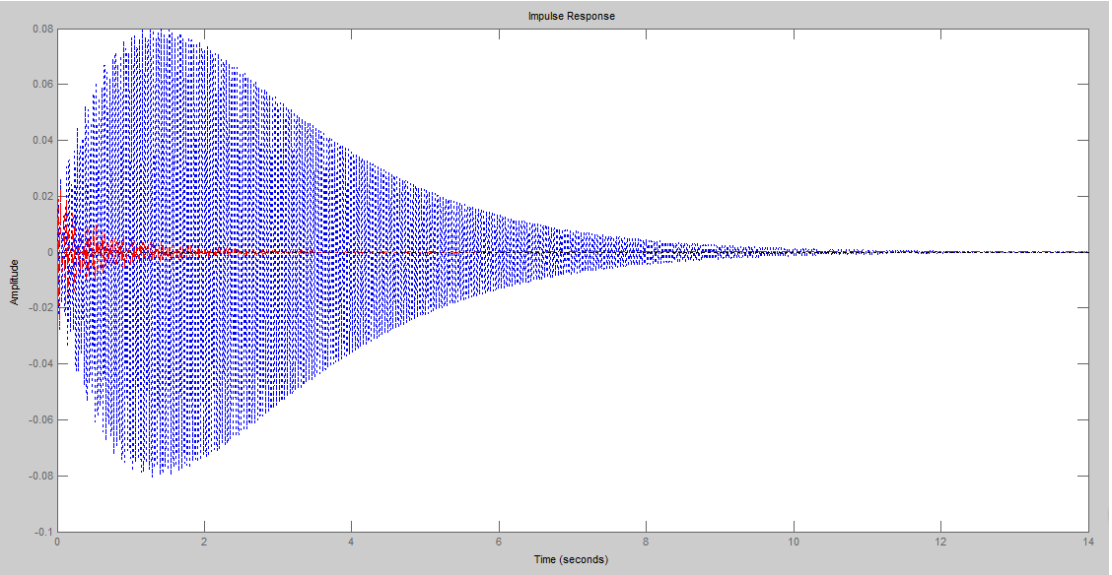

Figure 6.1 SISO vibration control at transducer 1 (K11) open-loop and closed-loop impulse signal simulation result

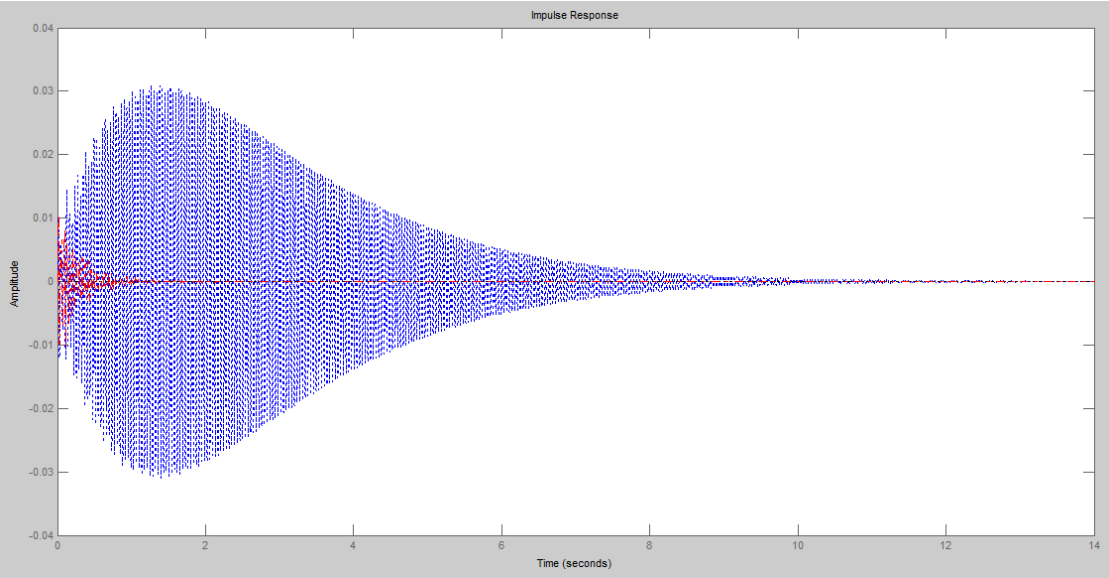

Figure 6.2 SISO vibration control at transducer 2 (K22) open-loop and closed-loop impulse signal simulation result

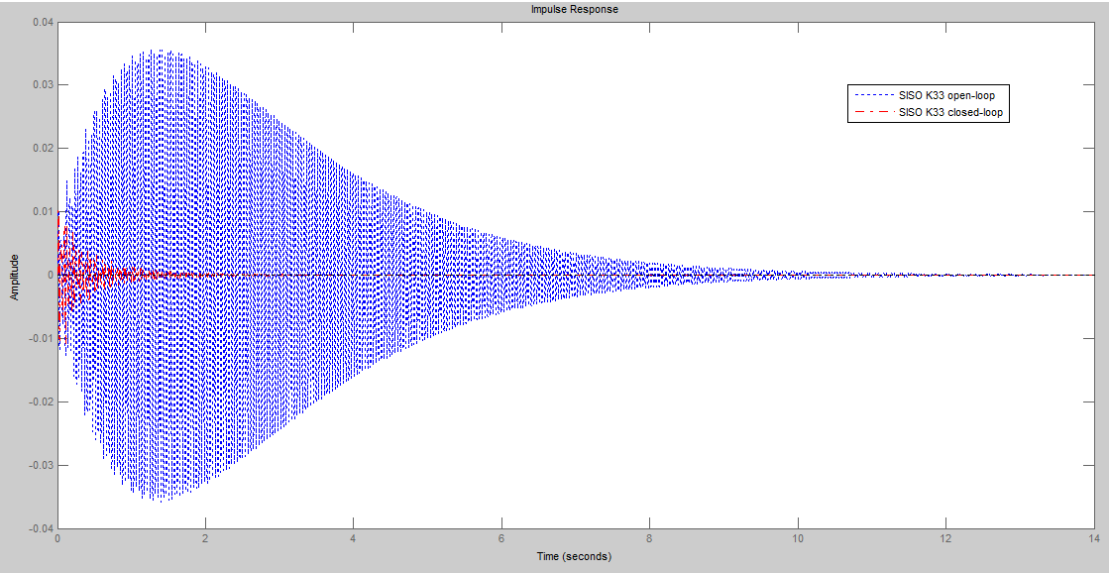

Figure 6.3 SISO vibration control at transducer 3 (K33)open-loop and closed-loop impulse signal simulation result

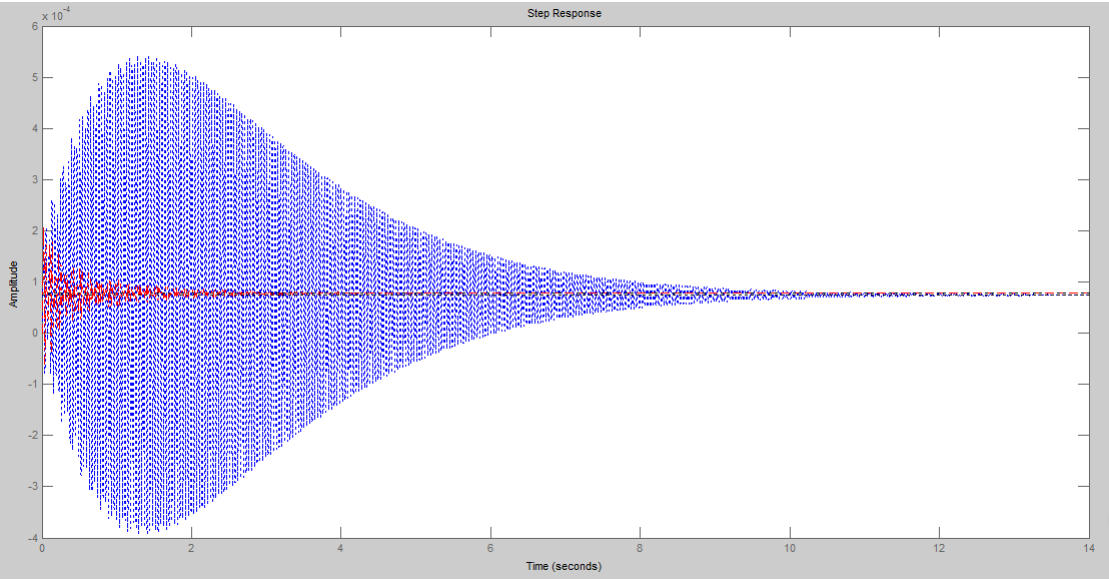

Figure 6.4 SISO vibration control at transducer 1 (K11) open-loop and closed-loop step signal simulation result

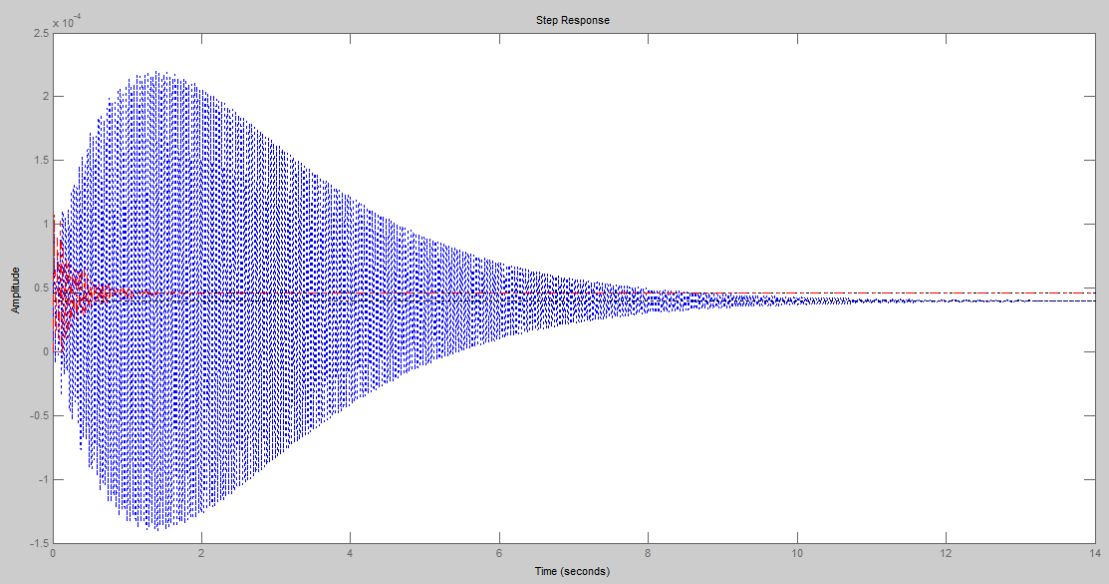

Figure 6.5 SISO vibration control at transducer 2 (K22) open-loop and closed-loop step signal simulation result

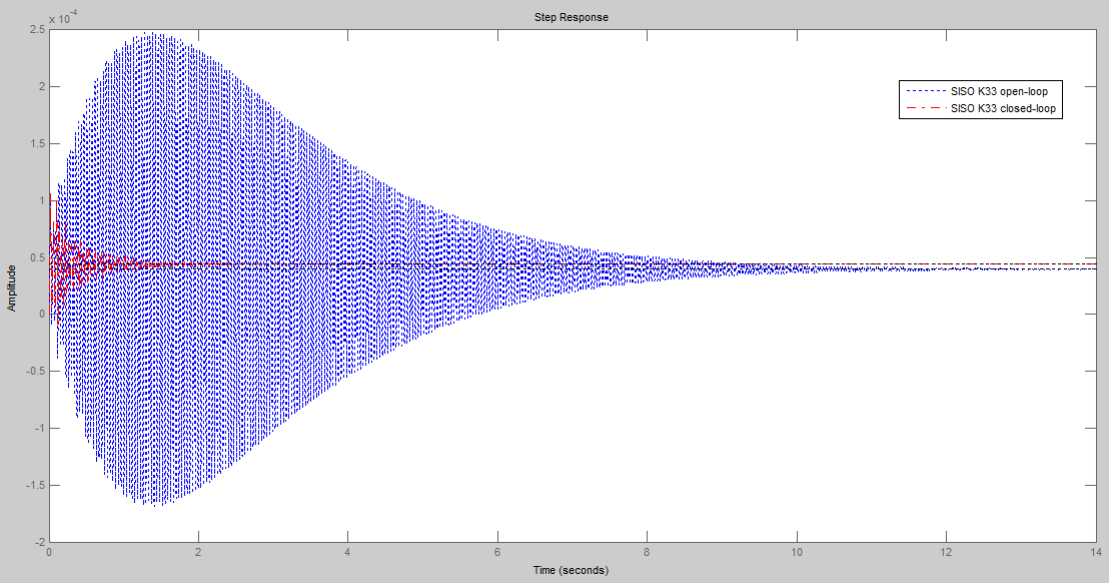

Figure 6.6 SISO vibration control at transducer 3 (K33) open-loop and closed-loop step signal simulation result

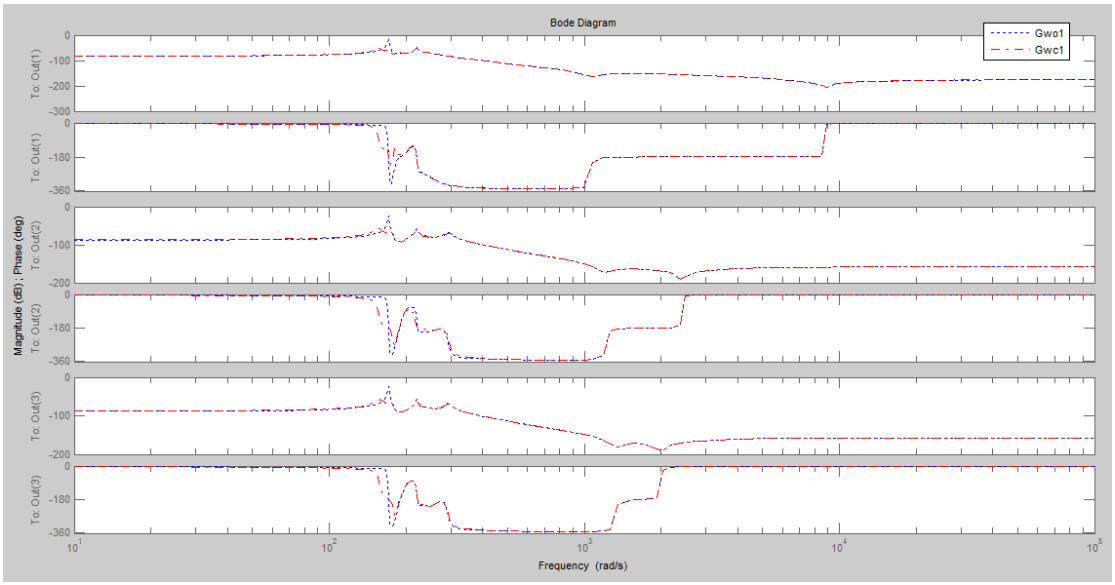

Figure 6.7 three SISO controller open-loop and closed-loop simulation result

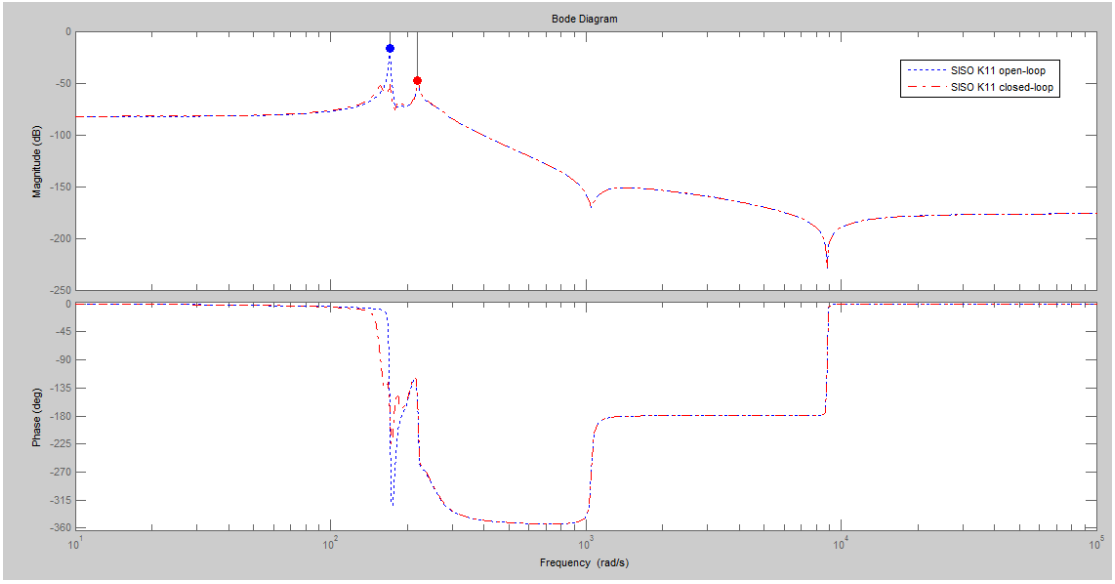

Figure 6.8 SISO vibration control at transducer 1 (K11) open-loop and closed-loop simulation result (1)

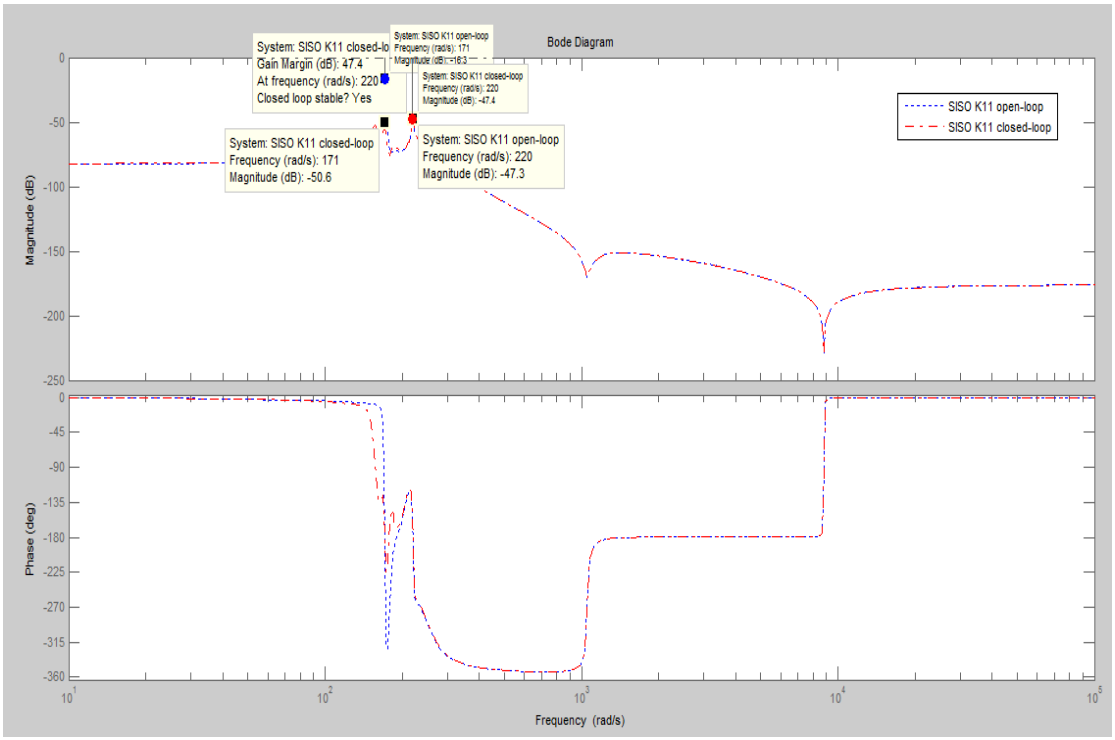

Figure 6.9 SISO vibration control at transducer 1(K11) open-loop and closed-loop simulation result (2)

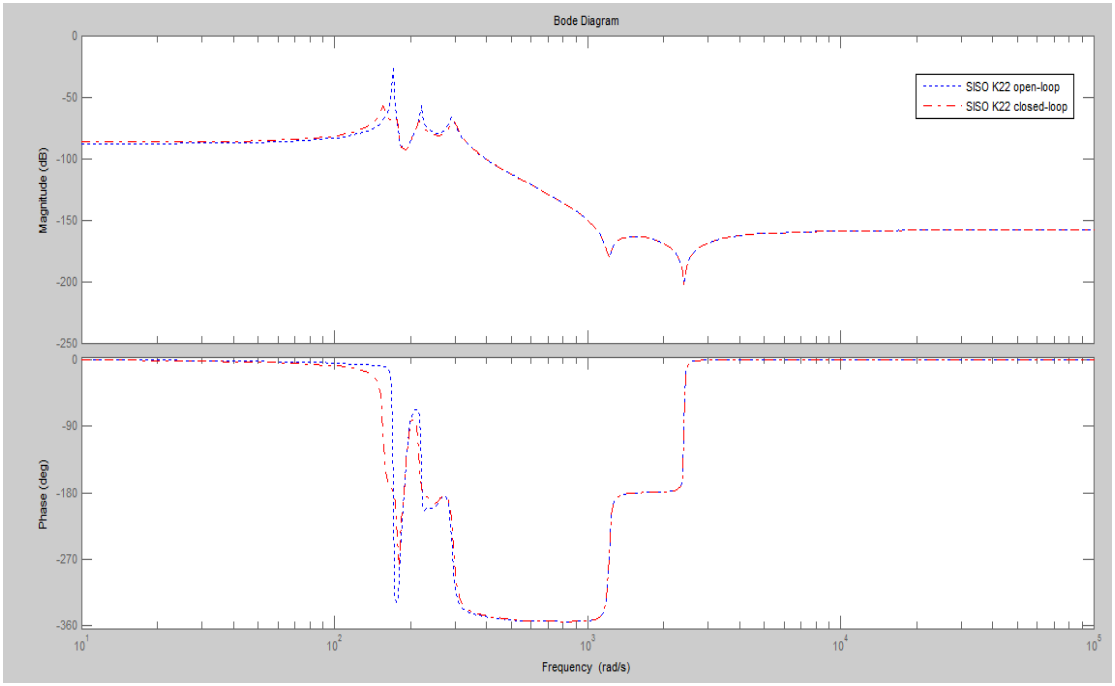

Figure 6.10 SISO vibration control at transducer 2 (K22) open-loop and closed-loop simulation result (1)

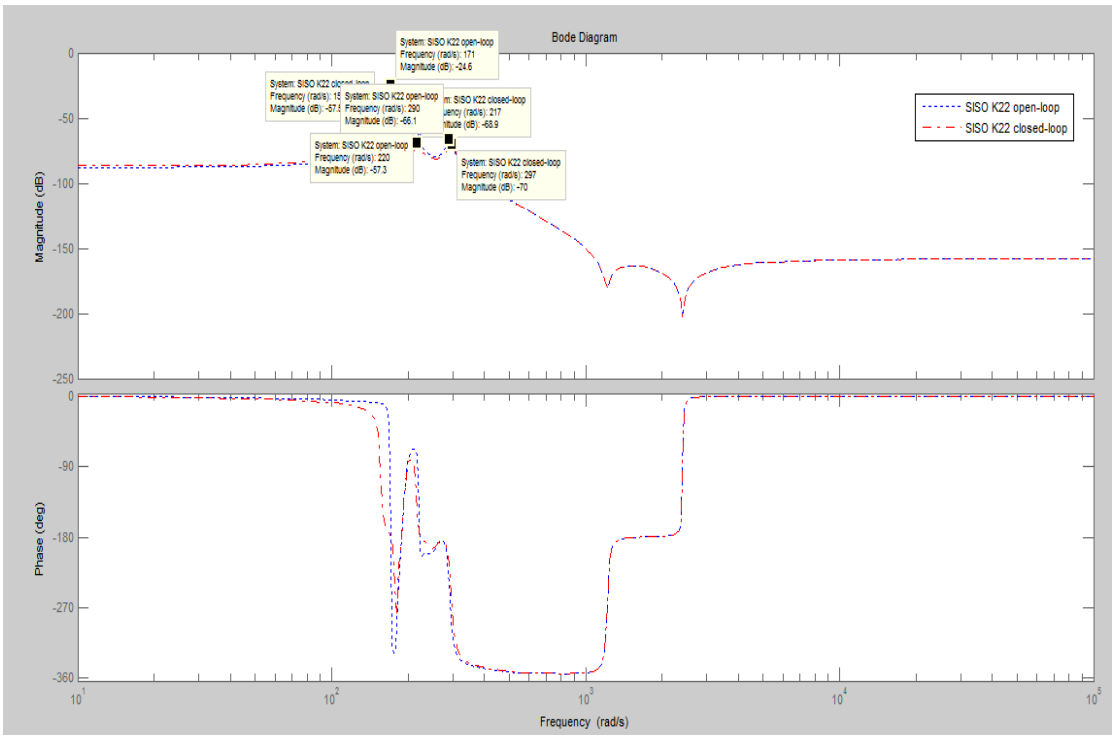

Figure 6.11 SISO vibration control at transducer 2 (K22) open-loop and closed-loop simulation result (2)

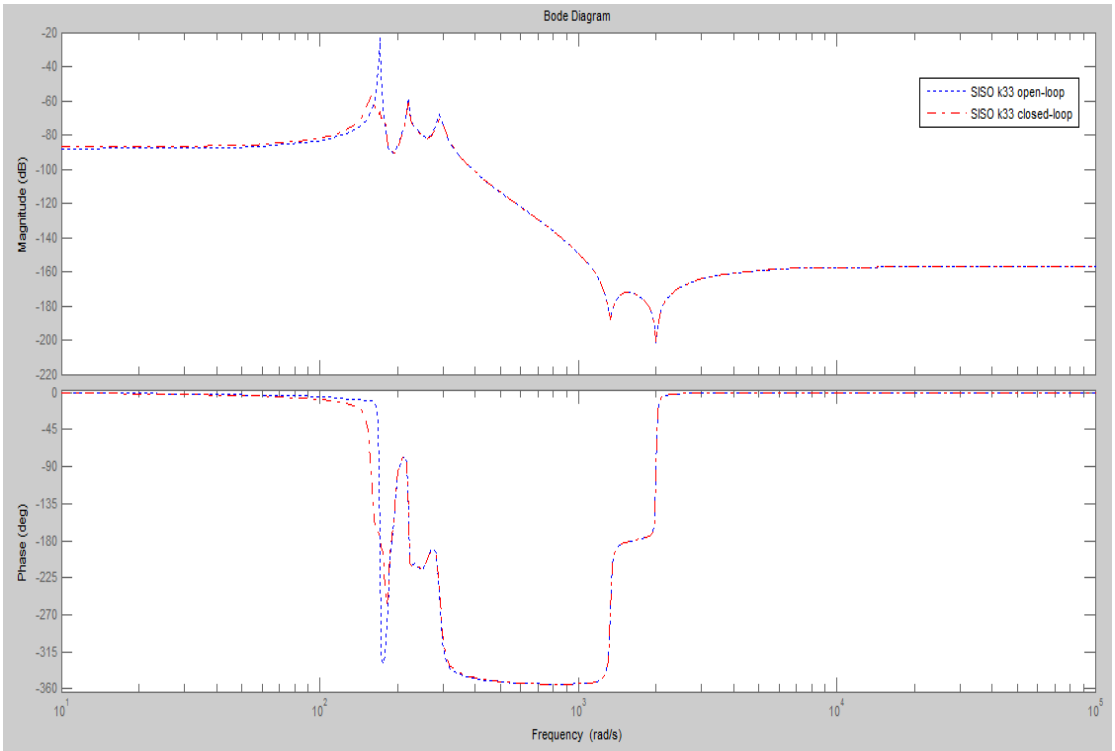

Figure 6.12 SISO vibration control at transducer 3 (K33) open-loop and closed-loop simulation result (1)

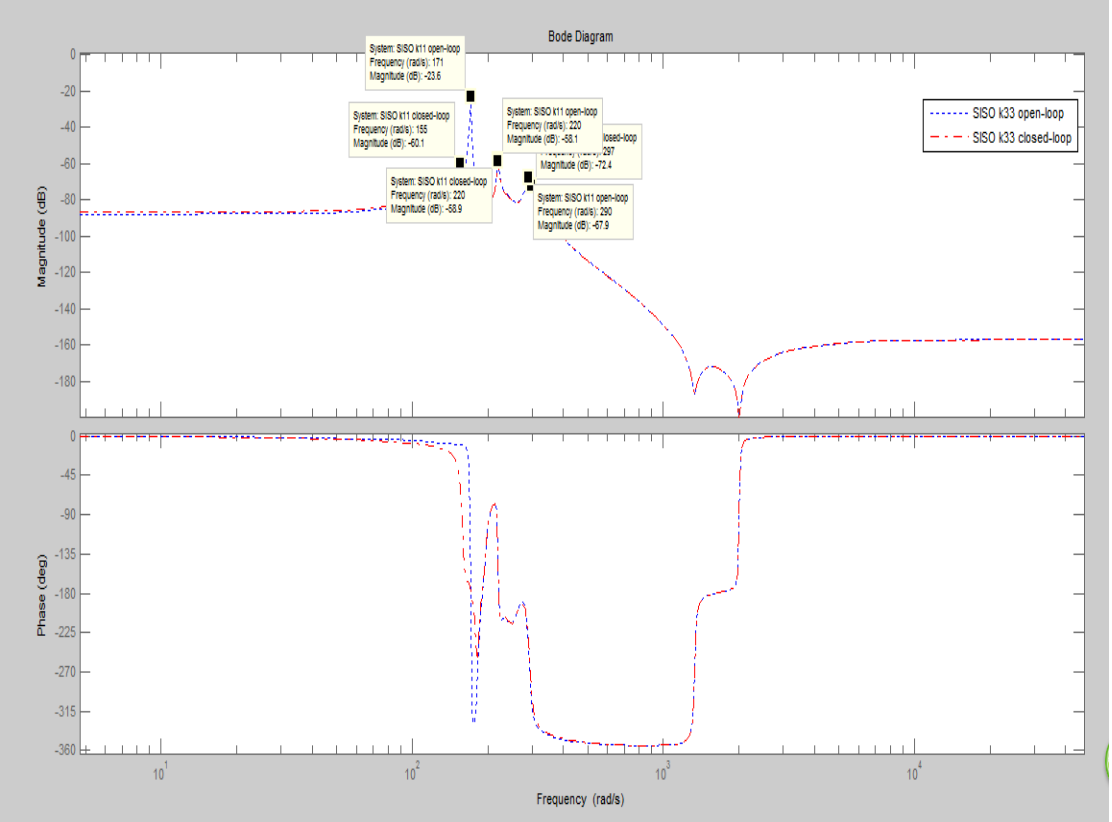

Figure 6.13 SISO vibration control at transducer 3 (K33) open-loop and closed-loop simulation result (2)

	Mode 1					
		ω (rad/s)	Peak (dB)	Attenuation (dB)	Gain Margin(dB)	Close-loop Stability
transducer 1	Open-loop	171 (27.1Hz)	-16.3	34.3	16.4	stable
	Close-loop	171 (24.5Hz)	-50.6			

	Mode 2					
		ω (rad/s)	Peak (dB)	Attenuation (dB)	Gain Margin(dB)	Close-loop Stability
	Open-loop	220 (35.01Hz)	-47.3	0.1		stable
	Close-loop	220 (35.01Hz)	-47.4		47.4	

Table 6.1 SISO PPF closed-loop frequency domain result at transducer 1

	Mode 1					
		ω (rad/s)	Peak (dB)	Attenuation (dB)	Mini Stability Margin(dB)	Close-loop Stability
transducer 2	Open-loop	171 (27.1Hz)	-24.6	32.9	24.6	stable
	Close-loop	156 (25.6Hz)	-57.5		68.7 (171Hz)	
	Mode 2					
		ω (rad/s)	Peak (dB)	Attenuation (dB)	Mini Stability Margin(dB)	Close-loop Stability

	Open-loop	220 (35.01Hz)	-57.3	11.6		stable
	Close-loop	217 (35.01Hz)	-68.9			
	Mode 4					
		ω (rad/s)	Peak (dB)	Attenuation (dB)	Mini Stability Margin(dB)	Close-loop Stability
	Open-loop	290 (46.2Hz)	-66.1	3.9		stable
	Close-loop	297 (47.27Hz)	-70			

Table 6.2 SISO PPF closed-loop frequency domain result at transducer 2

transducer 3	Mode 1					
		ω (rad/s)	Peak (dB)	Attenuation (dB)	Mini Stability Margin(dB)	Close-loop Stability
	Open-loop	171 (27.1Hz)	-23.6	36.5	23.3	stable
	Close-loop	155 (24.67Hz)	-60.1			

	Mode 2					
		ω (rad/s)	Peak (dB)	Attenuation (dB)	Mini Stability Margin(dB)	Stability
	Open-loop	220 (35.01Hz)	-58.1	0.8		stable
	Close-loop	220 (35.01Hz)	-58.9		60.6	
	Mode 4					
		ω (rad/s)	Peak (dB)	Attenuation (dB)	Mini Stability Margin(dB)	Stability
	Open-loop	290 (46.2Hz)	-67.9	4.5		stable
	Close-loop	297 (47.27Hz)	-72.4			

Table 6.3 SISO PPF closed-loop frequency domain result at transducer 3

6.2 Multi-mode MIMO PPF Controller Simulation

MIMO PPF controller are used to control the first four vibration modes of simulation plate structure model using MATLAB. Firstly, simulation plate structure model and MIMO PPF controller are connected as feedback closed-loop system. Secondly, dynamics correction model from shaker to transducer is connected to feedback closed-loop system as in Fig2.21. Thirdly, the parameters of the controller are chosen as Tab 5.3. Fourthly, sinusoid signals which contain resonant frequencies of first four modes of simulation plate structure model are applied to the shaker. Fifthly, Open-loop dynamics which is between shaker to plate without controller is compared to closed-loop dynamics which is between shaker to plate with controller. Time domain and frequency domain cases are designed to test the ability of MIMO PPF controller to attenuate multi-mode vibration when the controller centre frequencies match the resonant frequencies of the plate.

The simulation results show that the open-loop and closed-loop dynamics between shaker and plate.

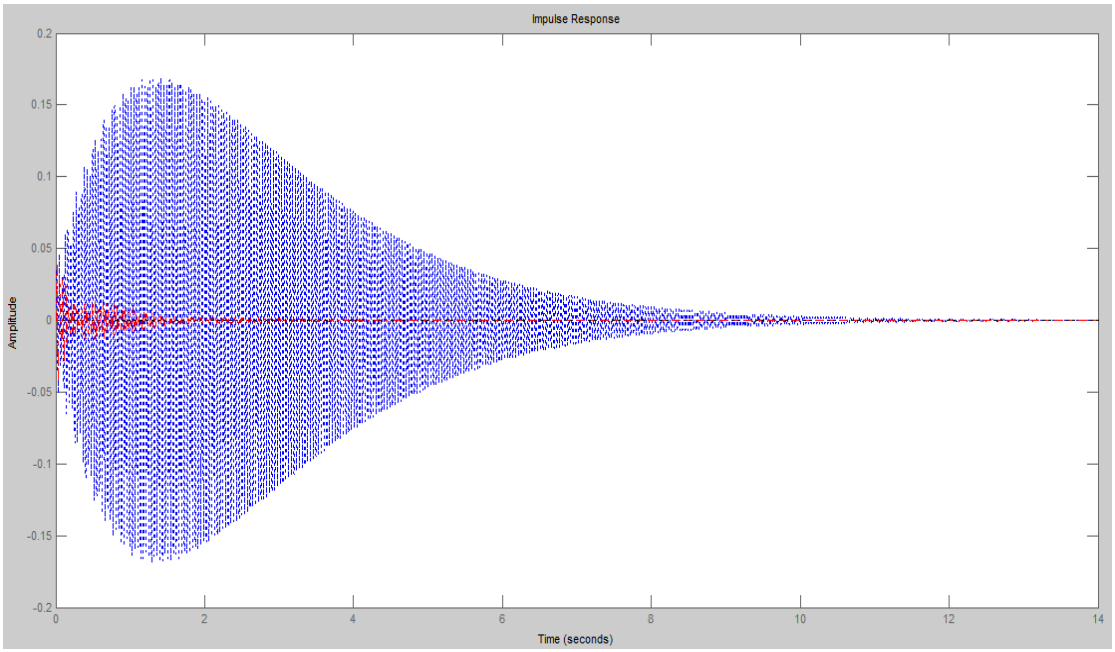

Figure 6.14 MIMO Controller open-loop and closed-loop (Gwo(1,1),Gwc(1,1)) impulse signal simulation result at transducer 1

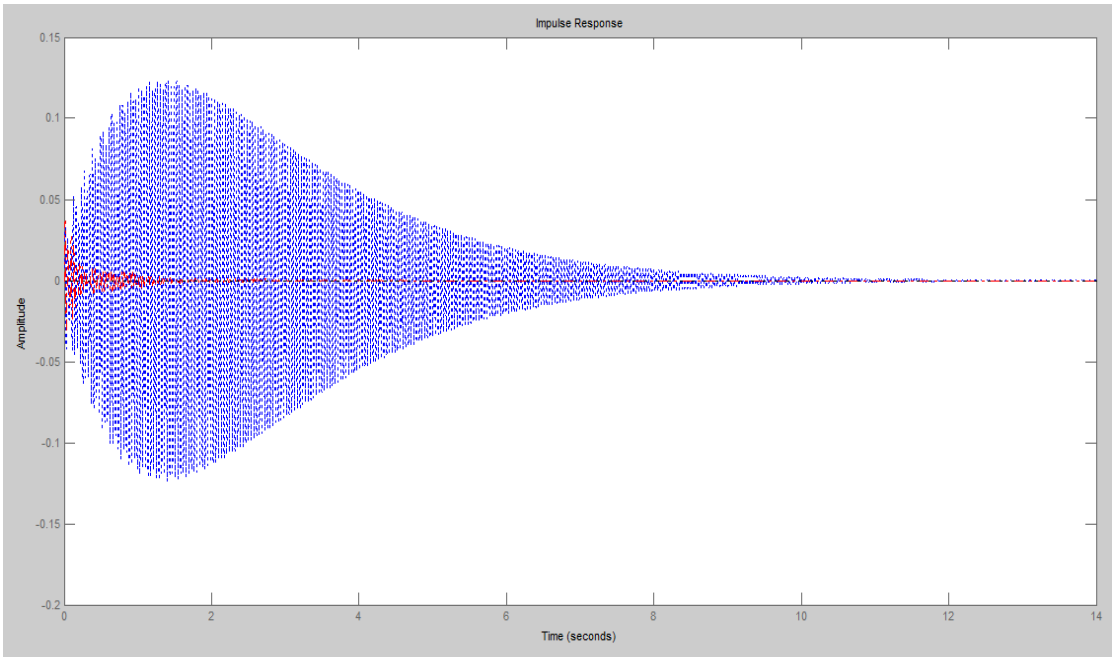

Figure 6.15 MIMO Controller open-loop and closed-loop (Gwo(2,1), Gwc(2,1)) impulse signal simulation result at transducer 2

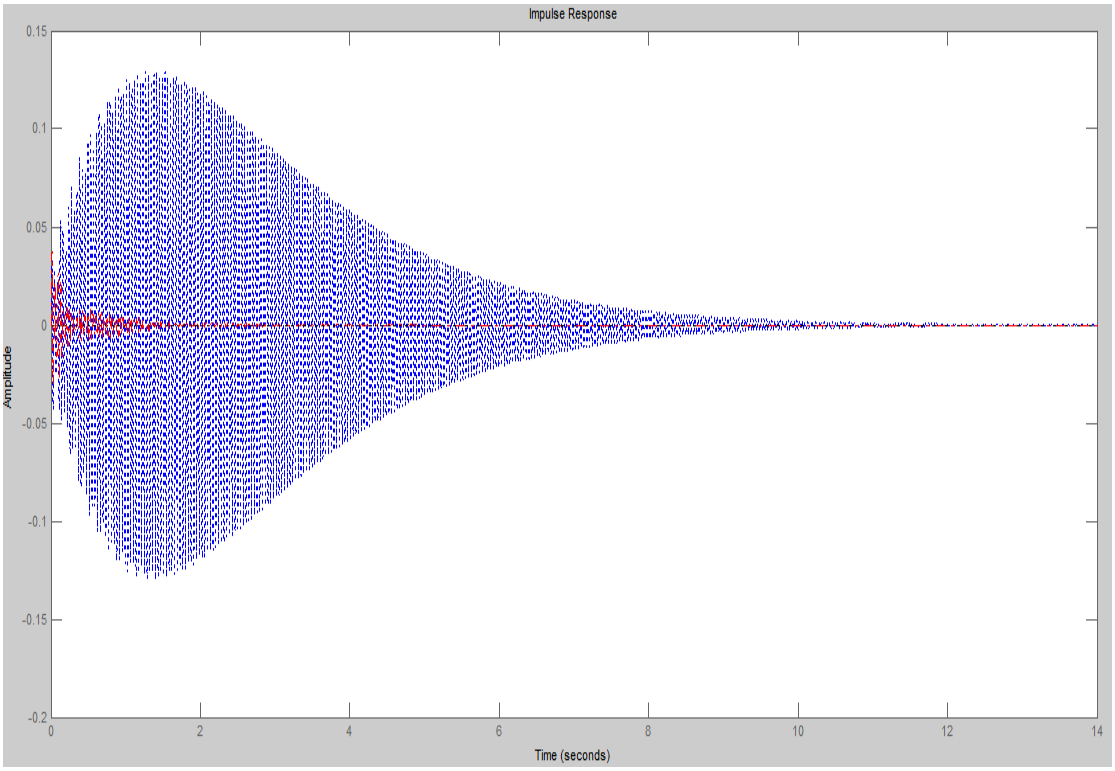

Figure 6.16 MIMO Controller open-loop and closed-loop (Gwo(3,1), Gwc(3,1)) impulse signal simulation result at transducer 3

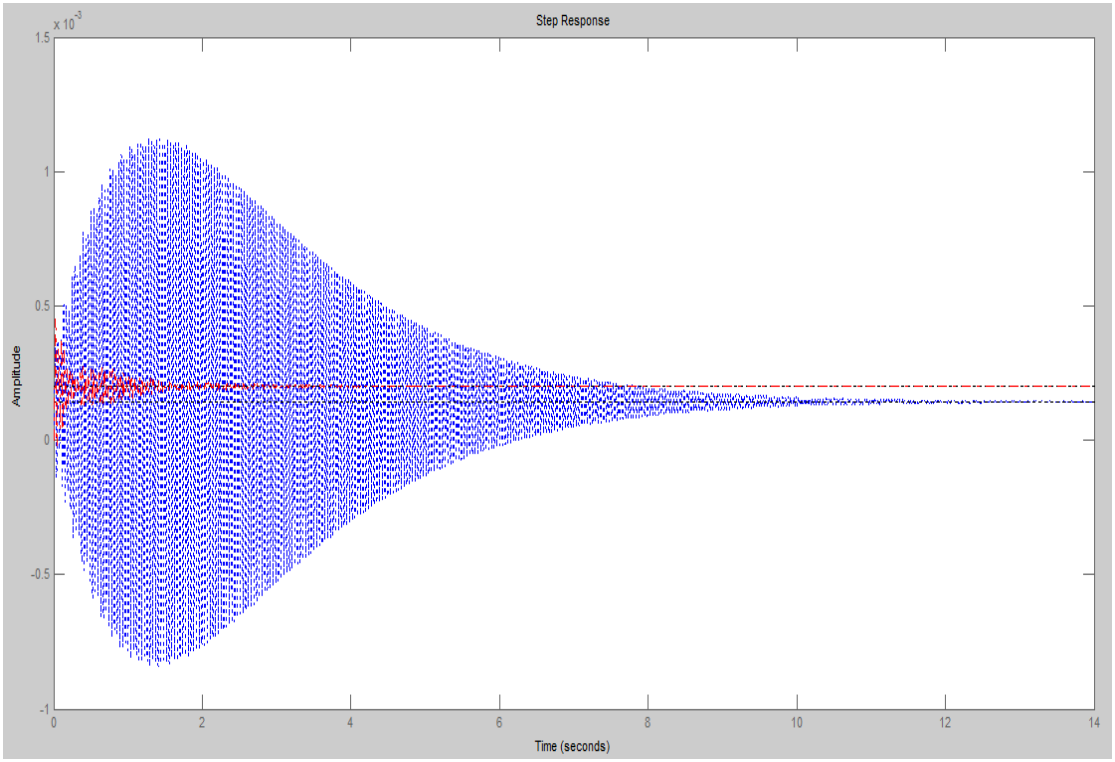

Figure 6.17 MIMO Controller open-loop and closed-loop (Gwo(1,1), Gwc(1,1)) step signal simulation result at transducer 1

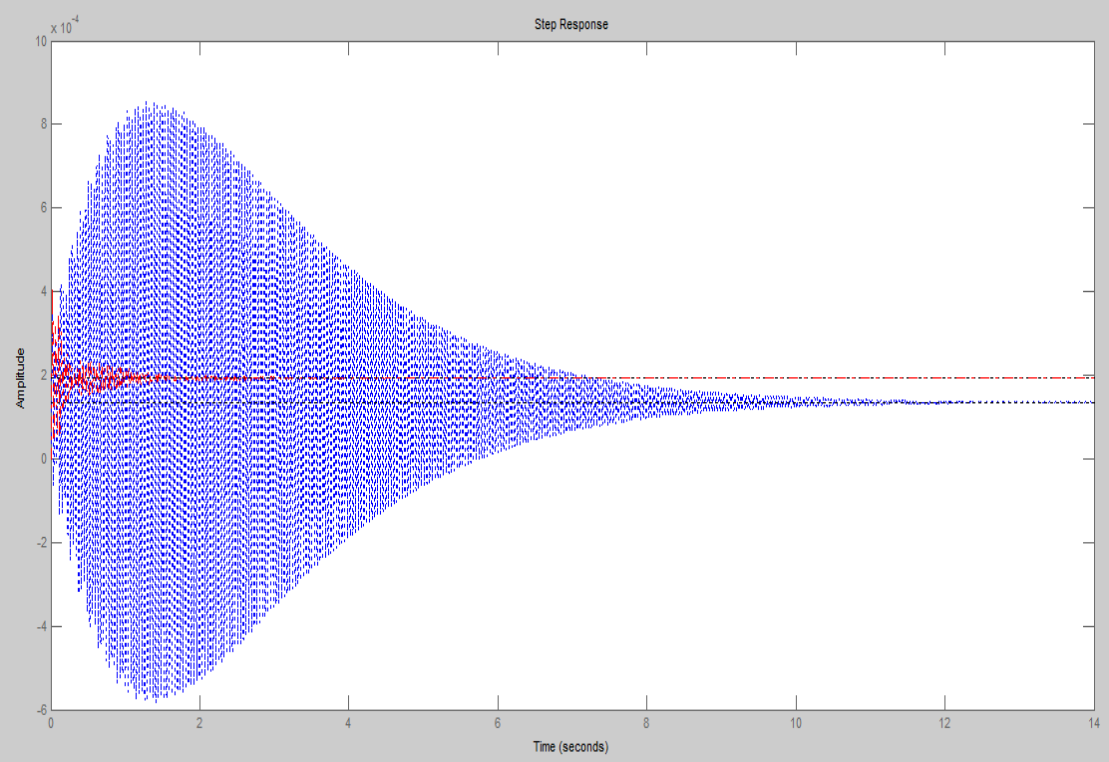

Figure 6.18 MIMO Controller open-loop and closed-loop (Gwo(2,1), Gwc(2,1)) step signal simulation result at transducer 2

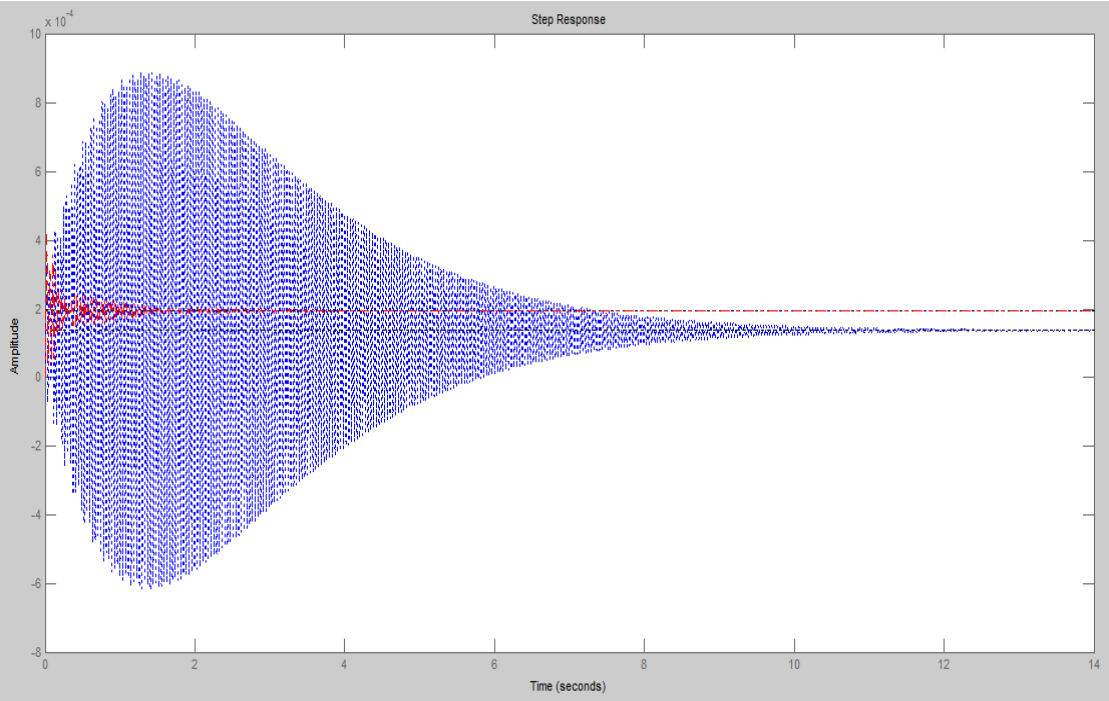

Figure 6.19 MIMO Controller open-loop and closed-loop (Gwo(3,1), Gwc(3,1)) step signal simulation result at transducer 3

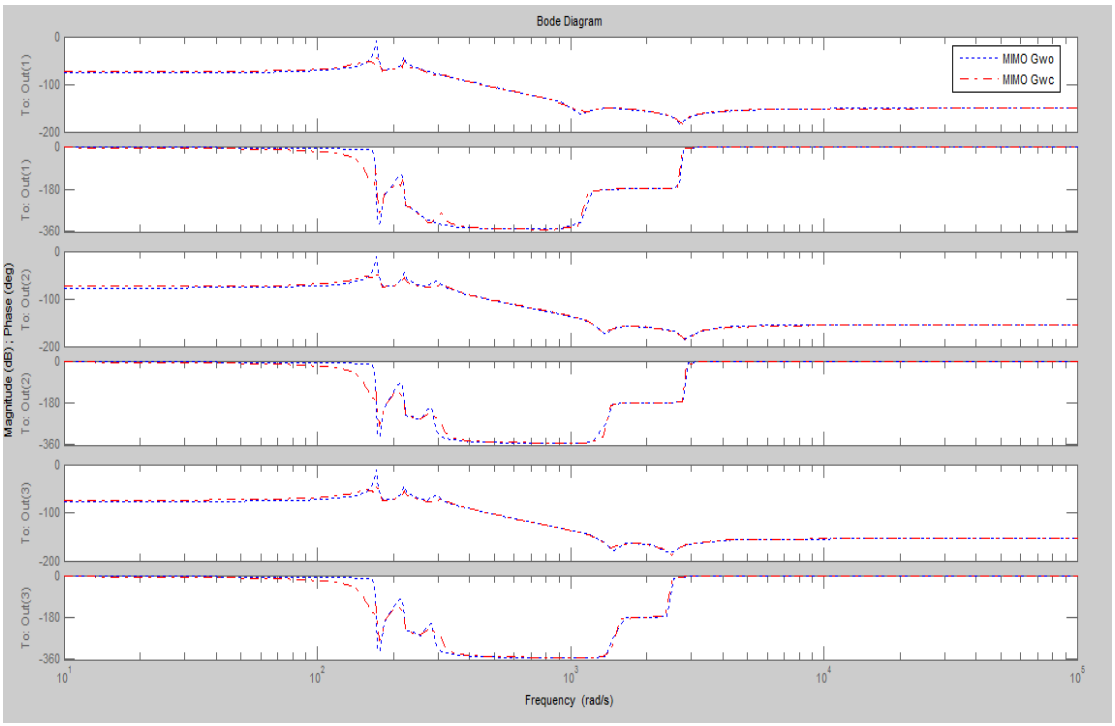

Figure 6.20 MIMO Controller open-loop and closed-loop simulation result

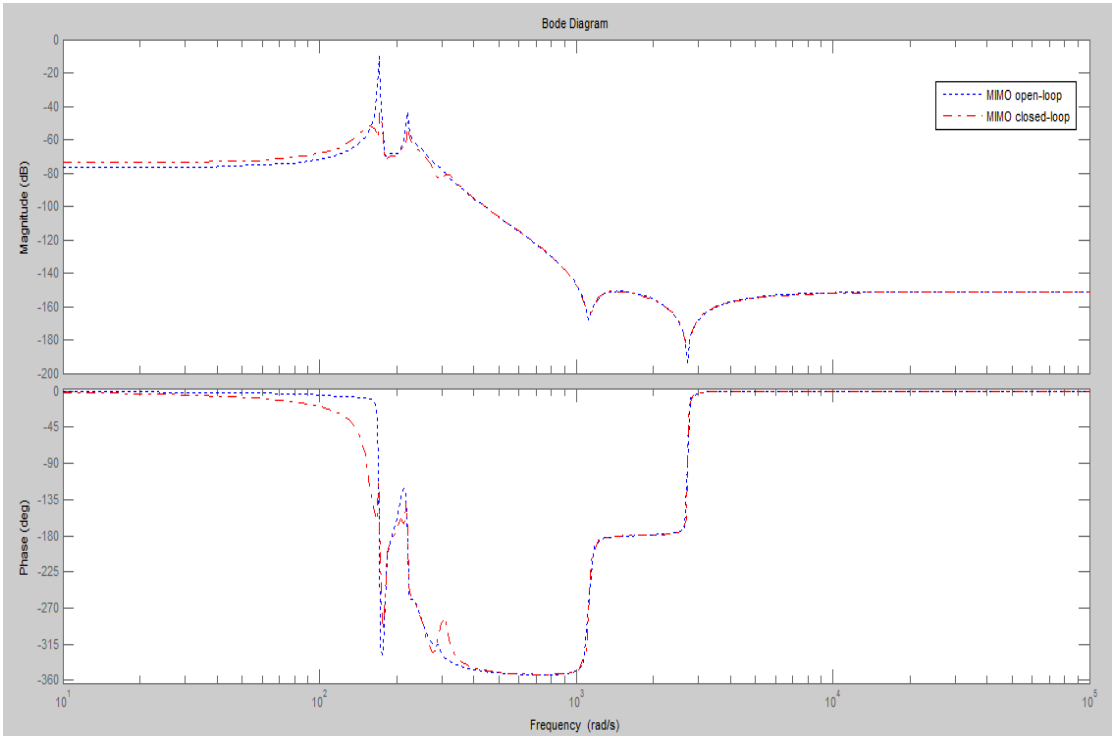

Figure 6.21 MIMO Controller open-loop and closed-loop (Gwo(1,1), Gwc(1,1))simulation result (1) at transducer 1

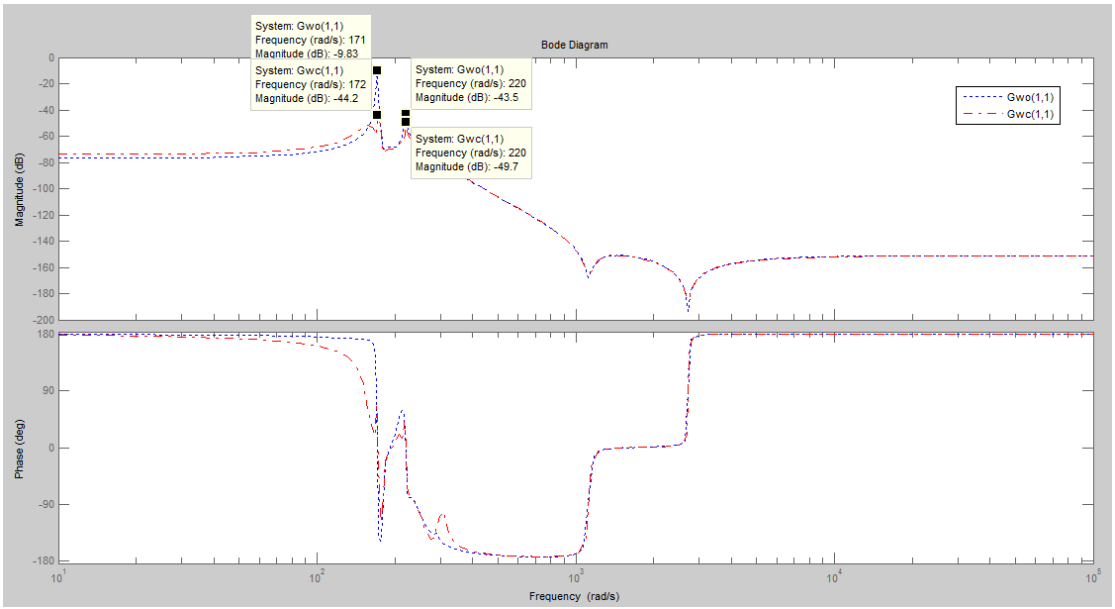

Figure 6.22 MIMO Controller open-loop and closed-loop (Gwo(1,1), Gwc(1,1))simulation result (2) at transducer 1

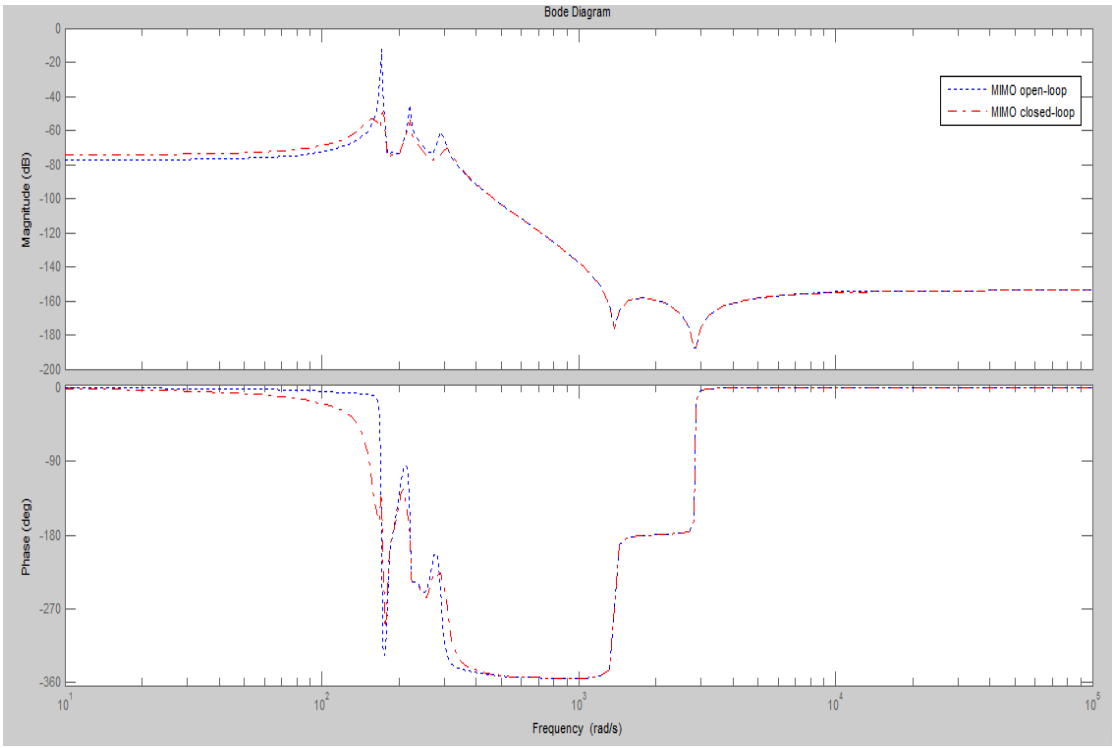

Figure 6.23 MIMO Controller open-loop and closed-loop (Gwo(2,1), Gwc(2,1))simulation result (1) at transducer 2

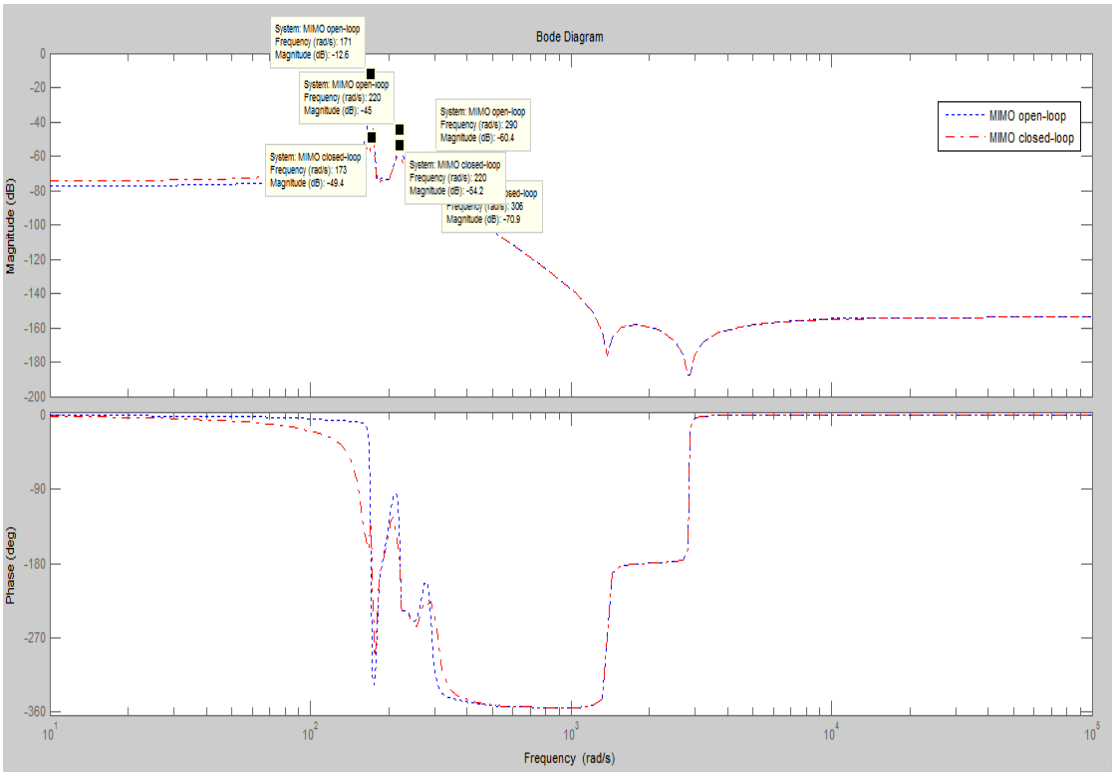

Figure 6.24 MIMO Controller open-loop and closed-loop (Gwo(2,1), Gwc(2,1))simulation result (2) at transducer 2

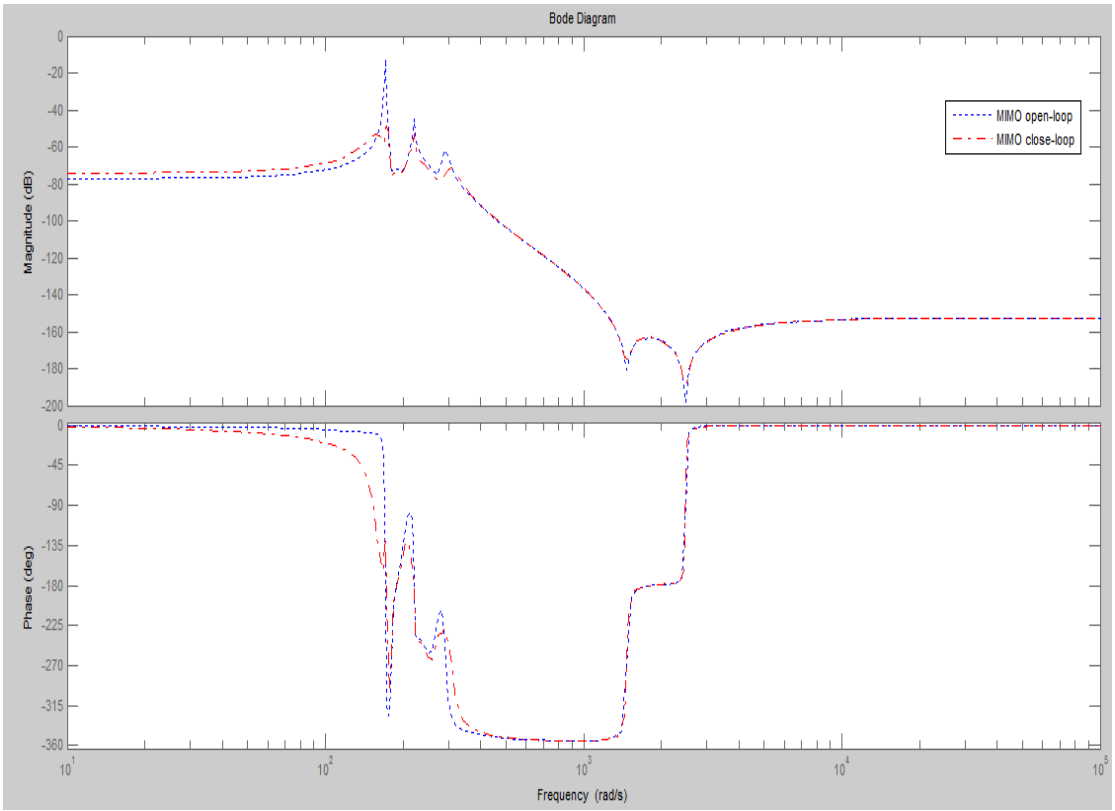

Figure 6.25 MIMO Controller open-loop and closed-loop (Gwo(3,1), Gwc(3,1))simulation result (1) at transducer 3

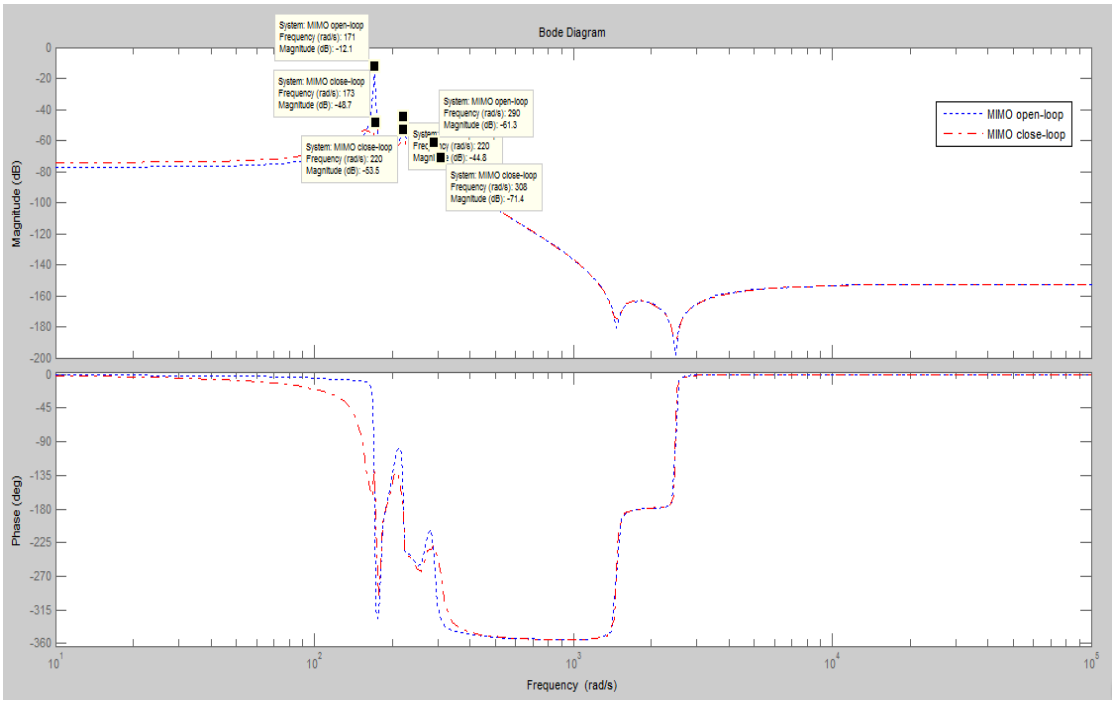

Figure 6.26 MIMO Controller open-loop and closed-loop (Gwo(3,1), Gwc(3,1))simulation result (2) at transducer 3

transducer 1	Mode 1					
		ω (rad/s)	Peak (dB)	Attenuation (dB)	Mini Stability Margin(dB)	Close-loop Stability
	Open-loop	171 (27.1Hz)	-9.83	34.37	9.86	stable
	Close-loop	172 (27.2Hz)	-44.2			
	Mode 2					
		ω (rad/s)	Peak	Attenuation	Mini Stability	Close-loop

			(dB)	(dB)	Margin(dB)	Stability
	Open-loop	220 (35.01Hz)	-43.5	5.8		stable
	Close-loop	220 (35.01Hz)	-49.7		44.7 (172 rad/s)	

Table 6.4 MIMO PPF closed-loop frequency domain result at transducer 1

transducer 2	Mode 1					
		ω (rad/s)	Peak (dB)	Attenuation (dB)	Mini Stability Margin(dB)	Close-loop Stability
	Open-loop	171 (27.1Hz)	-12.6	36.8	12.6	stable
	Close-loop	173 (27.3Hz)	-49.4		49 (172 rad/s)	
	Mode 2					
		ω (rad/s)	Peak (dB)	Attenuation (dB)	Mini Stability Margin(dB)	Close-loop Stability
	Open-loop	220 (35.01Hz)	-45	9.2		
	Close-loop	220	-54.2			

		(35.01Hz)				
	Mode 4					
		ω (rad/s)	Peak (dB)	Attenuation (dB)	Mini Stability Margin(dB)	Close-loop Stability
	Open-loop	290	-60.4	10.4		
	Close-loop	308	-70.8			

Table 6.5 MIMO PPF closed-loop frequency domain result at transducer 2

Transducer 3	Mode 1					
		ω (rad/s)	Peak (dB)	Attenuation (dB)	Mini Stability Margin(dB)	Close-loop Stability
	Open-loop	171 (27.1Hz)	-12.1	36.6	12.2	stable
	Close-loop	173 (27.3Hz)	-48.7		48.3 (172 rad/s)	
	Mode 2					
		ω (rad/s)	Peak (dB)	Attenuation (dB)	Mini Stability Margin(dB)	Close-loop Stability
	Open-	220	-44.8	8.7		

	loop	(35.01Hz)				
	Close-loop	220 (35.01Hz)	-53.5			
	Mode 4					
		ω (rad/s)	Peak (dB)	Attenuation (dB)	Mini Stability Margin(dB)	Close- loop Stability
	Open-loop	290 (46.2Hz)	-61.3	10.1		
	Close-loop	308 (49.02Hz)	-71.4			

Table 6.6 MIMO PPF closed-loop frequency domain result at transducer 3

6.3 Summary

As explained in Chapter 2, at transducer 1, the mode shape for mode 2 and mode 4 is too small, but at mode 2, the mode shape of shaker is very big, so only mode 1 and mode 2 can be seen in the dynamics between shake and transducer 1 in the figure after superposition. Similar at transducer 2 and 3, only mode 1, 2, 4 can be seen after superposition.

For multi-mode three SISO PPF controller, according to compare the open-loop and closed-loop dynamics between shaker and plate, the result can be seen through Figure 6.1-6.13 and Table 6.1-6.3 which three SISO PPF controller achieved. It is shown a good result at mode 1 for all of three controllers, but at mode 2 and mode 4 only a little bit attenuation.

For multi-mode MIMO PPF controller, according to compare the open-loop and

closed-loop dynamics between shaker and plate, the result can be seen through Figure 6.14-6.26 and Table 6.4-6.6 which MIMO PPF controller achieved. It is shown a better result at mode 1to mode 4 comparing with multi-mode three SISO PPF controller.

Chapter 7

Experiment

Experimental studies are used to verify the results of the simulation studies. The proposed PPF SISO and MIMO resonant controllers are implemented on a dSpace DS1103 data acquisition and control board using MATLAB, Simulink and Real-Time Workshop software.

7.1 Self-sensing

To measure the back-emf voltage without using any additional sensors, a technique called 'self-sensing' was used [126]. The transducer is then used for actuation and sensing at the same time, which means that actuation and sensing are performed collocated. Figure 7.1 shows an electrical model of an electromagnetic transducer in series with a measurement resistor R_m [139].

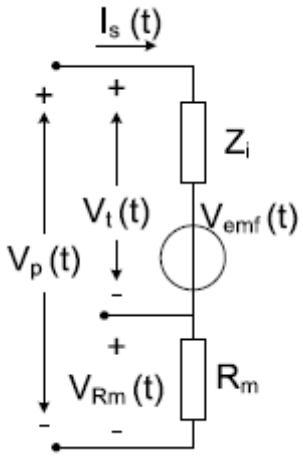

Figure 7.1 principle of the self-sensing technique used to measure the back-emf voltage V_{emf}

From this figure, it can be seen that:

$$V_t(t) = V_{Zi} + V_{emf} \quad (7.1)$$

V_{emf} is now easily found:

$$V_{emf}(t) = V_t(t) - V_{Zi} = V_t(t) - Z_i \cdot I_s(t) = V_t(t) - Z_i \cdot \frac{V_{R_m}(t)}{R_m} \quad (7.2)$$

This is shown in a block diagram in Figure 7.2. When implemented in MATLAB Simulink this time domain block diagram is converted to the frequency domain.

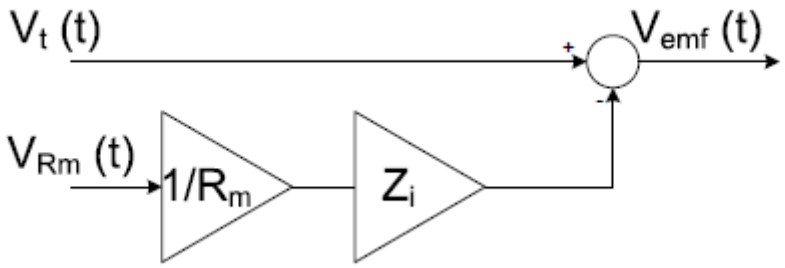

Figure 7.2 block diagram for the calculation of the back-emf voltage

The internal transducer impedance Z_i is known as this was characterised (Chapter 2.2) and because R_m is known, the back-emf voltage can be calculated by measuring the voltage across the transducer $V_t(t)$ and across the measurement resistor V_{R_m} (t). A 1 Ω measurement resistor with a power rating of 5 W was chosen to be used in series with the transducer such that the current owing through the transducer would not be limited severely and thereby also limiting the input voltage $V_p(t)$ (Figure 7.2) necessary for applying a certain voltage $V_t(t)$ across the transducer. Three of these block diagrams are placed in the `Self sensing' block to accomodate for the three control transducers [139].

7.2 Electronics

7.2.1 dSpace

To be able to acquire the back-emf voltage and to output the reference transducer voltage, a dSpace DS1103 Controller Board was used to interface with the system. This board provides 16 16-bit analog-to-digital (AD) converters, 4 12-bit AD converters and 8 14-bit digital-to-analog (DA) converters. When running a simulation externally in MATLAB Simulink, the onboard DSP is used for the signal processing and acquisition

and output of the various signals via its AD and DA converters. The continuous model in Simulink is then discretized and run at a sampling rate of 10 kHz, which was found to be sufficient by looking at the representation frequency sinusoidal signal. A sampling rate of 1 kHz would show a staircase approximation of the same sinusoid, which is undesired. For a list of the AD and DA converters used, refer to Table 7.2. Only the 16-bit AD converters were used instead of the 12-bit, to minimize the quantisation error [139].

Signal	Symbol	T 1	T 2	T 3
Reference voltage	V_{in}	DACH1	DACH3	DACH5
Transducer voltage	V_t	ADCH1	ADCH7	ADCH13
Measurement resistor voltage	V_{Rm}	ADCH3	ADCH9	ADCH15

Table 7.2 AD and DA converters on the dSpace DS1103 used for signal acquisition and reference voltage output

A low-pass antialiasing and reconstruction filters with cutoff frequencies of 10 kHz were added to the system.

7.2.2 Interfacing circuits

The MATLAB Simulink model needs the transducer and measurement resistor voltages to calculate the back-emf and a control signal. Subsequently, the output voltage needs to be put across the transducer. Figure 7.3 shows a block diagram of one of the interface circuits used to power the control transducers as well as to measure the transducer and measurement resistor voltage. Because there are three control transducers, this circuit was built in triplicate. In this figure, U_1 represents the OPA548 power operational amplifier and U_2 and U_3 represent the generic uA741 operational amplifier configured as a differential amplifier with a gain of 1. R_m indicates a measurement resistor used for calculating the current owing through the transducer and is specific for each circuit, because the self sensing measurement depends on an accurate value of this resistance. Table 7.3 lists the different resistor values [139].

Circuit	Symbol	Value [Ω]
1	R_{m1}	1.0000
2	R_{m2}	0.9859
3	R_{m3}	0.9935

Table 7.3 specific measurement resistor value for each interface circuit

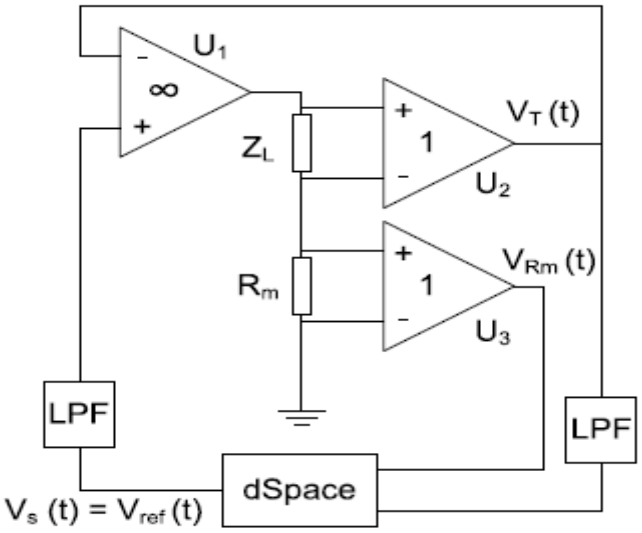

Figure 7.3 The interface circuit used to power the control transducer and to measure its voltage and the measurement resistor voltage for the purpose of self sensing

The transducer voltage $V_t(t)$ measured across the transducer which is represented by Z_L and measurement resistor voltage V_{R_m} (t) are acquired by the dSpace AD converters and after calculating the back-emf voltage V_{emf}, the control signal is output by the dSpace DA converter. This is the reference voltage which is placed across the transducer, using the negative feedback loop via U2. Simple first order low-pass filters (LPF) with a cut-off frequency of 1500 Hz (using a 1 kΩ resistor and 100 nF capacitor) were placed at the input of the transducer voltage measurement and after the dSpace output to reduce high frequency noise. The V_{R_m} input was not filtered as this was not necessary and even deteriorated the signal [139].

7.2.3 Additional electronics

To induce vibrations in the system, the disturbance transducer was powered by a 50 W

Jaycar amplifier kit. A sinusoid signal was used as input signal, which frequency was chosen from 20 to 50 Hz.

7.3 Multi-mode SISO PPF Controller Experiment Implemented Result

Three SISO PPF controller are used to control the first four vibration modes of simulation plate structure model. Firstly, Three SISO PPF controller are formed in MATLAB Simulink. Secondly, sinusoid signals which contain resonant frequencies of first four modes of simulation plate structure model are applied to the shaker one by one. Thirdly, Open-loop dynamics which is between shaker to plate without controller is compared to closed-loop dynamics which is between shaker to plate with controller. Time domain cases are designed to test the ability of three SISO PPF controller to attenuate multi-mode vibration when the controller centre frequencies match the resonant frequencies of the plate. The following is the multi-mode three SISO vibration control experiment results for every mode at each transducer.

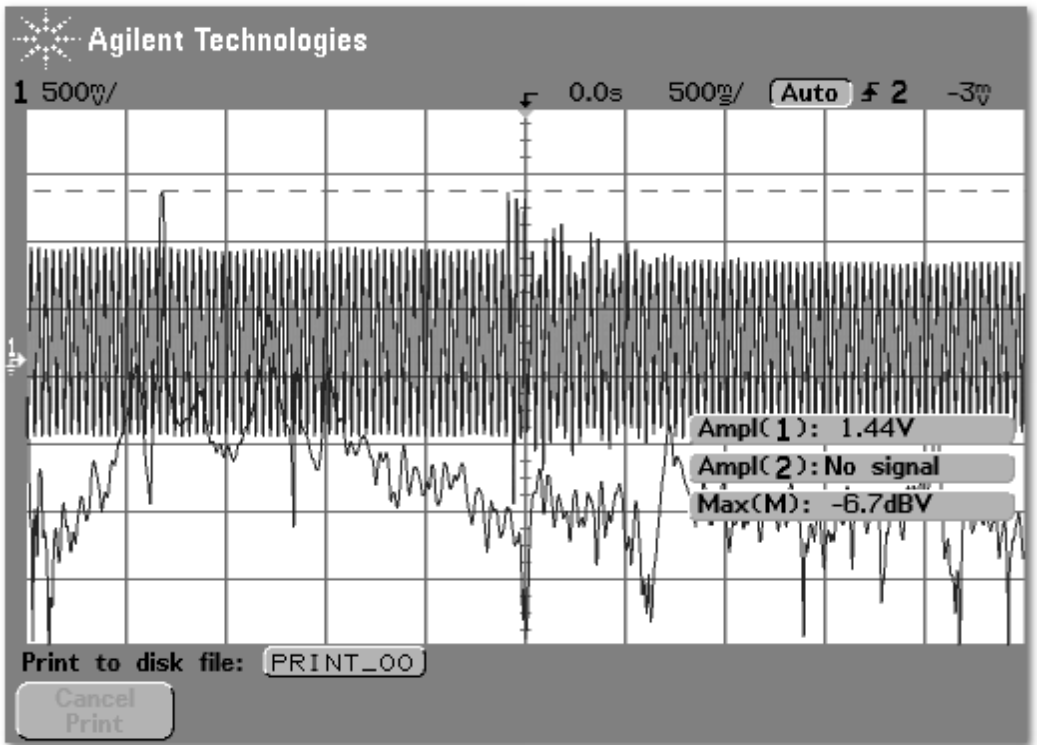

Figure 7.4 SISO vibration control at transducer 1 first mode 27.1 Hz before control

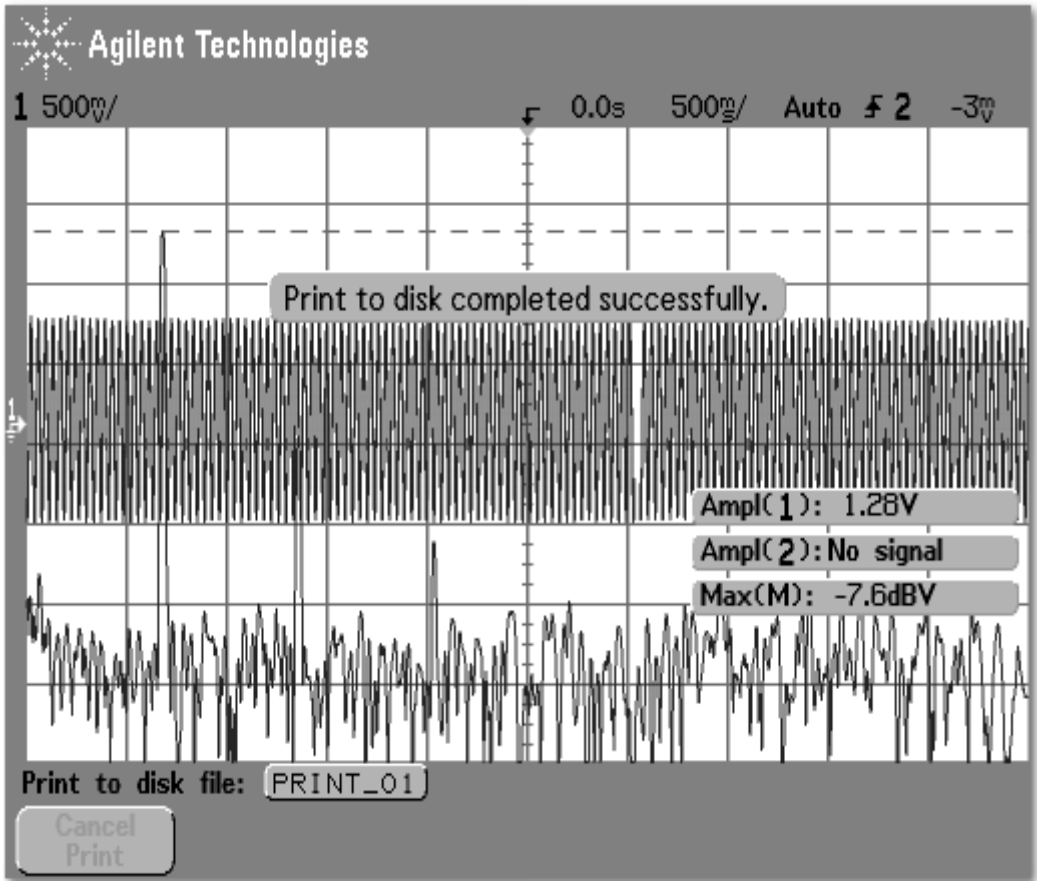

Figure 7.5 SISO vibration control at transducer 1 first mode 27.1 Hz after control

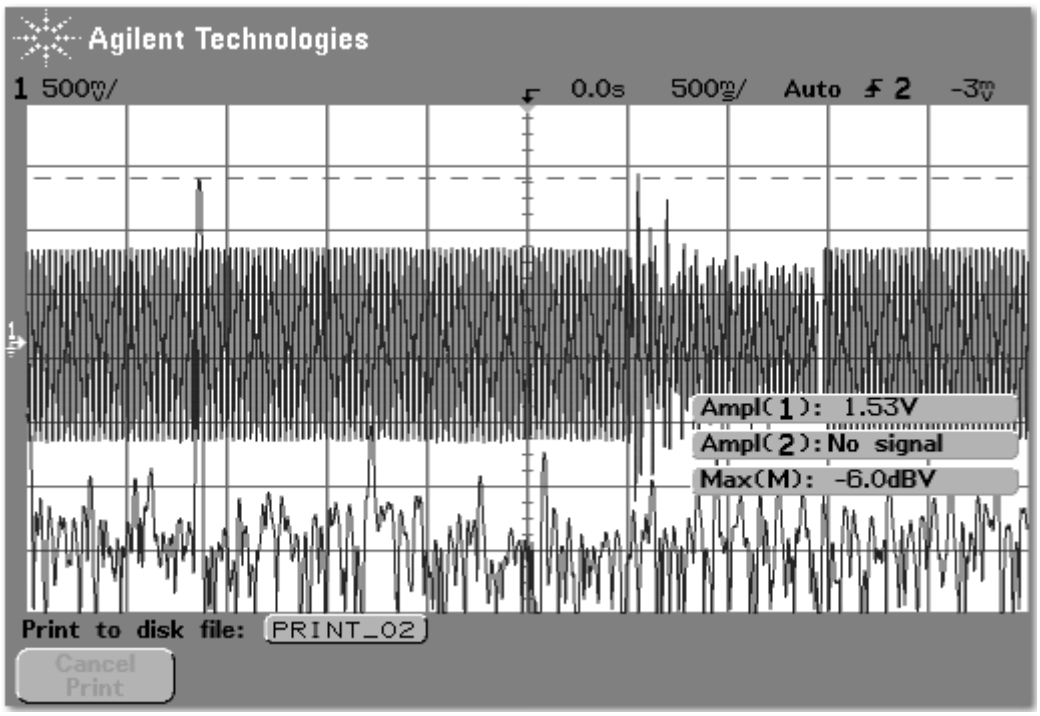

Figure 7.6 SISO vibration control at transducer 1 second mode 34.4 Hz before control

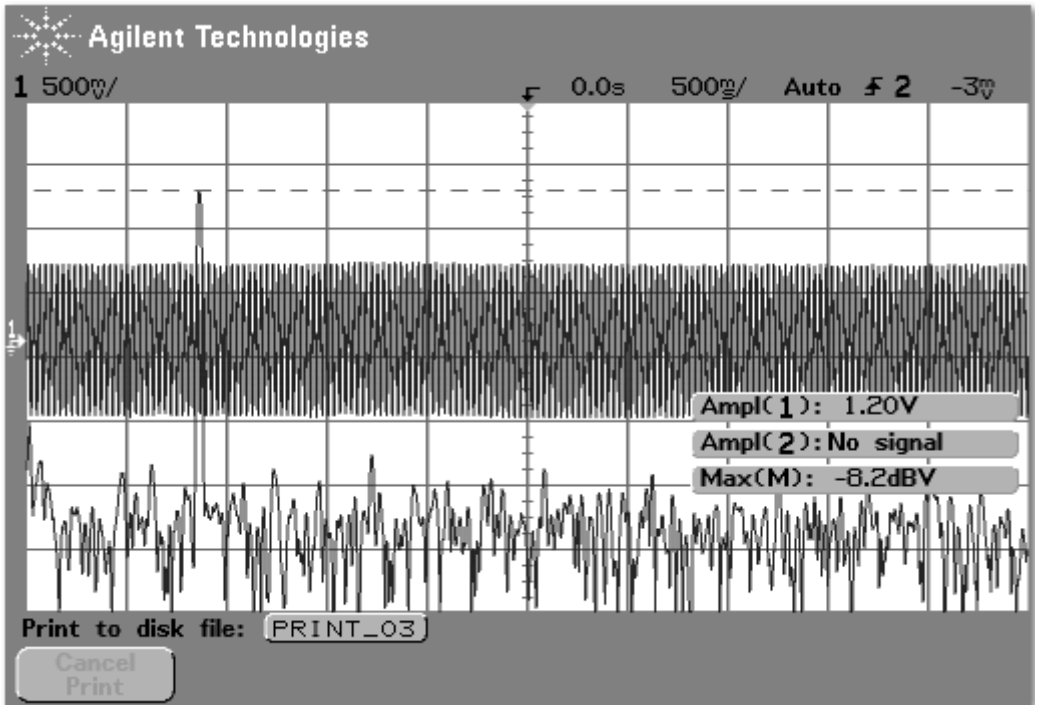

Figure 7.7 SISO vibration control at transducer 1 second mode 34.4 Hz after control

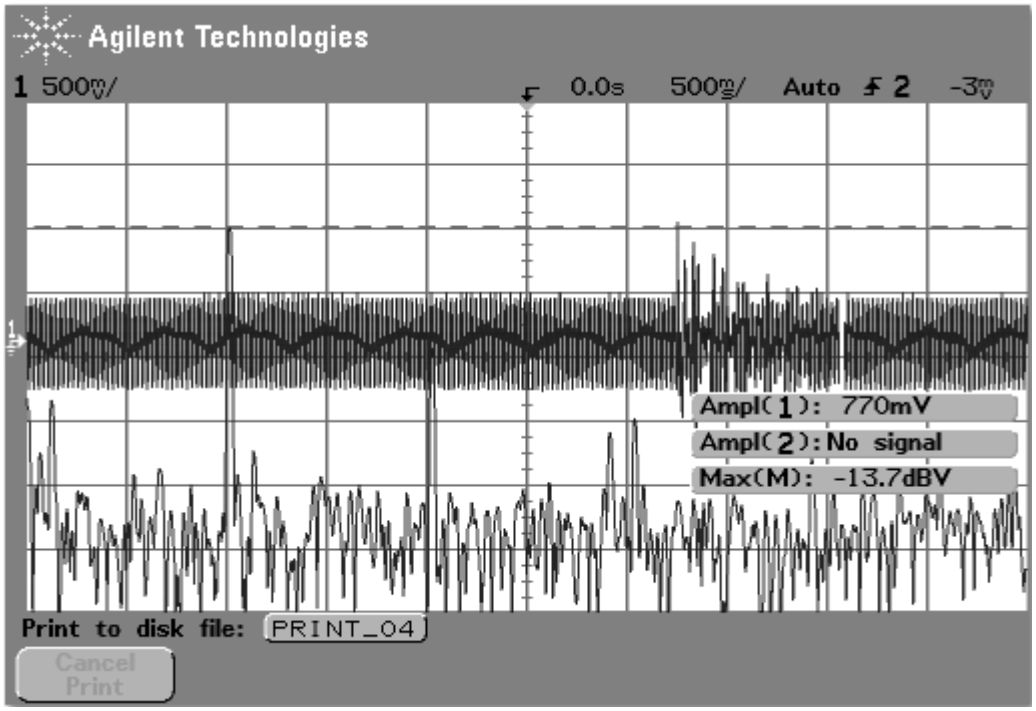

Figure 7.8 SISO vibration control at transducer 1 third mode 40.5 Hz before control

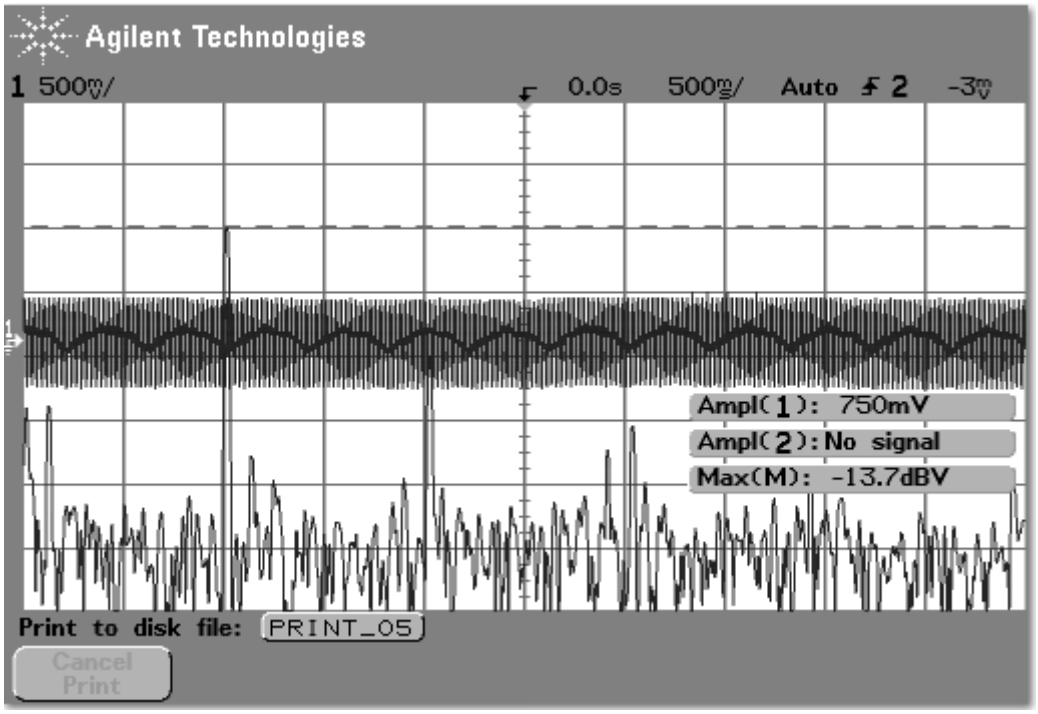

Figure 7.9 SISO vibration control at transducer 1 third mode 40.5 Hz SISO after control

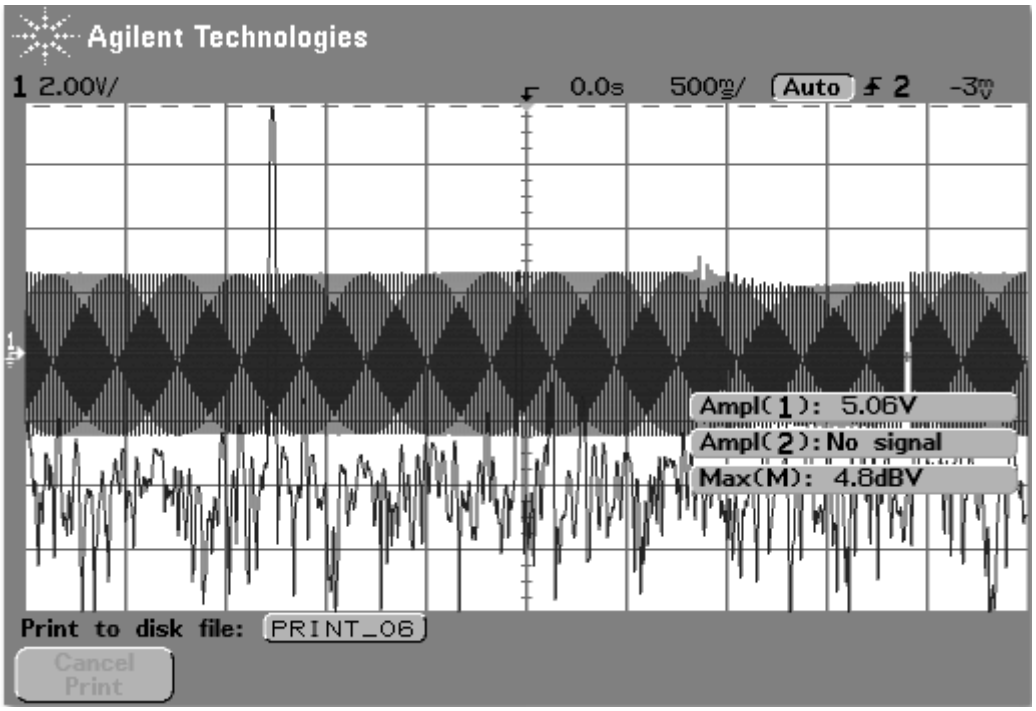

Figure 7.10 SISO vibration control at transducer 1 forth mode 49.2 Hz before control

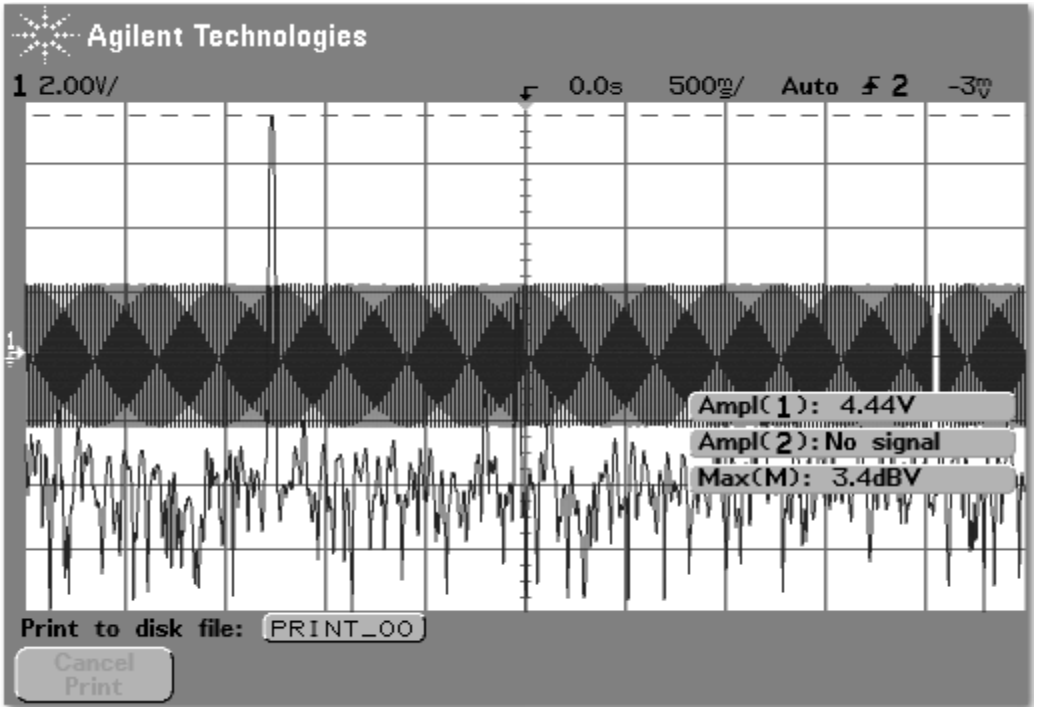

Figure 7.11 SISO vibration control at transducer 1 forth mode 49.2 Hz after control

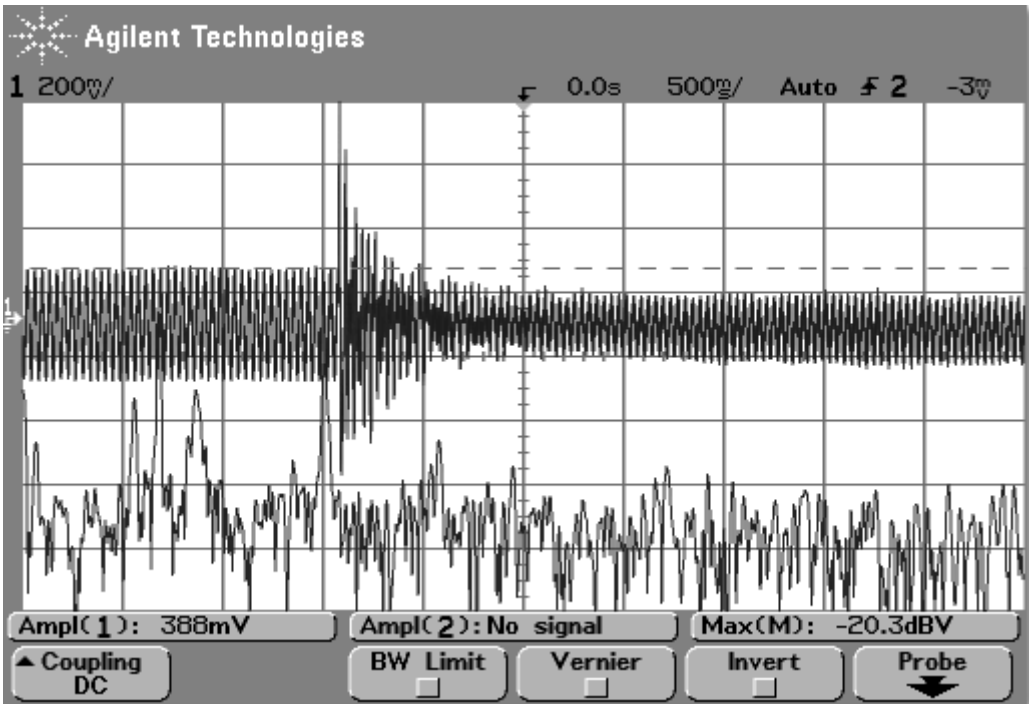

Figure 7.12 SISO vibration control at transducer 2 first mode 27.1Hz before control

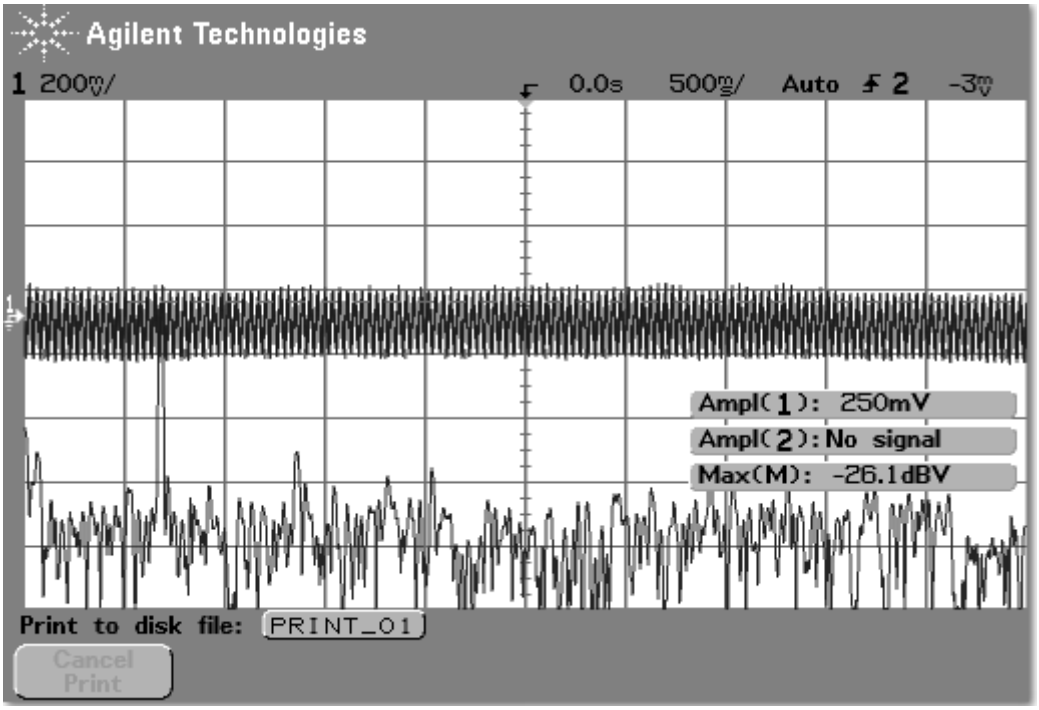

Figure 7.13 SISO vibration control at transducer 2 first mode 27.1Hz SISO after control

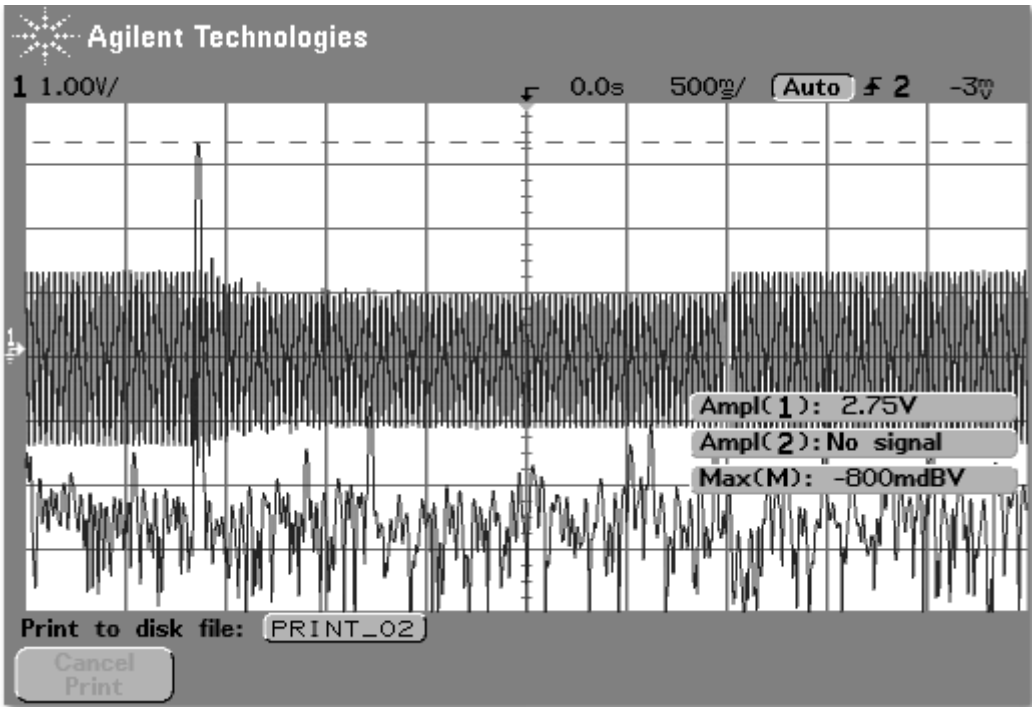

Figure 7.14 SISO vibration control at transducer 2 second mode 34.4 Hz before control

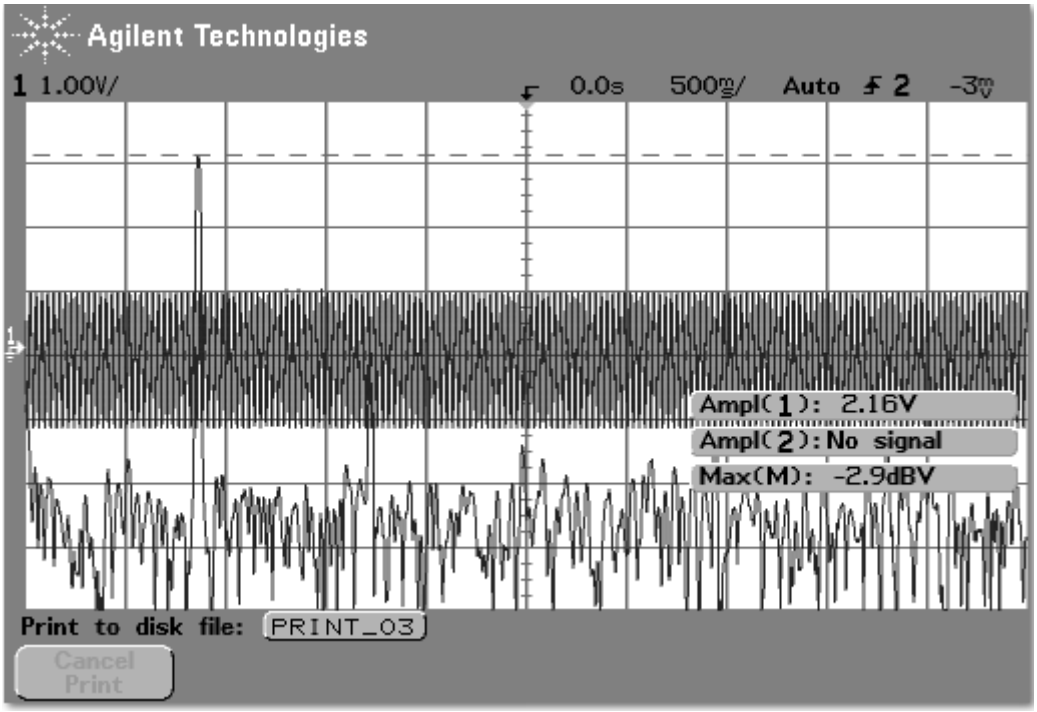

Figure 7.15 SISO vibration control at transducer 2 second mode 34.4 Hz after control

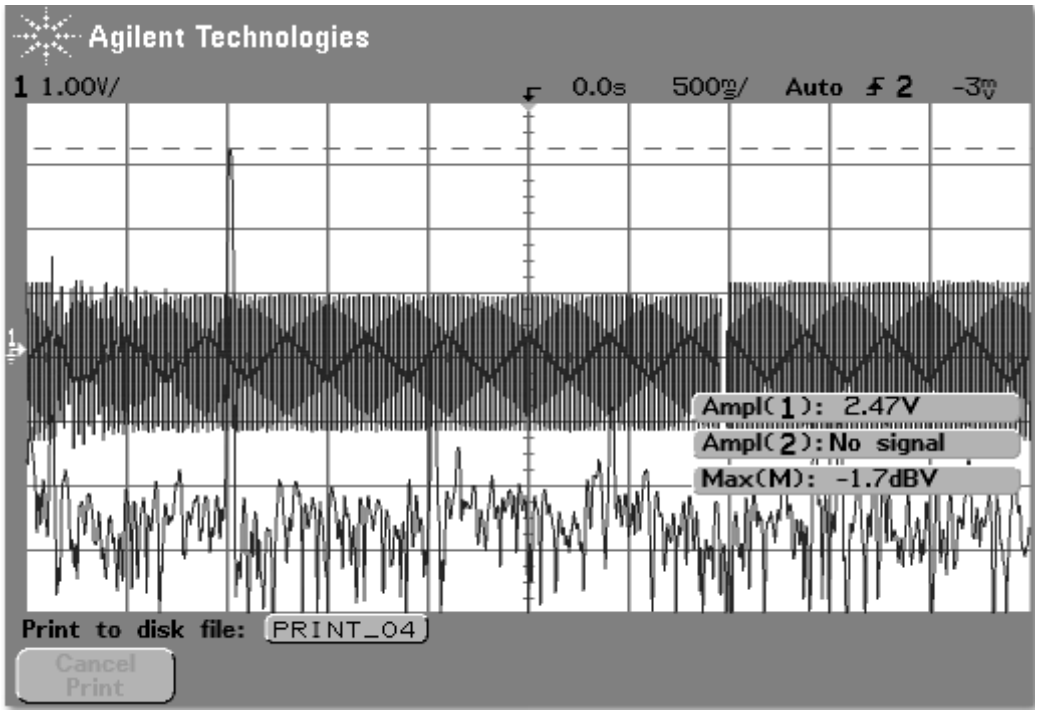

Figure 7.16 SISO vibration control at transducer 2 third mode 40.5 Hz before control

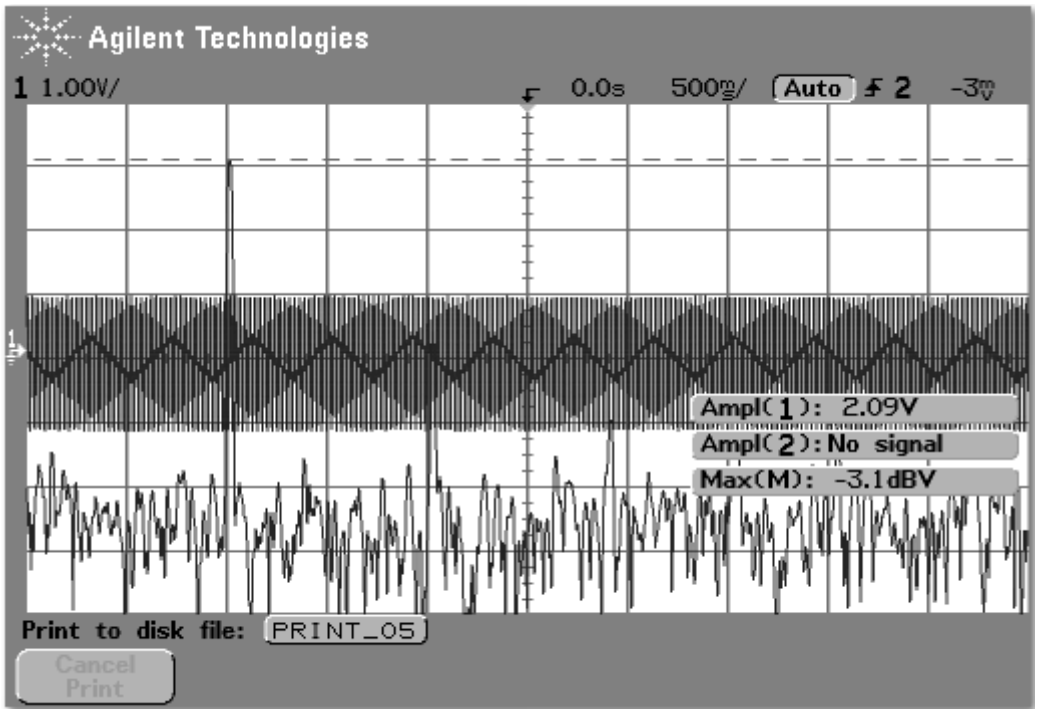

Figure 7.17 SISO vibration control at transducer 2 third mode 40.5 Hz after control

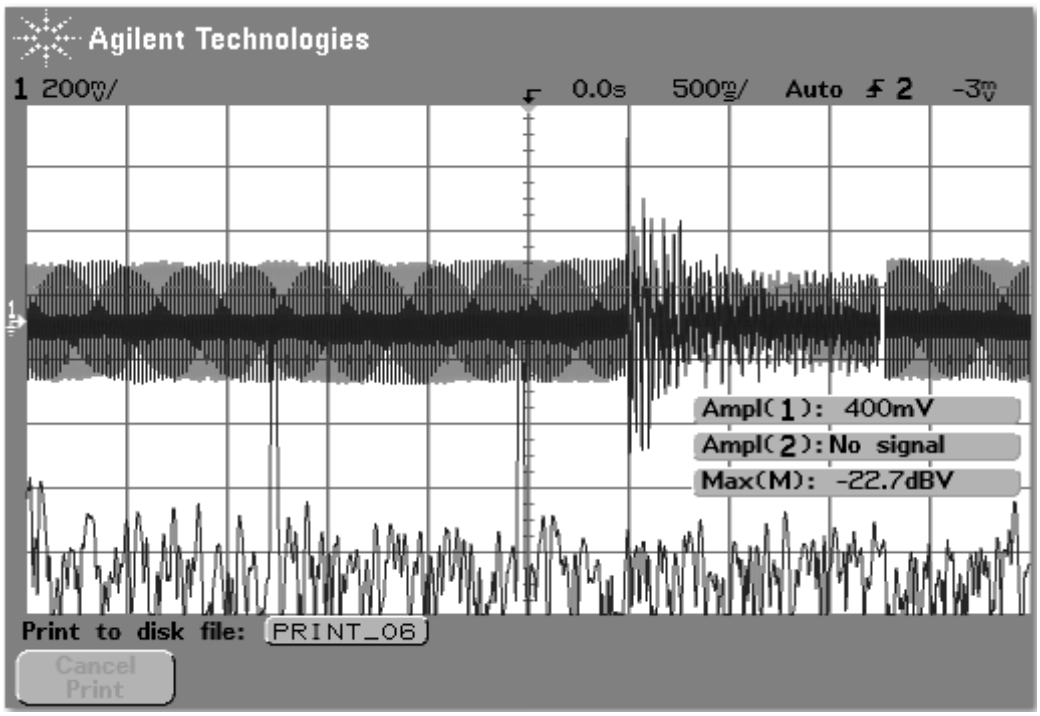

Figure 7.18 SISO vibration control at transducer 2 forth mode 49.2 Hz before control

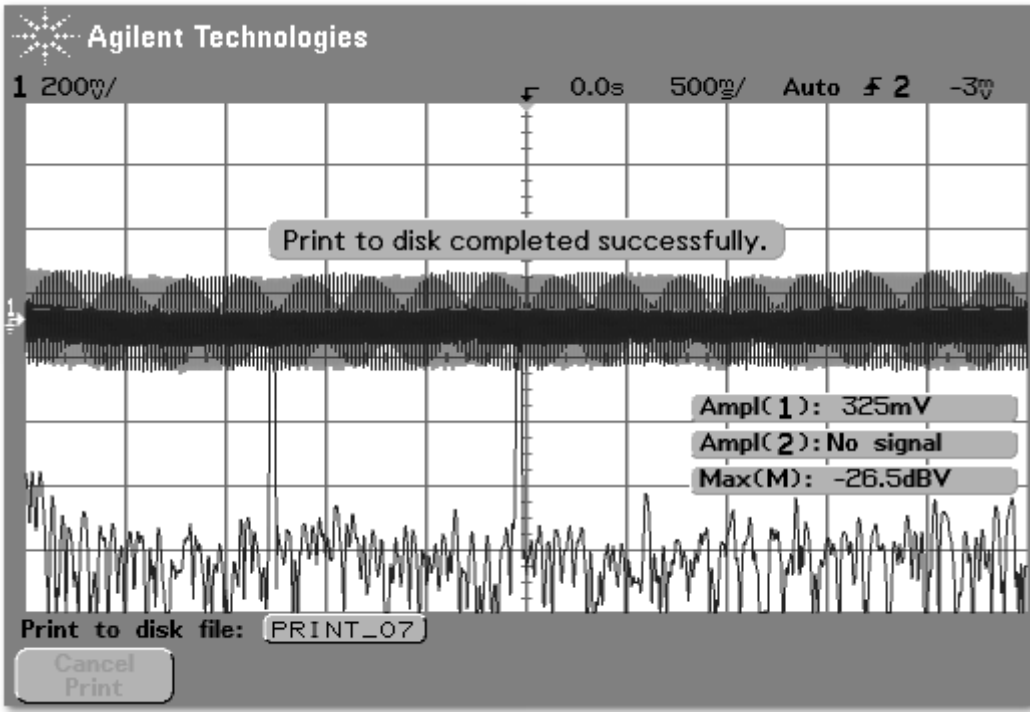

Figure 7.19 SISO vibration control at transducer 2 forth mode 49.2 Hz after control

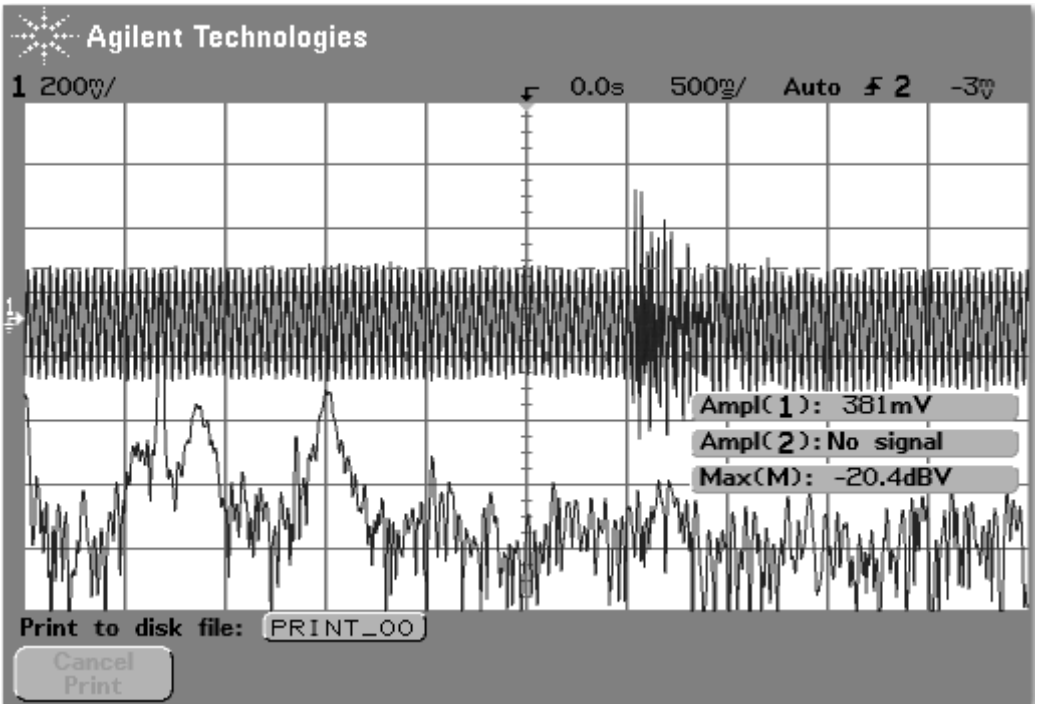

Figure 7.20 SISO vibration control at transducer 3 first mode 27.1Hz before control

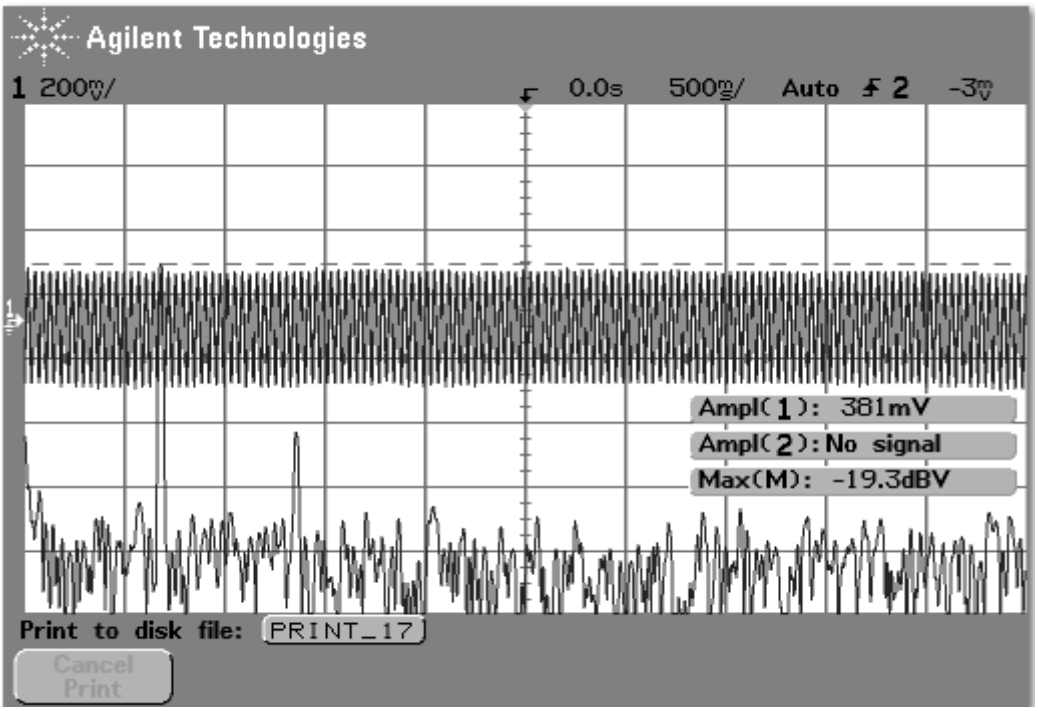

Figure 7.21 SISO vibration control at transducer 3 first mode 27.1Hz after control

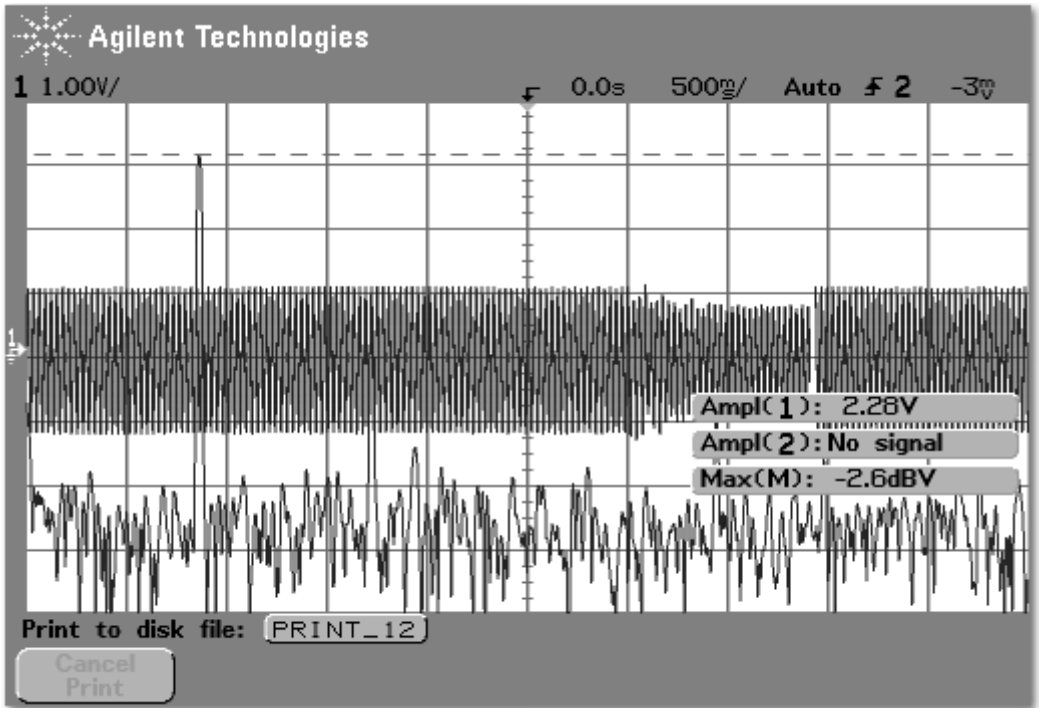

Figure 7.22 SISO vibration control at transducer 3 second mode 34.4 Hz before control

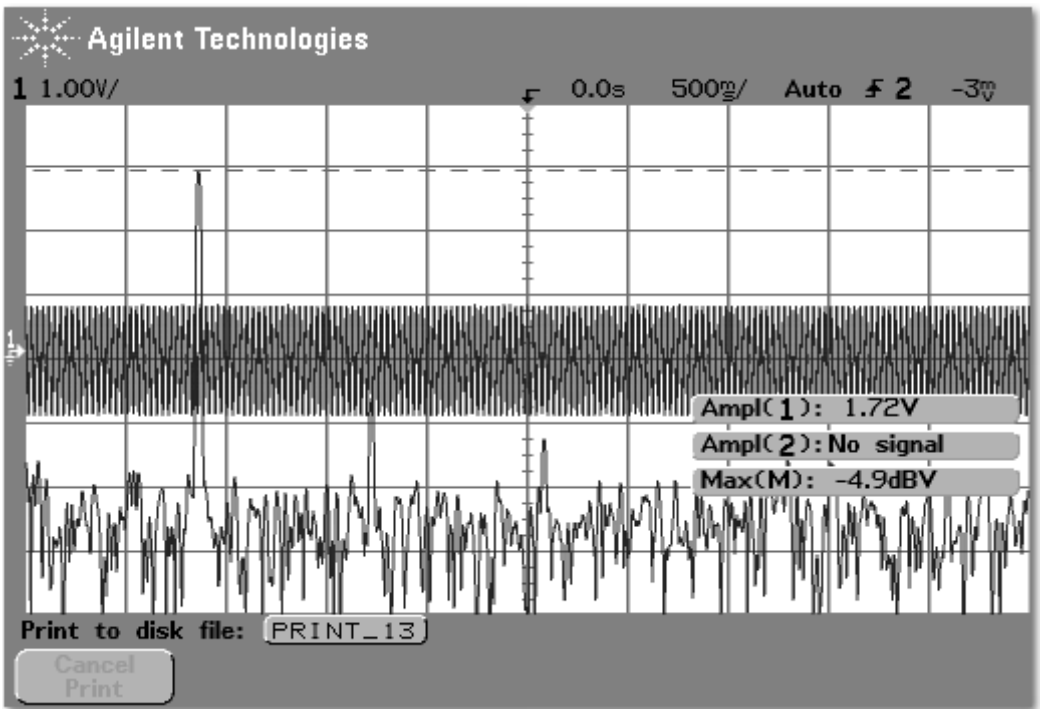

Figure 7.23 SISO vibration control at transducer 3 second mode 34.4 Hz after control

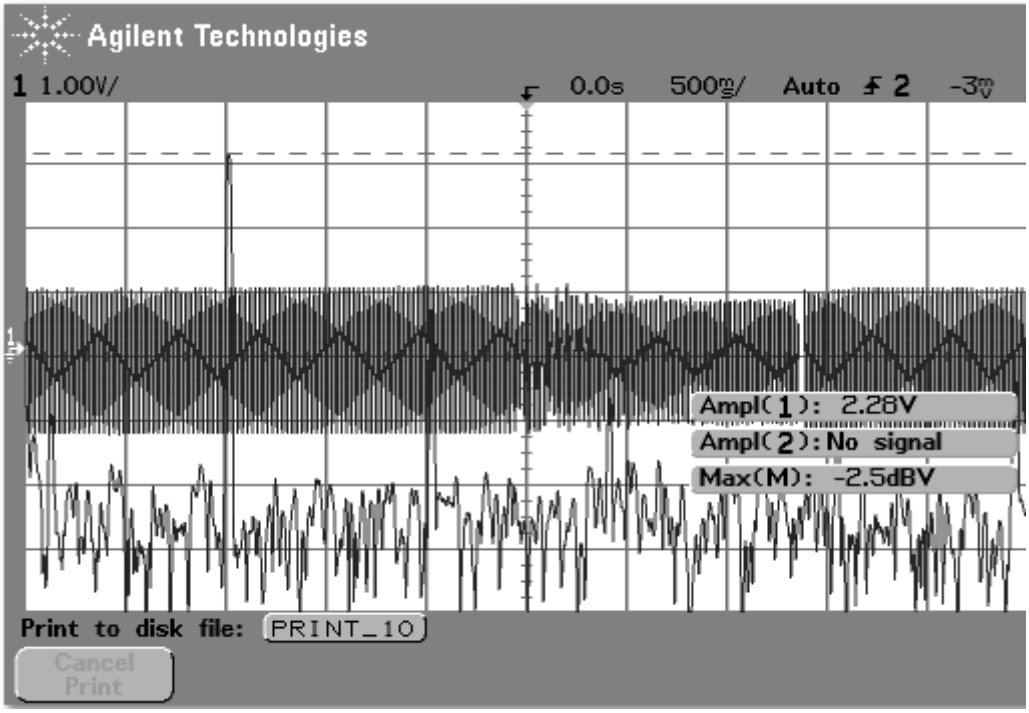

Figure 7.24 SISO vibration control at transducer 3 third mode 40.5 Hz before control

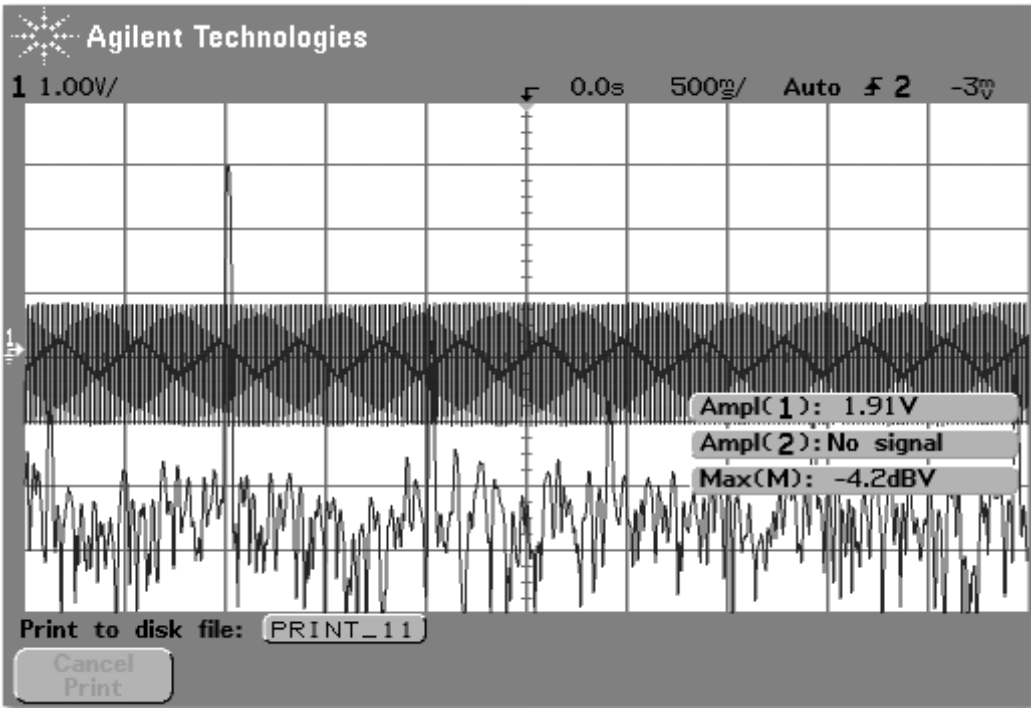

Figure 7.25 SISO vibration control at transducer 3 third mode 40.5 Hz after control

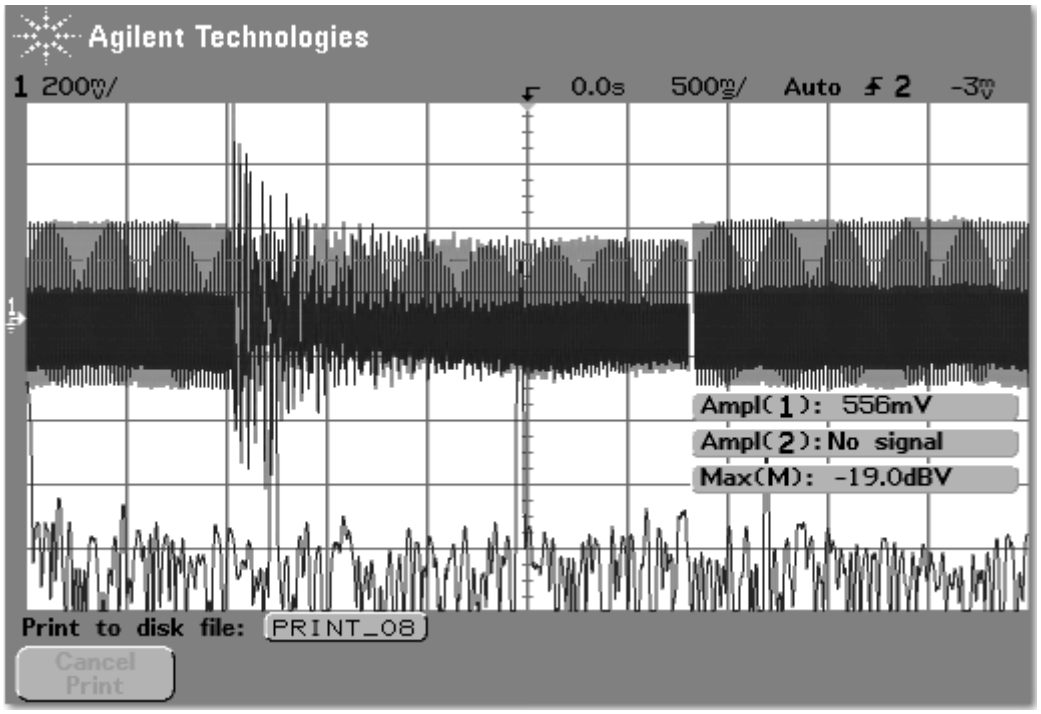

Figure 7.26 SISO vibration control at transducer 3 forth mode 49.2 Hz before control

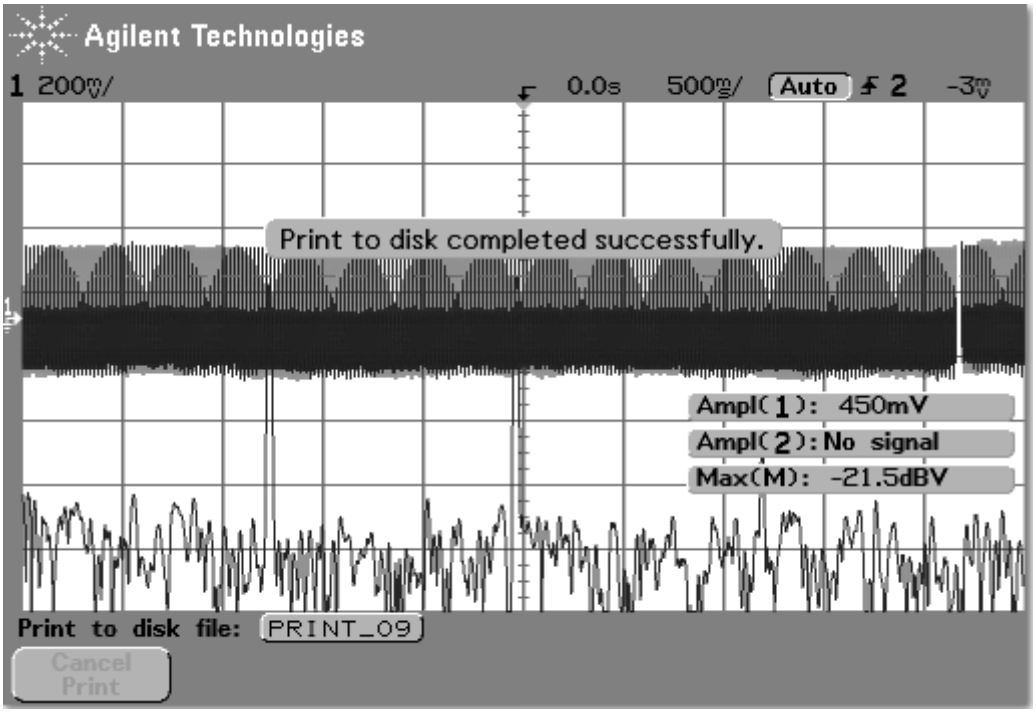

Figure 7.27 SISO vibration control at transducer 3 forth mode 49.2 Hz after control

Sinusoid signal which is swept from 20 Hz to 50 Hz is applied to the shaker, sampling time is 0.1s. Open-loop dynamics which is between shaker to plate without controller is compared to closed-loop dynamics which is between shaker to plate with controller.

Frequency domain cases are designed to test the ability of three SISO PPF controller to attenuate multi-mode vibration when the controller centre frequencies match the resonant frequencies of the plate . The following is the multi-mode three SISO vibration control experiment result at each transducer.

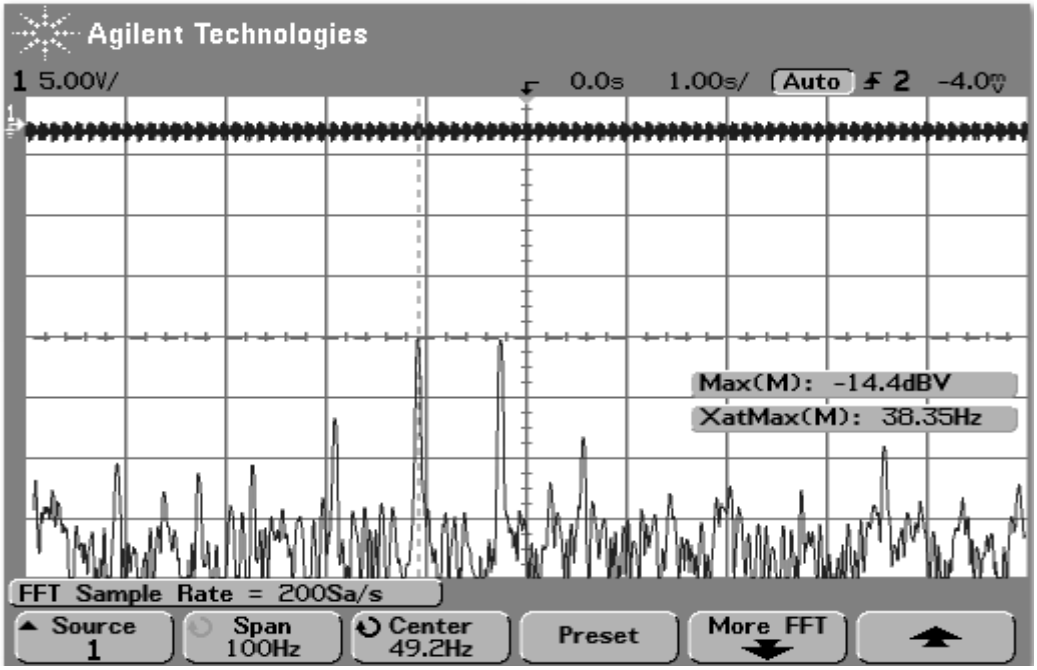

Figure 7.28 SISO vibration control for sweep signal at transducer 1 before control

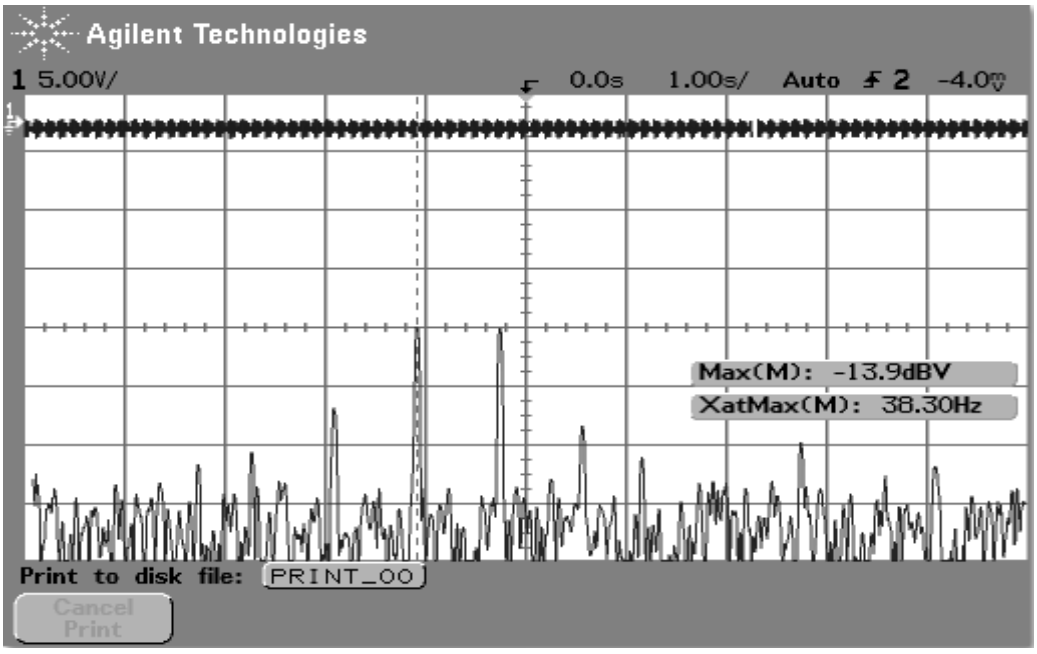

Figure 7.29 SISO vibration control for sweep signal at transducer 1 after control

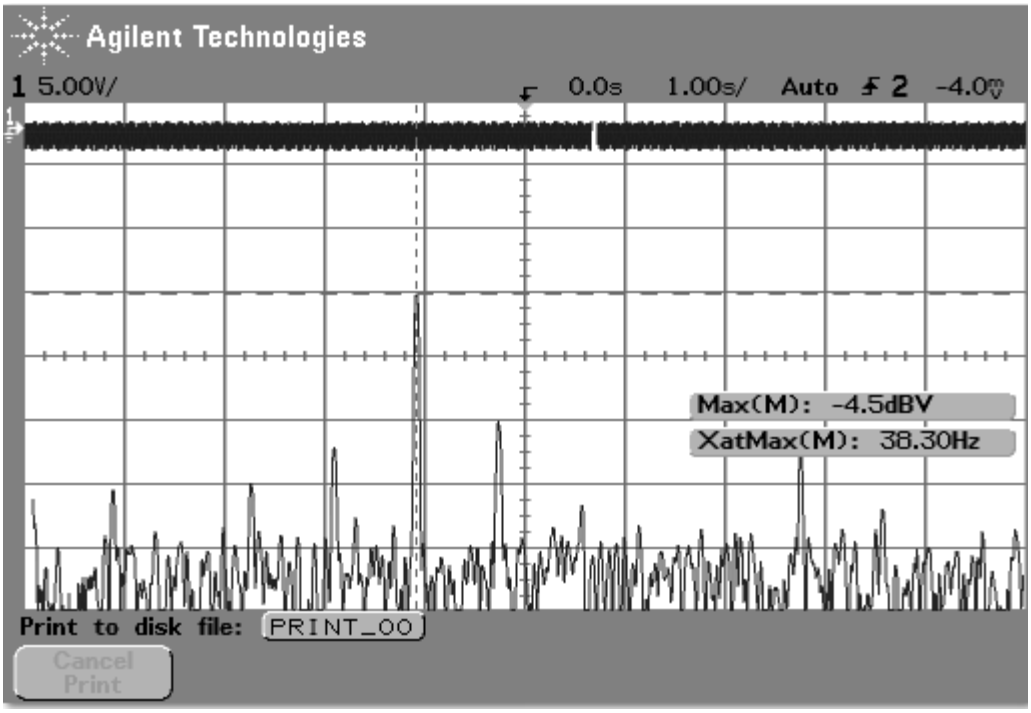

Figure 7.30 SISO vibration control for sweep signal at transducer 2 before control

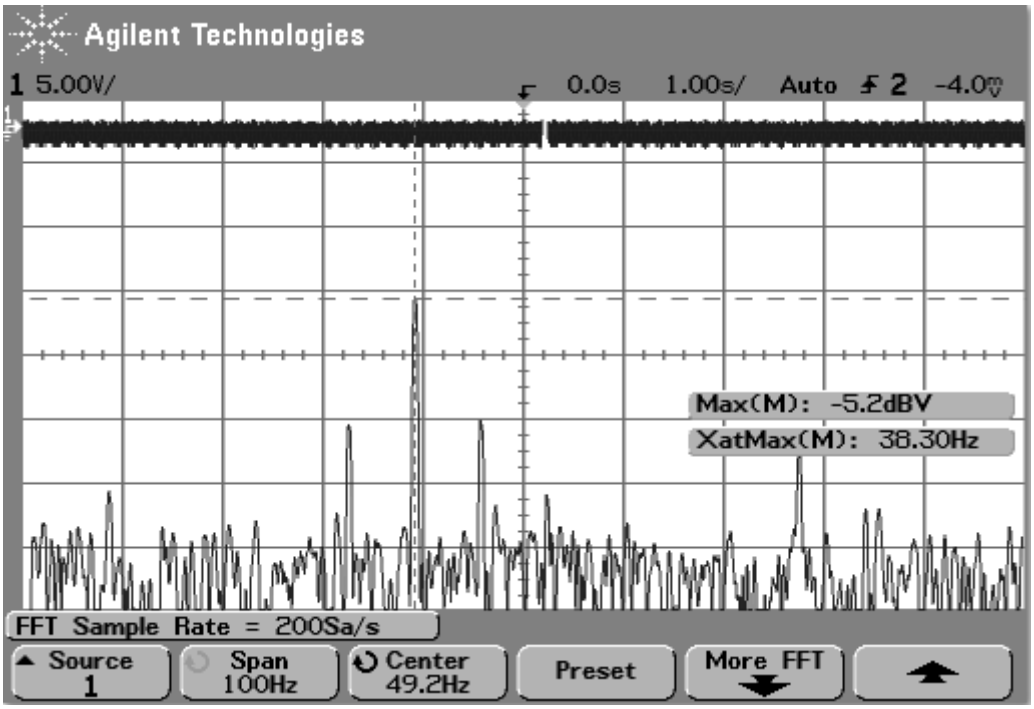

Figure 7.31 SISO vibration control for sweep signal at transducer 2 after control

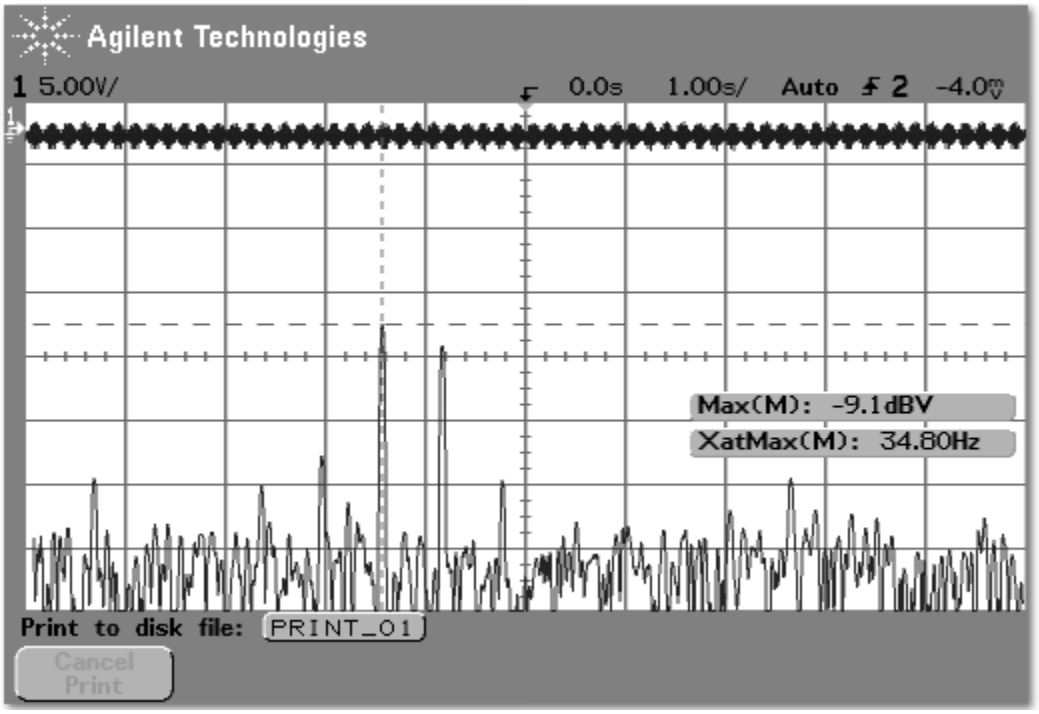

Figure 7.32 SISO vibration control for sweep signal at transducer 3 before control

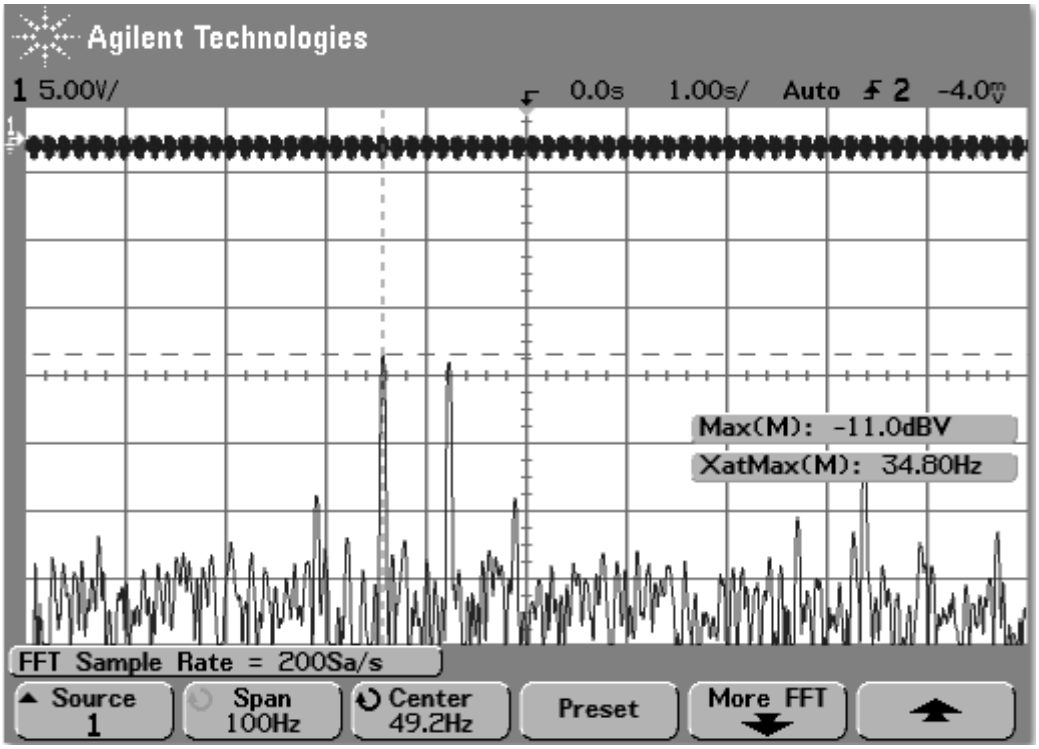

Figure 7.33 SISO vibration control for sweep signal at transducer 3 after control

The final experimental results for three SISO PPF controller are given in the Table 7.4.

			frequency (Hz)			
			27.1	34.4	40.5	49.2
transduer 1	Acceleration (g)	before	1.44	1.53	0.77	5.06
		after	1.28	1.2	0.75	4.44
	reduce rate (%)		**11.11%**	**21.569%**	**2.5974%**	**12.253%**
	Max Peak (dB)	before	-6.7	-6.0	-13.7	4.8
		after	-7.6	-8.2	-13.7	3.4
	reduce(dB)		**0.9**	**2.2**	**0**	**1.4**
transduer 2	Acceleration (g)	before	0.388	2.75	2.47	0.4
		after	0.25	2.16	2.09	0.325
	reduce rate(%)		**35.57%**	**21.45%**	**15.38%**	**18.75%**
	Max Peak (dB)	before	-20.3	-0.8	-1.7	-22.7
		after	-26.1	-2.9	-3.1	-26.5
	Reduce (dB)		**5.8**	**2.1**	**1.4**	**3.8**
transduer 3	Acceleration (g)	before	0.381	2.28	2.28	0.556
		after	0.381	1.72	1.91	0.45
	reduce rate(%)		**0**	**24.561%**	**16.228%**	**19.065%**
	Max Peak (dB)	before	-20.4	-2.6	-2.5	-19
		after	-19.3	-4.9	-4.2	-21.5
	Reduce (dB)		**-1.1**	**2.3**	**1.7**	**2.5**

Table 7.4 SISO vibration control experimental results

The parameters of the three SISO PPF controller are given in Table 7.5.

		Mode 1	Mode 2	Mode 3	Mode 4
Controller	control	g1=6.9	g2=2.19E-02	g3=1.54E-03	g4=1.05E-03

K11	gain				
	damping	zc1=5.87E-02	zc2=0.351	zc3=0.295	zc4=0.243
Controller K22	control gain	g5=0.345	g6=6.58E-02	g7=1.54E-03	g8=1.05E-03
	damping	zc5=5.87E-02	zc6=3.51E-01	zc7=2.95E-01	zc8=2.43E-01
Controller K33	control gain	g9=3.45E-01	g10=2.19E-01	g11=1.54E-03	g12=1.05E-03
	damping	zc9=5.87E-02	zc10=3.51E-01	zc11=2.95E-01	zc12=2.43E-01

Table 7.5 multi-mode SISO PPF controller experimental parameter result

7.4 Multi-mode MIMO PPF Controller Experimental Implemented Result

MIMO PPF controller are used to control the first four vibration modes of simulation plate structure model. Firstly, MIMO PPF controller are formed in MATLAB Simulink. Secondly, sinusoid signals which contain resonant frequencies of first four modes of simulation plate structure model are applied to the shaker one by one. Thirdly, Open-loop dynamics which is between shaker to plate without controller is compared to closed-loop dynamics which is between shaker to plate with controller. Time domain cases are designed to test the ability of MIMO PPF controller to attenuate multi-mode vibration when the controller centre frequencies match the resonant frequencies of the plate. The following is the multi-mode MIMO PPF vibration control experiment results.

		Mode 1	Mode 2	Mode 3	Mode 4
Controller 1	control gain	g1=0.103E	g2=6.58	g3=1.54E-03	g4=1.06
	damping	zc1=0.006	zc2=0.818	zc3=0.987	zc4=0.013
Controller 2	control gain	g5=2.94E-04	g6=2.34E-02	g7=1.96E-02	g8=1.62E-02
	damping	zc5=0.001	zc6=0.668	zc7=0.029	zc8=0.086
Controller 3	control gain	g9=1.47E-02	g10=2.34E-02	g11=3.93E-02	g12=1.62E-02
	damping	zc9=2.94E-02	zc10=4.68E-02	zc11=1.96E-0	zc12=1.62E-02

Table 7.6 multi-mode MIMO PPF controller parameter result

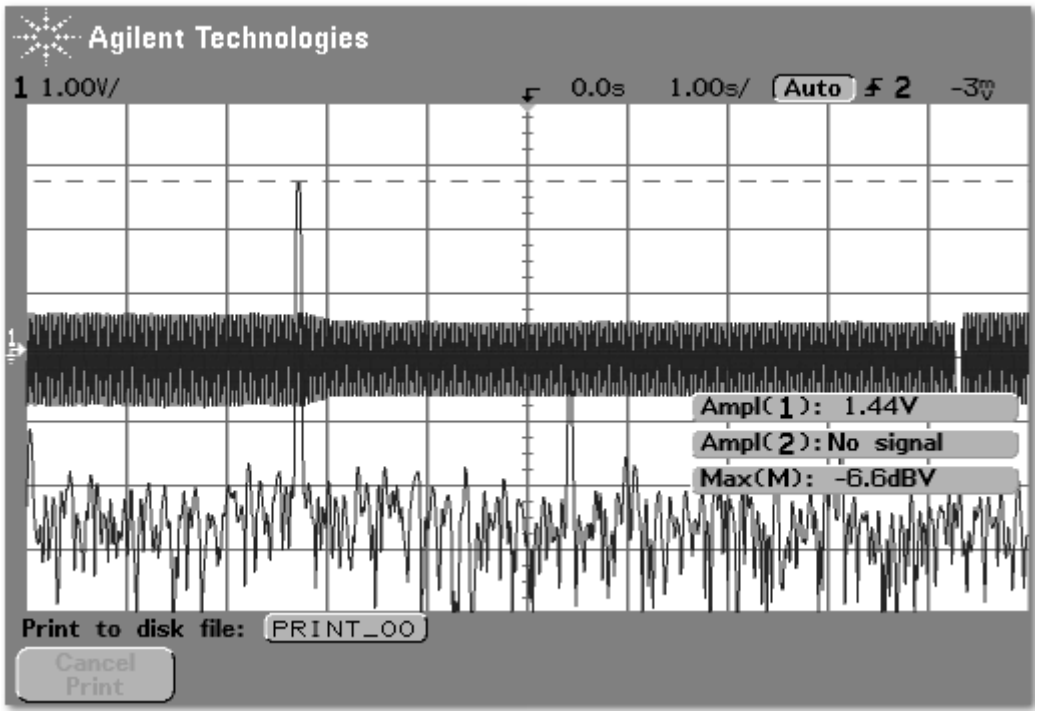

Figure 7.34 MIMO vibration control at transducer 1 first mode 27.1 Hz before control

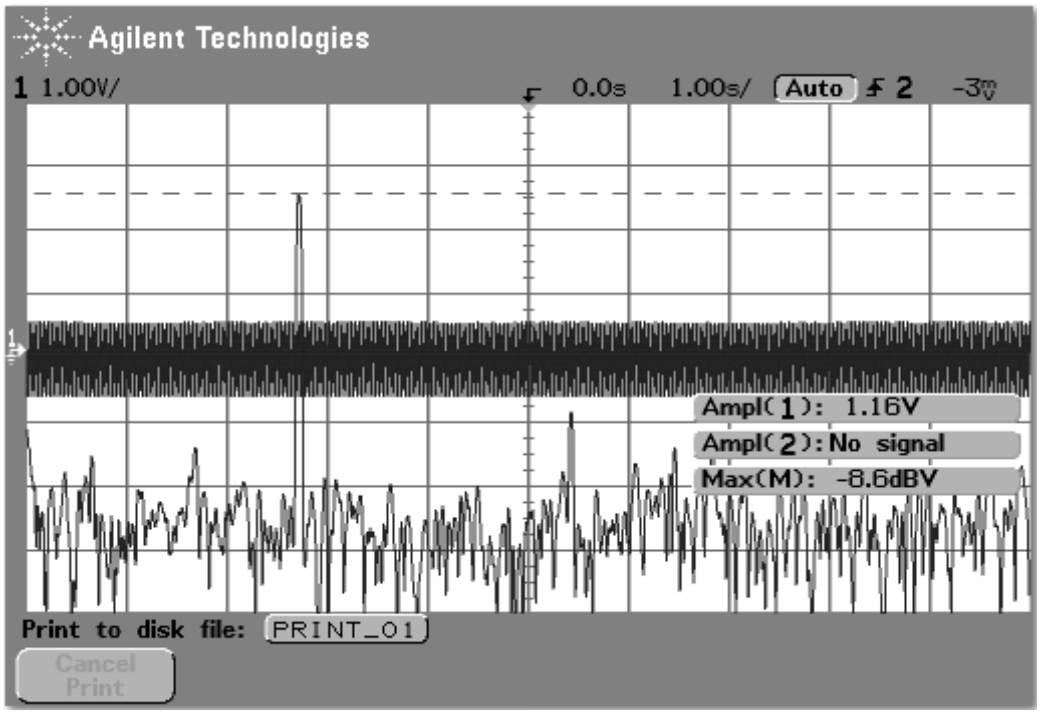

Figure 7.35 MIMO vibration control at transducer 1 first mode 27.1 Hz after control

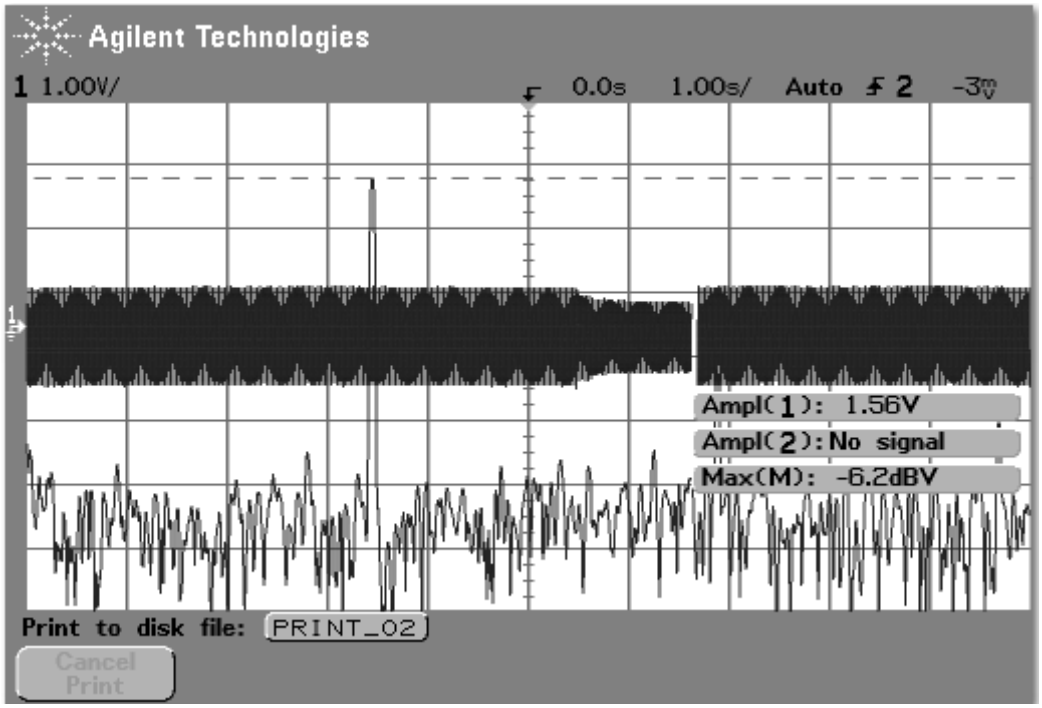

Figure 7.36 MIMO vibration control at transducer 1 second mode 34.4 Hz before control

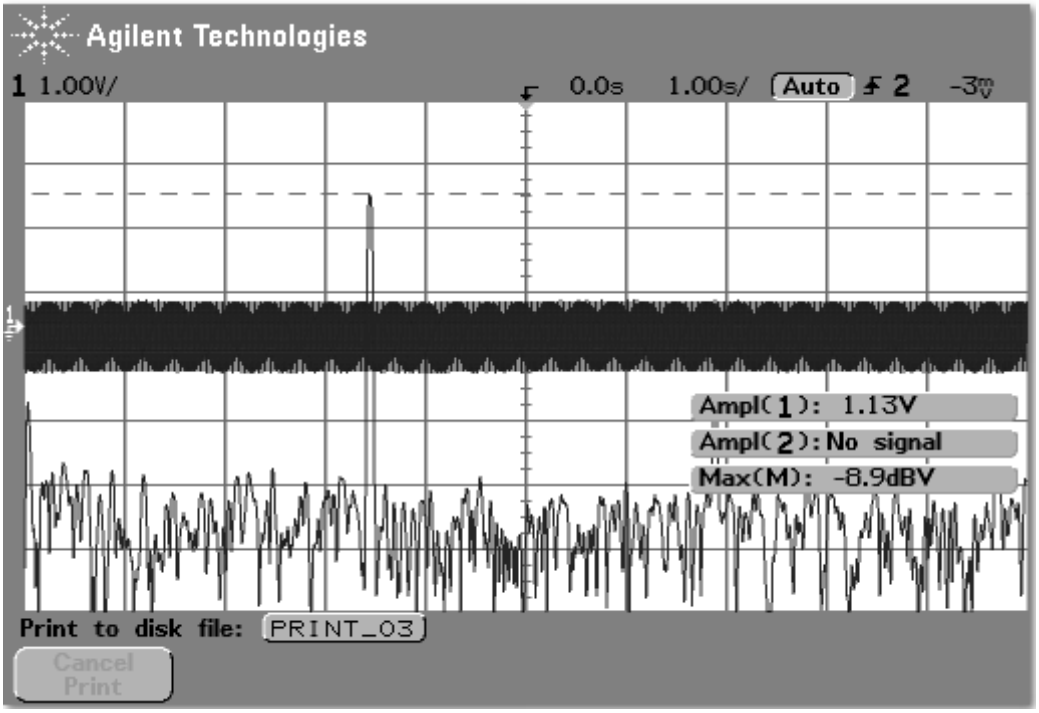

Figure 7.37 MIMO vibration control at transducer 1 second mode 34.4 Hz after control

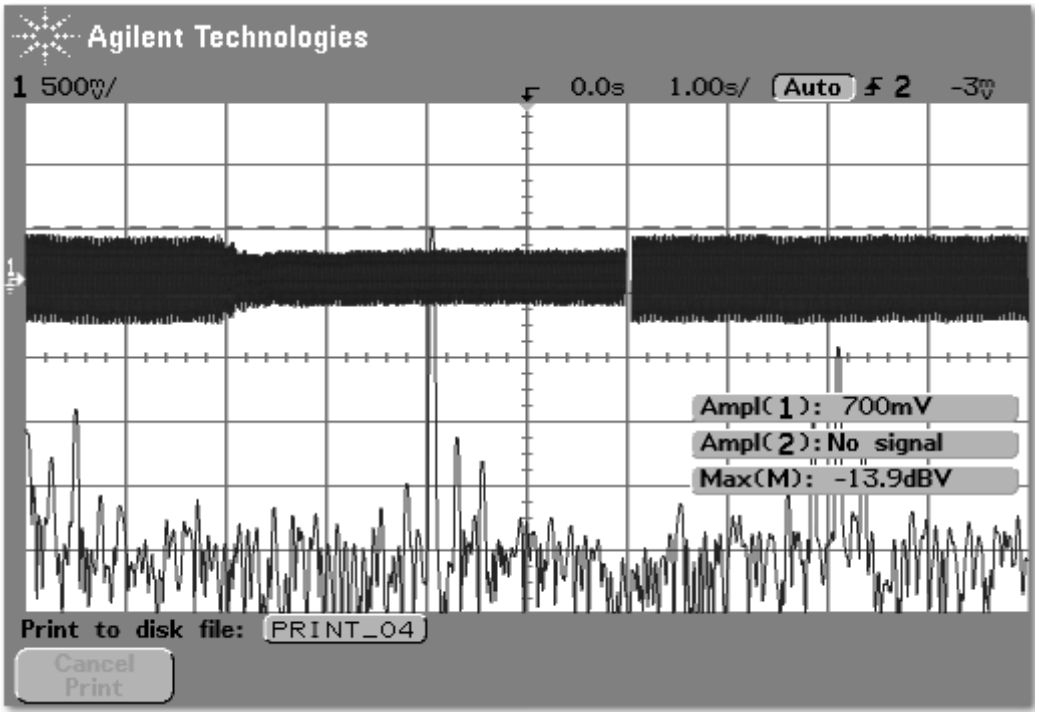

Figure 7.38 MIMO vibration control at transducer 1 third mode 40.5 Hz before control

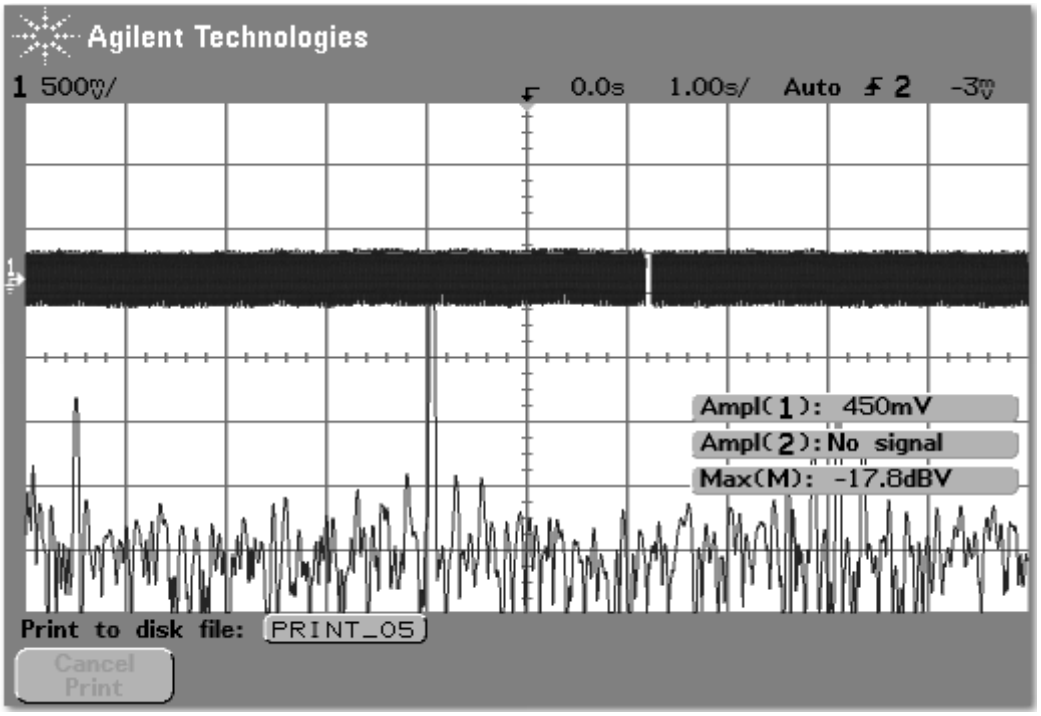

Figure 7.39 MIMO vibration control at transducer 1 third mode 40.5 Hz after control

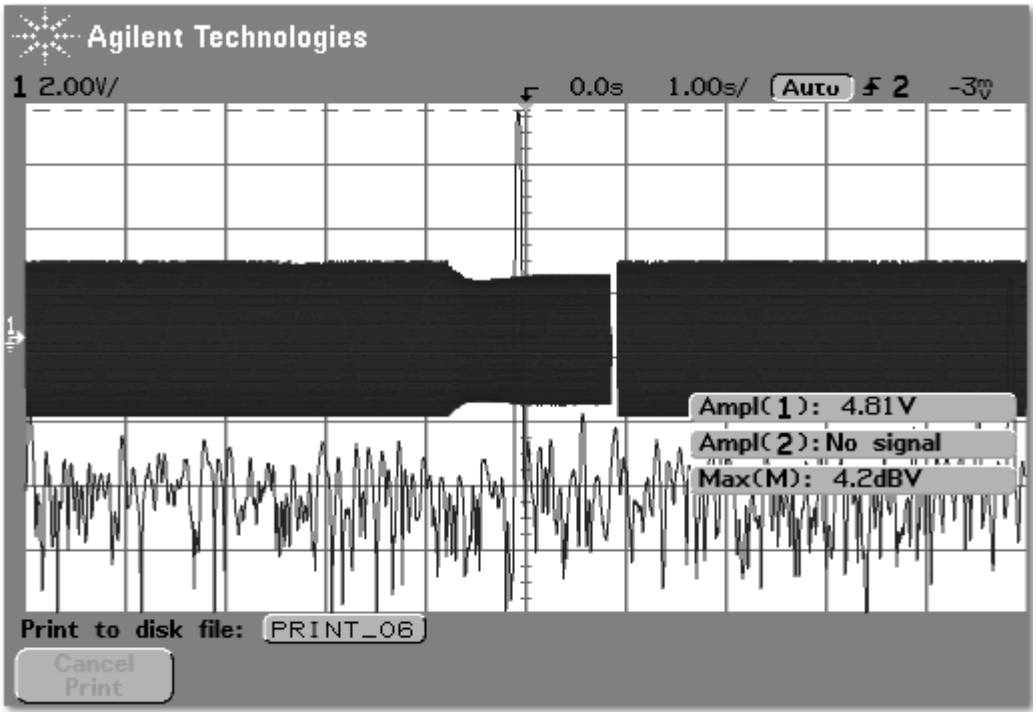

Figure 7.40 MIMO vibration control at transducer 1 forth mode 49.2 Hz before control

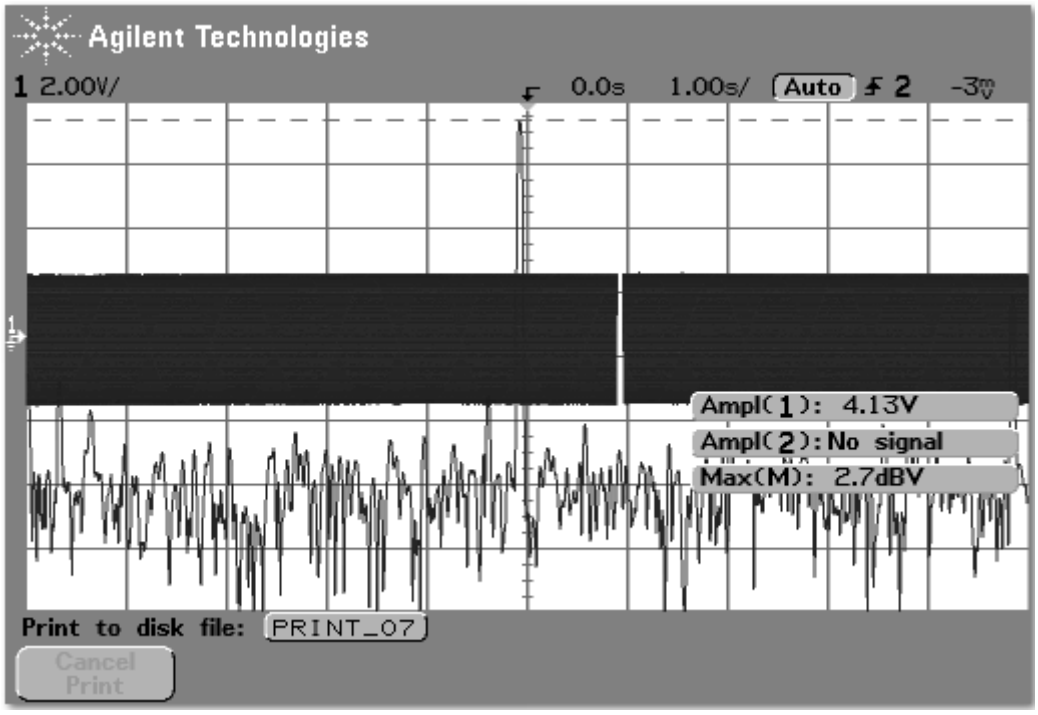

Figure 7.41 MIMO vibration control at transducer 1 forth mode 49.2 Hz after control

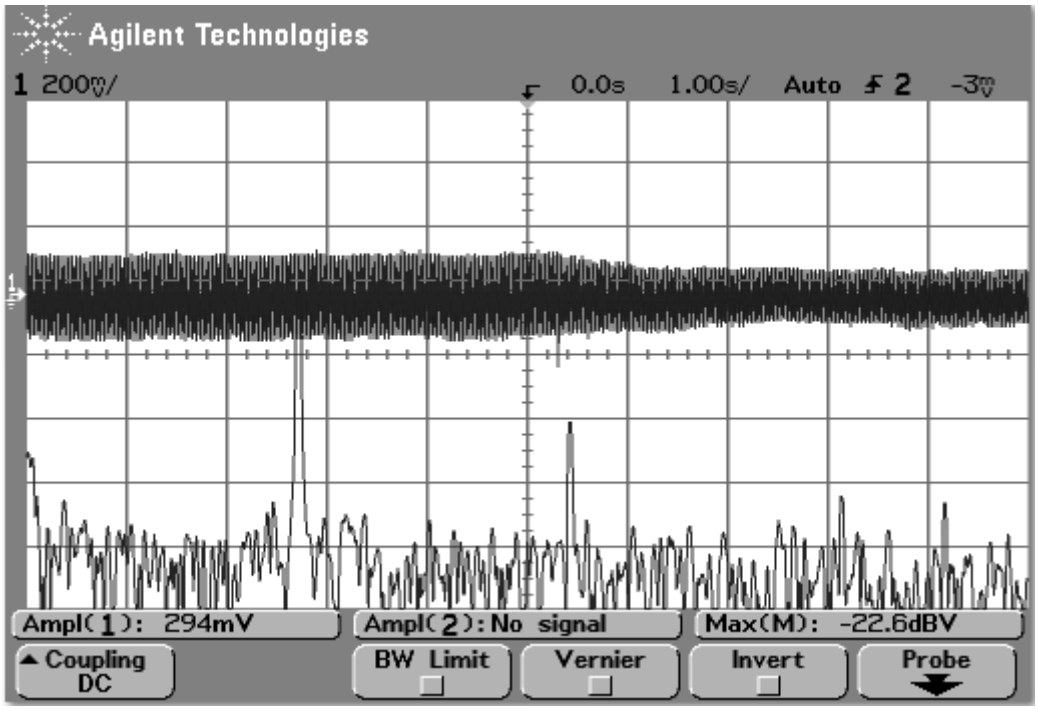

Figure 7.42 MIMO vibration control at transducer 2 first mode 27.1Hz before control

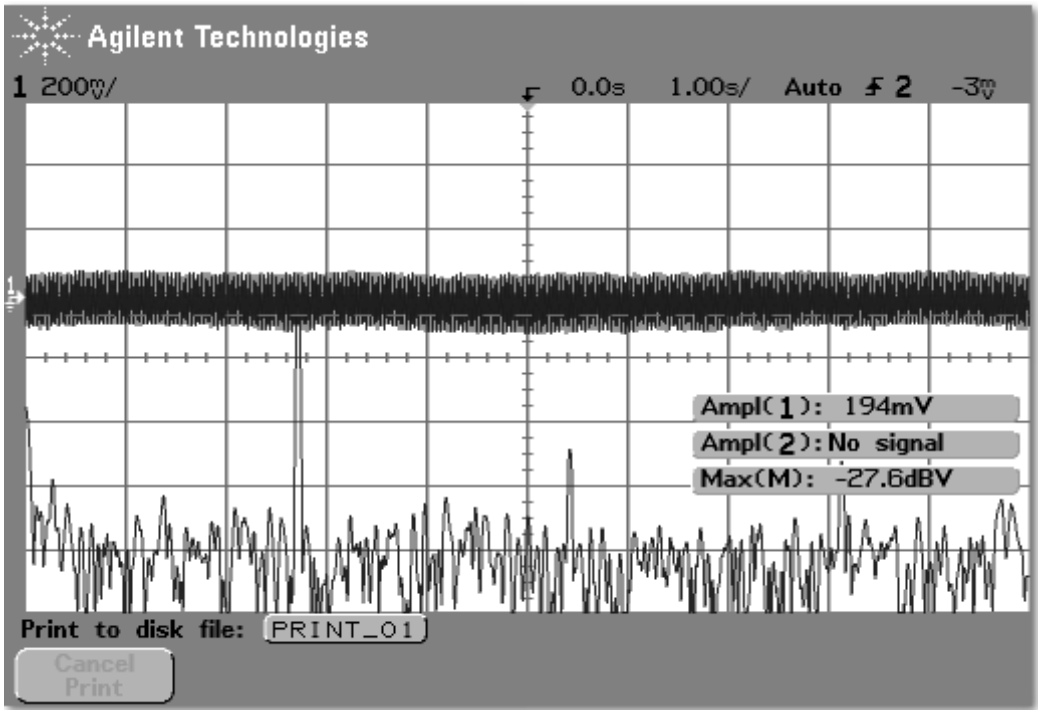

Figure 7.43 MIMO vibration control at transducer 2 first mode 27.1Hz after control

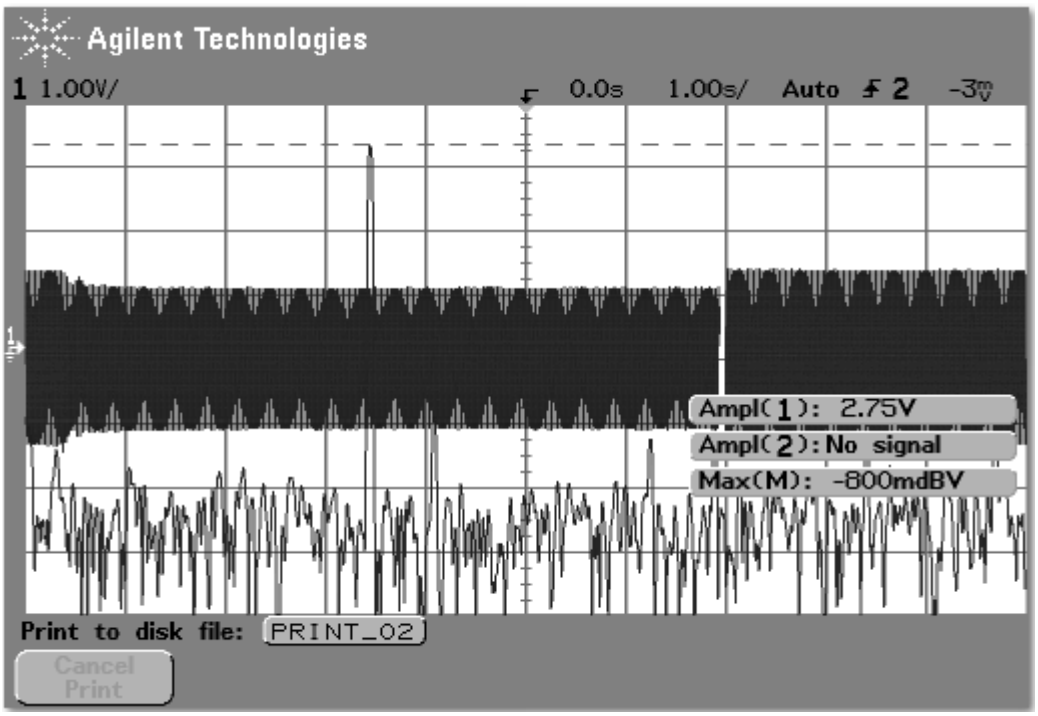

Figure 7.44 MIMO vibration control at transducer 2 second mode 34.4 Hz before control

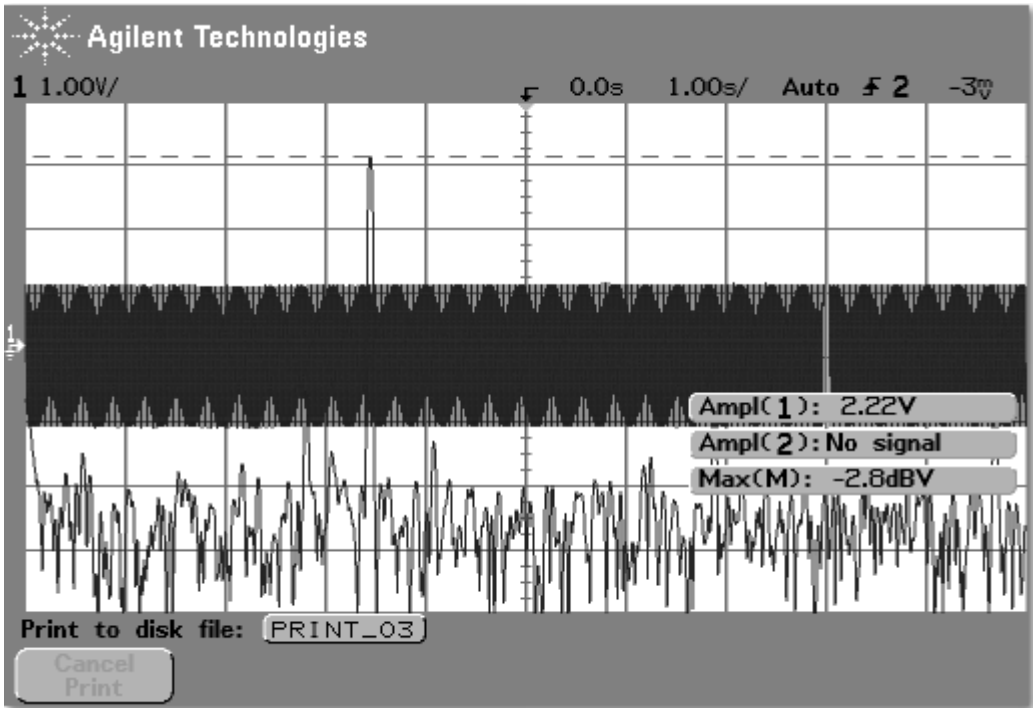

Figure 7.45 MIMO vibration control at transducer 2 second mode 34.4 Hz after control

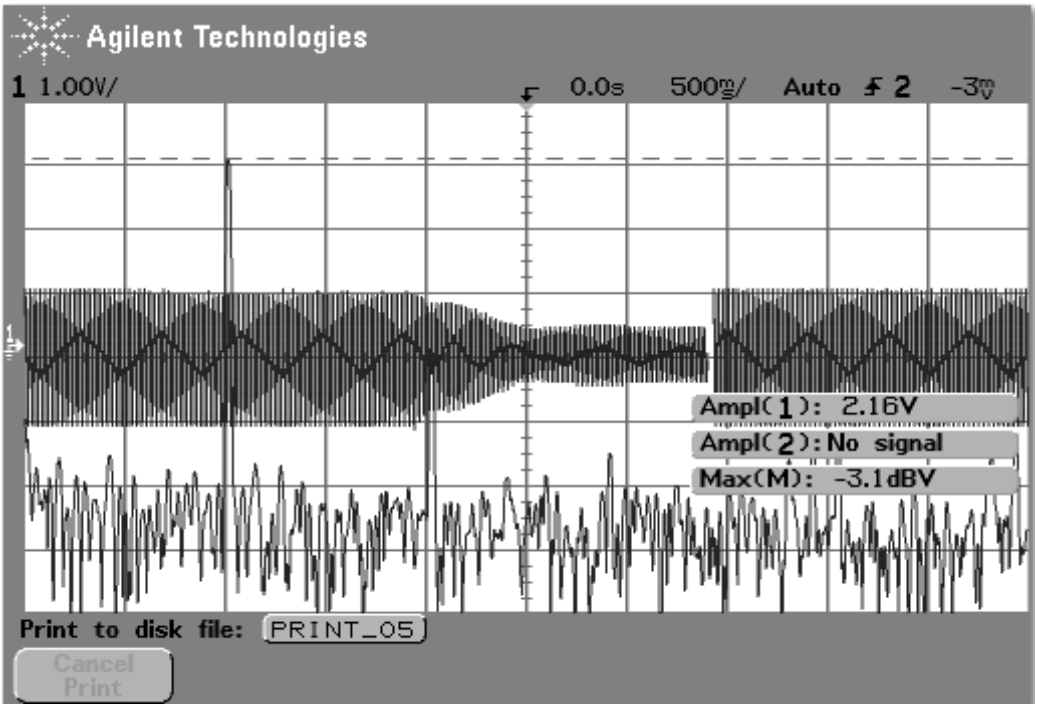

Figure 7.46 MIMO vibration control at transducer 2 third mode 40.5 Hz before control

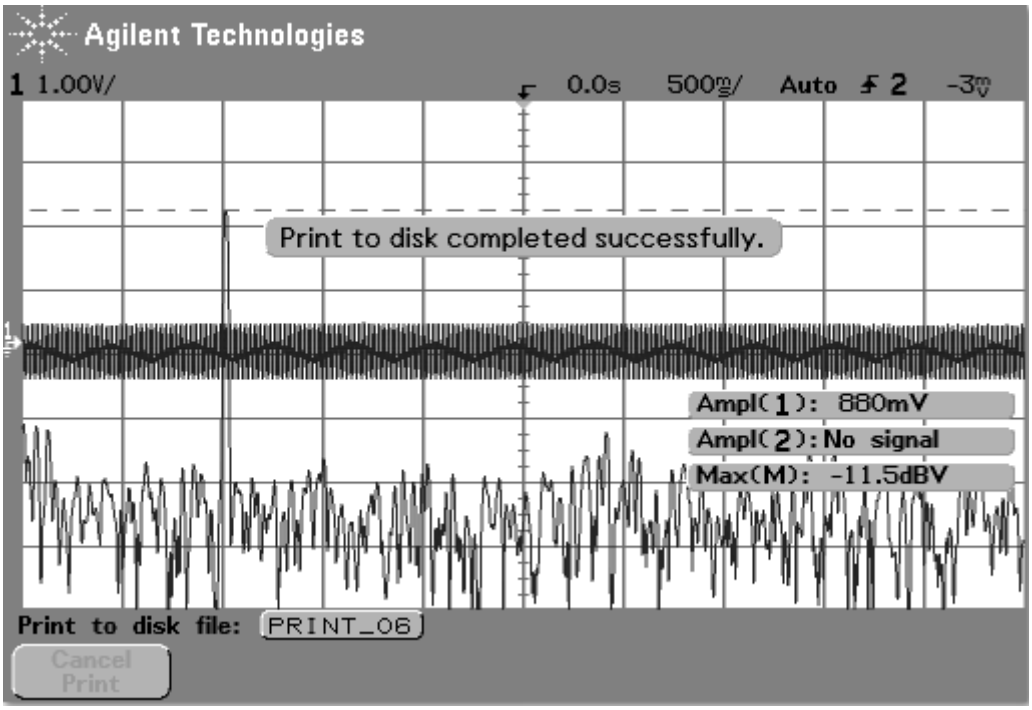

Figure 7.47 MIMO vibration control at transducer 2 third mode 40.5 Hz after control

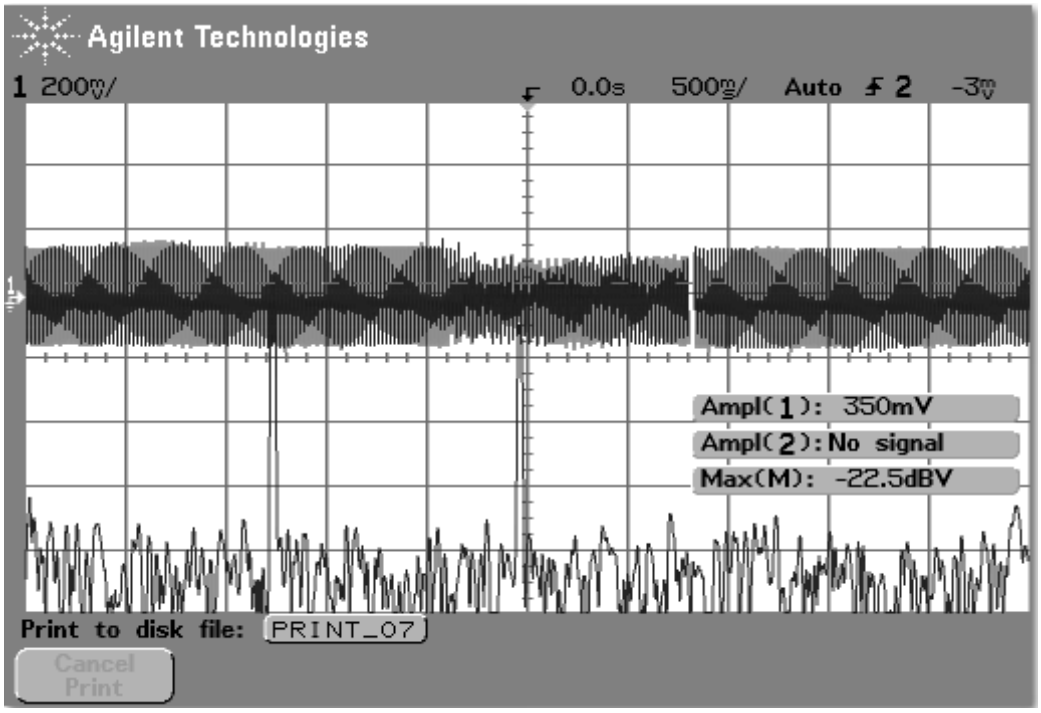

Figure 7.48 MIMO vibration control at transducer 2 forth mode 49.2 Hz before control

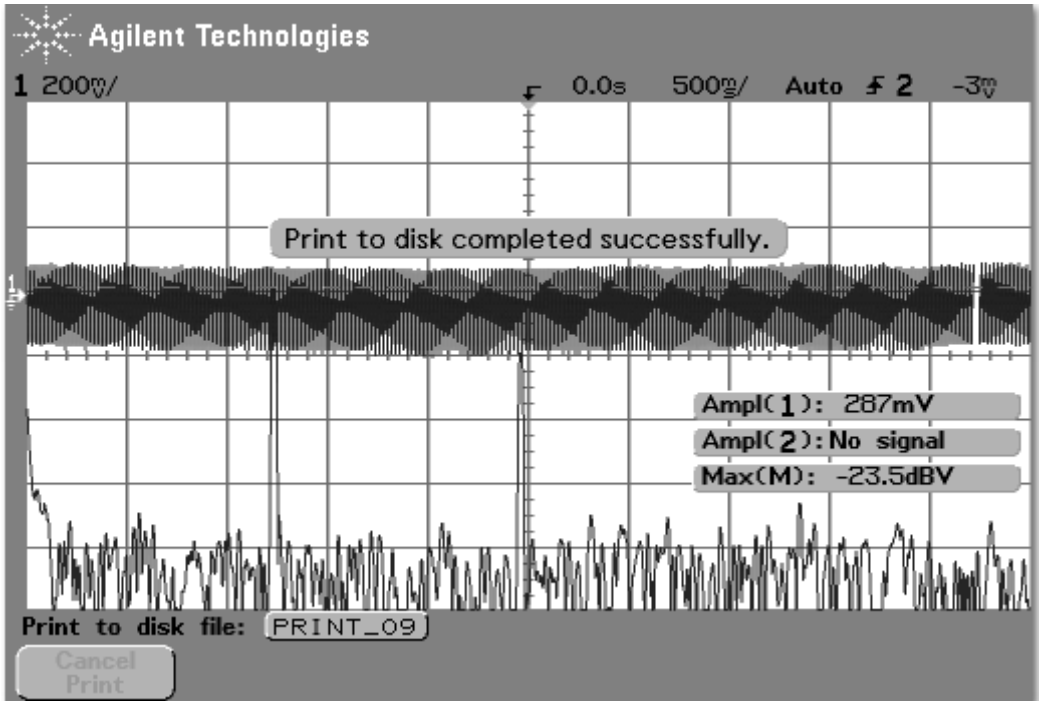

Figure 7.49 MIMO vibration control at transducer 2 forth mode 49.2 Hz after control

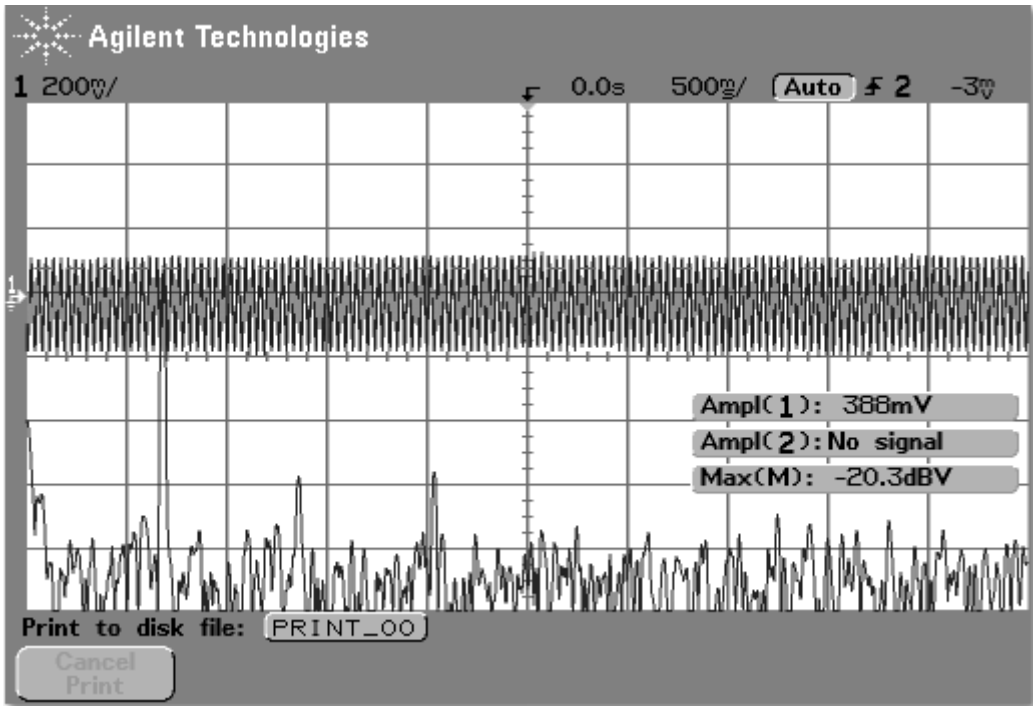

Figure 7.50 MIMO vibration control at transducer 3 first mode 27.1Hz before control

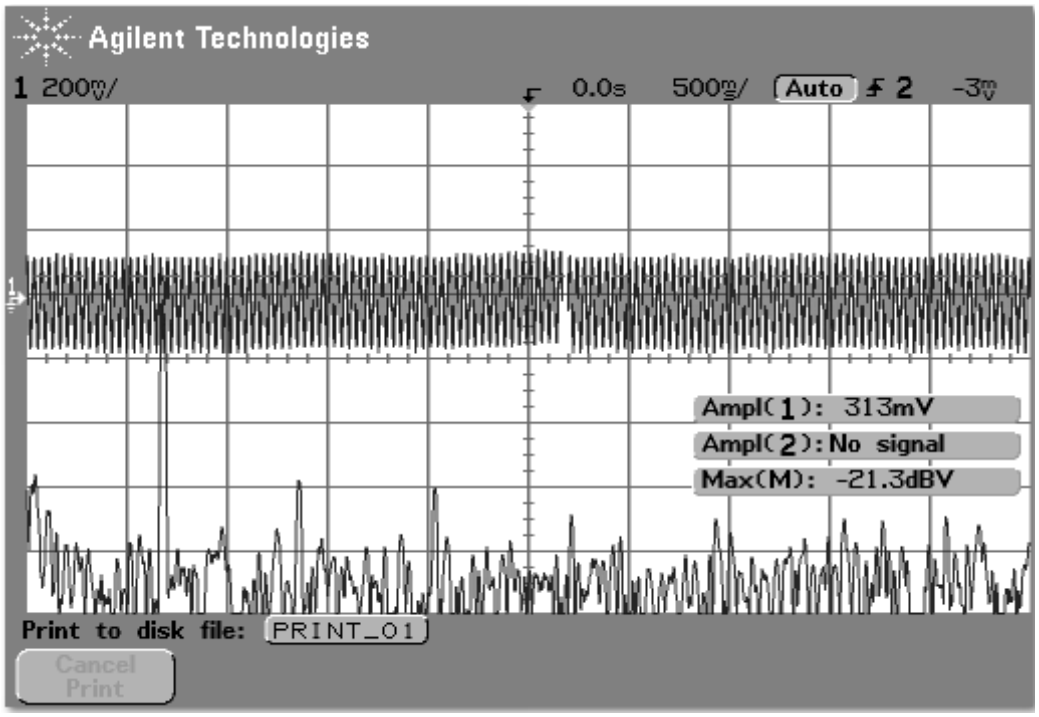

Figure 7.51 MIMO vibration control at transducer 3 first mode 27.1Hz after control

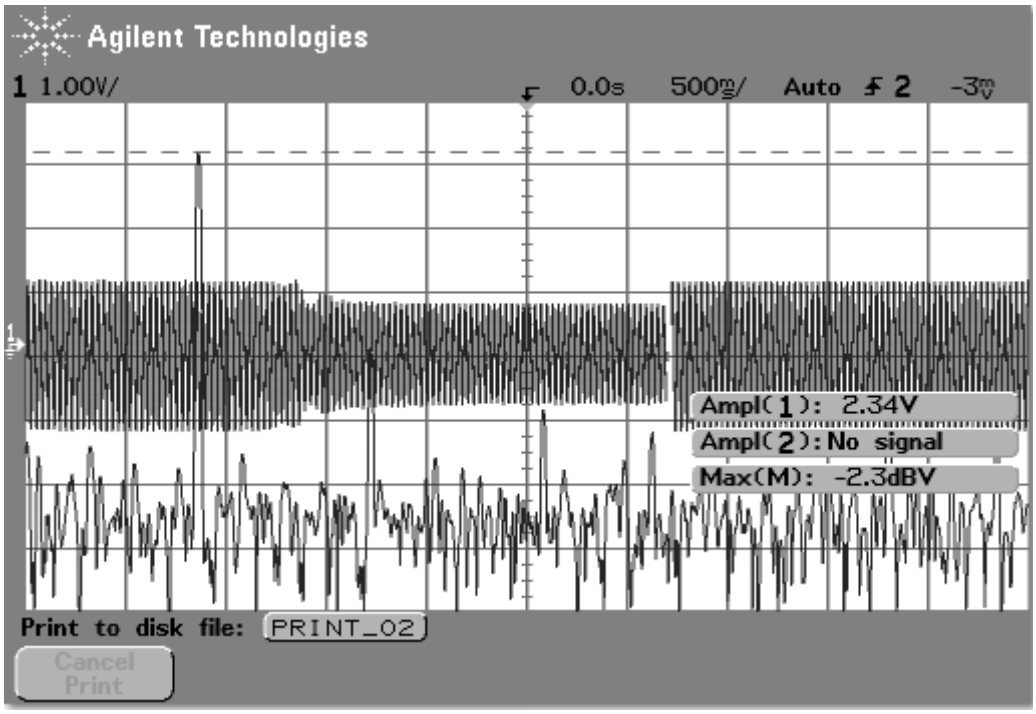

Figure 7.52 MIMO vibration control at transducer 3 second mode 34.4 Hz before control

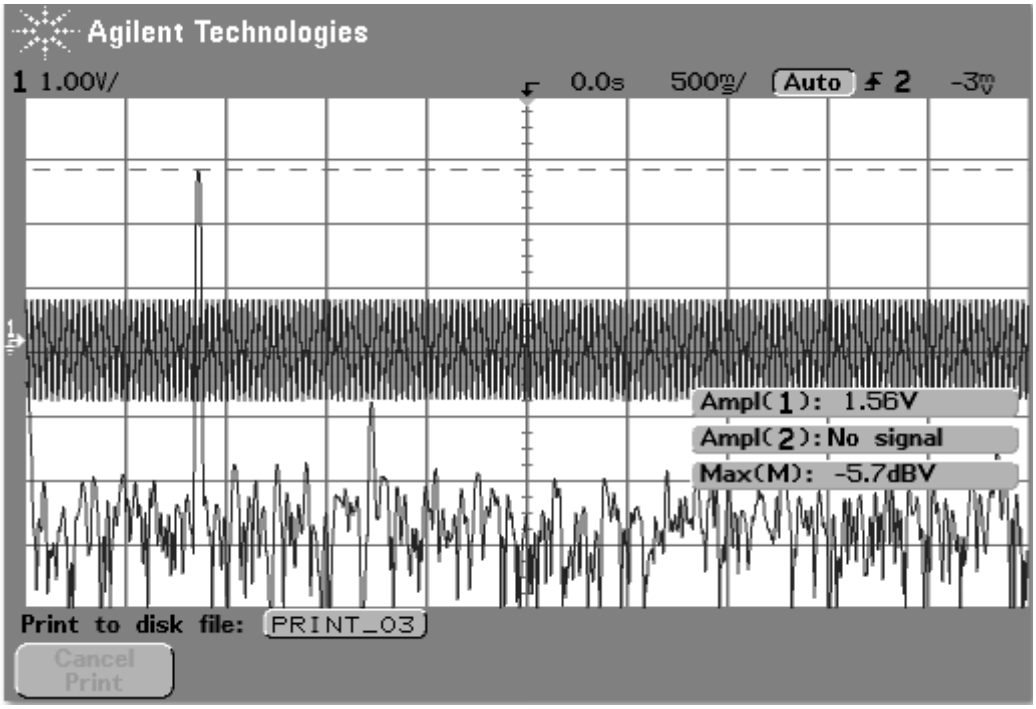

Figure 7.53 MIMO vibration control at transducer 3 second mode 34.4 Hz after control

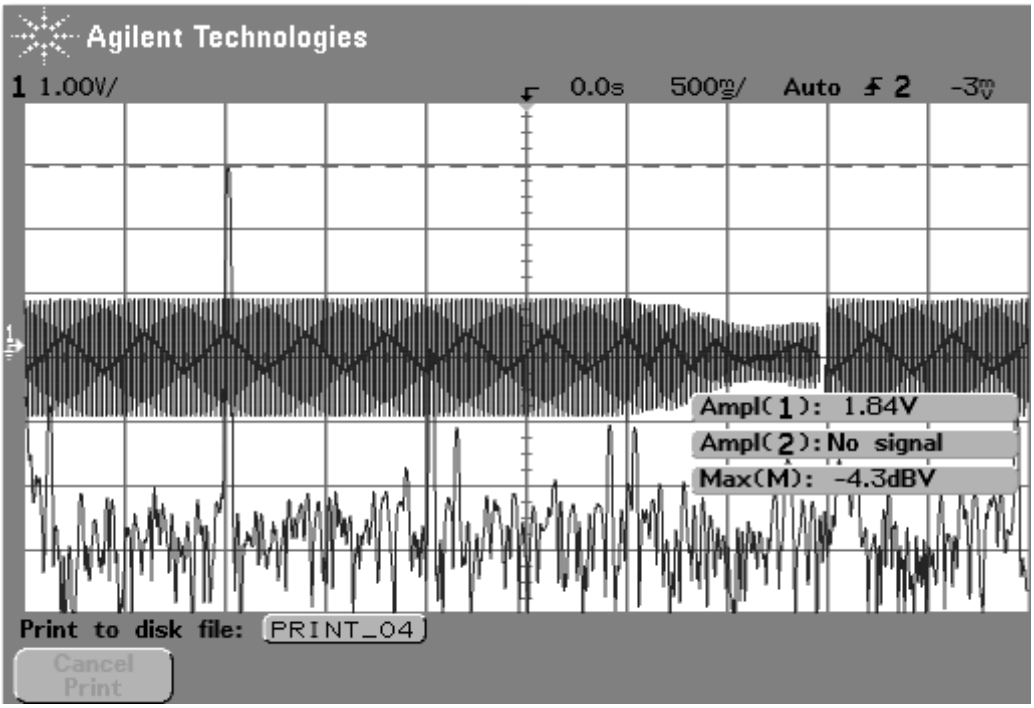

Figure 7.54 MIMO vibration control at transducer 3 third mode 40.5 Hz before control

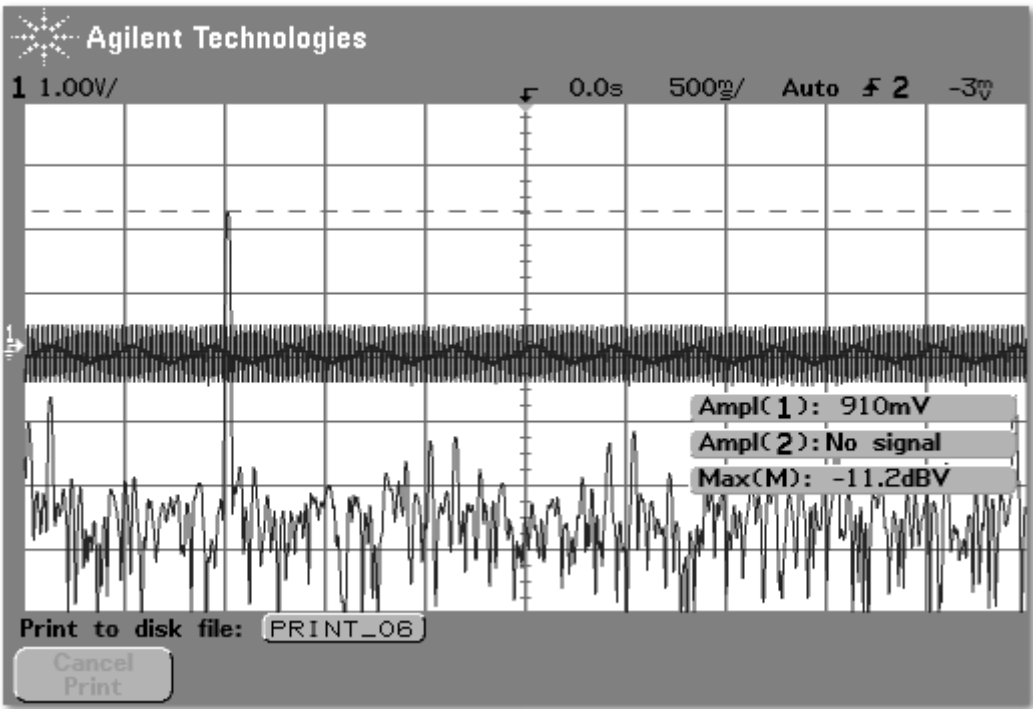

Figure 7.55 MIMO vibration control at transducer 3 third mode 40.5 Hz after control

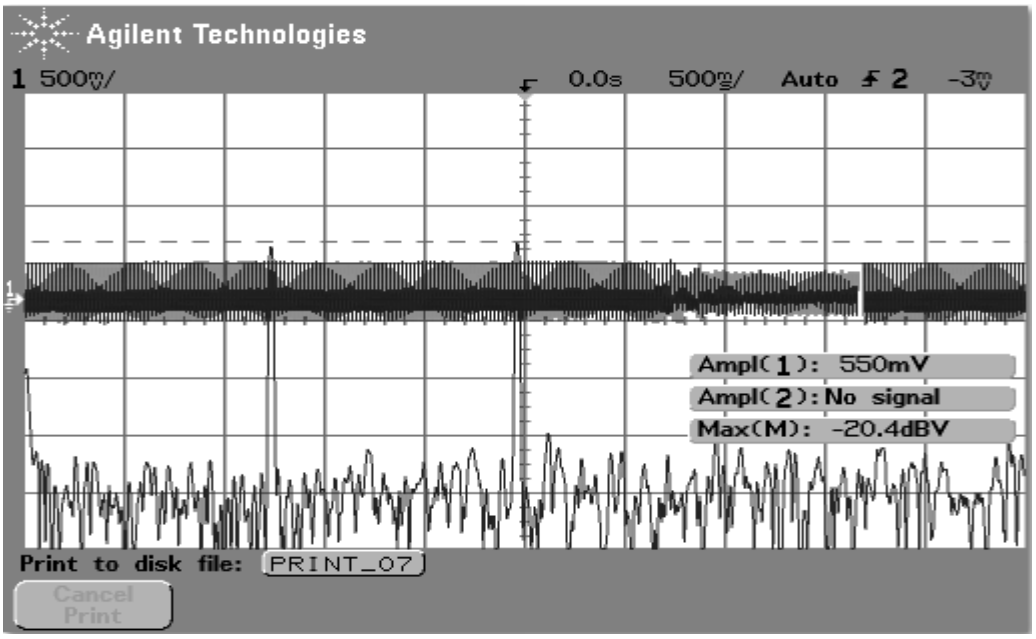

Figure 7.56 MIMO vibration control at transducer 3 forth mode 49.2 Hz before control

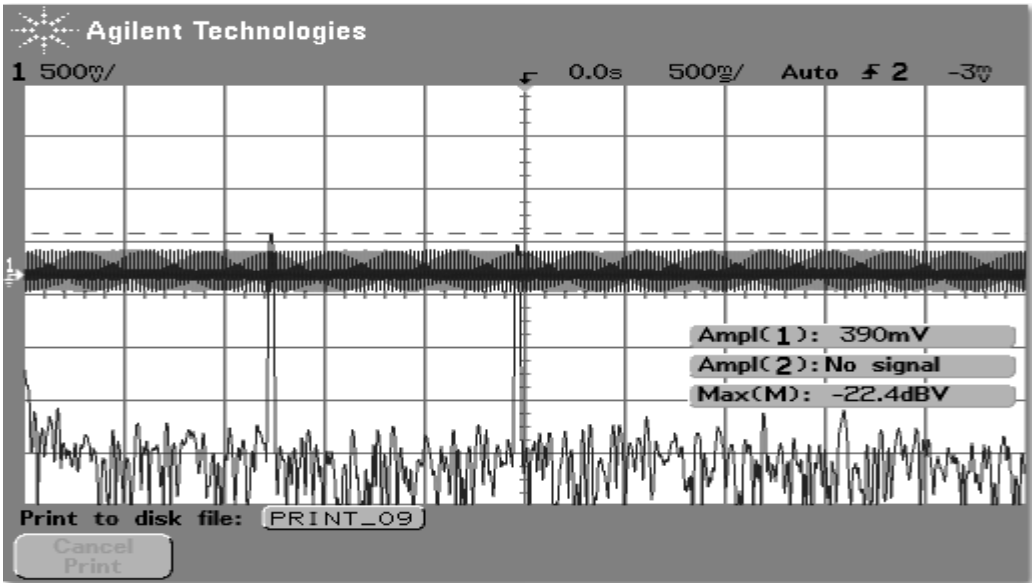

Figure 7.57 MIMO vibration control at transducer 3 forth mode 49.2 Hz after control

Sinusoid signal which is swept from 20 Hz to 50 Hz is applied to the shaker, sampling time is 0.1s. Open-loop dynamics which is between shaker to plate without controller is compared to closed-loop dynamics which is between shaker to plate with controller. Frequency domain cases are designed to test the ability of MIMO controller to attenuate multi-mode vibration when the controller centre frequencies match the

resonant frequencies of the plate . The following is the multi-mode MIMO vibration control experiment result at each transducer.

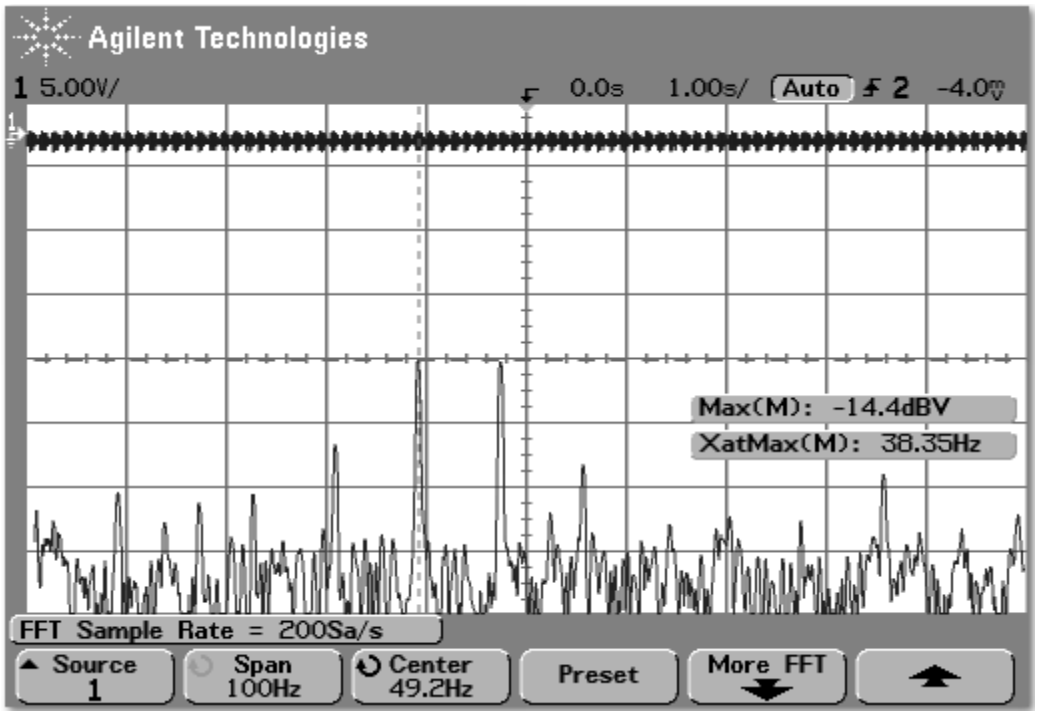

Figure 7.58 MIMO vibration control for sweep signal at transducer 1 before control

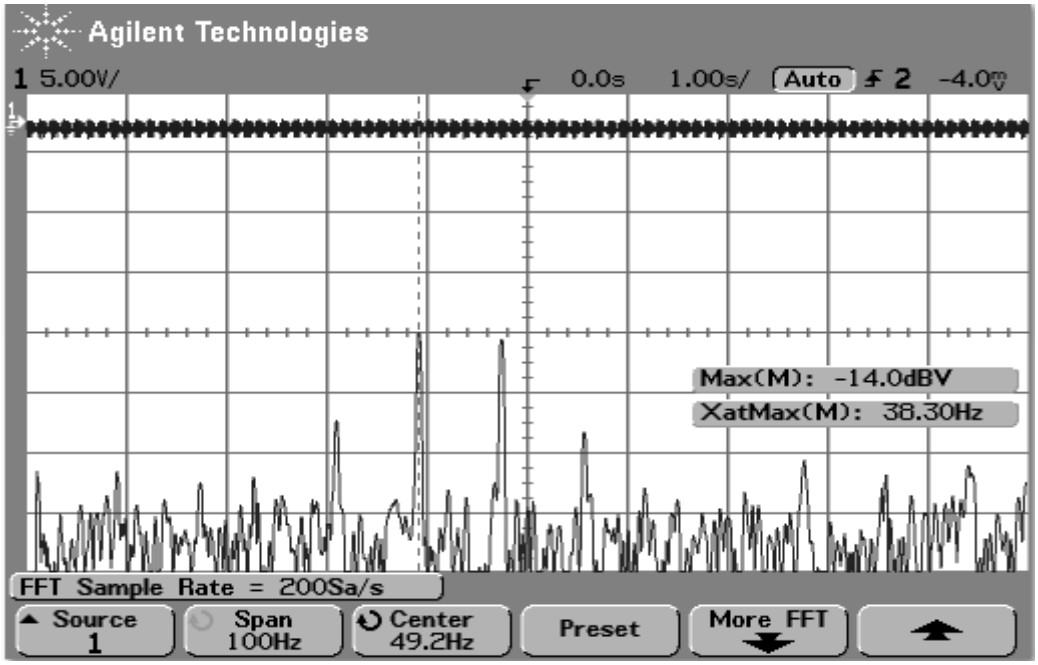

Figure 7.59 MIMO vibration control for sweep signal at transducer 1 after control

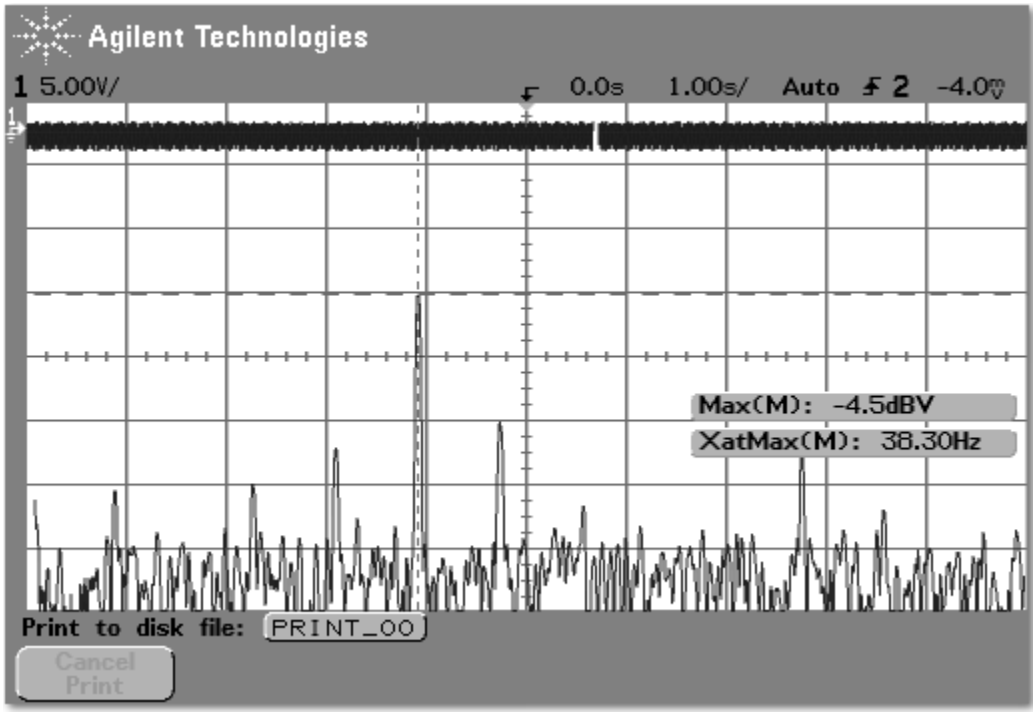

Figure 7.60 MIMO vibration control for sweep signal at transducer 2 before control

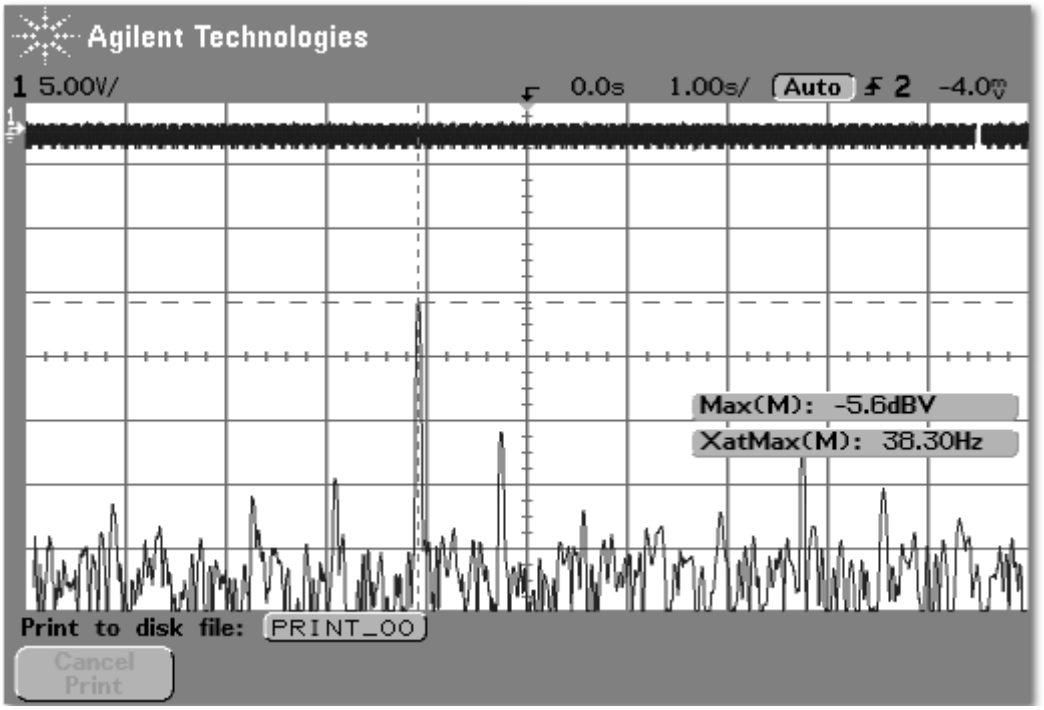

Figure 7.61 MIMO vibration control for sweep signal at transducer 2 after control

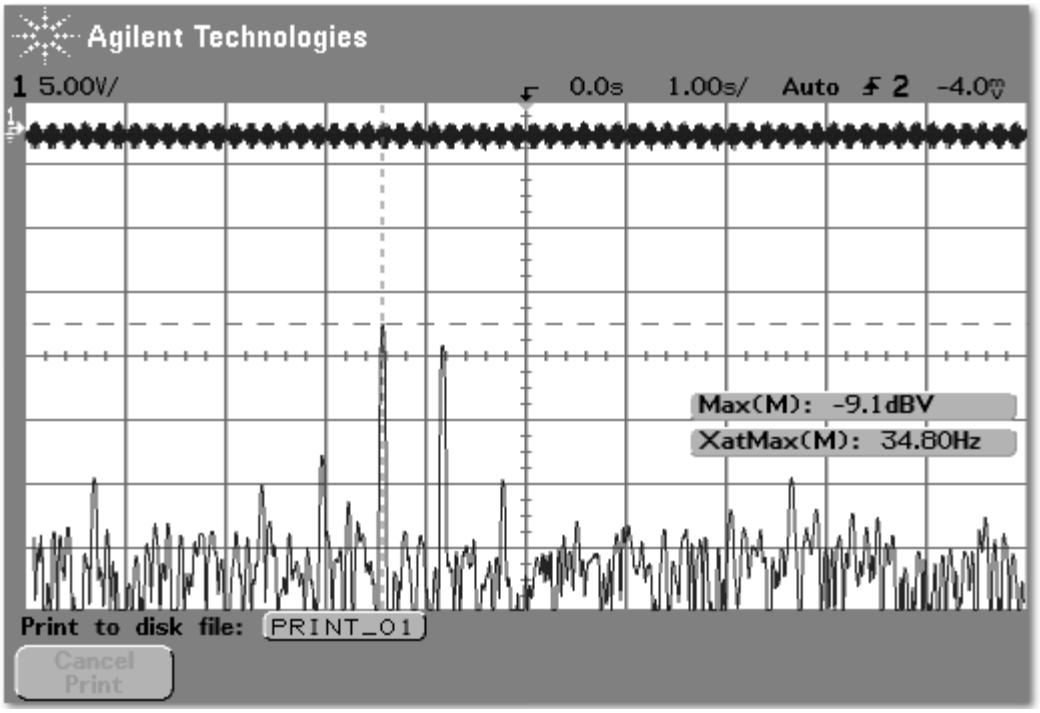

Figure 7.63 MIMO vibration control for sweep signal at transducer 3 before control

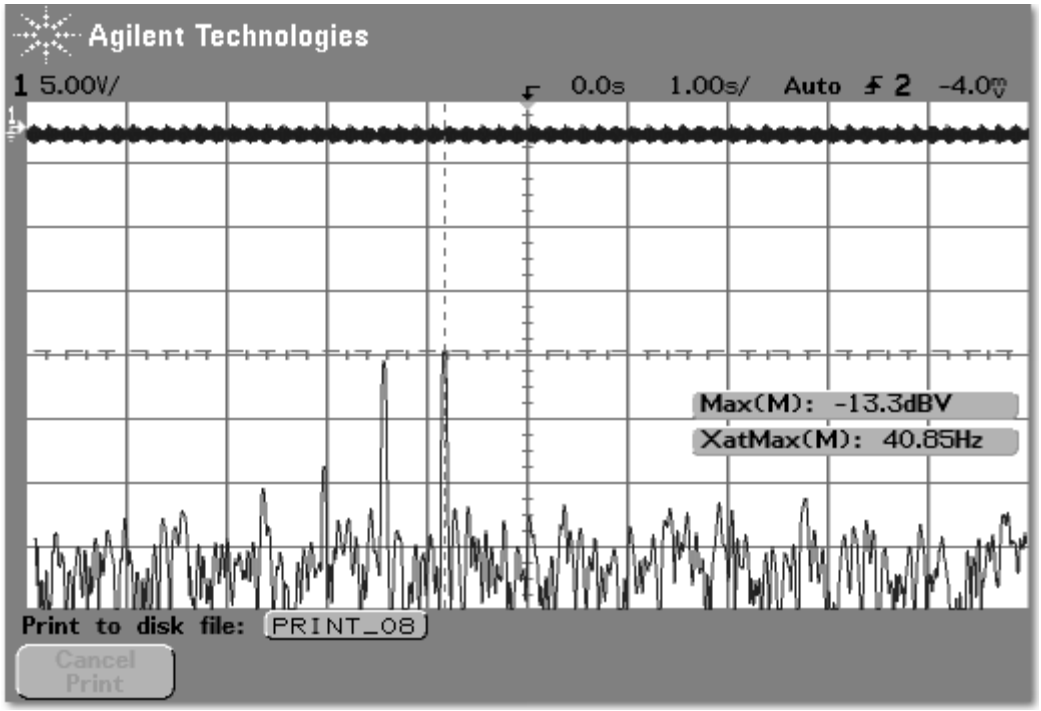

Figure 7.63 MIMO vibration control for sweep signal at transducer 3 after control

The parameters of the MIMO PPF controller are given in Table 7.7.

			frequency (Hz)			
			27.1	34.4	40.5	49.2
transduer 1	Acceleration (g)	before	1.44	1.56	0.7	4.81
		after	1.16	1.13	0.45	4.13
	reduce rate (%)		**19.444%**	**27.64%**	**35.714%**	**14.137%**
	Max Peak (dB)	before	-6.6	-6.2	-13.9	4.2
		after	-8.6	-8.9	-17.8	2.7
	reduce(dB)		**2**	**2.7**	**3.9**	**1.5**
transduer 2	Acceleration (g)	before	0.294	2.75	2.16	0.35
		after	0.194	2.22	0.88	0.287
	reduce rate(%)		**34.01%**	**19.27%**	**59.26%**	**18%**
	Max Peak (dB)	before	-22.6	-0.8	-3.1	-22.5
		after	-27.6	-2.8	-11.5	-23.5
	Reduce (dB)		**5**	**2**	**7.6**	**1**
transduer 3	Acceleration (g)	before	0.388	2.34	1.84	0.55
		after	0.313	1.56	0.91	0.39
	reduce rate(%)		**19.33%**	**33.333%**	**50.543%**	**29.091%**
	Max Peak (dB)	before	-20.3	-2.3	-4.3	-20.4
		after	-21.3	-5.7	-11.2	-22.4
	Reduce (dB)		**1**	**3.4**	**6.9**	**2**

Table 7.7 multi-mode MIMO vibration control experimental results

7.5 Summary

Although we try to derive the mathematical model which has the same dynamics response as the experimental plant, the parameters of the multi-mode SISO and MIMO PPF controllers in the experimental study are still different from the ones in simulation study because during modelling, we simplified the structure of transducer which is more complicated with electromagnetic and nonlinear characters in the fact.

For multi-mode three SISO PPF controller, the open-loop and closed-loop time domain and frequency domain results can be seen through Figure 7.4-7.33 and Table 7.4, 7.5.

It can be seen in the figure that at the beginning of turning on controller, there was a noise happened.

From a mathematical point of view, when the control is off, the transfer function is simply that of a monic vibrating system subjected to an arbitrary impulse. When the control comes on, the transfer function that describes the input-output relationship between the sensor and actuator takes over, however, its denominator remains the same, while its numerator will be altered [64].

Physically, this is due to the fact that for the collocated sensor/actuator pair (in the experiment, sensor and actuator is the same one) there will be some direct energy transmission from the actuator to the sensor. Thus the sensor voltage is made up of two components, some of the response due to the actuator, and some direct transmission of the force due to the collocation of the actuator [64].

However, this is not a problem for the PPF control law, as it was proven to be stable even in the presence control law of feed through in Chapter 5.3.

For sweep signal multi-mode three SISO vibration control result, it did not show the attenuation at each mode as in simulation.

For multi-mode MIMO PPF controller, the open-loop and closed-loop results can be seen through Figure 7.34-7.63 and Table 7.5, 7.6. It is shown a better result comparing with multi-mode three SISO PPF controller and there is no noise happened at the beginning of turning on controller.

For the first mode, the performance of multi-mode MIMO PPF controller is not good, because there is only one transducer (transducer 1) at that side, but there are two degrees of freedom at the corners (bending and torsion which could be seen in the ANSYS result Fig 2.13), one transducer is not enough to control two degrees of freedom vibration at the same time.

Same with mode 3 and mode 4, the performance of multi-mode MIMO controllers was decreased because only one transducer is not enough to control two degrees of freedom vibration at the same time.

For sweep signal multi-mode MIMO vibration control result, due to the limitation of oscilloscope which can only read the max(M) result, it could get the exactly attenuation result at each mode, but the attenuation at each mode still can be seen from the figure.

Chapter 8

Conclusion and Future Work

8.1 Outcomes of the Research

Because the increasing demand for improving dynamic performance, the operating efficiency, and the amount of material which is used in mechanical structures, many designers employ lightweight materials to reduce the cross sectional dimensions of those structures.

Due to the side-effect of employing lightweight materials and reducing the cross sectional dimensions, the structures become more flexible and more susceptible to the detrimental effects of unwanted vibration, particularly when they operate at or near their natural frequencies or when they are excited by disturbances that coincide with their natural frequencies.

The design and implementation of a high performance vibration controller for a flexible structure can be a so important task. In order to complete the task and achieve better performance, in this thesis, the author did the following things:

- Firstly, based on experimental, analytical and numerical three kinds of analysis methods, an infinite-dimensional and a very high-order mathematical transfer function model for distributed parameter plate structure is derived, using modal analysis and numerical analysis results. A 47 modes plate model was given as the simulation model.
- Secondly, traditional balanced model reduction method is used to decrease the dimensions and orders of the plate simulation model.
- Thirdly, a four modes feed-through truncated plate model which minimizing the effect of other truncated modes on spatial low-frequency dynamics of the system by adding a spatial zero frequency term to the truncated model is provided.

Numerical software MATLAB is used to compare the feed-through truncated plate model with balanced reduction plate model.

- Fourthly, both multi-mode SISO and MIMO PPF active control laws based upon positive position feedback is proposed, developed and studied for the flexible plate structure with bonded three self-sensing magnetic transducers which guarantee unconditional stability of the closed-loop system similar as collocated control system. The proposed multi-mode SISO and MIMO PPF controllers can be tuned to the chosen first four modes of the plate structure and increased the damping of the plate so as to minimize the chosen resonant responses. Stability conditions for scalar and multivariable case of PPF controllers are derived, multivariable case which allow for a feed-through term in the model is also derived, which is needed to ensure little perturbation in the in-bandwidth zeros of the model. In order to derive optimal controller parameters, a minimization criterion based on the H_∞ norm of the closed-loop system is solved by a genetic algorithm.
- Fifthly, the proposed multi-mode MIMO PPF controller, compared with multi-mode SISO PPF controller, which is validated in both simulations and experimental implementation, is an effective solution to suppress the vibration of distributed parameter plate structure.

According to literature review, the proposed multi-mode active vibration control methodology for plate structure using H_∞ optimization MIMO positive position feedback based genetic algorithm is the first time, similar method only can be found such as SISO PPF using H_∞ optimization based on genetic algorithm applied on beam structure[65], MIMO PPF using H_∞ optimization and pole optimization applied on beam structure[1, 3] .

8.2 Future Work

Within the scope of the research project documented herein, the development and implementation of multi-mode active vibration control methodology for plate structure using H_∞ optimization positive position feedback based genetic algorithm is focused on an MIMO basis. Due to the limited time and other restrained conditions, some parts of the experimental study may need to improve in the future.

- Firstly, the outcomes of this thesis provide a basis for further research application and is recommended for future work for the implementation of ***adaptive*** active vibration control methodology using H_∞ optimization MIMO positive position feedback based genetic algorithm which can be applied to multi-mode vibration control of a large class of flexible structures with varying and unknown parameters or loading conditions.
- Secondly, as discussed in Chapter 7.5, for the first mode, the performance of multi-mode MIMO PPF controller is not good enough because there is only one transducer (transducer 1) at that side, one transducer is not enough to control two degrees of freedom vibration (bending and torsion which could be seen in the ANSYS result Fig 2.13) at the same time. So another transducer which could be added to the plant is recommended for future work. And the author also did a simulation in ANSYS with four transducers. It is can be seen that the vibration suppression is better than three transducers.

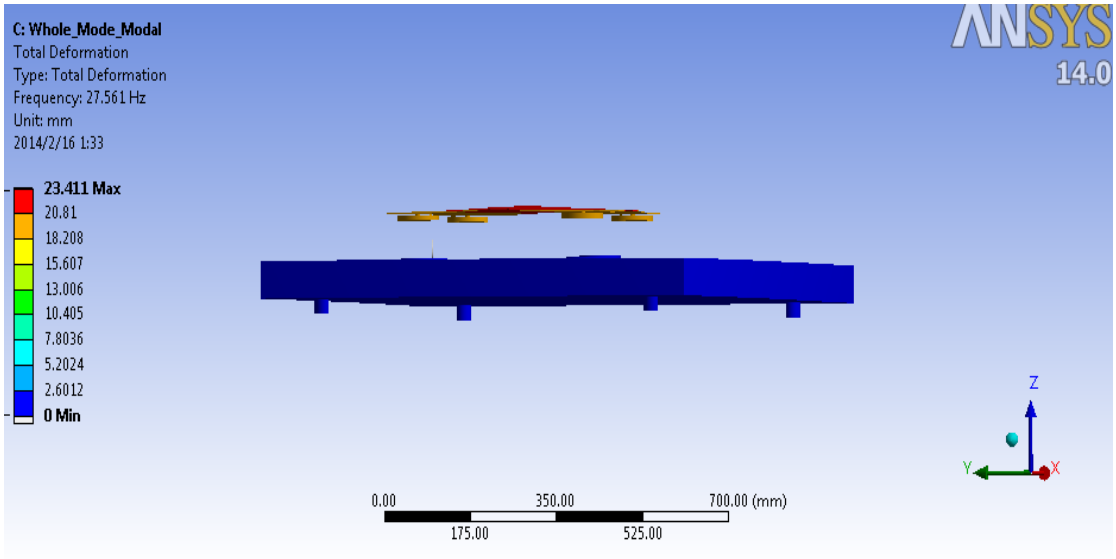

Figure 8.1 Modal Analysis mode shape of first mode with four transducers

- Thirdly, because the whole system was set up several years ago for the research study of honours degree student, four electromagnetic transducers which the frequency range is 20−200 Hz were bought before, the author could not find the similar size and similar frequency range transducer in the market during experimental study. If the fifth electromagnetic transducer which is added to the mechanical plant is heavier than others, the parameters of the whole mechanical

plant may change hugely, for example, the frequency of the first mode may drop down and below 20 Hz, which is beyond the frequency range of the transducer, or just a little bit over 20Hz, which is in the strongly nonlinear output area of the electromagnetic transducer and very hard to control the vibration of plate . So it is recommended for future that make a same size and same frequency range transducer by hand if could not find in the market, either.

- Fourthly, because the limitation of electromagnetic transducer, such as the frequency range only between 20−200 Hz, the limitation of the oscilloscope which can only read the max(M) result, piezoelectric sensor and actuator, signal analyzer are recommended for future experimental study to instead of the old equipments.
- Fifthly, as stated in 1.5.3 of Chapter 1, PPF combine with Genetic Algorithms (GA), the optimal control position of the three control transducers is also recommended for future work, which could be derived through GA calculation.
- Sixthly, although the author try to derive the mathematical model which has the same dynamic response as the experimental plant, the parameters of the multi-mode SISO and MIMO PPF controllers in the experimental study are still different from the ones in the simulation study because during modelling, the author simplified the structure of the transducer which is more complicated with electromagnetic and nonlinear characters in the fact. So it is recommended to remodel the transducer and minimize the effect to the whole system for future work.

Bibliography

[1] Moheimani, S. O. R., Vautier, B. J. G., & Bhilkkaji, B. (2005, December). Multivariable PPF control of an active structure. In Decision and Control, 2005 and 2005 European Control Conference. CDC-ECC'05. 44th IEEE Conference on (pp. 6824-6829). IEEE

[2] Halim, D., & Moheimani, S. O. (2004). Reducing the effect of truncation error in spatial and pointwise models of resonant systems with damping. Mechanical systems and signal processing, 18(2), 291-315

[3] Moheimani, S. R., Vautier, B. J., & Bhikkaji, B. (2006). Experimental implementation of extended multivariable PPF control on an active structure. Control Systems Technology, IEEE Transactions on, 14(3), 443-455

[4] Tjahyadi, H. (2007). Adaptive multi mode vibration control of dynamically loaded flexible structures (Doctoral dissertation, Flinders University)

[5] P Micheau and P. Coirault. Adaptive controller using filter banks to reject multi-sinusoidal disturbance. Automatica, 36:1659–1664, 2000.

[6] D.J. Inman. Engineering Vibration. Prentice Hall, USA, 1996.

[7] Andre Preumont, Kazuto Seto. Active control of structures, UK, 2008

[8] Dorf, R. C. (1991). Modern control systems. Addison-Wesley Longman Publishing Co., Inc..

[9] Genta, G. (2009). Vibration dynamics and control. Springer.

[10] Haugen, F. (2010). Basic Dynamics and Control. Porsgrunn: TeachTech.

[11] Belgacem, W., Berry, A., & Masson, P. (2012). Active vibration control on a quarter-car for cancellation of road noise disturbance. Journal of Sound and Vibration, 331(14), 3240-3254

[12] Yong, S., Zhiyuan, G., Shouwe, G., Jincong, Y., & Xiaojin, Z. (2010, July). FXLMS algorithm based multi channel active vibration control of piezoelectric flexible beam. In Intelligent Control and Automation (WCICA), 2010 8th World Congress on (pp. 4845-4850). IEEE.

[13] Li, D. S., & Cheng, L. (2010). The design of synthesized structural acoustic sensors for active control of interior noise with experimental validation. Journal of Sound and Vibration, 329(2), 123-139

[14] Preumont, A. (1999). Vibration control of active structures: an introduction. Meccanica, 34(2), 139-139.

[15] C.R. Fuller, S.J. Elliott, and P.A. Nelson. Active Control of Vibration. Academic Press, London, 1996.

[16] Iwamoto, H., Tanaka, N., & Hill, S. G. (2012). Feedback control of wave propagation in a rectangular panel, part 2: Experimental realization using clustered velocity and displacement feedback. Mechanical Systems and Signal Processing.

[17] Li, S. (2011). Active modal control simulation of vibro-acoustic response of a fluid-loaded plate. Journal of Sound and Vibration, 330(23), 5545-5557

[18] Kim, S. M., & Oh, J. E. (2013). A modal filter approach to non-collocated vibration control of structures. Journal of Sound and Vibration

[19] Meirovitch, L., Van Landingham, H. F., & Öz, H. (1977). Control of spinning flexible spacecraft by modal synthesis. Acta Astronautica, 4(9), 985-1010

[20] Meirovitch, L., Baruh, H., & OZ, H. (1983). A comparison of control techniques for large flexible systems. Journal of Guidance, Control, and Dynamics, 6(4), 302-310

[21] Moheimani, S. O. R., Fleming, A. J., & Behrens, S. (2001). Highly resonant controller for multimode piezoelectric shunt damping. Electronics Letters, 37(25), 1505-1506

[22] Pota, H. R., Moheimani, S. R., & Smith, M. (2002). Resonant controllers for smart structures. Smart Materials and Structures, 11(1), 1

[23] Aphale, S. S., Fleming, A. J., & Moheimani, S. R. (2007). Integral resonant control of collocated smart structures. Smart Materials and Structures, 16(2), 439.

[24] Pereira, E., Moheimani, S. O. R., & Aphale, S. S. (2008). Analog implementation of an integral resonant control scheme. Smart Materials and Structures, 17(6), 067001.

[25] Mahmood, I. A., Moheimani, S. R., & Bhikkaji, B. (2008). Precise tip positioning of a flexible manipulator using resonant control. Mechatronics, IEEE/ASME Transactions on, 13(2), 180-186.

[26] Pereira, E., Aphale, S. S., Feliu, V., & Moheimani, S. R. (2011). Integral resonant control for vibration damping and precise tip-positioning of a single-link flexible manipulator. Mechatronics, IEEE/ASME Transactions on, 16(2), 232-240

[27] Halim, D., & Moheimani, S. R. (2001). Spatial resonant control of flexible structures-application to a piezoelectric laminate beam. Control Systems Technology, IEEE Transactions on, 9(1), 37-53

[28] Goh, C. J. (1983). Analysis and control of quasi distributed parameter systems (Doctoral dissertation, California Institute of Technology).

[29] Goh, C. J., & Caughey, T. K. (1985). On the stability problem caused by finite actuator dynamics in the collocated control of large space structures. International Journal of Control, 41(3), 787-802

[30] Fanson J L, An experimental investigation of vibration suppression in large space structures using positive position feedback, PhD Thesis California Institute of Technology,November,1986

[31] J. L. Fanson, and T. K. Caughey, "Positive Position Feedback Control for Large Space Structures," AIAA Journal, vol. 28, no. 4, pp.717-724, 1990

[32] Song G, Schmidt S P and Agrawal B N, Experimental robustness study of positive position feedback control for active vibration suppression, J. Guidance, VOL. 25, NO. 1: ENGINEERING NOTES, 2001

[33] Baz, A., Poh, S., & Fedor, J. (1989). Independent modal space control with positive position feedback. Dynamics and control of large structures, 553-567

[34] Poh, S., & Baz, A. (1990). Active control of a flexible structure using a modal positive position feedback controller. Journal of Intelligent Material Systems and Structures, 1(3), 273-288.

[35] Goh, C. J., & Lee, T. H. (1991). Adaptive modal parameters identification for collocated position feedback vibration control. International Journal of Control, 53(3), 597-617.

[36] Caughey, T. K. (1995). Dynamic response of structures constructed from smart materials. Smart Materials and Structures, 4(1A), A101

[37] Baz, A., & Poh, S. (1996). Optimal vibration control with modal positive position feedback. Optimal control applications and methods, 17(2), 141-149

[38] Baz, A., & HONG, J. T. (1997). Adaptive control of flexible structures using modal positive position feedback. International journal of adaptive control and signal processing, 11(3), 231-253

[39] Wang, L. (2003, October). Positive position feedback based vibration attenuation for a flexible aerospace structure using multiple piezoelectric actuators. In Digital Avionics Systems Conference, 2003. DASC'03. The 22nd (Vol. 2, pp. 7-C). IEEE.

[40] Shan, J., Liu, H. T., & Sun, D. (2005). Slewing and vibration control of a single-link flexible manipulator by positive position feedback (PPF). Mechatronics, 15(4), 487-503.

[41] Hong, C., Shin, C., & Jeong, W. (2010). Active vibration control of clamped beams using PPF controllers with piezoceramic actuators. Proc. 20th Int. Congr. on Acoustics (Sydney, Australia, ICA 2010 23–27 August 2010).

[42] Ahmed, B., & Pota, H. R. (2011). Dynamic compensation for control of a rotary wing UAV using positive position feedback. Journal of Intelligent & Robotic Systems, 61(1-4), 43-56.

[43] Chuang, K. C., Ma, C. C., & Wu, R. H. (2012). Active suppression of a beam under a moving mass using a pointwise fiber bragg grating displacement sensing system. Ultrasonics, Ferroelectrics and Frequency Control, IEEE Transactions on, 59(10), 2137-2148.

[44] Shin, C., Hong, C., & Jeong, W. B. (2012). Active vibration control of clamped beams using positive position feedback controllers with moment pair. Journal of mechanical science and technology, 26(3), 731-740.

[45] Bang, H., & Agrawal, B. N. (1994). A generalized second order compensator design for vibration control of flexible structures. In AIAA/ASME/ASCE/AHS/ASC Structures, Structural Dynamics, and Materials Conference, 35th, Hilton Head, SC (pp. 2438-2448).

[46] Mahmoodi, S. N., Aagaah, M. R., & Ahmadian, M. (2009, June). Active vibration control of aerospace structures using a modified positive position feedback method. In American Control Conference, 2009. ACC'09. (pp. 4115-4120). IEEE

[47] Hu, Q., Xie, L., & Gao, H. (2006, December). A combined positive position feedback and variable structure approach for flexible spacecraft under input

nonlinearity. In Control, Automation, Robotics and Vision, 2006. ICARCV'06. 9th International Conference on (pp. 1-6). IEEE.

[48] Hu, Q., Xie, L., & Gao, H. (2007). Adaptive variable structure and active vibration reduction for flexible spacecraft under input nonlinearity. Journal of Vibration and Control, 13(11), 1573-1602.

[49] Kim, S. M., Wang, S., & Brennan, M. J. (2011). Comparison of negative and positive position feedback control of a flexible structure. Smart Materials and Structures, 20(1), 015011.

[50] Bhikkaji, B., Ratnam, M., Fleming, A. J., & Moheimani, S. R. (2007). High-performance control of piezoelectric tube scanners. Control Systems Technology, IEEE Transactions on, 15(5), 853-866.

[51] Chen, L., He, F., & Sammut, K. (2002). Nonlinear modal positive position feedback for vibration control in distributed parameter systems. In Annual Conference.

[52] Qiu, Z. C., Zhang, X. M., Wu, H. X., & Zhang, H. H. (2007). Optimal placement and active vibration control for piezoelectric smart flexible cantilever plate. Journal of Sound and Vibration, 301(3), 521-543.

[53] Song, G., Qiao, P. Z., Binienda, W. K., & Zou, G. P. (2002). Active vibration damping of composite beam using smart sensors and actuators. Journal of Aerospace Engineering, 15(3), 97-103

[54] Song G, Schmidt S P and Agrawal B N, Experimental robustness study of positive position feedback control for active vibration suppression, J. Guidance, VOL. 25, NO. 1: ENGINEERING NOTES, 2001

[55] Long, Z., & Guangren, D. (2012, May). A robust vibration suppression controller design for space flexible structures. In Control and Decision Conference (CCDC), 2012 24th Chinese (pp. 4020-4024). IEEE.

[56] Baz, A., & HONG, J. T. (1997). Adaptive control of flexible structures using modal positive position feedback. International journal of adaptive control and signal processing, 11(3), 231-253

[57] Kwak, M. K., & Han, S. B. (1998, July). Application of genetic algorithms to the determination of multiple positive-position feedback controller gains for smart

structures. In 5th Annual International Symposium on Smart Structures and Materials (pp. 637-648). International Society for Optics and Photonics.

[58] Kwak, M. K., & Shin, T. S. (1999, June). Real-time automatic tuning of vibration controllers for smart structures by genetic algorithm. In Proceedings of SPIE- The International Society for Optical Engineering (Vol. 3667, pp. 679-690)

[59] Kwak, M. K., & Heo, S. (2000, June). Real-time multiple-parameter tuning of PPF controllers for smart structures by genetic algorithms. In SPIE's 7th Annual International Symposium on Smart Structures and Materials (pp. 279-290). International Society for Optics and Photonics

[60] Kwak, M. K., Heo, S., & Jin, G. J. (2002, July). Adaptive positive-position feedback controller design for the vibration suppression of smart structures. In SPIE's 9th Annual International Symposium on Smart Structures and Materials (pp. 246-255). International Society for Optics and Photonics

[61] Rew, K. H., Han, J. H., & Lee, I. (2002). Multi-modal vibration control using adaptive positive position feedback. Journal of intelligent material systems and structures, 13(1), 13-22

[62] Orszulik R and Shan J., Active Vibration Control using Adaptive Positive Position Feedback, AIAA Guidance, 2009

[63] Orszulik R and Shan J., Vibration control using input shaping and adaptive positive position feedback , J. Guidance, 2011

[64] Orszulik, R., & Shan, J. (2011, June). Multi-mode adaptive positive position feedback: An experimental study. In American Control Conference (ACC), 2011 (pp. 3315-3319). IEEE

[65] Orszulik, R. R., & Shan, J. (2012). Active vibration control using genetic algorithm-based system identification and positive position feedback. Smart Materials and Structures, 21(5), 055002

[66] Han, J. H., & Lee, I. (1999). Optimal placement of piezoelectric sensors and actuators for vibration control of a composite plate using genetic algorithms. Smart Materials and Structures, 8(2), 257

[67] Qiu, Z. C., Zhang, X. M., Wu, H. X., & Zhang, H. H. (2007). Optimal placement and active vibration control for piezoelectric smart flexible cantilever plate. Journal of Sound and Vibration, 301(3), 521-543.

[68] Dosch, J. J., Leo, D. J., & Inman, D. J. (1992). Comparison of vibration control schemes for a smart antenna. In Decision and Control, 1992., Proceedings of the 31st IEEE Conference on (pp. 1815-1820). IEEE

[69] Meyer, J. L., Harrington, W. B., Agrawal, B. N., & Song, G. (1999). Vibration suppression of a spacecraft flexible appendage using smart material. Smart Materials and Structures, 7(1), 95.

[70] Friswell, M. I., & Inman, D. J. (1999). The relationship between positive position feedback and output feedback controllers. Smart Materials and Structures, 8(3), 285

[71] Song, G., Schmidt, S. P., & Agrawal, B. N. (2000). Active vibration suppression of a flexible structure using smart material and a modular control patch. Proceedings of the Institution of Mechanical Engineers, Part G: Journal of Aerospace Engineering, 214(4), 217-229

[72] Song, G., Qiao, P. Z., Binienda, W. K., & Zou, G. P. (2002). Active vibration damping of composite beam using smart sensors and actuators. Journal of Aerospace Engineering, 15(3), 97-103.

[73] Fei, J., & Fang, Y. (2006, August). Active feedback vibration suppression of a flexible steel cantilever beam using smart materials. In Innovative Computing, Information and Control, 2006. ICICIC'06. First International Conference on (Vol. 1, pp. 89-92). IEEE.

[74] Nam, Y., Park, J., Jang, H., Park, H., & Kim, J. (2006, October). Experiments on the Vibration Suppression of a Piezoelectric Beam using a Self-sensing Mechanism. In Computer Aided Control System Design, 2006 IEEE International Conference on Control Applications, 2006 IEEE International Symposium on Intelligent Control, 2006 IEEE (pp. 1121-1126). IEEE.

[75] Shan, J. (2007, August). Comparison of Two Vibration Control Methods for Flexible Manipulator with PZT Actuators. In Mechatronics and Automation, 2007. ICMA 2007. International Conference on (pp. 3220-3225). IEEE

[76] Wang, W., & Yang, Z. (2009). A compact piezoelectric stack actuator and its simulation in vibration control. Tsinghua Science & Technology, 14, 43-48

[77] Petersen, I. R. (2011, November). Negative imaginary systems theory in the robust control of highly resonant flexible structures. In Australian Control Conference (AUCC), 2011 (pp. 1-6). IEEE

[78] Ma, C. C., Chuang, K. C., & Pan, S. Y. (2011). Polyvinylidene fluoride film sensors in collocated feedback structural control: Application for suppressing impact-induced disturbances. Ultrasonics, Ferroelectrics and Frequency Control, IEEE Transactions on, 58(12), 2539-2554.

[79] Denoyer, K. K., & Kwak, M. K. (1996). Dynamic Modelling and Vibration Suppression of a Swelling Structure Utilizing Piezoelectric Sensors and Actuators. Journal of Sound and Vibration, 189(1), 13-31.

[80] Kwak, M. K., & Heo, S. (2007). Active vibration control of smart grid structure by multiinput and multioutput positive position feedback controller. Journal of Sound and Vibration, 304(1), 230-245.

[81] Han, J. H., & Lee, I. (1999). Optimal placement of piezoelectric sensors and actuators for vibration control of a composite plate using genetic algorithms. Smart Materials and Structures, 8(2), 257.

[82] Kwak, M. K., Heo, S., & Jeong, M. (2009). Dynamic modelling and active vibration controller design for a cylindrical shell equipped with piezoelectric sensors and actuators. Journal of Sound and Vibration, 321(3), 510-524.

[83] Tzou, H. S., & Tseng, C. I. (1990). Distributed piezoelectric sensor/actuator design for dynamic measurement/control of distributed parameter systems: a piezoelectric finite element approach. Journal of sound and vibration, 138(1), 17-34.

[84] Tzou, H. S. (1992). A new distributed sensor and actuator theory for “intelligent” shells. Journal of sound and vibration, 153(2), 335-349

[85] Kar, I. N., Miyakura, T., & Seto, K. (2000). Bending and torsional vibration control of a flexible plate structure using H∞-based robust control law. Control Systems Technology, IEEE Transactions on, 8(3), 545-553

[86] Zhang, Y. H., & Zhang, X. N. (2011, December). Active vibration control of a stiffened plate with a piezoelectric actuator. In Piezoelectricity, Acoustic Waves and Device Applications (SPAWDA), 2011 Symposium on (pp. 264-268). IEEE.

[87] Julai, S., & Tokhi, M. O. (2010, September). SISO and SIMO active vibration control of a flexible plate structure using real-coded genetic algorithm. In Cybernetic Intelligent Systems (CIS), 2010 IEEE 9th International Conference on (pp. 1-6). IEEE.

[88] Ojeda, X., Mininger, X., Gabsi, M., & Lécrivain, M. (2008). Noise cancellation of 6/4 switched reluctance machine by piezoelectric actuators: Optimal design and placement using genetic algorithm.

[89] Qiu, Z. C., Wu, H. X., & Ye, C. D. (2009). Acceleration sensors based modal identification and active vibration control of flexible smart cantilever plate. Aerospace Science and Technology, 13(6), 277-290.

[90] Qiu, Z. C., Zhang, X. M., Wu, H. X., & Zhang, H. H. (2007). Optimal placement and active vibration control for piezoelectric smart flexible cantilever plate. Journal of Sound and Vibration, 301(3), 521-543.

[91] Aoki, Y., Gardonio, P., & Elliott, S. J. (2008). Rectangular plate with velocity feedback loops using triangularly shaped piezoceramic actuators: Experimental control performance. The Journal of the Acoustical Society of America, 123, 1421.

[92] Zilletti, M., Elliott, S. J., Gardonio, P., & Rustighi, E. (2012). Experimental implementation of a self-tuning control system for decentralised velocity feedback. Journal of Sound and Vibration, 331(1), 1-14.

[93] Ma, K. (2003). Adaptive non-linear control of a clamped rectangular plate with PZT patches. Journal of Sound and Vibration, 264(4), 835-850.

[94] Ma, K., & Ghasemi-Nejhad, M. N. (2007). Adaptive input shaping and control for simultaneous precision positioning and vibration suppression of smart composite plates. Smart Materials and Structures, 16(5), 1870.

[95] Zhiyuan, G., Tinggao, Q., Quanzhen, H., & Xiaojin, Z. (2009, December). Control channel identification method and experimental research on FXLMS vibration control. In Computational Intelligence and Software Engineering, 2009. CiSE 2009. International Conference on (pp. 1-4). IEEE

[96] Julai, S., & Tokhi, M. O. (2012). Active vibration control of flexible plate structures with distributed disturbances. Journal of Low Frequency Noise, Vibration and Active Control, 31(2), 123-150.

[97] Caruso, G., Galeani, S., & Menini, L. (2003). Active vibration control of an elastic plate using multiple piezoelectric sensors and actuators. Simulation Modelling Practice and Theory, 11(5), 403-419.

[98] Li, P., Cheng, L., Li, Y. Y., & Chen, N. (2003). Robust control of a vibrating plate using μ-synthesis approach. Thin-walled structures, 41(11), 973-986.

[99] Fraanje, R., Verhaegen, M., Doelman, N., & Berkhoff, A. (2004). Optimal and robust feedback controller estimation for a vibrating plate. Control engineering practice, 12(8), 1017-1027.

[100] Zhang, W., Qiu, J., & Tani, J. (2004). Robust vibration control of a plate using self-sensing actuators of piezoelectric patches. Journal of intelligent material systems and structures, 15(12), 923-931.

[101] Shimon, P., & Hurmuzlu, Y. (2007). A theoretical and experimental study of advanced control methods to suppress vibrations in a small square plate subject to temperature variations. Journal of sound and vibration, 302(3), 409-424.

[102].Shimon, P., Richer, E., & Hurmuzlu, Y. (2005). Theoretical and experimental study of efficient control of vibrations in a clamped square plate. Journal of Sound and Vibration, 282(1), 453-473.

[103] Zhu, X., Liu, J., Huang, Q., & Gao, S. (2009, August). Robust H∞ control in active vibration control of piezoelectric smart structure. In Electronic Measurement & Instruments, 2009. ICEMI'09. 9th International Conference on (pp. 3-694). IEEE

[104] Yucelen, T., & Pourboghrat, F. (2007, November). Adaptive H∞ optimal control strategy based on nonminimal state space realization. In ASME IMECE (Vol. 7).

[105] Saunders, W. R., Cole, D. G., & Robertshaw, H. H. (1994). Experiments in piezostructure modal analysis for MIMO feedback control. Smart Materials and Structures, 3(2), 210.

[106] Kapuria, S., & Yasin, M. Y. (2010). Active vibration suppression of multilayered plates integrated with piezoelectric fiber reinforced composites using an efficient finite element model. Journal of Sound and Vibration, 329(16), 3247-3265.

[107] Butler, R., & Rao, V. (1995, December). State space modeling and control of MIMO smart structures. In Decision and Control, 1995., Proceedings of the 34th IEEE Conference on (Vol. 4, pp. 3534-3539). IEEE.

[108] Proulx, B., St-Amant, Y., & Cheng, L. (1998, July). Active control of plates using integrated piezoceramic elements of various shape: modeling and experiments. In 5th Annual International Symposium on Smart Structures and Materials (pp. 735-746). International Society for Optics and Photonics.

[109] Seto, K., MINGZHANG, R., & Doi, F. (2001). Modeling and feedback structural acoustics control of a flexible plate. Journal of vibration and acoustics, 123(1), 18-23.

[110] Kim, Y. S., Kim, I., Lee, C., & Moon, C. Y. (1999, June). Active suppression of plate vibration with piezoceramic actuators/sensors using multiple adaptive feedforward with feedback loop control algorithm. In 1999 Symposium on Smart Structures and Materials (pp. 553-564). International Society for Optics and Photonics.

[111] Yang, J., & Chen, G. (2012). InputOutput Stability Theory-Based Sliding Mode Control of Flexible Circular Plate Vibration. Advanced Science Letters, 7(1), 393-399.

[112] Yang, J., & Chen, G. (2012). Computed Force-Based Sliding Mode Control for Vibration of Flexible Rectangular Plate. Advanced Science Letters, 6(1), 385-390.

[113] Moheimani, S. R., Halim, D., & Fleming, A. J. (2003). Spatial Control of Vibrations: Theory and Experiments. World scientific.

[114] L. Meirovith. Fundamentals of Vibrations. McGraw-Hill, 2001

[115] L. Meirovitch. Principles and Techniques of Vibrations. Prentice-Hall, USA, 1997

[116] Paranjape, A. A., Guan, J., Chung, S. J., & Krstic, M. (2013). PDE boundary control for flexible articulated wings on a robotic aircraft.

[117] Ole Dossing Brüel and Kjær, March 1988.Structural Testing, Part Ⅱ:Modal Analysis and Simulation.Danmark.

[118] Ulrike Zwiers, Spring 2007. First Steps in Vibration Analysis Using ANSYS

[119] David Herrin, Modal and Harmonic Analysis using ANSYS. Department of Mechanical Engineering, University of Kentucky.

[120] S. O. R. Moheimani. Experimental verification of the corrected transfer function of a piezoelectric laminate beam. IEEE Transactions on Control Systems Technology, 8(4):660-666, July 2000.

[121] Glover, K. (1984). All optimal Hankel-norm approximations of linear multivariable systems and their L,∞-error bounds†. International Journal of Control, 39(6), 1115-1193.

[122] B. D. O. Anderson G. Obinata. Model Reduction for Control System Design.

Springer-Verlag, 2000.

[123]S. O. R. Moheimani, H. R. Pota, and I. R. Petersen. Spatial balanced model reduction for flexible structures. Automatica, 32(2):269-277, February 1999.

[124] R. L. Clark, “Accounting for out-of-bandwidth modes in the assumed modes approach: Implications on colocated output feedback control,” Trans. ASME J. Dynamic Syst., Measurement, Contr., vol. 119, pp. 390–395, 1997.

[125] Caughey, T. K., Goh, C. J., “Analysis and Control of Quasi-Distributed Parameter Systems,” Dynamics Laboratory Report DYNL-82-3 (1982), California Institute of Technology, Pasadena.

[126] Hanson, B., Levesley, M., Self-sensing applications for electromagnetic actuators, Science Direct, Sensors and Actuators A 116 (2004) 345-351, June 2004